Aston University

If you have discovered material in AURA which is unlawful e.g. breaches copyright, (either yours or that of a third party) or any other law, including but not limited to those relating to patent, trademark, confidentiality, data protection, obscenity, defamation, libel, then please read our Takedown Policy and contact the service immediately

THE DEVELOPMENT OF A SOLAR WALL MODULE USING A SELECTIVE SURFACE

By

CHRISTOPHER G. LLOYD

A thesis submitted for the Degree of

DOCTOR OF PHILOSOPHY

THE UNIVERSITY OF ASTON IN BIRMINGHAM

November 1983.

THE UNIVERSITY OF ASTON IN BIRMINGHAM

The development of a solar wall module using a selective surface.

Submitted for the degree of Doctor of Philosophy.
By: Christopher George Lloyd.

Summary
A need was indicated for the identification of a possible new solar energy product to improve the sales potential of a metal film with a selective surface, manufactured by the industrial sponsor of this project (INCO).

A possible way of overcoming the disadvantageous economics of solar energy collection was identified. This utilised the collection of solar energy by the walls of buildings constructed in such a manner as to allow the transfer of energy into the building, whilst providing adequate thermal insulation in the absence of sunlight. The actual collection element of the wall, being metallic, is also capable of performing the function of a low temperature heating system in the absence of sunlight. As a result of this, the proposed system, by displacing both the wall and central heating system which would otherwise be necessary, demonstrates economic benefits over systems which are constructed solely for the purpose of collecting solar energy.

The necessary thermodynamic and meteorological characteristics and data are established, and applied to a typical urban site in the North of England, for a typical average year, with and without a shading device incorporated into the construction.

It is concluded that the proposed system may offer considerable benefit in reducing the effective heating season in all orientations of wall.

KEYWORDS Solar Energy, Wall, Passive, Selective.

ACKNOWLEDGEMENTS.

The author wishes to thank the members of the project supervisory team for their help and support.

A particular thank you must also be offered to my wife for her patience, understanding and contribution to the production of this thesis.

CONTENTS

CONTENTS

CONTENTS

LIST OF TABLES

LIST OF FIGURES

1. Introduction.

The need to reduce the energy production requirements of industry commerce and society has prompted many investigations in the past. The possible use of ambient energy sources has been studied extensively, especially since the oil crisis which resulted from conflict in the Middle East in the mid 1970's.

Ambient energy in the form of solar, wind, wave and geothermal sources may prove attractive in the future, but the prime source of both wind and wave energy is solar radiation, and so it is hardly surprising that this form of ambient energy has been closely considered.

Solar energy poses several problems for those who wish to employ it for specific purposes, but the two which must be dealt with before any practicable use can be made of it are its dilute nature, and variability. The relatively dilute nature of the solar resource is discussed in Chapters 1.5. and 3.2. The availability of solar energy varies by day, season, latitude, altitude and climate. It seems that, for solar heating, where ever and whenever solar energy is least abundent, it is most required, and vice-versa. These characteristics combine to produce a situation whereby the cost of building something for the express purpose of collecting solar energy must be very carefully considered and the equipment involved must be justified on an economic basis.

This thesis describes a research project which was directed towards the identification of a solar energy product capable of accommodating, in part at least, the forgoing constraints. Furthermore, the project was required to employ the product of the sponsor company, and provide an avenue for further work which will hopefully lead to a product development to the benefit of the sponsor.

To establish such a possible course of action, it has been necessary to consider in some detail the collection of solar thermal energy, and the thermodynamic phenomena which lead to losses and inefficiencies in its use.

A "solar wall module" is identified as demonstrating characteristics of economy and shape which appear to offer a possible approach, and a computer model which predicts the thermodynamic behaviour of such a wall module was developed from theoretical and experimental criteria and data.

Actual performance of the module was simulated using a computer program to model the effects of latitude, longitude, altitude, orientation, season, time of day, type of day and air temperature. This model also accommodates the use of variable shading as a means of reducing excessive heat gains in the summer. As a result of this, it is possible to establish maximum energy contribution values per annum, dependent upon orientation and shading control.

Costing analysis based upon the alternative costs of conventional walls and central heating systems indicates that the solar wall module in its final form may well have an installed cost similar to, or less than, the conventional alternative. As a result of this, any solar energy contribution to the building in which the modules are installed will prove of immediate economic benefit.

The thesis concludes with a summary of the work still to be done to develop a product from this research.

2. Background

2.1. Project Background

The industrial sponsor of this project is INCO International Ltd. This company is based in Canada and is primarily concerned with the mining and processing of nickel, copper and precious metals although the latter two are essentially secondary to nickel production. The Company is also deeply involved in the manufacture of nickel based products i.e. stainless steels and Nimonic alloys.

When the project started in October 1980 the activities of INCO spanned 36 countries, employing 52,650 people worldwide; this position has been eroded in the last three years as the recession has had its effect upon metals producers. The project was based at INCO's European Research and Development Laboratory (ERDC) which served the Company's European needs for research and development, and provided a repository of expertise. ERDC also undertook research into areas not directly related to existing business but which offered business prospects for the future, or possible diversification; such "seed" projects were funded upon a corporate basis.

The project was based in the "Materials and products Research Group" the manager of which was the project industrial supervisor. INCO Limited had developed a continuous electrodeposition process for the manufacture of nickel foil, and a process whereby a selective absorbing surface was produced on the foil. The resulting product "Maxorb", had found a place in the production of solar flat plate collectors. The advantage to the collector manufacturer is an increase in the efficiency of his product, and this has resulted in sales of "Maxorb", notably in continental Europe. It was felt that sales potential could be increased for "Maxorb" and possibly plain nickel foil.

The then Director of the European Research and Development Centre (ERDC) of INCO, and the Interdisciplinary High Degrees Section of Aston University had discussed the possibility of an IHD post graduate project based at ERDC. It was decided that a project designed to identify applications for "Maxorb", and/or foil would meet a current need of INCO, and provide a suitable project for IHD purposes.

The writer was accepted as a postgraduate research student at Aston University, and employed by INCO Limited with Science and Engineering Research Council sponsorship. The project was given a preliminary title of "The Use of Metal Foils" and commenced on 3rd November, 1980.

The production and sale of INCO nickel foils was undertaken by MPD Technology Ltd; a wholly owned subsidiary of INCO. MPD was established to meet the need for diversification and was based at the ERDC site. The scope of MPD business was: super-plastic forming, nickel foil, "Maxorb" solar foil, battery electrodes, and hydrogen storage by metal hydrides.

2.2. Project objectives

When the project was conceived INCO was already involved in the production of nickel foil; at that time it was thought that this involvement would be expanded into the production of foil based articles, possibly employing other metals.

The trading position of INCO deteriorated due to the general industrial recession and such hopes have faded as the Company has found it necessary to husband its resources in the hope of better circumstances in the future. This restriction became evident at an early stage in the project, and it was decided to concentrate upon the INCO foil product known as "Maxorb" as a possible vehicle for the project. The reason for this was the high capital cost of the production equipment for this material, and the need for continuous production runs to maintain profitability. "Maxorb" had already found a market in the production of flat plate solar collectors, but the company felt that the future of this market was uncertain, and that possible alternatives should be sought.

"Maxorb" is a specialised product, and is described in more detail in chapter 2.3. and Appendix 1 and the nature of selective surfaces is described in Chapter 3. Its particular properties effectively restrict its use to Solar Energy applications.

It is essential that "Maxorb" is applied to a flat surface, as indicated by Neal and Musa (1981) as this assists the speed and ease of application and helps to prevent the formation of air pockets and other inclusions. It had been found in practice that an absorber plate of a flat plate collector was seldom flat in this sense, unless specifically designed so. This was a limitation on potential sales because the product was often offered as a means of increasing the efficiency of existing collector designs.

These considerations led to an early objective of the project as follows:

"To identify a way of increasing the potential future sales of "Maxorb" by investigating possible solar applications involving large flat surface areas."

2.3. Maxorb Foil.

A resume' of the properties of "Maxorb" foil is given in M.P.D.'s technical literature shown as Appendix 1.

The production of "Maxorb" foil is a result of two INCO developments which were initially unrelated. The first was foil production by continuous electrodeposition, the second a spectrally selective surface, (see Chapter 3) produced on nickel. This process is highly confidential, being unique to INCO.

The two processes combined to result in "Maxorb" foil, a thin foil of nickel, typically 13 microns thick, with a highly efficient spectrally selective surface. The foil is produced in ribbon form 150 or 500 mm in width, and provided with a pressure sensitive silicon adhesive on the reverse side. The market for "Maxorb" is wholly related to the solar industry and the normal method of application is by roller onto the surface of a solar collector absorber plate.

The surface to which "Maxorb" is to be applied must be clean and relatively free from surface and geometrical discontinuities; this may present difficulties in application.

The 1981 sales of "Maxorb" foil of 25,000 m^2 were expected to break down to 55% European sales, 25% sales to America, and 20% to the developing countries.

2.3.1. The application of Selective Surfaces.

Selective surfaces can be produced by three main routes at the present time: (See also Chapter 3).

1. Selective Paints.

   Duffie and Beckman (1980) give an example of an iron-manganese-copper oxide paint employing a silicon binder, with $\alpha = 0.92$, and $\epsilon = 0.13$. However, such products are not yet proven or commercially available.

2. Direct application.

   Selective surface treatments, chemical and electro-chemical, may be applied directly to solar absorbers and the costs of this process range from £5 to £12/m^2 dependent upon the surface quality. The method suffers from the materials handling problems of moving complete absorbers as indicated by Jones (1979). "Maxorb" may be applied in this manner, and usual values of emittance and absorbtance obtained

3. Selective Foil.

   "Maxorb" has only one competitor in the selective foil market, a black chrome on copper foil manufactured by Berry Solar Products of New Jersey, U.S.A. The claims by Berry indicate a performance equivalent to "Maxorb", although the claimed 0.02 emissivity factor must be considered with some scepticism when compared with the accepted values of .013-.09 indicated by Toloukian (1970) for polished copper. The material commands a selling price slightly in excess of the £5/m^2 for "Maxorb" and is believed to have a good market in the U.S.A.

"Maxorb" enjoys a good reputation for consistent quality, as indicated by Kenna (1981) and has been found to be an attractive and economic means of increasing the thermal efficiency of single glazed flat plate solar collectors.

In this form, "Maxorb" offers performance somewhat better than would have been achieved had a non selective collector been double glazed, i.e. provided with a second screen. A selective surface offers little benefit when used with double screens due to the high emittance of the inner screen, as indicated by Kenna (1981).

2.4. The Solar Market.

a. Active heating systems.

The oil crisis of the early 1970's prompted a worldwide interest in alternative energy sources and, as indicated by Tabor (1982), solar applications were given an unprecedented impetus. Flat plate collectors represent by far the most common solar energy application, and although the total market for energy related products is undefined, the market for flat plate collectors can provide an indication of recent trends.

The market in Europe since the mid 1970's has been summarised by Stammers (1982), and Figure 2.1. shows the European sales of flat plate collectors from 1975 to 1981. The spectacular rise in installed area up to 1980 is very evident, as is the fall in 1981, which is believed to have continued throughout 1982 and 1983.

The reason for this fall is not clear, neither are the motives of the purchasers of solar systems; as indicated in Chapter 2.5. there is little financial incentive. Certainly there seems to have been a recognition by the U.K. Government, as indicated by recent research policy, that active solar systems are not going to produce significant energy savings in the United Kingdom, Government support for this aspect of solar energy applications has largely ceased.

Some work has been conducted to establish the nature of purchasers of solar energy systems in the U.K. Batty (1982) identifies a social stratum of interest increasing with social class. This is also identified by Norton et al (1982), Batty (1982) also identifies an apparent

correlation between interest in solar heating and concern about the energy crisis, expressed by the more educated sectors of society.

Manning (1982) observes an "implied discount rate" for the purchase of systems, which is inversely proportional to the level of personal income. In other words, those with greater wealth are more likely to find the investment in solar energy systems attractive. This supports the suggestions above, and it appears therefore that the present market for solar systems is primarily associated with the more wealthy and educated members of society; for whom the risk of purchase is less important.

This does not explain the reason for the recent drop in solar system sales, which may be a result of any combination of the following;

a) The market, being restricted to the wealthy, is becoming saturated.

b) The original urgency of the energy crisis is becoming eroded with time, and is no longer perceived as an immediate threat.

c) The effects of economic recession mitigate against speculative investment in solar systems.

d) The withdrawal of Government support has resulted in a fall in consumer confidence.

e) Bad publicity following the poor performance of incorrectly installed systems.

Whatever the reason for the observed decline in sales, it would be folly to regard the present market as typical.

Thring (1982) has compared the potential growth of solar energy systems with other technological developments, especially central heating. In the authors view, such comparisons must be viewed with caution. The developments cited all offered something which was not previously available, or made it more convenient. For example, central heating allowed greater comfort; television provided entertainment, private cars gave convenience and mobility. Unfortunately solar energy applications do not normally offer anything to the user which does not already exist, and in general solar systems must have a back up conventional system to make up for those occasions when solar availability is inadequate. It is true that in remote locations a solar system may provide an energy source which would otherwise be unavailable, but in most situations in the developed world, a solar system is essentially used to augment the input to a conventional system.

In the author's view, the only real incentive for the development of solar applications is the economic benefit of energy collection. If that benefit cannot be clearly perceived, there appears to be little incentive other than that of individual interest for some other reason.

Despite the above comments, there is considerable interest in solar energy by the populace at large. Sadler (1982) identifies considerable appeal in "natural energy" in his survey, and also identifies considerable potential in housing designed to maximise solar collection if additional costs can be minimised.

b. Passive Systems.

The passive use of solar energy may be more promising. There does seem to be good reason for believing that passive solar principles can be cost effective, although analysis can be troublesome as indicated by Everett (1982).

The problem in evaluating how effective passive solar applications can be is that of deciding how much extra they have cost. This is relatively straightforward when considering an add-on feature such as a conservatory, but when considering passive principles which affect the entire structure of a building the problem is much more complex. Most passive solar buildings have been experimental or developmental in nature and as a result, the costs of monitoring equipment and features can tend to mask the true cost of the building. The use of passive solar principles has increased greatly over the past few years to the extent that a full listing of such buildings is no longer feasible, although Oppenheim (1982) presents a synopsis of British applications.

It appears then that the market may well be restricted, and comprised of relatively affluent and educated persons. Such individuals are to be found in many areas of the world, and at first sight it would seem worthwhile seeking a market in areas of the world which enjoy a great deal of sunshine. This is not necessarily the case as in such areas, with high ambient temperatures, solar energy is relatively easy to collect. An abundance of sunshine renders the highly specialised selective surface less necessary, and the potential contribution of solar energy for space heating applications has been shown by McGregor (1982) to be reduced in comparison to more Northerly latitudes.

For these reasons of need for efficiency, affluence, education and potential contribution, the markets of particular interest for "Maxorb" are those of Northern Europe and North America, and similar counterparts in the southern hemisphere, where thermal conversion is concerned. These considerations do not apply to the electrical conversion of solar energy, where an abundant solar resource is a decided advantage.

2.5. The economics of solar thermal energy collection

Figure 2.2. shows the average annual energy falling upon a horizontal surface over the world. For a typical north European latitude, a mean annual value of approximately 1000K Wh/m^2 of energy is available for collection. No collection system is perfect, and Lof (1981) has indicated that an overall collection efficiency of 30% can be expected from a well designed thermal system. This indicates that an annual energy contribution of 300 KWh/m^2 can be expected from a thermal system.

Assuming that the whole of the contribution of the solar system displaces an otherwise necessary electrical input, this results in an annual value of approximately £15.00/m^2 year if an electricity cost of 4.99p per KWh is assumed. This unit cost is the peak domestic tarriff in 1983 in England. If comparison is made with gas or off peak electricity or solid fuel then the value of the energy collected is correspondingly reduced. As a further complication the solar energy is available out of phase with the need for heat to compensate for losses to the atmosphere. This means that solar energy thermal applications favour a use which allows the energy to be consumed as it becomes available. For active systems this has resulted in wide adoption for domestic hot water systems, and swimming pool heating. In terms of passive applications, the use of direct gain windows facing south allows sunlight in the late and early months of the year to contribute, as indicated by Jesch (1981).

Stammers (1982) reports an average total system installation and materials cost of £270 per square metre of collector for retrofit installations. Comparison of this figure with the £15 which the system can be expected to recoup per annum indicates a very approximate payback period of the order of 20 years.

The application of discounted cash flow techniques to the long term economics of solar systems can offer a more attractive view. These techniques employ a variety of criteria for comparison of investment as discussed by Manning (1982), but all are highly dependent upon assumptions about future inflation rates, energy costs, system life, maintenance and efficiency. The uncertainties of these assumptions make value judgements of solar economics also uncertain, but Long (1982) has shown that the effective cost of energy contribution by a domestic hot water installation lies between 14 and 7 pence per KWh. As a result of this, Long concludes that the installed cost of such systems is approximately twice as great as that required to give equality with electricity supply costs. Systems which combine domestic hot water, and space heating have been investigated by Thring (1982), who concludes that a group of 50 houses with shared interseasonal storage and advanced collectors may have a payback period of 15 years if the houses have high heat loads and the solar system displaces electricity costs.

Payback periods of 15 years, and effective energy costs twice that of electricity are not inducements to purchasers. It can be argued that a solar system may be self sustaining, i.e., the system provides sufficient payback over its life time to recoup its replacement cost. However, system lifetimes have not yet been long enough to demonstrate this.

It seems that the initial capital cost of installation for present active systems is too high. It is not easy to visualise this situation changing dramatically. Stammers (1980) indicates that the cost of these installations can be divided equally between the cost of the collector, the cost of ancillary equipment, and the actual cost of installation. The overall cost of the installation is highly dependent upon established techniques and standard components. Although it can be argued that the cost of the

actual collectors may be reduced as production efficiency is improved, this will not have a dramatic effect upon overall costs. Even if the collector cost is reduced by 50% this merely results in a system cost reduction of 17%.

Bearing in mind these additional system costs, it seems that almost anything which is constructed solely for the purpose of collecting solar energy in the UK and similar latitudes has unattractive economics.

The situation with passive solar heating appears to be more promising, as passive applications tend to employ architectural features which would have been required anyway but which are modified to provide an enhanced solar contribution. However this makes a strict economic analysis of solar passive applications very difficult to establish, as the dividing line between a solar energy feature and a utilitarian or architectural feature is not clear. For example, a conservatory is known to confer benefit in terms of solar energy, but it also has a very real value as a conservatory, the question is thus unclear. Jesch (1981) provides an overview of passive principles, but no economic evaluation, and this is generally the case in the literature on the subject.

2.6. The thermal efficiency of solar collectors.

Solar energy falling upon the outer glazing of a collector is partially reflected and absorbed by the glazing system, before being absorbed by the collector absorber.

The absorber is heated by this absorbed energy, and as a result loses energy to its surroundings by radiation, conduction and convection through the glazing system and collector enclosure.

These solar gains and losses will be considered in greater detail in Chapter 4, but for the moment it is clear that the higher the absorber temperature, the greater the energy loss, and therefore the lower the efficiency of collection. It follows that the collection of energy should involve temperatures as close as possible to the required demand temperature, as any increase above this results in an unnecessary loss of energy. From this point of view, the collection of energy in a high temperature fluid for subsequent distribution into a low temperature living space introduces losses which could be reduced if the energy is collected at or near its required temperature.

2.7. The conception of a solar wall module.

The considerations of the preceding sections lead to a pessimistic view of the future market for "Maxorb" for flat plate collectors only. The market is seen as relatively restricted, possibly due to the disadvantageous economics of solar energy in the latitudes of interest i.e. Northern Europe. Recent market trends show an overall fall in sales and there appears to be no realistic means by which the excessive capital cost of active solar installations can be reduced.

An examination of current developments in flat plate technology also indicates that the evacuated tube collector as indicated by Hutchins et al (1982) may begin to challenge the flatplate collector with a selective surface for high efficiency applications. This type of collector benefits from the production technology of fluorescent lamp manufacture and the projected collector cost of £100/m^2 compares favourably with the average £90 cost of a flat plate collector. "Maxorb" is not ideally suited to use in evacuated tubes as the maximum operating temperature under coolant failure conditions may exceed the temperature capability of "Maxorb". In addition the area of the collection surface is reduced in comparison to flat plate collector designs, which reduces demand for "Maxorb" and increases the unit costs.

The potential of conventional passive applications for "Maxorb" is also found to be limited by the need for a protected environment for its selective surface. The Trombe wall for example requires that air circulates past the absorber and into the airspace thus contaminating the selective surface with dust. One possibility of a passive application is that of the glazed wall, as indicated by Mason (1982). In this latter application, the application to existing walls is difficult as the wall surface must be prepared, battened and glazed. The actual application of "Maxorb" to the wall also presents problems unless weather conditions are very good with dry still air, or the wall is protected by some temporary structure to prevent the flapping of "Maxorb" in the breeze and problems with adhesion.

When considering solar energy, the author thought it necessary to view the solar gain as one component of overall energy use. In this context, the Building Research Establishment (1975) have established that as much as 50% of the prime energy demand of the U.K. is used for space heating purposes, and that 30% of heat loss from dwellings occurs through the walls. This has prompted the advocation of wall insulation as an effective conservation

measure. However walls are not ready acceptors of solar energy, as the insulating effect of the wall lies between the absorbing surface and the interior of the building, this effect is illustrated in Chapter 6 of this thesis. Ideally the insulation should lie between the absorbing surface of the wall and the atmosphere.

In considering the possible use of walls as collectors, it is apparent that the cost of the wall so produced, and the building so formed should not exceed that of conventional construction if possible. Furthermore, in the absence of sunlight, the 'U' factor of the wall should not exceed that required by the Building Regulations of $0.6\ w/m^2 o_c$, as discussed by Elder (1981).

These considerations lead to the development of a concept which the author has termed a solar wall module. The module consists of a box section construction as illustrated in Figure 2.3. The absorber of "Maxorb" is placed on the inner back surface of the box which forms a concrete slab, and a series of screens placed between it and the atmosphere. The screens are employed to restrict convection and radiation losses.

The potential advantages of this module concept were perceived as follows:

1) The provision of a flat extended surface suited the nature of "Maxorb".

2) Energy is collected and distributed at or near the end use temperature for space heating.

3) The module by displacing an otherwise necessary wall, benefits by the displaced cost.

4) The cost of an energy distribution system is discounted because the solar energy is directly available to the living space.

5) Even when insufficient solar energy is available to make a contribution, any incident solar energy will reduce the loss from the interior of the building and so be of value.

6) The "Maxorb" absorber may be employed as a heating element, in which case the Wall Module may fulfill the role of an otherwise necessary central heating system. This renders the usually obligatory solar back-up system redundant, and may well reduce the cost of a building by that of the displaced boiler, piping and radiators.

A corollary of the need to reduce costs is the need to consider the module as non load bearing to reduce the required thickness of the slab at the rear. This slab is seen as providing a measure of thermal storage, and necessary security for the inhabitants of the building.

Initial calculations indicated that the required 'U' factor could be achieved if 8 glass screens spaced approximately 25mm apart were used. This was encouraging, but rendered the module much too expensive.

As a result of this, the project followed an investigation of the potential of the module in relation to plastic screen materials and associated selectively reflecting surfaces.

2.8. Project problems

The project presented its own, not unexpected difficulties which may well be associated with any research programme. The unexpected also occurred with the simultaneous financial difficulties of the industrial sponsor and the University. The problems of the

former resulted in understandable financial stringency which had a direct result upon the nature of the project experimental work and project duration.

The problems of Aston resulted in difficulties with academic supervision which was in a state of flux as nominated persons found it necessary to seek alternative positions. In addition, the decision of the University Computer Centre to discontinue programming courses produced considerable problems for the author. Upon reflection, the author considers that the decision to employ a new computer facility at the computer centre was ill advised as the teething troubles of the system reduced its availability and flexibility greatly.

3. Selective Surfaces.

In the context of this project, the term "selective surface" is used to denote a surface which demonstrates a useful variation of radiation characteristics between the wavelengths associated with solar and thermal infra-red spectra.

Before discussing selective surfaces it is necessary to establish an understanding of radiant energy exchange between bodies:

3.1. Radiant energy exchange

It is not proposed to give an extended account of this subject. Duffie and Beckman (1980) provide a discussion particularly directed towards solar energy applications, and Sparrow and Cess (1978) provide a thorough appreciation of the theoretical basis of radiant energy exchange.

If we consider the situation of a body enclosed within an evacuated isothermal enclosure, it is clear that the exchange of energy between the enclosure and the body must take place by means of radiation. In a steady state condition, the body must adopt the same temperature as the enclosure.

If we now consider the body to be made of some material opaque to the radiation in question, then the exchange of energy must be constrained to the surface of the body. Under equilibrium conditions, the energy which leaves the surface of the body must exactly equal that which enters, and it follows that this balance is achieved by virtue of the surface radiative characteristics.

Those characteristics of a surface which are of interest are the emittance, absorptance and reflectance, although only the emittance can be regarded as a property of the surface alone.

The absorptance of a surface is defined as the proportion of incident energy which is absorbed by that surface. This proportion is dependent upon the wavelength of the incident radiation, its direction, and the nature of the surface. The dependence of absorptance upon an undefined incident radiation necessarily dictates that it is not a property of the surface alone.

Emittance of a surface is also dependent upon the nature of the surface and the direction under consideration, but the wavelength of radiation is determined by the temperature of the surface. Emittance is defined as the proportion of energy emitted in relation to that which would be emitted by a perfect radiating body, a "black body" at the same temperature. Being dependent only upon the surface itself, the emittance can be considered to be a property.

The reflectance of a surface is necessarily the proportion of incident energy which is not absorbed, and is thus dependent upon the absorptance.

The monochromatic directional emittance and absorptance properties can be integrated for all directions and wavelengths of interest to give hemispherical values, which are used in the practical analysis of real systems. Unless otherwise stated, all the values used in this thesis are hemispherical. Authors in the literature occasionally quote values for the emittance normal to the surface, and care should be taken to ensure that this can be related to the hemispherical value.

For materials which are opaque to radiation, there is a relationship between the hemispherical and normal emittance of a surface. Both Jacob (1949) and Sparrow and Cess (1979) illustrate this relationship which is shown in Figure 3.1. as being dependent upon the electrical conductivity of the material. The situation is not as clearly understood for materials which exhibit transparency to the radiation in question. In this case, the radiant characteristics can no longer be considered as being purely surface phenomena, and the relationship

between normal and hemispherical emittance has not been clearly established for thin polymer films. The National Physical Laboratory is preparing to determine hemispherical values by experiment (Dr. F. Clark, 1982).

From the above, the energy emitted by a body is given by

$$E = \epsilon \times Eb \times A \qquad 3.1.$$

Where ϵ = the hemispherical emittance of the surface, at the temperature in question.

E_b = The energy emitted per unit area by a perfect radiator.

A = The surface area of the body.

The energy absorbed by a body in an isothermal enclosure is given by

$$E = \alpha \times I \times A \qquad 3.2.$$

Where α = the hemispherical absorptance of the surface.

I = The unit intensity of incident radiation.
From which $\frac{I}{E_b} = \frac{\epsilon}{\alpha}$ = constant for equilibrium.

The relationship must be true for whatever surface is involved, including the perfect radiator, in which case the energy emitted is a maximum, and the corresponding energy absorbed must be a maximum, or:
$\alpha = 1$. Thus, for equilibrium, $\epsilon = \alpha$.

As indicated above, the absorptance of a surface is not a property, but is dependent upon the nature of the incoming radiation. If the incoming, and emitted radiation are at significantly different wavelengths it is possible to devise surfaces with beneficial characteristics.

Such surfaces are said to be spectrally selective. In fact, all surfaces are selective to some extent, as the emissivity of real surfaces varies with temperature and hence the wavelength.

Selectivity relates not only to absorptance and emittance, but also to transmittance. The transmittance of a body is necessarily that energy which is neither reflected nor absorbed. However this is not a purely surface effect but is a characteristic of the material. The classic selective transmitter of radiant energy is glass, which transmits solar radiation but absorbs thermal infra red.

3.2. Solar and Thermal-Infra-Red Spectra.

Selective surfaces find a place in solar energy applications because the solar spectrum lies largely at shorter wavelengths than the thermal infra red spectrum of bodies at the operating temperature of low to medium temperature solar devices.

The nature of solar radiation will be discussed more fully in Chapter 6, and a full presentation of the matter can be found in Henderson (1970) or Kondratyev (1969). The fact which is of interest in relation to solar applications is that 98% of solar energy lies below a wavelength of 3 μm, and corresponds closely to the energy spectrum of a black body at a temperature in the region of 5700 K, see Figure 3.2.

Alternatively, the spectrum of energy emitted by a body at the sort of temperature encountered in solar applications lies predominantly at wavelengths greater than 3 μm.

The energy of radiation emitted by a black body at the wavelength is given by Planck's Law:

$$E_\lambda = \frac{2\pi h C_o^2}{\lambda^5 (e^{hC_o/\lambda kT} - 1)} \qquad 3.3.$$

Where h is Planck's constant and k is Boltzmans constant. The groups $2\pi hC_o^2$ and hC_o/k are termed Planck's first and second radiation constants C_1 and C_2 with values of 3.7405×10^{-16} Wm^2 and 0.0143879 m K respectively. $E\lambda$ is the energy emitted per unit area per unit time per unit wavelength interval at the wavelength λ. Real surfaces are not 'black' in the sense of perfect emitters, but are in reality 'grey' i.e. they exhibit less than perfect characteristics at any particular wavelength, and Planck's relationship is modified as follows:

$$E\lambda' = \frac{\epsilon\lambda \times C_1 \lambda^{-5}}{e^{C_2/\lambda T} - 1} \qquad 3.4.$$

Where $$\epsilon\lambda = \frac{E\lambda'}{E\lambda}$$

Where $\epsilon\lambda$ is the monochromatic emittance at the wavelength in question.

Figure 3.3. shows a graph of the distribution of energy radiated by a black body at various temperatures.

The locus of the maximum radiant energy emitted is given by Wien's displacement law:

$$\lambda max T = 2897.8\ \mu m\ K \qquad 3.5.$$

As can be seen, the lower operating temperatures result in a spectrum shift to longer wavelengths, and for a body at 200C, 99% of the radiated energy lies at wavelengths greater than $3\mu m$. It is this relative displacement of the solar and thermal infra-red spectra which allows the possibility of surfaces which demonstrate markedly different absorptance/emittance characteristics in each regime.

There are two types of selectivity which are of interest to us; the first is selectivity which allows high absorptance of energy in the solar spectrum, combined with a low emittance in the thermal infra red spectrum. The second surface type is one which demonstrates transparency to solar radiation, and low emittance i.e. low absorptance and high reflectance in the thermal infra red. The former type, of which "Maxorb" is an example, is employed as the absorber of solar collectors, whilst the latter by providing the so called "heat mirror effect" is now finding use in glazing applications.

The following sections briefly discuss the ways in which these two types of surface may be produced, a more comprehensive discussion may be found in Lampert (1981), for heat mirror type surfaces, and Koltun (1981) for both heat mirror and absorbing coatings.

3.3. Spectrally selective absorbing surfaces.

The potential of selective surfaces was first explored by Tabor (1956) who saw the folly of attempting to reduce the convective heat losses from solar collectors without also reducing the radiant component of heat loss. The objective in producing a selective surface is to have a high solar energy absorptance, combined with a low thermal infra red emittance. For this latter purpose, we are essentially restricted to the consideration of metallic surfaces, as non metallic materials have high emissivities ranging from .85 to .95. One exception to this is the case of transparent materials in which the radiation characteristics are a bulk phenomenon.

The problem then is to develop a surface coating which will allow the essentially low emittance characteristics of a metallic substrate to predominate at long wavelengths, whilst presenting a high absorptance at short wavelengths. This can be achieved either by coating a polished metal surface with a thin optically dark surface, or by converting the surface of the metal to a compound having appropriate properties. Whichever is considered, the surface so treated must be essentially transparent to radiation at wavelengths greater than 3μm.

Some work has been done in attempting to establish an effective self selective material by the doping of metallic surfaces with impurities to produce a drop in the reflectivity of surfaces due to the collective vibration of electrons. Seraphim (1978) reviews this possibility, but at the present time, no commercially available material has been produced.

This means that consideration must be given to multiple layers of materials in what are termed reflector-absorber tandems. There are two possible ways in which such tandems can be employed; a selective reflecting surface over an absorbing substrate, or conversely, a selectively absorbing surface over a reflecting substrate. Some highly doped semi conductors can provide the former alternative, but they do not give good overall absorptance. The selective absorbing surface is easier to produce as it is required to absorb high energy photons, whilst transmitting low energy photons. This is a much more natural state of affairs, and this form of tandem stacking has been investigated most thoroughly.

We have to consider then, the provision of a surface upon a metallic substrate, the surface being essentially black. Seraphim (1978) demonstrates the intrinsic limitations imposed by the optical properties of the sort of semiconductor which has found use in these applications, typically nickel-zinc sulphide and chromium oxide. Unfortunately such materials which have a satisfactory transparency wavelength window also have a high refractive index in excess of 3. As a result of this, valuable absorptance in the solar spectrum is sacrificed due to reflection.

As a consequence of this unfortunate correlation between refractive index and absorption cut off, it is necessary to consider ways in which the effect of this can be minimised. Two such ways have been identified, the first is the use of interference coatings or absorber-reflector tandems. The second is a topological or wavefront discrimination. The former method similar to the blooming of opti-

cal lenses depends upon the use of non absorbing dielectric layers to achieve reflection supression. Seraphim (1978) gives an example of a series of 4 layers in an interference stack. This was a molybdenum substrate, with a semi transparent molybdenum layer sandwiched between layers of aluminium oxide. This surface which was developed for aero-space applications, had an absorptance of 0.85, and emittance of 0.11 at 500°C. The high cost of production, and subsequent degradation with time due to interface diffusion and corrosion indicate that such material stacks will not find common use in solar applications. Nevertheless, the interference component of reflection suppression can play a role if the thickness of a black coating is carefully controlled, although this requires at least two surface treatments.

The topological approach to reflection suppression is to produce multiple reflections at the surface of the material by having a rough or matt surface texture. Hutchins (1981) describes how cavities have a significant role to play. On a larger scale, corrugations may be introduced to enhance this effect.

3.3.1. Commercially available absorbing surfaces

As indicated by Hutchins (1981), the surfaces in use for solar applications demonstrate several of the mechanisms for achieving selectivity as discussed in the previous section, but little is known of the proportions of each absorbing phenomenon which contribute to the total effect for a given surface. All the available coatings are absorber reflector tandems, with a highly reflecting substrate. These surfaces additionally depend upon surface texture and interference effects to enhance their properties.

The manufacture of surfaces with consistent characteristics requires close control of thickness, texture and constituent materials. Quality control and process control are particularly difficult with the result that relatively few materials have been produced which also

demonstrate adequate resistance to corrosion and degradation with time. No successful paint type application has yet been devised, and the three most used surfaces, nickel black (nickel-zinc-sulfide) chrome black (chromium oxide) and copper oxide are all the result of chemical or electro chemical processes and all break down at elevated temperatures approaching 300°C, see also Mason (1983).

3.3.2. Effectiveness of a selective absorber.

The effectiveness of a selective surface can be judged from the ratio of the solar absorptance to the emittance at the temperature in question, selective surfaces with a metal substrate all demonstrate an increase in thermal emittance with temperature and it is necessary therefore to ensure that this variation is accounted for. Koltun (1981) has prepared a table reproduced as table 3.1., in which the emittance, absorptance and α/ϵ ratio for various selective surfaces are shown, similar tables can be found in Duffie & Beckman (1980) and Meinel & Meinel (1978). The same information for "Maxorb" is also included.

It is apparent from table 3.1. that the most effective surfaces appear to be interference stacks. However these structures demonstrate very low emittance at the cost of reduced absorptance. The benefit of this low emittance may be outweighed by the reduced absorbtance, dependent upon the other energy transport coefficients which are acting upon the surface. If for example the heat transfer due to conduction and convection is significantly greater than that due to radiation, then the reduced radiation component will have little effect, and the reduced absorbtance will be detrimental.

3.4. Spectrally Selective Reflecting Surfaces.

The use of such surfaces which transmit energy in the solar spectrum, but reflect thermal infra red radiation is of value as a "heat mirror". The surface must be considered in conjunction with a substrate which is transparent to solar radiation.

Two uses have been proposed for such materials, either as a means of reducing the radiant heat loss through a window, or of reducing the heat gain through a window. This is achieved by having the reflecting surface towards the interior or the exterior of the building in question.

Lampert (1981) presents a valuable review of recent developments in reflecting film technology. Progress in the deposition of metal and metal oxide films upon various substrates has resulted in many possible heat mirror coatings, some 170 coating types are listed by Lampert and a selection is given in table 3.2. The technology employed is already developed, brief mention will be made of 3 of the techniques.

a. Chemical Vapour Deposition (C.V.D.)

This gaseous reactive technique for deposition may employ the hydrolysis of metallic chlorides, or the pyrolysis of organo-metallic or metal salts. These techniques require a heated substrate, and are restricted to use with glass, and further restricted to low alkali or fused silica glass in the case of pyrolysis. The surfaces so produced are generally of Indium oxide, Silicon oxide or Tin oxide. Recent developments in plasma assisted CVD may lead to effective low temperature pyrolysis techniques.

b. Physical Vapour Deposition.

The deposition of an evaporated vapour on a cooled surface in a vacuum is well known, and large commercial coaters have been in use in industry for many years. The need for evacuation naturally renders the technique relatively complicated in comparison to CVD techniques. Materials are boiled or sublimed by resistance heating, inductive heating, or electron beam heating in a vacuum of 10^{-2} Pa or less.

A very similar process is employed in reactive evaporation, where a background gas pressure is maintained as a reactive atmosphere. Oxides and nitrides can be produced in this manner. This system also allows the use of R.F. sputtering which has the advantage of being directional, and so less wasteful of material, but is also slow. Magnetron sputtering, in which stray electrons are prevented from being involved in the process by the use of a magnetic field, allows lower operating temperatures.

c. Ion Plating.

Ion plating is a process in which purposeful ion bombardment is used to promote film growth by using the substrate as a cathode either in vacuum, or with a reactive atmosphere.

The materials most often employed are Indium, Indium/Tin, or Silicon Oxides, although potential exists for Antimony compounds and Cadmium Stanate. In fact all the transparent semi-conductors may offer some potential. Unprotected metal films offer good thermal performance, but are inherently fragile and prone to corrosion.

Indium Oxide is of particular interest. Polyester coated with Indium Oxide is produced experimentally by Dr. R. Howson at Loughborough University, (Howson et al 1979). Samples of this material have been made available to the author for experimental purposes. This material is produced by reactive magnetron sputtering in an oxygen atmosphere. This material on 75mm polyester film has a solar energy transmission (normal) of 0.8 and a thermal infra red emittance of 0.3 (normal). This data was supplied by Dr. Howson for the samples which he provided, and checked by ICI Plastics Division, who also provided data for other candidate materials as indicated in table 3.3. given by Stay (1982).

3.5. Limitations of Selective Surfaces.

It would seem that the use of a surface with selective properties would assist in preventing heat loss from objects and, in sunlight, providing a heat gain. Unfortunately this is not necessarily the case; under normal circumstances the heat loss from a body is the combined result of radiant, convective and conductive effects. In the case of a body in moving air at moderate temperatures, as indicated in Chapter 4, the convective heat loss is somewhat greater than the radiative component. In consequence there is little incentive to reduce the radiative component of the loss unless convection is also suppressed. Furthermore, the properties of the selective surface are neutralised by such extraneous factors as dust, excessive moisture, corrosion and deposited films.

These limitations of selective surfaces dictate their use in solar energy applications (where selectivity relates to the solar/thermal infra red spectra) and where the surface can be provided with a protected environment. The need for incident solar radiation demands that this protection is provided by a translucent material which must fulfil the dual role of environmental protection and convection suppression.

4. Aspects of Heat Transfer

The performance of the proposed module as an effective insulating medium is determined by the manner in which energy is transmitted through it. This is true not only of steady state conditions, but also of variable temperature and energy inputs. This chapter is concerned with the way in which these energy flows can be analysed and their effects optimised.

4.1. Heat Transfer in a Closed Cell

The module is visualised as a series of closed vertical cells, and heat transfer across such a cell takes place by radiation, convection, and conduction. With an inner cell medium of air, which itself does not contribute significantly to the radiation component of transfer, the convective/conductive effects can be considered independently of the other radiative effect.

4.1.1. Radiant Heat Transfer.

The basic mechanism of radiant heat transfer is explained in Chapter 3 as a means of describing the properties of selective surfaces.

The condition ot radiation transfer between the faces of a closed cell is considered in its simplest form as that of two infinitely large parallel plates, each at a different constant temperature. The theoretical heat transfer coefficient for such an arrangement is given by several authors, including Duffie and Beckman (1980) and Holman (1972) for opaque diffusely reflecting plates:

$$Q = \frac{\sigma (T_2^4 - T_1^4)}{\frac{1-\epsilon_1}{\epsilon_1 A_1} + \frac{1}{A_1} + \frac{1-\epsilon_2}{\epsilon_2 A_2}} \qquad 4.1.$$

Where
T = Temperature - K
ϵ = Hemispherical emittance
A = Plate area - m^2
σ = Stephan Boltzman constant.
Q = Energy flow. Watts

In this case, the areas of the two plates are equal, and the energy flow per unit area is given by.

$$Q = \frac{\sigma(T_2^4 - T_1^4)}{\frac{1-\epsilon_1}{\epsilon_1} + 1 + \frac{1-\epsilon_2}{\epsilon_2}} \qquad 4.2.$$

$$= \frac{\sigma(T_2^4 - T_1^4)}{1/\epsilon_1 + 1/\epsilon_2 - 1} \qquad 4.3.$$

This expression is regularly quoted without definition. It will be shown that the basis of this derivation is of considerable importance when considering transparent plates and multiple cells. Sparrow and Cess (1977) present electrical analogue methods for assessing radiation networks, but for the relatively simple case under consideration this is not necessary.

Consider two plates at different temperatures, the net heat transfer will result from the difference between the total energy falling upon each surface. The energy falling upon each surface is denoted as G_1 and G_2 respectively. Each surface will also radiate, according to its temperature and emittance, an energy termed E_1 and E_2, and will reflect a proportion of the energy falling upon its surface given by $\rho_1 G_1$, and $\rho_2 G_2$ where 'ρ' is the reflectivity of the surface. This situation is shown diagramatically in Figure 4.1.

The energy falling upon each plate is then given by

$$G_1 = \rho_2 G_2 + E_2 \qquad 4.4.$$

$$G_2 = \rho_1 G_1 + E_1 \qquad 4.5.$$

Transposing;

$$G_1 (1 - \rho_1 \rho_2) = \rho_2 E_1 + E_2 \qquad 4.6.$$

$$G_2 (1 - \rho_1 \rho_2) = \rho_1 E_2 + E_1 \qquad 4.7.$$

and

$$G_2 - G_1 = \frac{\rho_1 E_2 + E_1 - \rho_2 E_1 + E_2}{(1 - \rho_1 \rho_2)} \qquad 4.8.$$

but $\rho = 1 - \alpha = 1 - \epsilon$ for an opaque material and

$E = \sigma \epsilon T^4$

Then $$G_2 - G_1 = Q = \sigma \frac{((1-\epsilon_1)\epsilon_2 T_2^4 + \epsilon_1 T_1^4) - ((1-\epsilon_2)\epsilon_1 T_1^4 + \epsilon_2 T_2^4))}{1 - (1-\epsilon_1)(1-\epsilon_2)} \qquad 4.9.$$

$$= \frac{\sigma(\epsilon_1 \epsilon_2)(T_2^4 - T_1^4)}{\epsilon_2 + \epsilon_1 - \epsilon_2 \epsilon_1} \qquad 4.10.$$

$$= \frac{\sigma (T_2^4 - T_1^4)}{1/\epsilon_1 + 1/\epsilon_2 - 1} \qquad 4.11.$$

The author has found this visualisation to be very useful, as it allows individual equations to be established for each surface in question, in relation to the other surfaces.

Extending the analysis a little further, if the faces of the cell are not opaque, but are partially transparent, as indicated in figure 42.. then the equations for each face become:

$$G_1 = \rho_2 G_2 + E_2 + \tau_2 G_3 \qquad 4.12.$$

$$G_2 = \rho_1 G_1 + E_1 + \tau_1 G_0 \qquad 4.13.$$

Where τ = Transmittance of the cell wall. These equations define the energy flow through the cell dependent upon the external energy flows which are incident upon it.

Extending still further, for finite cells, we must take into account the effect of the edges of the cell, and the resulting disruption of the simple case. Figure 4.3. shows this situation, and the resulting equations are:

$$G_1A_1 = \rho_2 G_2 F_A A_1 + \tau_2 G_4 F_A A_1 + \rho_s G_3 F_c A_2 + (\epsilon_2 T_2^4 F_A A_1 + \epsilon_s T_s^4 F_B A_2)\,\sigma \quad 4.14$$

$$G_2A_1 = \rho_1 G_1 F_A A_1 + \tau_1 G_o F_A A_1 + \rho_s G_3 F_c A_2 + (\epsilon_1 T_1^4 F_a A_1 + \epsilon_s T_s^4 F_c A_2)\,\sigma \quad 4.15$$

$$G_3A_2(1-\rho_s F_D) = \rho_1 A_1 G_1 F_B + \rho_2 A_1 G_2 F_B + \tau_1 G_o F_B A_1 + \tau_2 G_4 F_B A_1 + (\epsilon_s A_2 F_D T_s^4 + \epsilon_1 T_1^4 F_B A_1 + \epsilon_2 T_2^4 F_B A_1)\,\sigma \quad 4.16$$

Where subscript 's' indicates the side of the cell.

A_1 = the area of the opposing faces m^2

A_2 = the total area of the sides m^2

F_A = the view factor of one opposing face with respect to the other

F_B = the view factor of one face with respect to the sides

F_c = the view factor of the sides with respect to the face

F_D = the view factor of the sides with respect to themselves

G_3 = the total radiant energy falling upon the sides

The form of these last 3 equations seems cumbersome, but they are ideal for matrix manipulation, as will be demonstrated in Section 3 of this chapter.

4.1.2. Conductive and Convective Heat Transfer.

The conduction and convection within a closed vertical cell have been studied by several researchers since the original work of Mull and Reiher reported by Jacob (1949).

The general form of the derived correlations is:

$$Nu = a\ G_r^{\,b} \qquad 4.17$$

Where Nu = Nusselt Number, or the ratio of the heat transfer coefficient divided by the thermal conductivity of the air space.

Gr = Grasshoff number = Rayleigh number divided by the prandtl number = Ra/Pr

a,b = regression constants.

A summary of the early work in this area is discussed by Sharples and Page (1979) who develops the following expressions for use in relation to cavity walls for building purposes.

a) For slopes from horizontal to 70° heating from below

$$Nu = 1 + 1.44\left(1-\frac{1708}{R_a \cos\beta}\right)^{+}_{x} \frac{\left(1-(\sin 1.8\beta)^{1.6}\times 1708\right)}{R_a \cos\beta} + \left(\left(\frac{Ra\cos\beta}{5830}\right)^{\frac{1}{3}}-1\right)^{+} \qquad 4.18$$

Where: $)^{+}$ indicates that the term is considered to be zero if negative.

β = Slope from the horizontal in degress.

Ra = Rayleigh Number = $\frac{g \beta \Delta t \delta^3}{\nu \alpha}$

Where

β = Volumetric coefficient of expansion of air, assumed to be $1/K$

Δt = Temperature difference between the plates K

α = The kinematic viscosity of air at the mean temperature.

g = Gravitational constant 9.81 m/s^2

ν = Coefficient of diffusivity of air at mean temperature m^2/s

δ = Distance between the plates m

b) For slopes from 70° to the vertical

Nu = Nu evaluated at 70°

Duffie and Beckman (1980) also recommend this relationship.

This relationship is not entirely satisfactory as its basis is the work of Hollands (1975) which did not purport to cover slopes in excess of 60°. Additionally, this relationship does not provide any correlation with the aspect ratio of the gap which has been found to be a variable by Raithby et al (1977). In the context of cavity walls which would normally exhibit large aspect ratios, this is not important, but may well be in relation to the wall module, as shown in Figure 4.3. and described in Section2.7.

The latest experimental work reported by Hollands (1981) accommodates both these objections, and offers the following correlations for vertical cells.

a) For aspect ratio = 5 and Ra $< 2 \times 10^7$

$$N_u = \left(1+\frac{(0.193Ra^{\frac{1}{4}})}{(1+(1800Ra)1.29)}^{3}\right)^{\frac{1}{3}} \text{ or } 0.0605\,Ra^{\frac{1}{3}} \qquad 4.19.$$

Whichever is the greater

b) For aspect ratios = 10 and $Ra < 1.5 \times 10^7$

$$Nu = (1 + (.125\,Ra^{0.28})^9)^{1/9} \text{ or } 0.061\,Ra^{\frac{1}{3}} \qquad 4.20$$

Whichever is the greater.

c) Aspect ratio = 20 and $Ra < 1.3 \times 10^6$
Aspect ratio = 40 and $Ra < 4 \times 10^5$
Aspect ratio = 80 and $Ra < 2.5 \times 10^4$
Aspect ratio = 110 and $Ra < 10^4$

$$Nu = (1 + (.064\,Ra^{\frac{1}{3}})^p)^{1/p} \qquad 4.21$$

Where p = 6.5 for A=20 and $= 0.31A^{.81}$ for aspect ratios greater than 40.

These relationships are extremely cumbersome to apply, and the author has been unable to establish an effective cross correlation to evaluate the value at intermediate aspect ratios.

The solution to this problem was found by digital computation. The technique involves evaluating the heat flow for a given cell at both of the aspect ratios above and below the cell aspect ratio under consideration. The heat flow at the cell aspect ratio is then determined by linear interpolation.

Figure 4.4. shows the result of this computation for a typical cell temperature range. In view of the smooth transition between the Hollands correlated points, the author has employed this linear correlation model rather than employing a more sophisticated polynomial correlation. The computer program to achieve this is incorporated as a subroutine in Appendix 4.1.

The experimental results of Holland were produced in test cells which had the edge temperature controlled to be the mean of the plate temperatures. In a practical situation, this may not be the case, and corrections may be required, as discussed in Chapter 5.8.

The curves shown in Figure 4.4. are of considerable value, as they indicate that the heat transfer across a cell has a well developed heel at a gap of approximately 25mm. In consequence, any gap greater than this will confer little benefit in reducing heat flow.

Figure 4.5. shows the variation of heat flow with temperature for a 25mm gap. The derived nusselt number is also shown, and contrasted with that produced by the Holland (1975) correlation recommended by Sharples (1979). This latter relationship indicates a cut-off heat transfer condition at 4°C temperature difference for a single cell. This observation led the author to suppose that a 5 screen array was required to minimise convective heat flow with an overall temperature difference of 20°C. As can be seen from Hollands (1980), this supposition was entirely unjustified, and the subsequent analysis which demonstrated that a five screen array gave satisfactory characteristics was fortuitous.

4.1.3. Combined Heat Transfer

The combined convective, conductive and radiative heat transfer coefficients for a particular cell result in the overall heat transfer coefficient. The effects are additive i.e. the heat transfer coefficient of the cell in total is the sum of the individual coefficients. The heat flow in this case is given by:

$$Q = hr \times (T_1 - T_2) + h_c (T_1 - T_2) \qquad 4.22$$

Where hr = radiative heat transfer coefficient

h_c = convective heat transfer coefficient

The problem here is that the radiative heat transfer coefficient as recommended by Duffie and Beckman (1980) and others is given by:

$$hr = \frac{(T_1 + T_2)(T_1^2 + T_2^2)}{1/\epsilon_1 + 1/\epsilon_2 - 1} \qquad 4.23$$

This is a much simplified expression but still renders the evaluation of temperatures from a given heat flow very difficult. If one of the temperatures is known, then the other can be found by repeated iteration of the expression

$$Q = \frac{(T_1 + T_2)(T_1^2 - T_2^2) \times (T_1 - T_2) + h_c(T_1 - T_2)}{1/\epsilon_1 + 1/\epsilon_2 - 1} \qquad 4.24$$

This expression must be evaluated for an estimated value of the unknown temperature. The resulting overall heat transfer coefficient is evaluated, and this value used in conjunction with the known heat flow, and a second estimate of the unknown temperature made. This process is repeated until the estimated and evaluated temperatures are sufficiently similar.

This procedure works quite well for opaque screens when the infinite plate approximation is acceptable, but it is very difficult to apply if these conditions are not acceptable. An alternative method will be described in the next section of this chapter.

4.2. Heat Transfer through a Series of Cells

The preceding three sections have indicated the heat transfer regime through a single vertical cell. In the case of the module, we have a series of such cells.

Duffie and Beckman (1980) have considered the problem, and offer an analysis based upon Figure 4.6. In this analysis, a heat flow and absorber temperature are assumed. This heat flow is then employed cell by cell using the iterative method indicated in the previous section, until a screen temperature is arrived at. If this screen temperature results in a loss to the atmosphere which is different to that assumed, the heat flow is modified and the process repeated until the computed loss and heat flow are sufficiently similar.

This process is somewhat tedious but can be applied using simple computer techniques, and was used in a modified way for the initial evaluation of the proposed module incorporating glass screens. However it is of no value in computing the radiant heat transfer coefficients when partially transparent screens are involved, and a different technique is required. Whillier (1977) offers a series of algebraic relationships for two semi transparent screens and a third glass outer screen, but these relationships present considerable difficulty if the simple approximation of infinite plates is not assumed. Edwards (1977) suggests that in the analysis of solar radiation transmission the screens can be considered as an increasing stack, and the effective reflectivity of the stack computed as each element is added. This may well be satisfactory for solar spectrum radiation, but for thermal infra red radiation, the emitted energy of the screens and absorber complicates the analysis.

Returning to the analysis presented in Section 1 of this chapter, it is clear that the equations can be arranged for each surface so as to produce two matrices and associated vectors in terms of the total radiation falling upon each face of each screen, and the temperature of each screen. Figures 4.7. and 4.8. show these two matrices and the associated vectors. The matrix associated with the 'G' vector is termed the GCF matrix, and that associated with the T^4 vector the T_{4CF} matrix. It is clear then that these may be arranged as follows:

$$[GCF] \times [G] = - [T4CF] \times [T4] \qquad 4.25$$

$$\text{From which } [G] = - \text{INV}[GCF] \times [T4CF] \times [T4] \qquad 4.26$$

The required inversion of the GCF matrix is readily performed by computer, and the resulting 'G' vector can be computed for an assumed range of screen temperatures.

Similarly, a matrix solution can be applied to the convective components of heat transfer, and the conduction through each screen. This is a simple process and need not be resorted to because the convective component of each cell can be simply calculated from the assumed temperature field. With the convective component and radiative component identified, the overall heat transfer coefficient can be computed for each cell. If a heat flow is assumed this can then be used with each cell heat transfer coefficient to evaluate a second temperature field which is then used to repeat the procedure, until the heat flow through each cell matches the assumed value. The extreme values of the temperature vector so produced, in conjunction with the assumed heat flow results in the overall heat transfer coefficient for the entire array. This can be repeated for different assumed heat flows to produce a profile of the screen

array heat transfer coefficient for various temperature differences between the absorber and outer screen. This whole process can then be repeated for various types of screen and absorber material, and configurations of screen.

The application of this method will be discussed in Chapters 5 and 6 for experimental and simulation calculations.

Some corroboration of this matrix technique is provided by the parallel work of Hollands (1983) who develops a similar method of analysis, but without considering the sides of the enclosure.

4.3. Heat Transfer to the Atmosphere

The preceding sections have considered the analysis of the heat transfer from the absorber to the outer screen. The loss from the outer screen to the atmosphere, is the natural extension of that loss, and it follows that the energy entering the outer screen must equal that leaving it, and the heat transfer coefficient from the screen to the atmosphere is complementary to the heat transfer coefficient from the absorber to the outer screen.

The heat loss from the outer screen consists of two components, the convective or wind loss, and the radiative loss. This former loss is readily deduced, and provided that it is of a reasonable value does not affect the overall 'U' factor dramatically. This is shown by Cole and Sturrock (1977), and is due to the dominant effect of the low heat transfer coefficient from the absorber to the outer screen. Various correlations have been established for this, Duffie & Beckman (1980) recommend a value of:

$$h_w = 2.8 + 3V \quad \text{for vertical surface} \qquad 4.27$$

Where h_w = the wind heat transfer coefficient in Watts/$m^2{}^oC$

V = Wind speed metres/second.

Alternatively, Sharples (1980) suggests a relationship based upon building surface speeds derived for windward and leeward surfaces as follows:

$$h_w = 18.6 \times U_s^{0.605} \ W/m^2 K^{-1} \qquad 4.28$$

Where $U_s = 0.25 \times U$ for $U = 1$ to 2 metres/second.

$U_s = 0.5 \times U$ for $U > 2$ metres/second.

The above for windward surfaces.

and for leeward surfaces

$$U_s = 0.05U + 0.3 \text{ metres/second} \qquad 4.29$$

Where U = wind speed.

Because of the insensitivity of the module to the actual component of windspeed, the correlation suggested by Duffie and Beckman was adopted.

The radiative component of loss from the outer screen is much more complex. The problem relates to establishing an effective emissivity for the ground and atmosphere to compute the longwave radiation incident upon the outer screen. This has led some writers to imply an effective temperature for the atmosphere when computing the radiant heat loss. Duffie and Beckman (1980) suggest this course of action, and further suggest that the heat loss so computed is rationalised to a heat transfer coefficient by dividing by the difference between the air temperature and outer screen temperature. Such a procedure is simplistic, and implies that the screen temperature cannot fall below that of the air temperature. This is not the case, as under some conditions of atmosphere the radiant loss is sufficient to reduce the outer screen temperature to a value below that of the air. In this case the air in fact contributes to the energy input to the outer screen.

An energy balance for the module outer screen can be considered as follows:

$$h_w (T_s - T_{air}) + \sigma \epsilon_s T^4 = h_m (T_a^4 - T_s^4) + \sigma \epsilon_a T_{air}^4 + \sigma \epsilon_g T_g^4 + S \qquad 4.30$$

Where

T_s	=	Screen temperature K
T_{air}	=	Air temperature K
ϵ_s	=	Outer screen emittance
h_m	=	Heat transfer coefficient from the absorber to the outer screen.
ϵ_a	=	Effective atmospheric emittance
ϵ_g	=	Effective ground emittance
T_g	=	Ground temperature K
S	=	Solar energy absorbed by the outer screen in watts
T_a	=	Absorber temperature. K

From the above, the outer screen temperature can be evaluated by the iterative application of:

$$T_s = h_m \times T_{air} + h_w \times T_{ar} + (\epsilon_a T_{air}^4 + \epsilon_g T_g^4 - \epsilon_s T_{s'}^4 + s) \quad (h_w + h_m) \qquad 4.31$$

Where $T_{s'}$ is an iterated guess at the value of T_s.

Once the outer screen temperature is deduced, the heat loss from the module is found from the known heat transfer coefficient hm.

The above analysis works well when the heat transfer coefficient from the absorber to the room is large in comparison to that from the absorber to the outer screen. In the absence of an outer screen, when considering the losses from a conventional wall, an alternative analysis must be used, which will be explained in the next section.

The effective emittances of atmosphere and ground have been evaluated by Unsworth and Montieth (1975) as follows:

Emittance of the atmosphere

$$\epsilon_a = (0.7 + .09(.5 \times \mathrm{Ln} W_p)) \times .5 + .09 \times .35 \qquad 4.32$$

For bright sky conditions, and

$$\epsilon_a = (.952 + .0144 \times (.5 \mathrm{Ln} Wp)) \times .5 + .0144 \times .35 \qquad 4.33$$

For overcast conditions.

Where Wp = precipitable water content of the atmosphere.

The evaluation of Wp is considered in Chapter 6.

Emittance of ground

$$\epsilon_g = 0.5 \times \frac{T_g^4}{T_a^4} \qquad 4.34$$

4.4. Heat Transfer into the Room

The heat transferred from the rear surface of the module storage slab is similar to that discussed in the previous section, as it consists of convective and radiative components.

The convective component of heat transfer has been studied by Sharples (1980) who derives his data from the Ashrae (1977) data. In this case, the heat transfer coefficient is not augmented by wind, and a coefficient of 3 watts/$m^{2o}C$ is recommended as being typical for vertical walls.

The radiative heat loss presents more problems, as it depends upon the nature and temperature of the other walls of the room. However, assuming the room behaves as a black body with respect to module, the following expression can be used as discussed by Sharples (1980).

$$hr = 6\epsilon_m (T_m^2 + T_r^2)(T_m + T_r) \qquad 4.35$$

Where ϵ_m = Emittance of the module slab surface, taken as 0.95.

T_m = Module surface temperature K

T_r = Surface temperature of the room walls, taken as being the room air temperature. K

h_r = Radiative heat transfer coefficient $w/m^{2o}K$

4.5. Transient Analysis of the Module

Because the screen elements of the module are essentially light-weight constructions, the transient analysis of the module can be restricted to consideration of the storage slab. Various methods can be used; finite element and finite difference techniques can be readily applied, but the development of a partial differential equation solution presents problems due to the continuously varying boundary conditions of solar input and surface temperature. Some researchers have applied a fourier technique as indicated by Mathur (1978). The problem which is presented by the slab of the module can be considered as essentially a one dimensional heat flow, and the technique of finite differences was chosen as the simplest method. This technique is explored in detail by Croft and Lilley (1977), but is briefly explained as follows for one dimensional heat flow where the loss of heat from the edge of the slab is neglected.

Figure 4.9. illustrates a system of nodal points, equally dividing the thickness of the slab. Considering the situation of an inner node. The heat gained by an element of volume over a period of time is approximately:

$$H = \rho \times C_p \times \Delta \ell^3 (T_n - T_n^1) \qquad 4.36$$

Where H = The heat absorbed over the time in question by the volume of material associated with the node, in Joules.

ρ = The density of the material kg/m^2

C_p = Specific heat of the material J/kg

$\Delta \ell$ = Nodal distance

T_n = The temperature of the node at the beginning of the period in question. K

T_n^1 = Temperature of the node at the end of the period in question. K

The heat absorbed or lost by the material associated with the node must have been derived from its adjacent nodes, and this is found as being:

$$(T_n^1 - T_{n-1}^1) \times \frac{k}{\Delta \ell} \times \Delta \ell^2 \times \Delta t + (T_n^1 - T_{n+1}^1) \times \frac{k}{\Delta \ell} \times \Delta \ell^2 \times \Delta t \qquad 4.37$$

from which

$$\rho c_p \frac{\Delta \ell (T_n - T_n^1)}{\Delta t} = (T_n^1 - T_{n-1}^1) \times \frac{k}{\Delta \ell} + (T_n^1 - T_{n+1}^1) \times \frac{k}{\Delta \ell} \qquad 4.38$$

or $$\alpha (T_n - T_n^1) = (T_n^1 - T_{n-1}^1)\beta + (T_n^1 - T_{n+1}^1)\beta \qquad 4.39$$

where $\alpha = P_{cp} \Delta \ell / \Delta t$; $\beta = k/\Delta \ell$

Croft and Lilley proceed from this point to derive algebraic relationships for these nodal temperatures, but for computational purposes the author has found it to be more convenient to rearrange as follows:

$$-\beta T_{n-1}^1 + \alpha T_n^1 + 2\beta T_n^1 - \beta T_{n+1}^1 = \alpha T_n \qquad 4.40$$

Clearly, this will give a series of simultaneous equations for the unknown future nodal temperatures in terms of the known initial temperatures.

The situation with the surface nodes is a little more complicated, and can be established as follows referring again to Figure 4.9.

The energy into the nodal volume over a given time is by:

$$H' = \rho c_p \times \frac{\Delta \ell^3}{2} (T_s - T_s') \qquad 4.41$$

and the energy from the outside is given by:

$$H'' = (T_a - T_s^1) \times h_1 \times \Delta t + s \times \Delta t \qquad 4.42$$

where Δt is the time interval

where s = solar input, T_a = temperature of the outer cover

h_1 = module heat loss factor

The energy from the inner node is:

$$(T_{s+1} - T_s^1) \times \beta \times \Delta t \qquad 4.43$$

From these, the resulting nodal equation is

$$(\alpha/2 + \beta + h) T_s^1 - \beta T_{s+1}^1 = h_1 \times T_a + \alpha/2 \times T_s + S \qquad 4.44$$

A similar expression can be derived for the inner or room surface as being

$$-\beta T_{R-1} + (\alpha/2 + \beta) T_R 1 + h_2 = \alpha/2 \times T_R + h_2 \times T_a \qquad 4.45$$

These equations can be arranged into a coetticient matrix with associated future temperature vector and what is effectively a nodal heat gain vector, these are shown in Figure 4.10 for an eight node solution. The solution is found by simple matrix inversion of the temperature coefficient matrix.

It should be noted that the above description is termed a forward pass, in that the unknown temperatures are all in the future. This gives what are termed "implicit equations". An alternative is to employ a backward pass, in which the equations are set up assuming present conditions, and the future condition extrapolated. This gives rise to "explicit equations" which are more easily solved by manual means, but which also give rise to problems of computational stability, and consequent restriction of the time interval employed.

For the eight node implicit system shown, a time interval of 300 seconds was found to be acceptable.

5. Experimental Considerations.

It was apparent, from the lack of published data, that the heat transfer calculations associated with multiple screens which may be transparent to thermal infra-red radiation may be questionable. It was decided to conduct a series of experiments with the objective of demonstrating the validity of the calculations which are discussed in Chapter 4.

5.1. Choice of Type of Experiment

The classic way of determining the heat flow rates for this type of situation is that reported by Hollands (1975). Typically, a cell is created by metal plates of known emissivity, with edges capable of being maintained at the mean temperature of the plates. The plates are then subjected to a temperature differential by either a water jacket, or electrical heating, and the heat flow measured using heat flow transducers.

From a purely practical point of view, there were two reasons why this approach was not appropriate for this project. The first reason was one of cost, it had become apparent that INCO's trading position was deteriorating, and as a result the project had to proceed on very much a petty cash basis. The second problem was time, the time needed to procure and fabricate equipment as sophisticated as Hollands' own would have been prohibitive, as there was no possibility of extending the project beyond its three year projected timescale. As events have shown, this constraint was to prove even more onerous than was thought probable.

Bearing these factors in mind, it was decided to conduct the experiments upon a small scale replica of the module which would be well insulated to reduce incidental heat losses. The size of the replica was influenced by three considerations; firstly the width of "Maxorb"

available, secondly, the physical size for the purposes of the author lifting and manoeuvring it, and thirdly the wish to confirm Hollands' aspect ratio effect on the convective cell heat transfer coefficient.

The experimental module was designed as indicated in Figure 5.1. as a compromise between these requirements. The objective of the experiment was to heat the "Maxorb" absorber with a series of five screens in front of it, and to measure the thermal input and losses, and the temperature difference from the absorber to the outer screen. This would provide a basis on which the computational methods already discussed could be demonstrated.

5.2. Energy input and Measurement.

Energy input to the absorber was provided by making an electric heater out of the "Maxorb" itself. This was achieved by scribing appropriate channels in the "Maxorb" to create a flat serpentine ribbon through which an electric current could be passed. By measuring the current used, and the voltage across the input terminals, the energy input could be easily determined. In this way it was possible to avoid costly calorimetry or heat flux tranducers.

Figure 5.2. shows a diagram of the "Maxorb" heater so produced. To provide rigidity, and to ensure an even temperature profile over the absorber surface, it is stuck onto an aluminium plate. The first plate employed was 1mm thick, but this was found to result in a temperature variation of $1.7^{\circ}C$ over the plate which was thought to be excessive. The problem was overcome by using a 10 mm thick plate and a plate carrier of balsa wood rather than plywood.

This method of energy input and measurement proved to be successful, and contributed to the reproducibility of the experimental procedure as indicated in Section 5.7.

5.3. Temperature Measurement

It was apparent that the measurement of temperature would be as critical as that of the energy input measurement. The nature of the experiment precluded the use of standard thermometers. Thermocouples were considered to be insufficiently sensitive to produce the 0.1°C sensitivity thought to be required. This sensitivity was necessary if measurements of individual cell temperature variations down to .2°C were to be possible.

It was decided to employ a temperature transducer marketed by Analogue Devices Ltd., known as the AD 590 and described in Analogue Devices (1981). This device employs the variation in transistor junction voltage as a temperature indicator. Furthermore it is remarkably unobtrusive and has an output current which is virtually independent of the impedance of the measuring circuit which avoids the problems of connecting cable compensation associated with thermocouples.

The one problem which the author anticipated with this device is its own self heating effect due to the current produced. This effect depends upon the heat sink with which it is associated, and is discussed further in Section 5.6.

In service these transducers have proved to be very reliable and only one of the twenty which were purchased failed to function.

The current output from the transducers which is in the order of $1\mu A/°C$ gives a voltage output of 1 mv/K when passed through a 1000 ohm resistor.

To allow the simultaneous use of a series of transducers an instrument was designed and constructed to accommodate 18 transducers, each one of which could be accessed by a pair of decade switches. The instrument also accommodated a stabilised d.c. power supply to drive the transducers with the required 5 volt input, and a digital thermometer.

5.4. Calibration.

There were three aspects of calibration required for the equipment employed, namely input energy measurement, heat loss measurement, and temperature measurement.

The calibration of heat input measurement was simply achieved by comparing the readings of the instruments used with those of instruments of known accuracy. It was found that although the voltmeter employed gave readings consistent within the accuracy of actually taking the reading from the pointer, the ammeter gave readings which were consistantly 5% low.

The evaluation of the thermal characteristics of the insulated boxes, and screen carrier was conducted in two stages. Firstly, the end box was calibrated by placing two identical boxes back to back, from which the heat flow from either box could be calculated when the heater was interposed and raised to various temperatures. In the second stage, the screen carrier heat loss characteristics were determined by placing the screen carrier between both end boxes, with identical heaters at either end. The heaters were then brought to various temperatures, and the associated temperature gradient of the screen carrier recorded. In this way the losses from the ends and the carrier could be isolated and characterised.

The calibration of the module configuration was established by making up a five glass screen configuration in the screen carrier. This allowed the individual screen temperatures and mean cell temperatures to be established, so characterising the edge losses from each cell, and providing a measure of screen temperatures which could be used to modify the computer program which would then be employed to compare computed results with other experimental results for different screen materials. It was necessary to employ glass screens for this purpose because of the difficulty of measuring the temperature of a thin plastic film which is transparent to thermal infra-red radiation.

Temperature calibration of the transducers was carried out in two stages. The first was to calibrate several transducers by comparison with NPL certified full depth mercury thermometers in an NPL calibration water bath. The most accurate of these transducers was then retained as a reference. Subsequent calibration was carried out by placing transducers in rosette fashion at the centre of the back face of the heater plate which represented a massive heat sink. The plate was then placed between the end boxes, brought to temperature, and allowed to achieve equilibrium before being allowed to cool down. During the cooling period comparative readings of the transducer temperatures were taken. The transducer readings had been previously set to zero with respect to the reference transducer at room temperature. The calibration curves so obtained were substantially linear, and their algebraic correlation equations are given in Results Sheet I.

5.5. Environmental Influences.

The first attempts to determine the thermal characteristics of the experimental equipment proved difficult to achieve any consistency of results. This was found to be the result of large fluctuations in air temperature due to central heating, persons opening and closing the workshop door, and apparent solar gains.

The answer to this lay in finding a relatively stable thermal environment, and an old test cell with thick concrete walls, and a double door entry system was found and refurbished. This test cell provided a maximum temperature variation of 1°C per day, but on most days there was no perceptible change.

To reduce the risk of spurious inputs to the equipment by room lighting, the wall which the equipment faced was painted matt black. Subsequent checks revealed that a period of twenty minutes elapsed between a person entering the test cell, and any perceptible change in the temperature readings of the equipment transducers. In consequence, all results were taken immediately upon entering the test cell.

5.6. Experimental Procedure

The procedure employed in all the experiments was as follows:

a) Assemble the apparatus and leave for 24 hours to achieve steady state conditions.

b) Adjust all temperature transducers to zero reading with respect to the reference transducer, which was placed in the centre of the primary hot plate.

c) Using a stabilised D.C. power supply, a voltage was applied to the "Maxorb" heating element, and the apparatus allowed to reach equilibrium for 24 hours. Experience showed that equilibrium was achieved more quickly if the temperature of the hot plate was boosted to 5°C greater than that expected from the voltage applied. This was repeated to give a series of five readings with hot plate temperatures up to 30°C above the room temperature. The disposition of the transducers for each experimental configuration is indicated in the appropriate results sheet in Appendix 2.

d) The equipment was stripped completely, and the process indicated in a), b) and c) above repeated.

In this way, it was expected to reduce variations in results which may have been introduced by time scale effects. To check this, several tests were allowed to continue over long week-ends, but no difference in result was noted. In general, if no change in the readings was observed over a two hour period then the apparatus could be regarded as stable.

5.7. Experimental Results.

After initial preparatory trials, and a period of heating to allow excess moisture to be driven off, the following series of experiments was undertaken for the purposes previously discussed.

a) With the end boxes, hot plate and carrier only. The joint between the boxes and the carrier was sealed using masking tape. Temperature transducers were placed at the centre rear face of the hotplate, and the centre inner faces of the hot box outer plywood sheets. The configuration and results obtained are indicated in Appendix 2, results sheet A.

b) With the end boxes, and screen carrier and two similar hotplates and carriers. Once again the joints were sealed with masking tape. The transducers in the screen carrier were sealed in a proprietry domestic sealing compound in channels cut into the inner surface of the screen carrier. The disposition of transducers and results are as indicated in Appendix 2, results sheet B.

c) With the end box, hot plate and carrier and screen carrier all sealed with masking tape. Five glass screens were inserted into the screen carrier, each separated by 25mm. temperature transducers were placed at the centre top and bottom of each inter screen cell so formed. The screens were sealed at the edges using a proprietary sealing compound. Results are shown in Appendix 2, results sheet C.

d) The experiment referred to in c) the previous paragraph was repeated, but the four inner glass screens were replaced by polythene. The polythene was supported on a wooden frame. Results are shown in Appendix 2, results sheet D.

e) The experiment indicated in the previous section was repeated, with the three inner screens of polythene, and the fourth screen of melinex with a reflective indium oxide layer as supplied by Dr. Howson of Laughborough University. This screen was again supported on a wooden frame. Results are indicated in Appendix 2, results sheet E.

f) The experiment was repeated with two inner polythene screens, followed by two screens of highly reflective aluminised polyester film supplied by ICI Limited, Plastics Division. Results are indicated in Appendix 2, results sheet F.

g) For comparison purposes a further experiment was conducted using a three inner polythene screens, and one outer glass screen. Results are shown in Appendix 2, results sheet G.

h) A further experiment with glass screens was conducted to assess the temperature drop across the glass screens, and results are shown in Appendix 2, results sheet H.

The measurement of glass screen temperature was done by taping a transducer to the surface of the glass screen using masking tape. To reduce the effect of thermal radiation on the transducers, a wad of fibreglass was then taped over the transducer.

For each assembly, the screens were cleansed of dust and finger-marks, using soapy water.

The results of the experiments a) to g) are summarised in graphical form in Figure 5.3. In this figure, the X axis which is labelled the reference temperature difference, is the temperature difference between the centre rear of the hot plate and the centre inner of the end box. This temperature difference is used in all the experimental data graphical plots.

The results of individual experimental configurations in Figure 5.3. show a satisfactory consistence, and are close to the mean regression lines computed from the data. As anticipated, the relatively transparent polythene screens show a greater thermal input than the opaque glass screen configuration, and the double aluminised screen configuration shows a lower power input than the single Howson Variant.

The multiple glass screen experiment shows an excellent reproducibility, with all the points from the three different experiments lying close to the mean regression line for each screen as indicated in Figure 5.4.

5.8. Analysis of Results

The experimental results were consistent and reproducible, but various heat loss effects must be taken into account in order to model the situation.

1. Heat losses from each cell edge.

The loss from each cell into the screen carrier can be estimated by determining a general radial heat transfer coefficient for the screen carrier, and applying this to each cell for each configuration. The resulting indicated heat loss from the cell is not that which actually occurs, but should be indicative of it. A further correction is required which will be discussed in the next section.

This screen carrier radial heat loss characteristic can be determined as follows:

a) For a given reference temperature difference, the heat loss H_e from the end boxes can be estimated from the results of experiment a) in Appendix 2.

$$H_e = -.00223 + .1337 \times \Delta t \qquad 5.1.$$

b) The heat loss from the screen carrier plus boxes

$= -.190 + .253\,\Delta t$ from experiment b) 5.2.

c) The heat loss from the carrier alone

$= -.188 + .1193x\,\Delta t$ 5.3.

d) The mean temperature difference from the inner surface of the carrier to the outer end box surface is given by regressed values from experiment b) as.

Wall temperature difference $= 0.8446\,\Delta t$ 5.4.

e) The screen carrier radial heat transfer characteristic is then:

$$\therefore \frac{188 + .1193\,\Delta t}{0.8446\,\Delta t} \qquad 5.5.$$

This value can then be employed with the 25mm gap to give a cell radial heat loss characteristic which can then be multiplied by the cell mean temperature to determine an indicative heat loss for the cell. The cell mean temperature can be determined from the transducers at the top and bottom of each cell.

The results of this procedure are indicated in Figures 5.5. to 5.8.

2. Further consideration of loss from the end boxes.

The loss from the end box as indicated by experiment a). must be modified in subsequent experiments to account for the increased heat loss arround the corner of the hot plate into the screen carrier which is operating at a lower temperature than the end box.

This is a complex problem, and was approached by using a two dimensional finite element technique. The author is grateful to Mr. D.C. Hickson for the use of a computer program for this purpose.

The nodal grid is shown in Figure 5.9. The temperature inputs for each screen configuration were determined from results at a reference temperature difference of 30°C. The temperature at inter-nodal points were determined by assuming that the temperature distribution between any three points was quadratic in form, and the corresponding isothermal lines were drawn.

An approximation to the increased heat flow into the screen carrier was then found by drawing squares between two isothermal lines. The heat flow is then considered as proportional to the number of squares as described by Kreith and Black (1980).

In this way, the additional heat flow was determined for each configuration, from which the additional loss could be established. The appropriate factors and isothermal lines are indicated in Figures 5.12 to 5.15 for each screen configuration.

3. Screen Edge Loss.

The loss from the screen edges was determined from the experimental screen temperatures and the radial loss factors described previously.

This was done by developing a computer program which computed the screen temperatures from the modified end box loss, and individual radial cell losses. These cell edge losses were then adjusted to produce the correct screen temperatures with a reference temperature difference of 30°C. If the computer model is accurate, it should also then compute screen temperatures at other reference temperature differences, and with other screen configurations.

This program is given in Appendix 4.1. with referances to the relevant chapters of this thesis.

4. Comparison of results and computation.

Figures 5.16 to 5.19 show the calculated screen temperatures compared to the screen temperatures recorded from the experiments. There is a close correspondence of calculated and experimental values, falling largely within the inner and outer screen temperatures recorded on either side of the screens indicating that the simulated approach is reasonable.

6. Computer Modelling of the Solar Wall Module.

6.1. Thermal losses from the Module.

In Chapter 5.8. a method for the analysis of heat losses through an array of screens was developed. The method employed factors to estimate the loss of energy from each screen interspace or cell; this was necessary because of the relatively low aspect ratio of 12.8 to 1 employed by the experimental equipment. However, in practice a ratio of 40:1 is expected, and additionally modules will be normally arranged in multiples along a wall. Where modules are not in multiple units, they will naturally face end to end with some other architectural feature which will itself demonstrate a temperature gradient similar to that of the module. For these reasons the edge losses of a full size module in situ can be expected to be much less, in proportion, than those associated with the experimental equipment, and for the purpose of the analysis of module thermal performance they have been neglected.

This allows a simplified matrix formulation in comparison to that developed in Chapter 5.8., the simplification results from neglecting the side wall loss terms in the radiation coefficient matrices. Additionally, the screens employed in the module will be of thin plastic film, typically 75μ or less. This means that the temperature variation across the screen is insignificant and can be neglected.

The radiation evaluation matrices which result from these simplifications are indicated in Figure 6.1. The analysis thereafter follows that indicated in Chapter 5.8. with the exception that the convective heat transfer coefficient is not altered to allow for an edge loss component.

The program developed to compute the heat transfer characteristics of the module is based upon that indicated in Chapter 5.8. and is given in Appendix 4.2.

The results of this analysis for various combinations of screen materials is summarised in Figure 6.2.

Several points of interest can be drawn from this figure:

1) The target loss coefficient of 0.6 w/m^2 C as required by the Building Regulations is attainable with 5 screens, namely PPHHG and below (fig 6.2).

2) The combination of highly transparent inner polythene or polypropylene screens is superior to the more opaque varieties of melinex or glass provided that a reflecting screen is incorporated subsequently.

3) The 'Maxorb' absorber is necessary to achieve 0.6 $w/m^{2o}C$, this cannot be done with a non-selective absorber.

4) The position of the reflecting screen is of great importance. The best position is furthest from the absorber due to the effect of the relatively high emittance of the reverse side of the reflecting screen. This can be seen by comparing the characteristic of HPPPG with that of PPPHG, the effect is accentuated in the case of transparent screens.

It is apparent that the most beneficial thermal characteristic is that associated with two inner polythene or polypropylene screens, followed by two reflective screens, and a glass outer screen. A glass outer screen has been maintained in all these comparisons for purely practical reasons, as it is assumed that such a material will be required as an external surface for purposes of longevity in service.

It is important to remember that the thermal characteristics as calculated above do not take into account any incident solar energy. The effect of such energy will be to reduce the loss characteristic for a given temperature difference as the energy absorbed by the screens raises the temperature of the screens and reduces the effective temperature differentials.

6.2. Solar Transmission Thermal Gain

In Chapter 4.2. the radiation heat transfer of a series of cells is explained, and a matrix solution developed

The situation with solar energy transmission is very similar as this is once again a radiant heat transfer phenomenon. The following differences apply:

a) The emitted radiation of the screens is not taken into account, as this lies in the thermal infra-red spectrum, and so does not materially contribute to processes in the solar spectrum. Chapter 3.1. explains this effect in more detail.

b) The surfaces of the screens are assumed to be specular, and so the radiation properties of the screen vary with the angle of incidence of the sunlight.

Referring to figure 4.2. it is evident that a series of simultaneous equations can be set up in terms of reflectance ρ and Transmittance τ for each screen and the absorber. However,the values of ρ and τ will vary according to the angle of incidence. The matrix resulting from this consideration in terms of ρ and τ is indicated in figure 6.3. and this matrix can be equated to the incident energy vector indicated. Simple matrix inversion then provides the individual components of solar energy upon each screen surface.

The variation in reflectance and transmission can be taken into account by considering these relationships in terms of the refractive indices and extinction coefficients of the screen materials. These relationships are as follows, and are given in more detail by Duffie and Beckman (1980).

For unpolarised radiation passing from a medium of refractive index n_1 to another medium of refractive index n_2, the perpendicular (r_s) and parallel (r_p) reflectances are given by:

$$r_s = \frac{\sin^2(\theta_2 - \theta_1)}{\sin^2(\theta_2 + \theta_1)} \qquad 6.1.$$

$$r_p = \frac{\tan^2(\theta_2 - \theta_1)}{\tan^2(\theta_2 + \theta_1)} \qquad 6.2.$$

Where $r = \frac{1}{2}(r_s + r_p)$ 6.3.

θ_1 = angle of incidence

θ_2 = angle of refraction

r_s = reflectance perpendicular to the plane of incidence

r_p = reflectance parallel to the plane of incidence

r = total reflectance

The angles θ_2 and θ_1 are related by Snells law:

$$\frac{n_1}{n_2} = \frac{\sin\theta_2}{\sin\theta_1} \qquad 6.4.$$

For normal incidence,

$$r_o = \left[\frac{n_1 - n_2}{n_1 + n_2}\right]^2 \qquad 6.5.$$

Where r_o = reflectance at normal incidence.

And if one medium is air with a refractive index of unity.

$$r_o = \left[\frac{n - 1}{n + 1}\right]^2 \qquad 6.6$$

This is the situation with one interface, in practical applications the light passing through a screen is subject to two such interfaces. The resulting attenuation of the radiation is the sum of two components, the first being the result of multiple reflections and the second being the result of absorption of the radiation by the material of the screen.

The reflective loss results in a transmittance which is the quotient of the radiation passing through the screen, divided by the initial radiation,

$$\text{or } \tau_r = \frac{1}{2}\left[\frac{1 - r_s}{1 + r_s} + \frac{1 - r_p}{1 + r_p}\right] \qquad 6.7.$$

Where τ_r = Transmittance for radiation only.

Thus, knowing the reflectance of a material at normal incidence, it is possible to calculate the refractive index of the material, as follows:

$$ro = 1 - \tau_r = 1 - \left[\frac{1 - ro}{1 + ro}\right] \qquad 6.8.$$

$$\text{and} \quad ro = \left[\frac{(n - 1)}{(n + 1)}\right]^2 \qquad 6.9.$$

From which "n" can be deduced.

The absorption of radiation through a partially transparent medium is described by Bouguers law which assumes that the loss in intensity of absorbed radiation is proportional to the intensity of the radiation and the distance travelled, or:

$$dI = IK\,dx \qquad 6.10.$$

Where dI is the radiation absorbed,

I is the local radiation intensity,

K is a constant for the material and radiation wavelength in question and is termed the extinction coefficient,

dx is the length of the light path through the medium.

From this, the transmittance due to absorption is given by:

$$Ta = e^{-KL/\cos\theta_2} \qquad 6.11$$

Where Ta = Transmittance due to absorption.

L = the medium thickness

The total transmittance is then given by:

$$T_t \simeq T_r \times Ta \qquad 6.12$$

Where T_t = the total transmittance.

Thus, knowing the total transmittance, and the reflectance of a material at normal incidence it is possible to find the refractive index and the extinction coefficient and thus determine the total transmittance of the same material at other angles of incidence.

It should be noted that the absorption assumption above does not apply to thin films of polythene and polypropylene which absorb radiation predominantly in discrete absorption bands which are rapidly saturated. However the analysis assuming Bouguers law results in a conservative estimate, and so has been retained.

The above analysis has been applied to a series of experimental data supplied by Stay (1982), and the results are given in Table 6.1. The analysis for the Howson reflective film was conducted by assuming that the indium oxide layer lay upon the known melinex sheet, with the IO_3 layer having a refractive index of 2.1 as reported by Howson (1979). The reported total normal transmittance was then employed to give an effective extinction coefficient/thickness quotient of 0.01635 for the IO_3 layer.

The above analysis was programmed in BASIC as shown in Appendix 4. 3.

Figure 6.4. shows the values of transmittance for the reference module design for all incidence angles. The figure also shows a normalised cosine curve. The area of the transmission curve up to the module shadow angle cut off is 95% of that of the cosine curve. This similarity of curves, is made use of in establishing the transmittance of the module to diffuse light in Appendix 3.

6.3. The Solar Resource and Weather

The thermal performance of the wall module as a building element is dependent upon the energy which it absorbs and the way in which that energy is then dissipated into the building, and the atmosphere.

It follows that the variation in solar availability, external air temperature, and internal or room temperature will determine the quantity of energy which the module can contribute, and the temperatures at which the module will be effective. Of these, the room temperature is affected by factors which have not as yet been considered, but have been discussed by Lebans (1980) and Fisk (1981) and include:

a) The thermal mass of the building.

b) The rate of air infiltration.

c) The level of incidental energy gains.

d) The rate of heat loss from the building by conduction through the floor, ceiling, walls and windows.

e) Direct solar gains through windows.

f) Variation in heating/cooling control.

These factors result in a complex analysis dependent upon the design of the building itself. Analyses have been conducted by Gordon & Zarmi (1981) Richardson & Berman (1981) which accommodate such factors, and Page (1979) has done considerable work in this area. The problem is that in the absence of a standard design of building it is difficult to analyse the benefit which might be expected from the module. Ideally, the performance of the module should be compared with a wall of conventional construction to assess its worth.

The author decided to remove the room temperature as a variable, by assuming it to be a constant temperature of 293K or 20°C. This is an arbitrary figure, and it may be that the figure of 16.5°C as recommended by the DoE (1) is more realistic. However the losses assuming 20°C will result in a slightly conservative figure for the contribution of the module. Similarly, the assumption that the room temperature remains constant will result in a conservative assessment of potential contribution if the actual use of heating allows an evening reduction in temperature.

In practice, the constant temperature approach implies either a massive building, or the removal and addition of heat from and to the building to maintain a constant temperature, or a combination of both.

This leaves the variability of solar input, and the variability of external air temperature to be considered as inputs to the performance of the module. The following section discusses the solar input conditions of the module.

The solar energy available to the module is subject to considerable variability. Duffie and Beckman (1980) provide a comprehensive guide to the origin of the variations which can be summarised as follows:

a) Variation due to the earth's orbital eccentricity about the sun.

b) The latitude of the site.

c) The diurnal variation of night to day.

d) The orientation and slope of the collecting surface.

e) The transmittance of the atmosphere to solar radiation.

f) The amount of cloud in the area.

The factors e) and f) above can be considered as the effect of the climate of the site in question.

A further difficulty in the assessment of available solar energy is the fact that the energy is available in two distinct forms. The first is the direct, or beam radiation which originates from the solar globe and is highly directional in nature, the second is diffuse energy which originates from the earth sky vault. The distribution of this energy about the sky vault varies with the type of day from a bright clear sky, to an overcast sky. These factors will be discussed under the appropriate section of this chapter.

For the purposes of assessing the performance of the module there are several requirements.

1) To establish the maximum temperature excursions of the module under direct sunlight conditions.

2) To determine the level of heat loss from the building through the module under poor sunlight conditions.

3) To establish the level of energy contribution to a building under average conditions.

The assessment of each of these conditions of solar input will be considered in the following sections of this chapter.

For the purposes of analysis, the site chosen is of some importance. For the purely practical reason of time limitation the analysis must be limited to one site. The UK site with most data available is Kew, but an analysis based upon Kew data would provide results which would be optimistic for more northerly latitudes. As a compromise,

Sheffield was chosen, as this provides a more northerly site, and Professor J. Page of the Department of Building Science of Sheffield University has conducted analysis of solar radiation levels which can be used for comparison.

6.3.1. Analysis of Bright Sunny Days.

a. Direct Sunshine

The first, and simplest part of this analysis is determining the relative position of the sun with respect to the surface under consideration.

Benford and Bock (1939) as reported by Duffie & Beckman (1980) have established that the angle of incidence of solar direct beam radiation upon a surface is given by.

$$\begin{aligned}\cos\theta = {} & \sin\delta \sin\phi \cos\beta - \sin\delta \cos\phi \sin\beta \cos\gamma \\ & + \cos\delta \cos\phi \cos\beta \cos\omega \\ & + \cos\delta \sin\phi \sin\beta \cos\gamma \cos\omega \\ & + \cos\delta \sin\beta \sin\gamma \sin\omega \end{aligned} \qquad 6.14$$

Where ϕ = Latitude

δ = Solar declination, i.e. the displacement of the sun from a normal to the earths axis.

β = The slope of the surface from the horizontal; 90° for a vertical surface.

γ = The asimuth angle of the surface, with zero as due south.

ω = The hour angle, i.e. the angle by which the sun is displaced from being at its highest point relative to the location. At 15° per hour morning negative afternoon +.

The solar declination is determined as indicated by Dogniaux (1973).

$$= 0.33281 + (-22.984x \text{ Cos } (\pi/183xJ) + 3.7872 \text{ SIN}(\pi/183 x J)$$

$$- .03499 \text{ Cos } (2\pi/183x J) + \cdot 03205 \text{ Sin } (2\pi/183 \times J)$$

$$- .1398 \text{ Cos } (3\pi/183x J) + .07187 \text{ Sin } (3\pi/183 x J) \quad 6.15$$

Where J is the day number from January 1st.

To establish the hour angle, it is necessary to take account of the variation in solar day length from that of 24 hours. This variation is provided by Dogniaux (1973) who gives the following for the equation of time (ET) hours.

$$ET = \frac{1}{60}\left\{0.00037 + (.43177 \text{ Cos } (\pi/183xJ) - 7.3764 \text{ SIN}(\pi/183xJ)\right.$$

$$-3.165 \text{ Cos } (2\pi/183xJ) - 9.3893(\text{SIN}\,2\pi/183xJ)$$

$$\left. + .07272 \text{ Cos } (3\pi/183xJ) - .24498(\text{SIN}\,3\pi/183xJ)\right\}$$

6.16

From which the local time is determined by:

$$\text{Local time} = \text{GMT} + \text{ET} \pm \frac{1}{15} \times \Delta \text{ longitude} \quad 6.17$$

Where Δ longitude is the difference in longitude of the site from the Greenwich meridian, west + ve, east - ve.

The solar altitude "h" is given by

$$\text{Sinh} = \text{Sin}\,\phi \;\text{Sin}\,\delta + \text{Cos}\,\omega + \text{Sin}\,\delta \;\text{SIN}\,\phi \quad 6.18$$

and the solar zenith angle or the angle of the sun from directly overhead by

$$\text{Cos } Z = \text{Sinh} \quad 6.19$$

From the forgoing, the sunrise and sunset from solar noon can be determined by:

$$SS = \pm \; {}^{1}/_{15} \times \text{Cos}^{-1} (-\tan \phi \;\; \tan \delta) \text{ hours} \qquad 6.20$$

It is thus possible to determine the direction of the sun for any time of day, and day of the year with respect to the surface in question.

In the absence of any atmosphere, the energy falling upon a surface can be determined from the solar constant, this being the intensity of solar radiation upon the earth. However, this value also varies and is described by Dogniaux (1973) in Watts/m^2 as

$$c = 1353 + (45.326 \text{ Cos } ({}^{\pi}/_{183}J) + 1.8037 \text{ Sin } ({}^{\pi}/_{183}J)$$

$$+ .88018 \text{ Cos } ({}^{2\pi}/_{183}J) + .09746 \text{ Sin } ({}^{2\pi}/_{183}J)$$

$$- .0.00461 \text{ Cos } ({}^{3\pi}/_{183}J) + .18412 \text{ Sin } ({}^{3\pi}/_{183}J) \qquad 6.21$$

Note the mean value of the solar constant indicated above as 1353 Watts/m^2 has been assessed as somewhat higher than this in recent years after measurement by space probes as indicated by Hickey et al (1982). For the purposes of this assessment the Author has decided to retain the older value as this is the basis for subsequent correlations which have not as yet been revised in the light of the new data.

Having established the energy which would be available on the surface outside the earths atmosphere, it is necessary to consider the effect of the atmosphere itself. The attenuation of sunlight by the atmoshphere is described in several works, but Kondratiev (1969) and Henderson (1970) cover the various absorption and scattering effects in detail.

The effect of the atmosphere is to reduce the direct component of the suns radiation, but to introduce a diffuse component due to light which is scattered back to the earth. This analysis continues by considering the effect upon the direct component followed by consideration of the diffuse effect.

Unsworth (1975) has established that the direct beam irradiance at the earths surface is effected by the following atmospheric factors.

a) The total water vapour and ozone content of the atmosphere

b) The length of the path of sunlight through the atmosphere

c) The level of aerosol droplets in the atmosphere

The water vapour content of the atmosphere is expressed in terms of the precipitable water depth, i.e. the depth of the water in a vertical column of the atmosphere it it were in liquid form. Unsworth (1975) reports this to be in the region of 5-33 mm for the U.K., with minimum values occuring with the low air temperatures of winter.

Rogers et al (1981) have analysed Metereological Office data for the United Kingdom, and fitted this to a Fourier series as follows:

$$W = 10.44 + (-6.468 \cos(\pi/183J) - 3.492 \sin(\pi/183J) + 1.056 \cos(2\pi/183J) + 2.049 \sin(2\pi/183J) - .128 \cos(3\pi/183J) + .579 \sin(3\pi/183J))$$

This expression provides the mean precipitable water content in millimetres for bright sky conditions in the United Kingdom.

The solar path length, also known as the effective air mass is given by $m = \frac{1}{\text{Sin}h}$, however this gives pessimistic values if employed for solar altitudes of less than 10^{o}; and Rogers et al have fitted a Fourier series to the Smithsonian Meteorological Tables (1951) to give

$$M = \exp (3.67985 - 24.4465 \text{ Sin}h + 134.017 \text{ Sin}^2h - 742.81 \text{ Sin}^3h + 2263.36 \text{ SIN}^4h - 3804.89 \text{ SIN}^5h + 2661{\cdot}05 \text{ Sin}^6h) \quad 6.23$$

The values for "M" must be corrected to take into account the altitude of the site, and Rogers et al have established a correction factor Cm as follows

$$Cm = \exp\left(\frac{alt}{1000}\left(-0.1174 - {\cdot}0017x \frac{alt}{1000}\right)\right) \quad 6.24$$

Where 'Alt' is the altitude of the site above sea level in metres.

The level of aerosols in the atmosphere, or the atmosphere turbidity is a local effect dependent upon pollution, and is defined by the atmospheric turbidity coefficient as indicated by Unsworth (1975). This coefficient is used to give a correction factor to the value of solar beam radiation arrived at by consideration of precipitable water and air mass conditions alone. This factor is given by

$$Tf = \exp(-Ta^m) \quad 6.25$$

Where Ta is the atmospheric turbidity coefficient.

Rogers et al (1981) have combined these factors into a Fourier expansion of the form

Solar beam normal radiation

$$= \quad T_f \times c \times \quad I \exp\left[\sum_{i=o}^{3}\left(\sum_{j=o}^{2} b_{ij}\, W^j\right) m^i\right] \; W/m^2 \qquad 6.26$$

Where the constant b_{ij} are given by the following table

j \ i	0	1	2	3
0	-12.964_7	-6.4211	-.46883	0.0844097
1	$.41282_8$	-0.801046	·220414	.0191442
2	-1.1209_6	1.53069	-.429818	.0374176

and I is the extraterrestrial solar direct beam intensity.

The turbidity coefficient Ta is a variable dependent on location, Souster (1977) has investigated the range of this coefficient and recommends the following monthly values for days which exhibit the highest 5% of daily total solar irradiation at Kew.

	Ta
January	.3
February	.35
March	.30
April	.4
May	.34
June	.25
July	.33

August	.36
September	.34
October	.31
November	.25
December	.17

Souster also recommends the following for alternate sites.

a) Remote inland rural sites in England and Wales. - Kew data - 0.07

b) Rural sites in England and Wales. - Kew data - 0.03

c) Outer suburban sites. - Kew data

d) Inner suburb sites. - Kew data + .05

e) Inner city sites. - Kew data + 0.1.

From the foregoing, we are in a position to estimate the beam component of sunlight incident upon any surface from the relationship:

$$\text{incident energy} = \text{normal beam energy} \times \cos\theta \qquad 6.27$$

in the case of a horizontal surface this becomes:

$$\text{energy incident upon horizontal surface} = \text{normal beam energy} \times \sin h \qquad 6.28$$

The various Fourier expansions referred to above would be very difficult to manipulate manually, but present no problems for digital computation.

b. Diffuse Radiation

The diffuse radiation of a clear sky is a complex phenomenon whereby a general diffuse level is augmented by a rise in the proximity of the solar disk, as explained by Duffie & Beckman (1980).

Souster, Rogers and Page (1978) have investigated this, and suggest that an approximation to the actual distribution can be made by considering the distinct distributions, one isotropic distribution, and a component deriving from the sun. The suggested analysis is as follows:

General background isotropic diffuse irradiation on a horizontal surface.

$$= \quad cb_o - b_1 \quad \times \text{beam irradiation on a horizontal surface.}$$

Circumsolar diffuse irradiation normal to the beam radiation

$$= \quad c\,C_o - C_1 \quad \times \text{beam irradiation upon a horizontal surface.} \qquad 6.29$$

Where c is the solar constant

Where the regression constants b_o, b_1, C_o and C_1 are given by:

$$b_j = \sum_{i=o}^{7} b_{ji} (\text{Sin } h)^i \qquad 6.30$$

$$c_j = \sum_{i=o}^{7} c_{ji} (\sin h)^i \qquad 6.31$$

and the coefficient b_{ji} and c_{ji} are determined from the following table.

i	b_{oi}	b_{1i}	c_{oi}	c_{1i}
0	2	.272	1	.4524
1	331.965	.371162	536.917	1.54901
2	-658.223	-9.33202	-802.612	-12.2948
3	4356.27	45.8221	3836.53	36.6472
4	-15563.0	-108.407	-12557.0	-60.8460
5	26253.8	137.668	20257.8	59.7328
6	-20505.8	-89.6616	-15276.3	-32.3132
7	6037.43	23.4606	4358.42	7.3817

For vertical surfaces. The energy falling on a vertical surface which results from the general background isotropic irradiation is half that value expected on a horizontal surface. This relationship is explained in Appendix 3. With the circumsolar component, the diffuse value is given by the product:

$$G_{cn} = \text{Circumsolar normal diffuse value} \times \cos\theta \qquad 6.32$$

Souster et al found that a further correction was required for surfaces which presented an obtuse angle to the sun.

This correction is given as

$$\Delta G = 0.2\, G_{cn}(1 - \cos\alpha)\, \sin 2(\gamma - 45) \times 2\, S_{in}\, h \cos h \qquad 6.33$$

$$\text{For } 135^\circ > \gamma > 45 \text{ or } -45^\circ > \gamma > -135^\circ \qquad 6.34$$

Otherwise $G = 0$

The information of this section was programed using BASIC, and a listing of the program with annotation is indicated in Appendix 4.4.

A comparison of the output of the program written by the author and that developed by Page and his associates at Sheffield University is given in Figure 6.5. The comparison indicates that the program gives very similar results to the Sheffield program Sun 3.

6.3.2. Overcast Sky Conditions.

The overcast sky results in diffuse light only, and the distribution of this over the sky vault is not isotropic, but reaches a maximum directly above the observer. It is possible to relate the energy falling upon a vertical surface from such a sky distribution to that falling upon a horizontal surface. This relationship is explained in Appendix 3.

Thus if it is possible to establish the energy expected to fall upon a horizontal surface from an overcast sky, it is also possible to relate this to the wall module.

Rogers et al (1979) in their research at Sheffield University have found that the solar radiation falling upon a horizontal surface in the United Kingdom can be related to the solar altitude as follows:

$$G_h = 2 + K \, \mathrm{Sin}(h) \ \mathrm{W/m^2} \qquad 6.35$$

The analysis of Rogers indicates that the variation of the factor 'K' over the year, and from place to place in the United Kingdom is less than might be expected, and this appears to be due to the seasonal and latitudinal compensation offered by the Sin(h)term. For Kew Rogers offers the following seasonal values for K, for average overcast days i.e. days upon which no beam component of radiation was observed.

Spring,	Summer,	Autumn,	Winter
230	170	260	218

Thus the solar radiation absorbed by the module absorber is given by

$$Gabs = Cor \times \bar{\tau}n \times Gh \qquad 6.36$$

Where Cor = The vertical -horizontal correction factor taking into account the self shading of the module as described in Appendix 3.

τn = The normal transmission coefficient of the module glazing system as indicated in Appendix 3.

These factors and the corresponding factors relating to the 10% worst overcast days were incorporated into Appendix 4.4. as subroutines AVCST and AVCST 10.

6.3.3. Air Temperature

As discussed in Section 6.3. the air temperature determines the rate of heat loss from the module, and hence the potential solar contribution. Each area of the country has an associated average temperature for a particular time of year, and such values can be found in Meteorological Office memorandum. However this information is very general, and ideally we would wish to know how the local air temperature varies with the type of radiation day, i.e. whether bright clear sky or overcast, and how the air temperature may be expected to vary over the day.

The CIBS Guide No A2 (1982) offers some information by providing banded temperature data, and associated solar data. The guide also offers a means of computing diurnal variations based upon a trigonometrical function. However, this data results in a tedious manual calculation, and ideally computer generated information would be preferable if this could be run as a subroutine of the solar data program referred to in the earlier sections of this program.

Fortunately, Page et al (1978) have produced an analysis of Meteorological Office data which suits this need admirably. Page has reduced the data to a series of Fourier expansions which describe the temperature in terms of the day type, latitude, air temperature mean monthly daily sunshine hours, the wind speed, and month number. Page also introduces a further month dependent relationship. In the following description the symbols used are:

lat	=	latitude
long	=	longitude
$\bar{t}$	=	monthly mean air temperature ^{o}C
n	=	monthly mean daily hours of sunshine
u	=	monthly mean wind speed. m/s
N	=	month number, 1 - 12 from January

FN = $4.62-2.3(MN) + 0.43(MN)^2 - 0.0267(MN)^3$ 6.37

MN = 1-6 for January to June and 6-1 for July to December.

alt = Altitude, metres above sea level.

The relationships established by Page are in Fourier form as follows.

$$t = a_f + a_1 \cos(W(T - \phi_1)) + a_2 \cos(2W(T - \phi_2)) \ ^\circ C \quad 6.38$$

Where a_f is the fundamental term

a_1 is the first harmonic

a_2 is the second harmonic

$W = \pi/12$

T = Local apparent time

ϕ_1 = First harmonic phase lag

ϕ_2 = Second harmonic phase lag

For bright sunny days, the above factors are given by

a_f = For Jan.Feb. Mar. Apr; $-3.63 + 2.01\bar{t} - .056\bar{t}^{-2} - .165$ long

= For May, June, July, Aug; $6.14 + .36\bar{t} + .025\bar{t}^{-2} - .347u$

= For Sep. Oct. Nov. Dec ; $-3.73 + 1.67\bar{t} - .023\bar{t}^{-2} - .165$ long 6.39

a_1 = For Jan. Feb. Mar. Apri ; $-0.49 + 4.32\ n/u + .003$ alt

= For May, June, July, Aug; $1 + n(1.61 - .28u + .042(\text{long} - 50))$

= For Sept. Oct. Nov. Dec ; $(2.79 + .006\text{alt})\ n/u$ 6.40

a_2 = For Jan. Feb. Mar. Apr; $-(.22 + (.455 - .074 \times a_1)a_1)$

= For May, June, July, Aug; $-(4.09 + 0.0013\ \text{alt} - 1.3N + .1N^2)$

= For Sept. Oct. Nov. Dec.; $-(.38 + (.404 - .050a_1)a_1)$ 6.41

ϕ_1 = $13 + .7a_1(FN)$

ϕ_2 = $0.5\ \phi_1$

u = wind speed m/s

For Average Days

$$a_f = \bar{t} \quad ^oC \qquad 6.42$$

a_1 = For Jan, Feb, Mar, Apr; $2.73\ n/U$

For May, June, July, Aug; $1+ n\ (0.85-0.125U)$

For Sep. Oct. Nov. Dec ; $2.73\ n/U - 0.488\ (n/U)^2$

6.43

a_2 = For Jan. Feb. Mar. Apr; $-(.1+(.4 -.1\ a_1)\ a_1)$

For May, Jun. July, Aug; 0

For Sep. Oct. Nov. Dec ; $-(.1+ (.43- .082\ a_1)\ a_1)$

6.44

$$\phi_1 = 13.0 + a_1\ (FN) \qquad 6.45$$

$$\phi_2 = 0.5\ \phi_1 \qquad 6.46$$

For Overcast Days

a_f = For Dec. Jan. Feb. Mar. Apr. May

If $\bar{t} > 2, .68\bar{t} + 1.5 + .2\ long + N/15$

otherwise $2.86 + .2\ long + N/15$ 6.47

For June, July, Aug. Sept. Oct. Nov.

$0.85\ \bar{t} + .9 + N/10$ 6.48

$$a_1 = 0.5 + .16n - .1\ (.9+ 1.4\ SIN\ \pi N/12\ )(U-3.7)+ .0013\ alt \qquad 6.49$$

$$a_2 = 0$$

$$\phi_1 = 15.6 -.1\ (U-4) - .1\ (N-1)\ hours \qquad 6.50$$

Given that the necessary input information is available, the above expressions allow the development of a simple computer program to establish the probable temperature profile of a day for each month of the year for each of the three day-types mentioned.

The inclusion of the monthly mean wind speed in the above presents something of a problem due to the variability of this value with local effects. For this reason, an annual wind speed of $6ms^{-1}$ derived from the CIBS guide number A2 as being that which will be exceeded for 25% of the time in most of central England. This basic figure is then subjected to the following factors.

$$U = 6 \times K \times Z^{a} \qquad 6.51$$

Where Z = height above ground, assumed to be 10m.

K and a are given as follows dependent upon the type of Terrain.

TERRAIN	K	a
Open flat country	.68	.17
Country with wind breaks	.52	.20
URBAN	.35	.25
CITY	.21	.33

These terrain features can be conveniently aligned with those described for the turbidity coefficient given in Section 6.3.1.

The above information is incorporated into Appendix 4.4. as a subroutine.

6.3.4. Average Solar Conditions.

a) Work of other authors.

The previous sections concerning bright clear days, and cloudy days represent the two extremes of day type. In reality, the monthly distribution of day types will include some clear days, some overcast, and a proportion of partially cloudy days. The manner in which to establish an average condition is not clear.

Liu and Jordan (1960) originally observed the importance of what they then described as a cloudiness index, and which has latterly been termed a clearness index, as the ratio of the average daily insolation upon a horizontal surface to that of the extraterrestrial irradiation at the same place, i.e.

$$\bar{K}_T = \bar{H}/H_o \qquad 6.52$$

Where $\bar{K}_T$ = clearness index,

$\bar{H}$ = insolation upon the surface

$\bar{H}_o$ = extraterrestrial radiation

In the above, a bar above the character indicates monthly mean values, daily values are represented without a bar, and hourly values employ lower case characters.

The values of '$\bar{H}$' are necessarily recorded data, and the values of $\bar{H}_o$ are calculated.

Liu and Jordan found that the cumulative distribution of days with a fraction less than K_T showed considerable similarity for locations with the same value of monthly clearness index $\bar{K}_T$, and the hourly distribution K_T, had been found to be very similar to the daily values, K_T, by Whillier (1953). A synopsis of this data can be found in Duffie & Beckman (1980).

These observations have led to various further correlations, Orgill and Hollands (1977) have established correlations based upon Canadian data, relating the ratio of diffuse to global irradiation to the clearness index; Bugler (1977) has in a similar manner related the ratio of global irradiation to diffuse irradiation with the ratio of global irradiation to that for a clear sky. This latter is itself related to the extraterrestrial radiation, and so the 'x' ordinate of Buglers correlation has an affinity with K_T. A similar type of correlation has been developed by Stauter and Klien (1979) for North American locations. Unfortunately the various data from these and other authors do not correlate well, and similar correlations for monthly mean values show considerable variation between authors as shown by Duffie and Beckman (1980).

Hollands and Huget (1983) present a useful discussion of this method of analysis, including the work of Bendt et al (1981). Hollands also presents refined estimates of the probability density function of the Lui and Jordan plots, and it may well be that this approach will be of value in the future when proven. However further investigation of the hourly diffuse values is required.

Page (1978) develops an analysis based upon regression equations of the type

$$\bar{H} = \bar{H}o \quad (a + b \frac{\bar{n}}{n_o} \quad) \qquad 6.53$$

Where $\bar{n}$ = number of hours bright sunshine

n_o = number of hours daylight

a and b = are constants dependent upon climate

Page further develops this to establish the relationship between diffuse and global horizontal values as follows:

$$\frac{\bar{Hd}}{H} = c + d\frac{\bar{H}}{Ho} \qquad 6.54$$

Where $\bar{Hd}$ = diffuse fraction of radiation

Ho = extraterrestrial radiation

c and d = constants, dependent upon climate

The problem with this approach is the lack of information concerning the required climatic constants, Page refines his equations further by adopting a means of assessing the ideal number of bright sunshine hours by assuming a standard clear atmosphere and calculating the maximum possible hours of bright sunlight which would then burn the recording card of a sunshine recorder. This results in an effective sunshine day length which Page employs to calculate the resulting modified sunshine fraction. This value is then employed to calculate "pseudo turbidity" values, which in turn are employed to calculate values of total direct irradiation.

This process is cumbersome and requires considerable computer time, and the use of correction factors which are not yet available. Page goes further to assume that the proportion of time represented by (1 - effective sunshine fraction) is comprised totally of overcast conditions. This results in the assumption that all days are either totally overcast, or bright and clear. This cannot be correct as many days are in fact partially cloudy.

b) Present Approach, Average Solar Conditions.

Having considered the approaches made by other authors, the author did not feel justified in adopting any of the methods presently available for the estimation of average conditions, and decided to resort to first principles in an attempt to develop a method for this analysis.

If consideration is restricted to the United Kingdom, there is a source of data which provides the basis for any solar energy considerations;

that is, the Meteorological Office (1980) data for daily global solar radiation. This data is published in chart form, and an example is given in Figure 6.6. and gives average insolation month by month. Thus the value for any location in the U.K. can be determined.

Similarly, the average number of bright sunshine hours is known for the United Kingdom and available in chart form in Meteorological Office publication (1974). As pointed out by Page (1979) these values are slightly conservative as they do not accommodate that period of bright sunshine falling below the threshold value of a sunshine recorder, or 200 watts/m^2 approximately.

The radiation intensity for sunny conditions can be readily determined as discussed previously, and in any given month, the proprotion of bright sunny days or periods can be established from Meteorological Office data. This allows an approximation of the mean monthly contribution from bright sky conditions to be made.

The solar radiation on overcast days can also be established fairly easily, but the proportion of overcast days is less easy to define. Barratt (1976) presents frequency distributions for a series of locations in the United Kingdom which suggest that the variation in cloudiness over large areas of the country may be very similar. This is confirmed by scanning the Meteorological data for total cloud cover given in Meteorological Office (1980). This data is shown in Figure 6.7. plotted for five locations in the north of England, and Kew.

The figure indicates that the mean proportion of overcast days per month is relatively constant over the country. The data does indicate a clearer coastal situation, but this has not been isolated. The mean value of the shaded area shown in Figure 6.7. has been adopted as a typical figure for the proportion of overcast days per month in this investigation.

With proportions established for the number of clear days, and overcast days, it follows that the proportion remaining must be that appropriate to partially cloudy days. In fact this is not the case, and some of the clear day proportion will infact be due to a partial cloud contribution, however there is no simple way in which to account for this.

The nature of the sky vault diffuse radiation distribution is not clear, some work has been conducted in this area, and is summarised by Page (1977), the following conclusions can be drawn.

1) The presence of broken cloud increases the sky vault radiation generally, and the diffuse radiation from such a sky is greater than that associated with over cast or clear sky conditions.

2) The intensity of sunlight increases towards the suns position in the sky.

The actual intensity of radiation is still in some doubt, and is assumed to be dependent upon cloud type. Louden (1965) indicates that the energy falling upon vertical surfaces under a partially cloudy sky is relatively insensitive to the amount of cloud, and further suggests that this energy can be considered as some multiple of that diffuse radiation which would have been available under bright sky conditions. Page (1977) suggests that this multiplication factor is 3. The author decided to check this from Meteorological Office data and the computed values of solar radiation as follows:

$$C_L = \left\{ \bar{H} - P_B - \bar{H}_B - P_{oc} \times \bar{H}_{oc} \right\} \Big/ \bar{H}_{BD} \quad (1 - P_B - P_{oc}) \qquad 6.55$$

Where C_L = multiplying factor of diffuse irradiation on clear days to give the partially cloudy value.

$\bar{H}$ = Global irradiation on a horizontal surface from Meteorological data.

$\bar{H}_B$ = Daily average total calculated global irradiation on a horizontal surface.

$\bar{H}_{oc}$ = Daily average calculated global irradiation for an overcast sky.

P_B = Proportion of clear days.

P_{oc} = Proportion of overcast day.

H_{BD} = The daily average diffuse irradiation for a clear day.

This multiplying factor, C_L, was computed for each month, and the results are indicated in Table 6.1. The values vary month by month from a minimum of 1.6 to a maximum of 2.8, and there appears to be a distinct demarcation between winter with its lower values, and spring/summer with higher values.

These multiplying factors were employed to calculate the corresponding thermal behaviour of the module for partially cloudy days. This was done by applying C_L to the diffuse component of radiation calculated as described in Chapter 6.3.1.

The analysis used by the author to establish average insolation conditions is admittedly less sophisticated than that employed by Page, or that based upon a probability function for the clearness index advocated by the other authors mentioned previously. However, the approach adopted does have the advantage of being based upon the measured average data for the United Kingdom, and ensures that the measured mean monthly energy falling upon a horizontal surface is not exceeded by the analysis. The relationship of the horizontal value, to that appropriate to a vertical surface is the same as that adopted by Page for bright sky and overcast sky conditions. The assumed multiplying factor for partially cloudy skies may or may not be valid, the author merely invokes it as a device to account for the remaining energy falling upon a horizontal surface after the known beam radiation and diffuse irradiation from overcast skies have been accounted for.

It should be noted that the EEC have established a program for developing a model to predict the inclined surface radiation for the EEC area, as described by Page (1981). This work is now completed, but not yet published, and its recommendations will be of considerable value in confirming the author's approach, or otherwise.

The results of the computations described, are discussed in the next chapter.

7. Results of Computer Modelling.

7.1. Seasonal Variation in Performance.

a) Bright Sunny Conditions.

When the computations described in the previous chapter are performed for the fifteenth day of each month, for various orientations of wall, the results can be summarised as shown in Figure 7.1. This figure shows a distinct drop of performance in the summer months for a south facing wall in bright sunlight. Page (1977) indicates a flattening of the summer south facing curve, but no reduction from the Spring and Autumn values for a vertical surface. The reason for the accentuated fall in the case of the module is due to the increased specular reflectance of the glazing at high solar elevations, and the self shading of the module as indicated in Appendix 4. This same reduction does not occur in west and east orientations due to the absorbed radiation in the morning or afternoon being the result of varying angles of incidence upon the module.

This effect of a self compensating summer reduction in performance may be of value in reducing summer excesses.

As can be seen, the maximum average bright sky thermal contribution which the module could be expected to deliver is slightly in excess of 1 kwh/m^2 per day. This occurring in the Spring and Autumn for a south facing wall and in mid summer in the case of East and West facing walls, for bright sunny days. It is also apparent that the module is capable of providing a contribution throughout the year on bright sunny days when facing south. East and West orientations result in a net sunny day loss from mid November to the end of January, whilst North facing orienta-

tions produce a net loss from the end of October to the middle of March.

b) Overcast Days.

By the nature of the model explained in Chapter 6, the thermal contribution of the module is independent of orientation in overcast conditions as the maximum mid summer contribution on such days is found to be approximately 300 Wh/m^2 day, although the maximum winter loss is reduced slightly in comparison to a north facing wall in bright sky conditions. This is due to the greater air temperature experienced with ample cloud cover.

c) Average Conditions.

Where the average condition performance is computed as indicated in Chapter 6, the results can be summarised as indicated in Figure 7.2. and shown in Table 7.1. The figure shows a general reduction in performance as compared to bright sky conditions, but, conversely, an increase in performance compared to overcast sky conditions. The flattening of the south facing curve is less pronounced than in the case of bright sky conditions, but it is significant that a southerly orientation still retains a net contribution over the year. The module with an east or west orientation retains its general form as for bright sunny days but with a drop in maximum performance to less than 1 Kwh/m^2 day in mid summer. Northerly aspects show an increase in contribution compared to bright clear conditions due to the increased diffuse radiation from sunlight reflected from broken clouds.

For purposes of comparison, the equivalent performance of a standard wall with the same 'U' value of the unilluminated module was calculated and is indicated in Figure 7.3. and

Table 7.2. The comparison of contribution available is quite clearly shown. This shows distinct advantages in total energy available, and in the reduction of heating season effectively to zero for a south wall and three to four months for other orientations. The standard wall indicated approximately eight months of net heat loss for all orientations and a negligible capability for contribution.

7.2. Summer Excesses, and Control

The forgoing sections indicate the potential of the wall module in comparison to a wall of conventional construction. The extra energy available is only of value if it can be used, and it is not normally required for space heating purposes during the summer months. This naturally indicates a need for some sort of control of the excess energy, which may take one or more of the following.

1) The controlled ventilation of the building.

2) The shading of the building to avoid summer insolation.

3) The utilisation of the excess energy via a heat pump for hot water services and/or process heating or similar application.

4) The storing of excess energy for interseasonal heating purposes.

5) The utilisation of some form of control system within the module to limit the absorption of solar radiation.

6) The utilisation of some form of control system to increase the out loss coefficient of the module.

These methods may all be applied in various ways, however the first four methods namely ventilation, shading heat upgrading and heat storage involve factors which are beyond the present scope of this project, and which depend upon the conditions of

a particular building. For example the ventilation of the building is dependent upon height, prevailing wind, type of construction, vent/wall ratios and usage. The use of complementary shading, possibly by seasonal foliage as described by Lebans (1980) or the use of architectural features is dependent upon the location of the building, and local topographical features. Seasonal storage is a complex subject, and although the possibility of rockstorage or latent heat storage as described by J.K.R. Page (1981(2)) cannot be ruled out, there are many inter relationships between the size and type of building and the requirement of the storage system. Similarly, the viability of upgrading the excess energy using a heat pump, is dependent upon the excess energy available, the required heat flow, and the cost of the heat pump itself. It should be noted that in this latter case, the expenditure upon the heat pump system must be justified by the savings in energy use as the system must merely augment a conventional system. As indicated in Chapter 2.5. the economics of a system which is dependent only upon displaced fuel costs may be questionable, but there is the possibility of also using the heat pump with heat exchangers to the atmosphere or some other heat source for the purposes of energy input in the absence of a solar contribution.

These variables require considerable analysis for each application and the author is of the view that any attempt in this project to establish the relative efficacy of application of such measures would be presumptuous given the timescale involved.

Despite this difficulty in defining the best combination of measures to accommodate summer excesses, the author considers that an effective control of module performance may well be necessary where other measures are inapplicable for some reason, and also provide a further degree of flexibility when other measures can be used.

Of the two methods of control of the module namely control of the solar input, or control of the thermal resistance of the module, the control of solar input is the more attractive for initial consideration. This is because the potential control over solar input is such as to reduce it to zero, whilst the control of the outloss coefficient is much less capable of being adjusted. In other words, the dominant effect which causes excessive summer heat gains is the solar input, not the rate of heat loss from the module.

Control of the solar input can be visualised as being activated either by some external agency, or as an automatic response of the module itself. The use of an external activation implies either something associated with the structure of the building itself, or something within the module which is activated by some mechanical penetration of the module shell, or some electrical device within the module. Shurcliff (1980) presents a comprehensive survey of the role of shutters and shades, many of which could be employed. The possible use of external shutters presents some concern for safety in high winds, but the use of internal shuttering or shading devices which are activated from the interior of the building warrants further attention.

Automatic self contained control of the module has obvious attractions in terms of simplicity of installation and operation. There appear to be two potential ways in which such an actuation could be brought about, namely by using the intensity of solar radiation, or by using the temperature of the module; as a control actuator these being the two operational variables. In these terms, the intensity of solar radiation, possibly using a photochromic effect may well be worth further investigation, but it may well be that a photochromic film would prevent absorption of energy, at the very time when it was required, and that different orientations of wall would require different photochromic materials. Such materials although in common use for other purposes, i.e. sunglasses, are still expensive and not yet commercially available in polymer film form.

The potential use of the module operating temperature as a control is readily visualised in the form of a simple lattice type blind actuated by a wax pellet, or ninotol wire. This presents some problems when visualising its use for extended periods of time, and ideally, a thermochromic effect using a polymer film would be preferable if such a material exists.

Chahroudi (1978) reported the development of a material known as "Cloud Gel" by Sunteck Research Associates in California. This material was claimed to provide an efficient thermochromic effect in sheet form, and achieved this by changing from being transparent to milk white over a temperature range of $3^{o}C$. The solar transmittance in the transparent phase was reported as .95, and 0.2 in the milky phase. This material would have obvious potential use in the module, and the author decided to analyse its effect upon module performance. Attempts to contact the manufacturers of this material have been unsuccessful and the author was fortunate in that the material was exhaustively examined in the "Energy Efficient Window Programme" of the United States Government Department of Energy. The report of these investigations given in Berkeley (1977) confirms the statements of the manufacturers, and further reports that a 50,000 cycle test of the material showed no degradation of properties. Interestingly, the material was not recommended for use on the basis of its optical qualities which were considered inappropriate for window glazing purposes. This is not a constraint for potential application in the solar wall module.

The author included a variable transmittance in the module performance program given in Appendix 4.4. to examine the effect of such a control screen on the problem of summer excess. The precise nature of cloud gel is not known, and no analysis of its thermal infra-red properties appears to be available; as a result, it is not possible to decide upon the best position for it in the array of screens, ideally it should be close to the absorber,

but this would be inadvisable if the emittance is high, as indicated by the comment in Chapter 5.8. To accommodate this the author modelled the effect of the control screen by assuming that it would be such as to operate over a 3°C variation of the outer surface of the module storage slab. This temperature varies less than that of the absorber and is thus approximated by the variation of the screens. Time constraints prevent the investigation of the effect of the control film in each possible screen position.

The bright, overcast and average sky conditions were computed for thermochromic screen activation temperatures of 2°C above room temperature, room temperature and 2°C below room temperature. The results of these calculations are given in Tables 7.3., 7.4. and 7.5, and Figures 7.4. and 7.5. It is clear that the curves for each sky condition retain their essential character, but are reduced in amplitude as the thermochromic screen set point is reduced. This indicates a considerable degree of flexibility in the amount of energy which the module, and hence the building can be designed to achieve. For example it may be to the designers advantage to delete a thermochromic screen for north facing walls, whilst incorporating a low set point screen for east and west or south facing walls.

The results of these calculations can be employed to give an approximate characteristic for the performance of the module in terms of thermochromic screen set point and orientation. Figure 7.6. shows the calculated average annual contribution in Kw hours for South, East and North facing modules dependent upon the thermochromic screen set point, and asymptotic to the values appropriate to the module without a thermochromic screen, and a standard wall. This figure may thus be utilised to provide an indication of module performance in any mode of operation. In practice, the author believes that a maximum screen set point of 2°C above room temperature would be appropriate to reduce temperature excursions unless some steps

were taken to deliberately remove heat from the building, in this case the maximum annual contribution of South, East and North facing modules can be seen to be 100 Kwh, 70 Kwh and 40 Kwh/m^2 respectively.

8. Economic Considerations.

8.1. Potential Value of the Module.

The potential value of the wall module can be considered as comprising two elements. The first of these elements is that of the energy which the module will save over a period of time. As previously indicated in Chapter 2.5. this potential saving is dependent upon the nature of the energy source which is assumed to be displaced, whether electricity, gas, oil or other. Furthermore, the assumed value will be dependent upon the orientation of the module, and its level of operation. If for example it is desired to maintain a reasonable summer equilibrium by operating with a low cut off temperature, then the potential energy to be collected is much reduced as the summer peak is not available.

The second element of value, is that associated with architectural and other features which the module displaces. There are two such features which are apparent; as indicated in Chapter 2.7. the module displaces the wall which would otherwise be required, and the central heating system which can be dispensed with.

As the potential fuel savings can be expected to be relatively small, it follows that the savings due to displacement should be significant. If these displacement savings alone can equate to the cost of the module, then any energy savings can be considered as pure profit from the use of the module, which will then demonstrate a negligible pay back period.

To establish a guide to these values, Spons Architects and Builders Price Guide (1983) provides some interesting information as follows:

1) The cost per m^2 of wall constructed of facing brick, and light weight concrete blocks with 13mm of plaster is approximately £40, including labour.

2) The cost of a central heating installation is estimated as £27.7 per m^2 of floor area.

Assuming a square office floor of 1000 m^2 with 3 metre high ceiling the total wall area is $\sqrt{(1000)} \times 3 \times 4$ m^2 or 380 m^2 assuming that the wall is 50% glazed, this results in a module wall area of 190 m^2. This area of module displaces a central heating cost of approximately £27.7 x 1000 which results in a displaced saving by the module of $\frac{£27,000}{190} = £145/m^2$

This figure will vary with the size and aspect ratio of the building floor in question.

The combined displaced savings of the module appear to provide a figure in the region of £180 per square metre of wall, and if the module can be produced and installed for less than this figure it can at least be considered as being cost effective in providing future energy needs for the building. Against this must be set the need to employ electricity as a heat source for central heating purposes.

8.2. Module Production Costs.

The actual cost of producing the solar wall module is impossible to quantify with precision. The cost will naturally be dependent to some extent upon the detailed design of the product, which in turn is dependent upon the results of further research and development. It is possible to achieve an indication of the probable overall costs by first establishing the cost of raw materials, and then estimating labour costs and installation costs.

On that basis, the cost of materials can be summarised as follows, for a 1 m^2 module.

	£	
Glass	5	
Precast box	20	(Ivimy 1983)
4 aluminium frames	12	(Walker 1983)
Maxorb	6	
Terminals	1	
Polythene	1	
Howson screens	2	
Cost of cloud gel	15	
Cost of ancillaries	2	
	62	

The cost of cloud gel is again difficult to quantify, the estimate of £15 is based upon the 1977 estimate by Berkely Laboratories.

The cost of assembly of the module is more difficult to quantify, but in the authors experience of assembling experimental equipment, the proposed module could be assembled on a production basis in two man hours. If a cost of £10/man hour is assumed, to cover overheads also, the assembly cost assuming simple hand tools is approximately £20.

To this figure must be added an estimate of installation cost. This again is very difficult to quantify but the module would be much less time consuming to install than an equivalent double skin wall, which is estimated by Spon (1983) to cost £20 in labour using this same figure as a conservative estimate of installation cost, the resultant sum total is:

Estimated installed cost of module

$£102/m^2$

If an alternative of twice the materials cost is used, the estimated module cost is then $£124/m^2$. To this must be added the cost of transport, which is largely dependent upon the relative locations

of the building site and production site, and would require evaluation on that basis.

A further saving of the module relates to its reduced weight in comparison to the conventional double skin wall, and consequent reduction in building strength requirements. The author proposes to neglect this element of cost saving as a counterbalance to the uncertainties in the above costing estimates.

The costing indicated above is not exhaustive, and cannot be so at the present stage of development of the module. There is a strong indication that the installed cost of the module may be no greater than that of the conventional equivalent practise, and may well be somewhat less.

If the cost of the module can be shown to be equal to or less than that of the conventional equivalent then any energy gains produced by the module are truly free. In the authors view, there is sufficient indication of this possibility to warrant further development as indicated in Chapter 9 to result in a detailed design for the module to allow a thorough costing exercise.

9. Further Work.

The present project has demonstrated the thermodynamic feasibility, and economic potentialities of the proposed solar wall module. Much work is still required before the module can be considered for widespread use. Important aspects are as follows.

1) Market potential.

The potential market for the module and possible user interest requires assessment. In the authors view, this should be accomplished before any further development is undertaken. With increased interest in passive design of buildings, the module could prove to be an important feature of construction.

2) Control membrane.

The control membrane discussed in Chapter 7.3. is of prime importance if the module is to provide a flexible application in varying orientations, building types and required behaviour. Although the membrane has been described and thoroughly tested, it has not been possible to identify any manufacturer. The potential production of this material, and its association with other materials requires investigation. However it is not the only possible method of control.

3) Infra red reflecting screens.

The material supplied by Dr. Howson, and described in Chapter 3 is produced only in small quantities at the present time. It is necessary for material of this type to be readily available at an appropriate cost.

4) The nature of an effective system for supplying electrical power to the "Maxorb" absorber requires detailed consideration.

5) The restriction of condensation within the module requires consideration.

6) The life of the module requires to be assessed, especially in respect of the degradation of the plastic materials employed in the screens. Although the mechanical requirements of the screens are slight, the optical properties of component materials over extended periods of time requires investigation.

7) The detailed design of the module as a building component for various construction methods and the best modular sizing system requires to be established.

8) It seems probable that if the preceding points can be satisfactorily resolved, then a trial building will be required to demonstrate the behaviour and installation of the module on a practical basis, the funding and design of such a building must be determined.

10. Conclusions.

1. The economic viability of solar energy collection for direct space and water heating in the United Kingdom is questionable when based upon the present costs of conventional energy sources where such sources are available. This is because the cost of erecting a structure of sufficient surface area, allied with necessary costs of installation storage and control, render too great an initial cost for reasonable rates of energy return. In the authors view, this is a major impediment to the future use of solar energy, and hence the future sales of "Maxorb" in flat plate collectors.

2. It is possible to design a system of construction which will allow the passage of solar energy into a building, whilst providing a satisfactory degree of thermal insulation to prevent heat loss from the building. Such a construction requires the judicious use of spectrally selective reflecting and transmitting surfaces in an array of screens. The positioning and spacing of the screens is critical in reducing radiative and convective heat loss through the system. Such a construction allows the use of large flat surface areas which are ideally suited to the application of "Maxorb". The system operates at or near ambient temperature, allowing high thermal efficiencies and the use of relatively inexpensive thermoplastic screen materials.

   The thermal characteristics of such a system can be determined by experiment and successfully simulated by computer program.

3. The use of a wall construction of this type, naturally offsets the excessively high summer heat gains due to reflection from its vertical outer glazing at high solar altitudes. Further reductions can be achieved by the incorporation into the screen array of a thermochromic screen which turns from translucent to opaque at a particular set temperature. Such a construction will allow a maximum average energy contribution of approximately 160 Kwh/m^2 per

annum for a south facing wall in the U.K., varying to a net loss, dependent upon the set point temperature of the thermochromic screen, and the orientation. These conclusions are based upon the work of other workers in the field, and solar weather data published by the U.K. Meteorological Office.

This type of construction therefore offers considerable thermal flexibility to the architect. In addition, the change of aspect of the module from dark to light as the thermochromic screen operates may also offer aesthetic opportunities in design.

4. This method of construction allows two elements of cost to be discounted in comparison to conventional construction. The first is the cost of the otherwise necessary wall, and the second is the cost of the otherwise necessary central heating system. This latter can be replaced by the solar wall module due to the presence of the "Maxorb" absorber which, being of nickel foil, can be employed as a heating element in its own right.

   On that basis, the cost of systems displaced by using the solar wall module is approximately £180 per m^2 for conventional commercial buildings.

5. The cost of producing and installing the solar wall module is estimated at approximately £100 - £125 /m^2 for a reasonable number of units in the region of 100. Substantial savings upon this estimate may be expected if high rates of production can be achieved.

6. It appears that the solar wall module can offer a cheaper method of construction than conventional practice if used in a non load bearing situation. In that case, any energy gains are an immediate economic gain, and as a result the solar wall module does not suffer from the disadvantageous economics of other solar energy collecting systems which may employ "Maxorb", i.e. flat plate collectors for active domestic hot water systems.

TABLES

Hemispherical radiative properties of selective absorbing surfaces of various types.

From Koltun (1981).

Radiative Properties of spectrally selective reflecting surfaces.

From Lampert (1981).

Material	Thickness mm	Solar Spectrum		Thermal (20°C)		
		Extinctn. Coefficient	Reflective Index	τ	α	ϵ
Glass	5	10	1.526	0	.1	.9
Polythene	$30*10^{-6}$	300	1.51	.869	.067	.064
Polypropylene	$30*10^{-6}$	300	1.51	.84	.067	.091
InO_2 (Howson)	———	———	———	.011	.184 .743	.805 .246
Metallised Polyester	$12*10^{-6}$	———	———	0	.525 .969	.475 .031
Melinex	$75*10^{-6}$	240	1.62	.261	.074	.665
Tedlar	$100*10^{-6}$	280	1.684	.25	.05	.7
"Maxorb"	$13*10^{-6}$	———	———	0	.92	.08

Table 3.3.

Radiative coefficients used in the computation of module performance and experimental analysis.

MONTH	J	F	M	A	M	J	J	A	S	O	N	D
Total energy on horizontal surface. Met. Office Whrs/Day	555	1097	2083	3402	4444	5138	4444	3888	2708	1527	763	444
Bright sunshine hours. Met. Office	1.25	2.25	3.25	4.75	5.5	6.25	5	4.75	3.5	2.75	1.5	1
Proportion of bright sunshine daily	.161	.234	.281	.345	.352	.374	.3	.323	.264	.261	.177	.137
Proportion of overcast days	.44	.41	.35	.3	.25	.22	.22	.25	.26	.33	.38	.43
Calculated bright sunshine W hrs.	743	1582	3147	4683	6111	6734	6475	5440	4349	2238	1103	698
Calculated overcast sunshine W hrs.	323	590	722	1075	1363	2300	2217	1865	1341	760	415	267
Proportionate bright sunshine W hrs.	120	370	884	1615	2151	2518	1942	1757	1148	584	195	95
Proportionate overcast sunshine W hrs.	142	241	252	322	340	553	427	432	348	250	157	114
Remaining unaccounted energy Whrs.	293	468	947	1465	1953	2067	2075	1699	1212	693	411	235
Value of diffuse irradiation on bright days Whrs	454	803	1108	1692	1926	1844	2037	1831	1505	935	534	326
Proportion of partially cloudy days.	.399	.356	.369	.355	.398	.406	.48	.427	.476	.409	.443	433
Bright sky diffuse multiplier for partial cloud	1.61	1.63	2.31	2.43	2.54	2.8	2.18	2.12	1.69	1.8	1.73	1.63

Table 6.1.

Evaluation of partially cloudy sky diffuse multiplier from observed and calculated data for a horizontal surface./m^2

Month		J	F	M	A	M	J	J	A	S	O	N	D
Bright Sky Conditions	S	487	818	1098	863	738	701	697	826	1006	1085	823	701
	E	-113	41	366	648	961	1195	1045	876	676	263	0	-108
	N	-161	-95	-2	106	209	296	266	230	155	31	-91	-169
	PR	.161	.234	.281	.345	.352	.374	.3	.323	.264	.261	.177	.137
Over-cast	ALL	-147	-102	-62	9.5	76	235	241	210	119	10	-82	-137
	PR	.44	.41	.35	.3	.25	.22	.22	.25	.26	.33	.38	.43
Partially Cloudy	S	188	340	609	769	832	938	755	738	539	493	292	116
	E	-58	75	412	780	1021	1184	954	839	517	261	40	-70
	N	-87	0	228	448	647	829	629	526	309	152	0	-89
	PR	.399	.356	.369	.355	.398	.406	.48	.427	.476	.409	.443	.433
Average Condition	S	89	270	510	573	609	695	624	633	553	487	243	65
	E	-105	-5	258	504	759	979	824	692	455	178	-13	-102
	N	-124	-64	87	199	350	499	434	350	219	73	-47	-118

Table 7.1. PR = Proportion

Evaluation of average sky contribution from bright sky, overcast sky and partially cloudy sky conditions for a module without a thermochromic screen. Whr/m^2 day

Month		J	F	M	A	M	J	J	A	S	O	N	D
Bright Sky Conditions	S	-173	- 127	- 55	- 22	14	57	70	70	48	- 5	- 98	-156
	E	- 207	- 176	- 114	- 59	2	64	68	46	6	- 61	-146	- 202
	N	-215	-193	- 150	- 105	- 56	- 2	8	- 6	- 39	- 87	-159	- 212
	PR	.161	.234	.281	.345	.352	.374	.3	.323	.264	.261	.177	.137
Over cast	ALL	-183	-170	- 147	- 118	- 86	- 43	- 6	- 14	- 41	- 78	- 128	- 166
	PR	.44	.41	.35	.3	.25	.22	.22	.25	.26	.33	.38	.43
Partially Cloudy	S	-176	- 131	- 73	- 23	+13	54	42	53	3	- 38	-105	- 153
	E	-176	-153	- 99	- 42	+7	54	44	47	- 3	- 53	- 117	- 161
	N	-180	- 164	- 120	- 75	- 23	27	18	18	- 23	- 67	- 124	- 165
	PR	.399	.356	.369	.355	.398	.406	.48	.427	.476	.409	.443	.433
Average Condition	S	-178	- 146	- 93	- 51	- 11	34	40	41.7	3.4	- 42	- 112	- 159
	E	- 184	- 165	- 120	- 70	- 18	36	40.2	32	- 10	- 63	- 126	- 168
	N	-186	- 173	- 138	- 98	- 50	0	9.7	2	- 31	- 76	- 131	- 171

Table 7.2. PR = Proportion

Table of average sky energy contribution from bright, overcast and partially cloudy skies for a standard wall, $U = 0.57$ $\alpha = 0.95$, Whr/m^2 day

Month		J	F	M	A	M	J	J	A	S	O	N	D
Bright Sky Conditions	S	319	431	521	458	444	455	446	460	527	538	457	405
	E	-113	41	312	426	520	592	547	514	457	251	-.4	-108
	N	-161	- 96	-12	71	142	199	179	164	114	21	- 92	-169
	PR	.161	.234	.281	.345	.352	.374	.3	.323	.264	.261	.177	.137
Over Cast	ALL	-147	-102	- 62	10	76	232	238	210	119	10	-82	-137
	PR	.44	.41	.35	. 3	.25	.22	.22	.25	.26	.33	.38	.43
Partially Cloudy	S	171	264	366	428	478	530	484	469	393	356	249	114
	E	-58	0	324	466	552	609	560	523	404	248	40	-78
	N	- 87	-7.7	211	345	444	522	458	411	285	152	-1	-89
	PR	.399	.356	.369	.355	.398	.406	.48	.427	.476	.409	.443	.433
Average Condition	S	55	152	259	313	365	437	417	400	357	289	159	33.0
	E	-105	-32	185	314	421	520	474	441	343	169	- 13	-84
	N	-124	- 37	54	161	268	370	340	300	206	17	-31	-116

Table 7.3. PR = Proportion

Evaluation of average sky contribution from bright sky, overcast and partially cloudy sky conditions for a thermachromic screen set point of 2°C above room temperature, Whr/m^2 day

Month		J	F	M	A	M	J	J	A	S	O	N	D
Bright Sky Conditions	S	200	294	358	312	297	307	299	313	366	388	304	278
	E	-113	20	185	270	353	418	381	354	302	166	-6	-108
	N	-161	- 96	- 12	71	142	199	179	164	114	21	- 92	-169
	PR	.161	.234	.281	.345	.352	.374	.3	.323	.264	.261	.177	.137
Over cast	ALL	- 64	- 42	- 22	0	14	34	36	37	23	2	- 31	- 59
	PR	.44	.41	.35	.3	.25	.22	.22	.25	.26	.33	.38	.43
Partially Cloudy	S	96	149	220	267	303	341	314	307	255	225	152	66
	E	- 60	40	194	294	352	391	362	342	263	160	24	- 70
	N	-88	- 12	124	213	282	336	298	271	190	104	- 8	- 89
	PR	.399	.356	.369	.355	.398	.406	.48	.427	.476	.409	.443	.433
Average Condition	S	6	79	159	202	238	286	277	269	240	195	89	0
	E	-106	- 23	100	197	278	348	314	297	227	110	- 22	-102
	N	-124	- 68	20	100	176	244	232	204	143	49	- 51	-117.9

Table 7.4. PR = Proportion

Evaluation of average sky contribution from bright, overcast and partially cloudy sky conditions. For thermochromic screen set point at room temperature. Whr/in^2 day.

Month		J	F	M	A	M	J	J	A	S	O	N	D
Bright Sky Conditions	S	54	124	200	164	151	164	155	169	219	221	149	100
	E	-150	- 70	36	106	184	249	214	192	142	39	- 74	-145
	N	-180	-135	- 76	-18	31	76	61	61	26	-35	-121	-184
	PR	.161	.234	.281	.345	.352	.374	.3	.323	.264	.261	.177	.137
Over cast	ALL	-161	-131	-101	-58	-19	44	53	53	16	-39	-104	-149
	PR	.44	.41	.35	.3	.25	.22	.22	.25	.26	.33	.38	.43
Partially Cloudy	S	-22	14	78	119	141	175	150	158	109	88	25	- 34
	E	-111	- 52	38	115	171	215	182	171	104	40	-47	-111
	N	-126	-80	- 0	55	104	132	125	114	65	11	-64	-121
	PR	.399	.356	.369	.355	.398	.406	.48	.427	.476	.409	.443	.433
Average Condition	S	- 71	-19	50	81	114	142	131	134	113	83	27	- 70
	E	-138	- 55	11	59	127	190	163	148	91	16	- 72	- 130
	N	- 149	-112	- 56	- 3	47	97	90	81	40	-15	- 88	- 139

Table 7.5. PR = Proportion

Evaluation of average sky contribution from bright, overcast and cloudy sky conditions.

For thermochromic screen set point of 2°C below room temperature. Whr/m^2 day.

FIGURES

Aston University

Illustration removed for copyright restrictions

Figure 2.1

European flat plate collector sales

(from Stammers (1982)).

Figure 2.2.
Annual mean daily solar irradiation over the globe W/m^2
From U.K. ISES (1976).

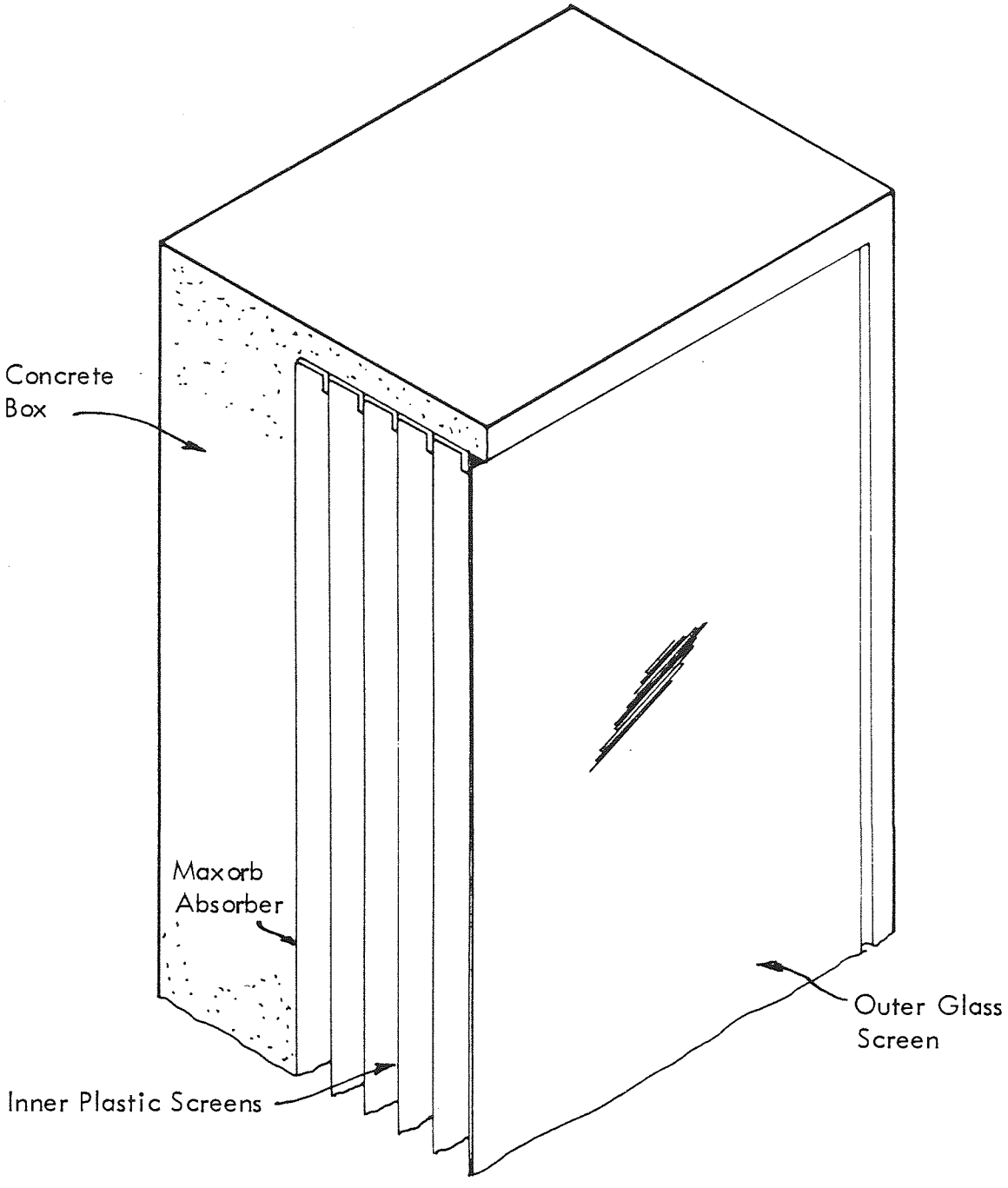

Figure 2.3 .

Cutaway section of the solar module

Aston University

Illustration removed for copyright restrictions

Graph showing the ratio of hemispherical emittance to normal emittance for various values of normal emittance for opaque materials

From Sparrow and Cess (1979)

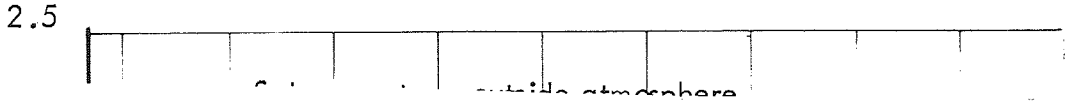

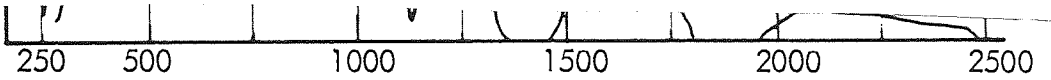

Figure 3.2.

Comparison of the spectrum of the sun and corresponding black body. From U.K. ISES (1976).

Figure 3.3.

Normalised spectral distribution of a black body at various temperatures.

From Duffie and Beckman (1980)

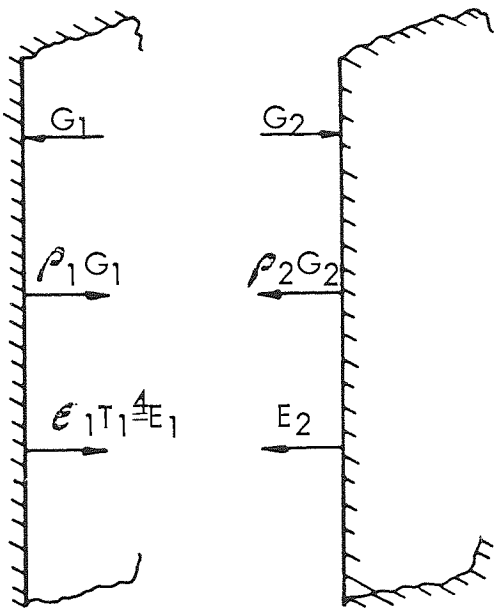

Figure 4.1.

Radiant energy exchange between two infinite parallel plates.

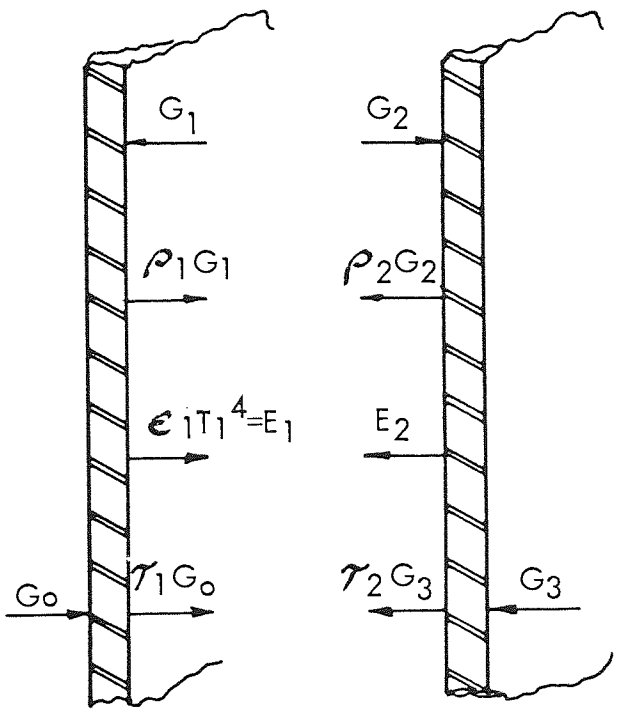

Figure 4.2.

Radiant energy exchange between two infinite parallel partially transmitting screens.

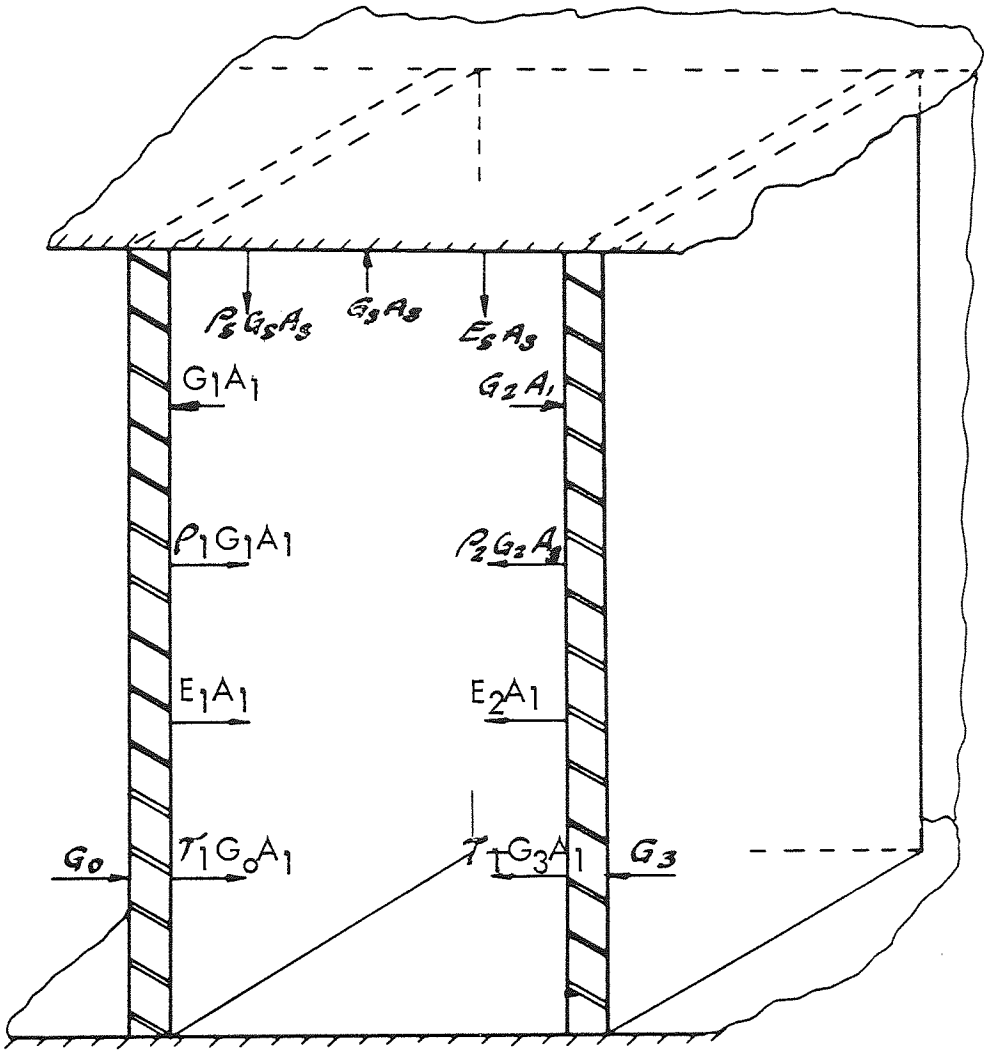

Figure 4.3.

Radiant energy exchange in a finite enclosure with partially transparent screens and opaque sides.

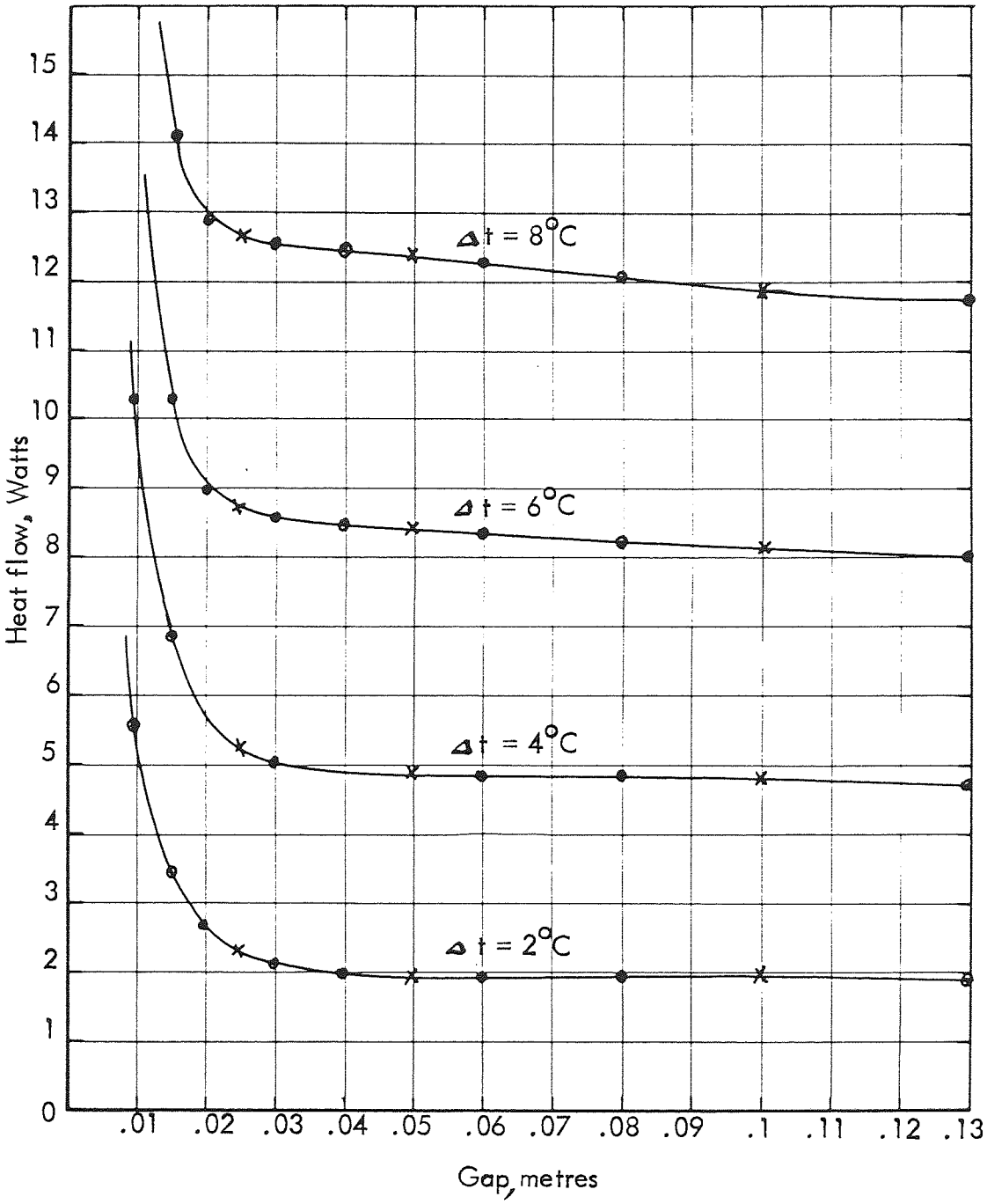

Figure 4.4.

Graph of heat flow due to conduction and convection across a 1 m^2 cell, with varying gap and aspect ratio. Hot screen at 20 C, various temperature differences.

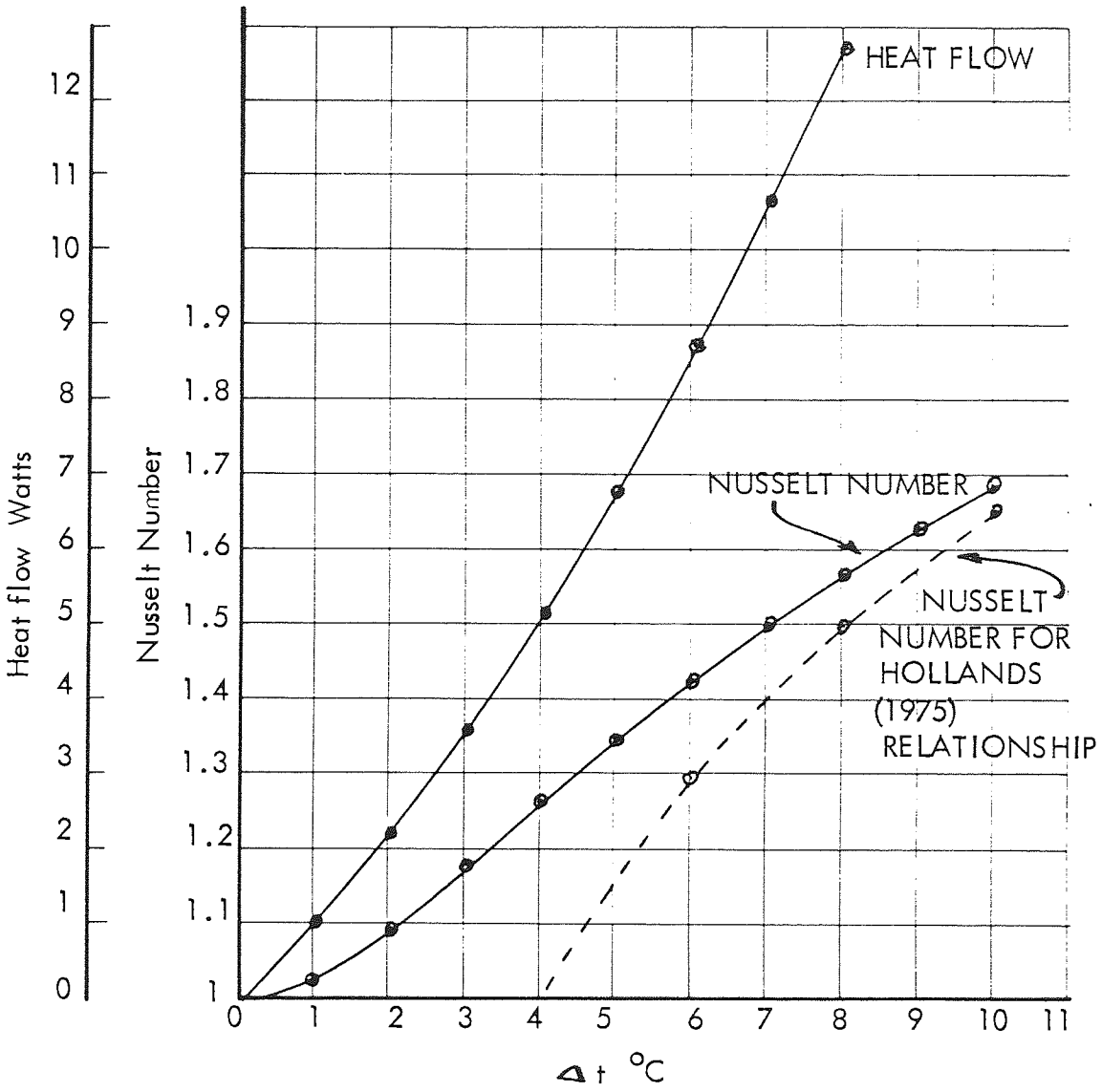

Figure 4.5.

Graph of Nusselt number and heat flow for a 1 m^2 cell with 25mm gap, versus temperature difference for a hot screen temperature of 20 C.

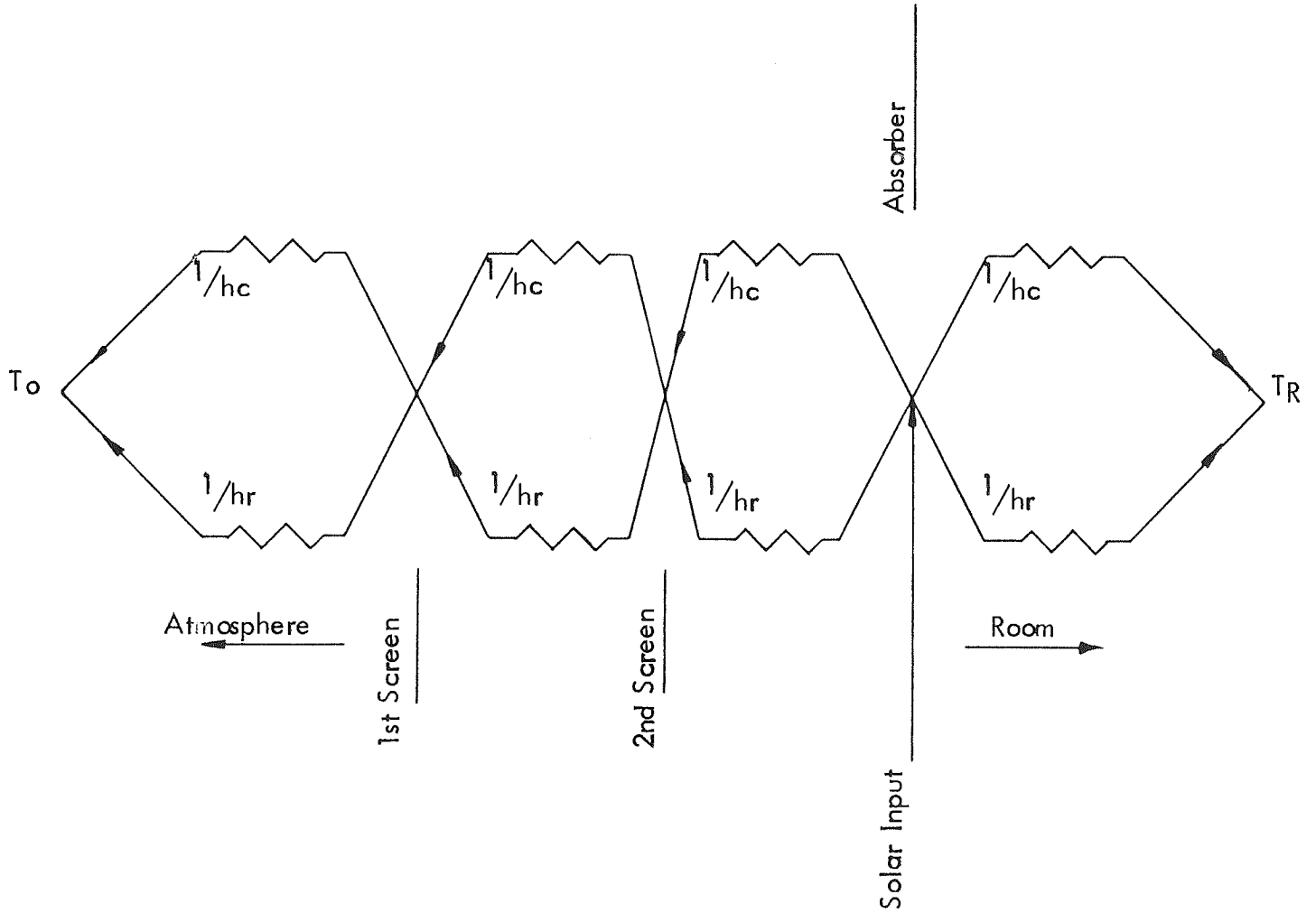

Figure 4.6.

Electrical resistance network analogue of combined heat flow through two opaque screens.

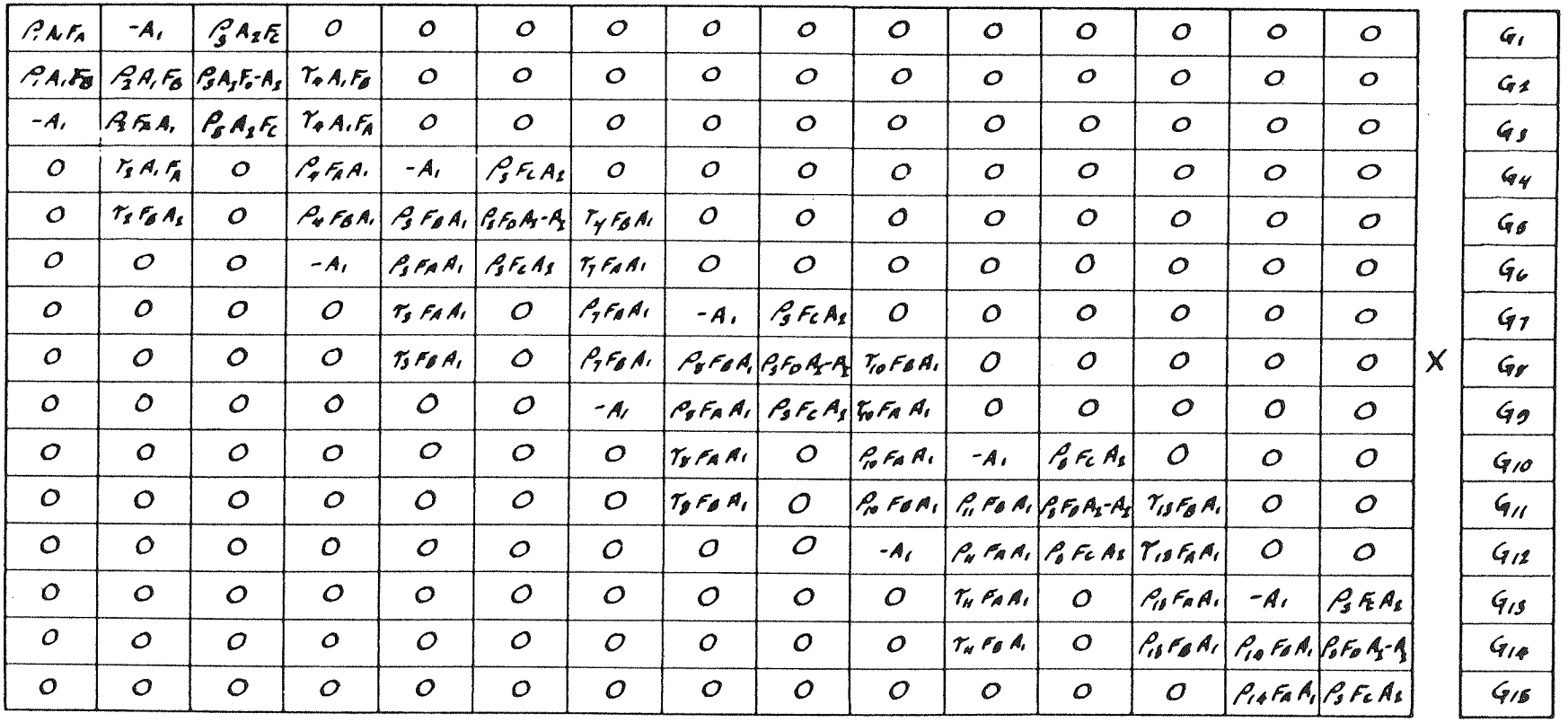

Figure 4.7.

Radiant coefficient matrix GCF.

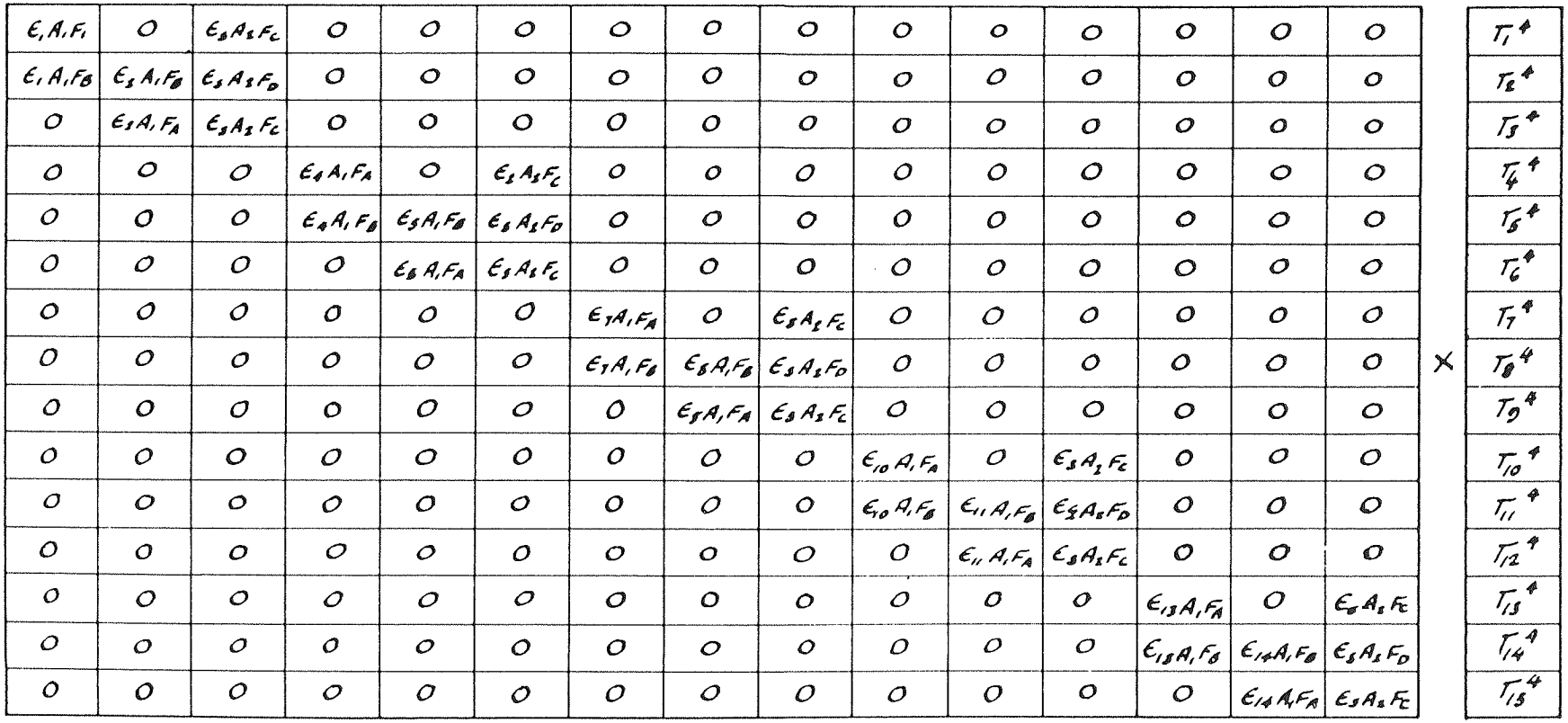

Figure 4.8.

Radiant coefficient matrix T4CF.

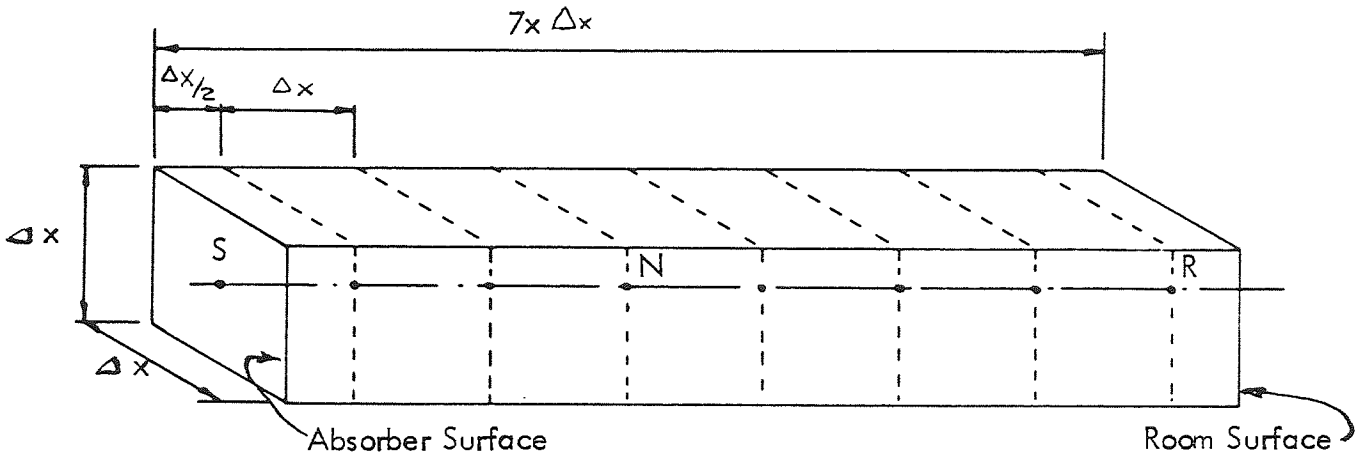

Figure 4.9.

Diagram of nodal and volume arrangement for finite difference analysis.

$\alpha/2+\beta+H_1$	β	0	0	0	0	0	0
$-\beta$	$\alpha+2\beta$	$-\beta$	0	0	0	0	0
0	$-\beta$	$\alpha+2\beta$	$-\beta$	0	0	0	0
0	0	$-\beta$	$\alpha+2\beta$	$-\beta$	0	0	0
0	0	0	$-\beta$	$\alpha+2\beta$	$-\beta$	0	0
0	0	0	0	$-\beta$	$\alpha+2\beta$	$-\beta$	0
0	0	0	0	0	$-\beta$	$\alpha+2\beta$	$-\beta$
0	0	0	0	0	0	$-\beta$	$\alpha/2+\beta+H_2$

$\times$

T_1^1
T_2^1
T_3^1
T_4^1
T_5^1
T_6^1
T_7^1
T_8^1

$=$

$H_1 \times T_{LOV} + \alpha/2 \times T_1 + SLR$
αT_2
αT_3
αT_4
αT_5
αT_6
αT_7
$\alpha/2 \times T_8 + H_2 T_R$

Figure 4.10

Matrices for the finite difference analysis of an 8 node slab.

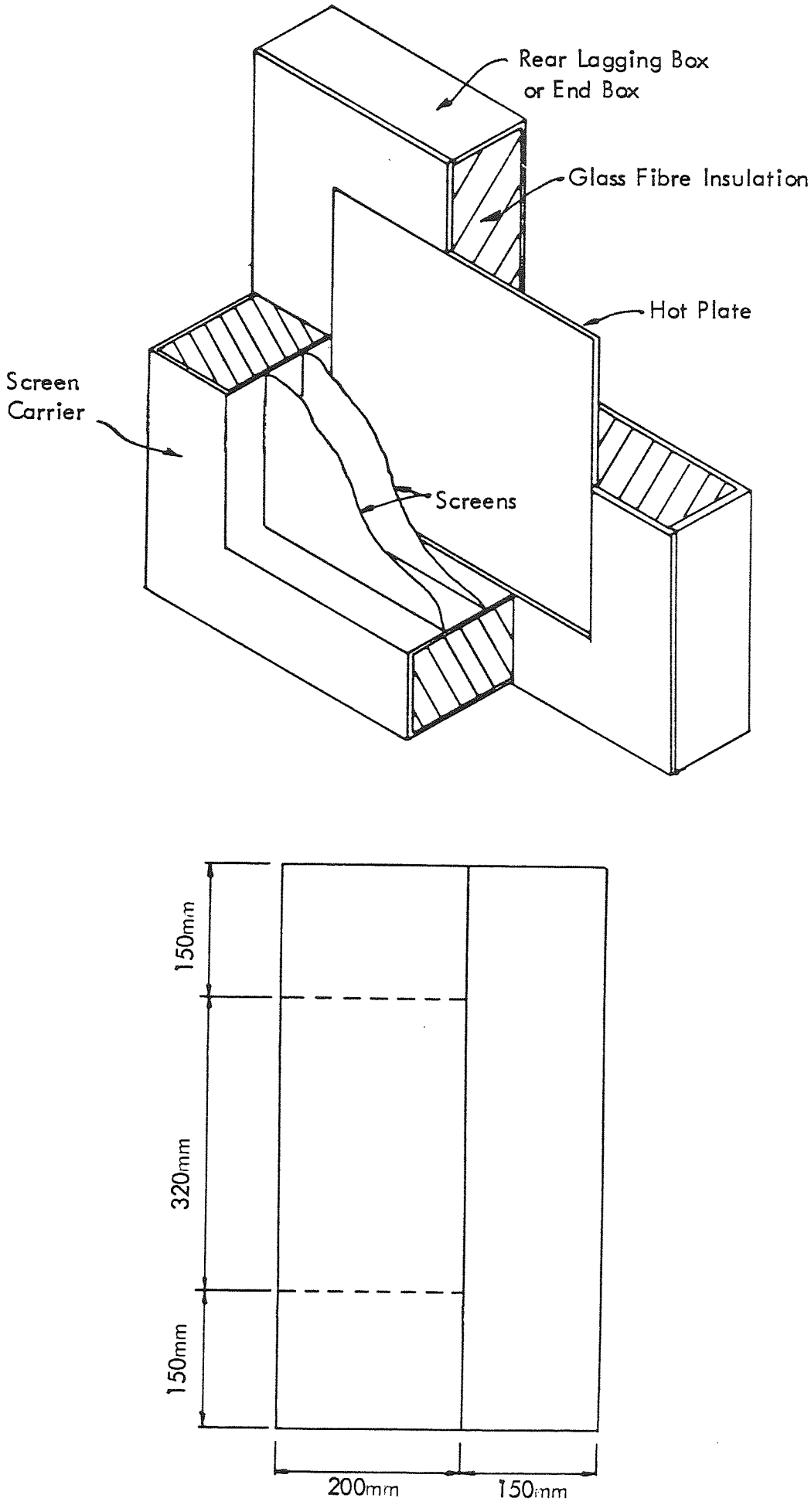

Figure 5.1.

Arrangement and dimensioning of experimental equipment.

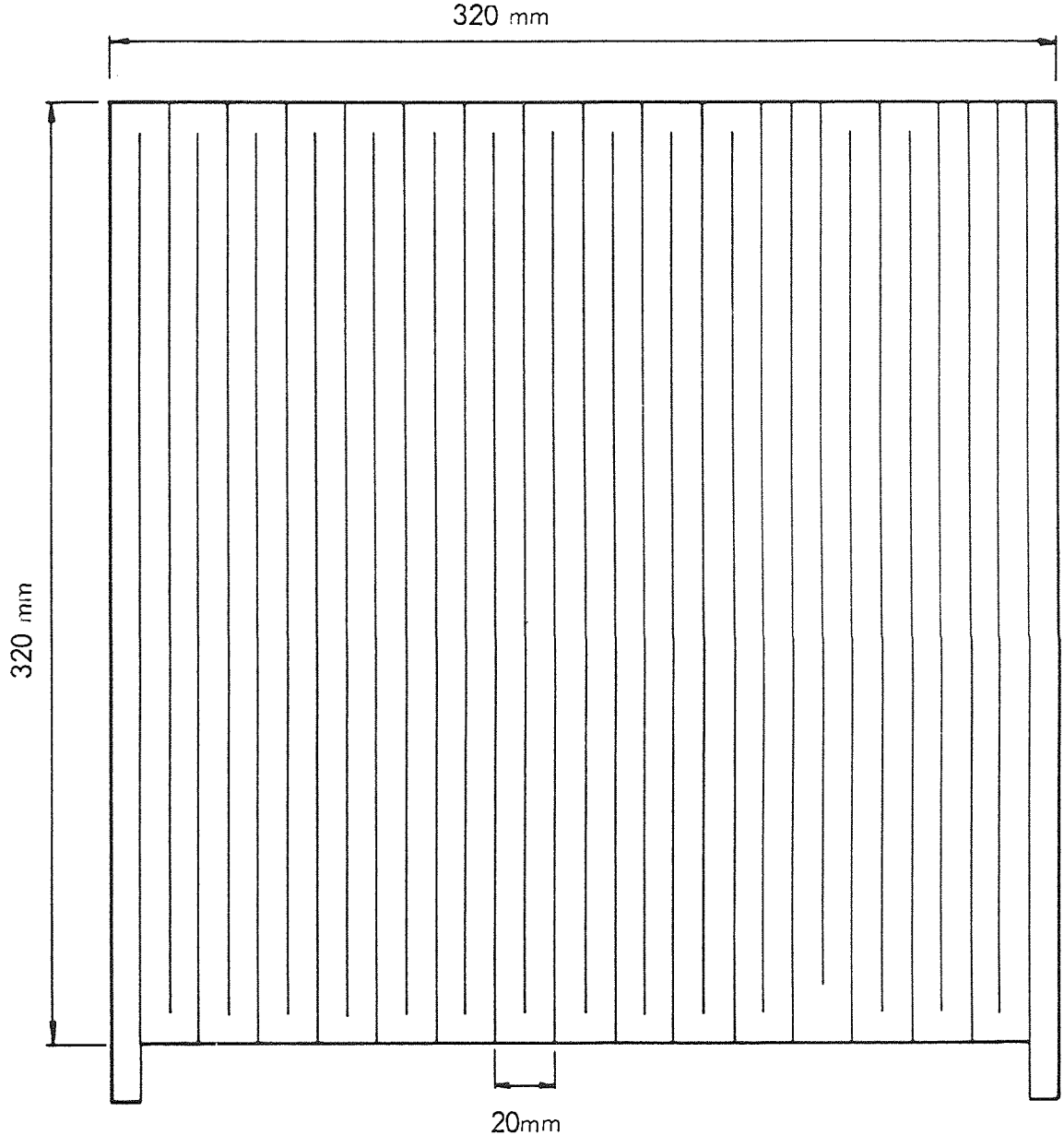

Figure 5.2.

Arrangement of "Maxorb" heater

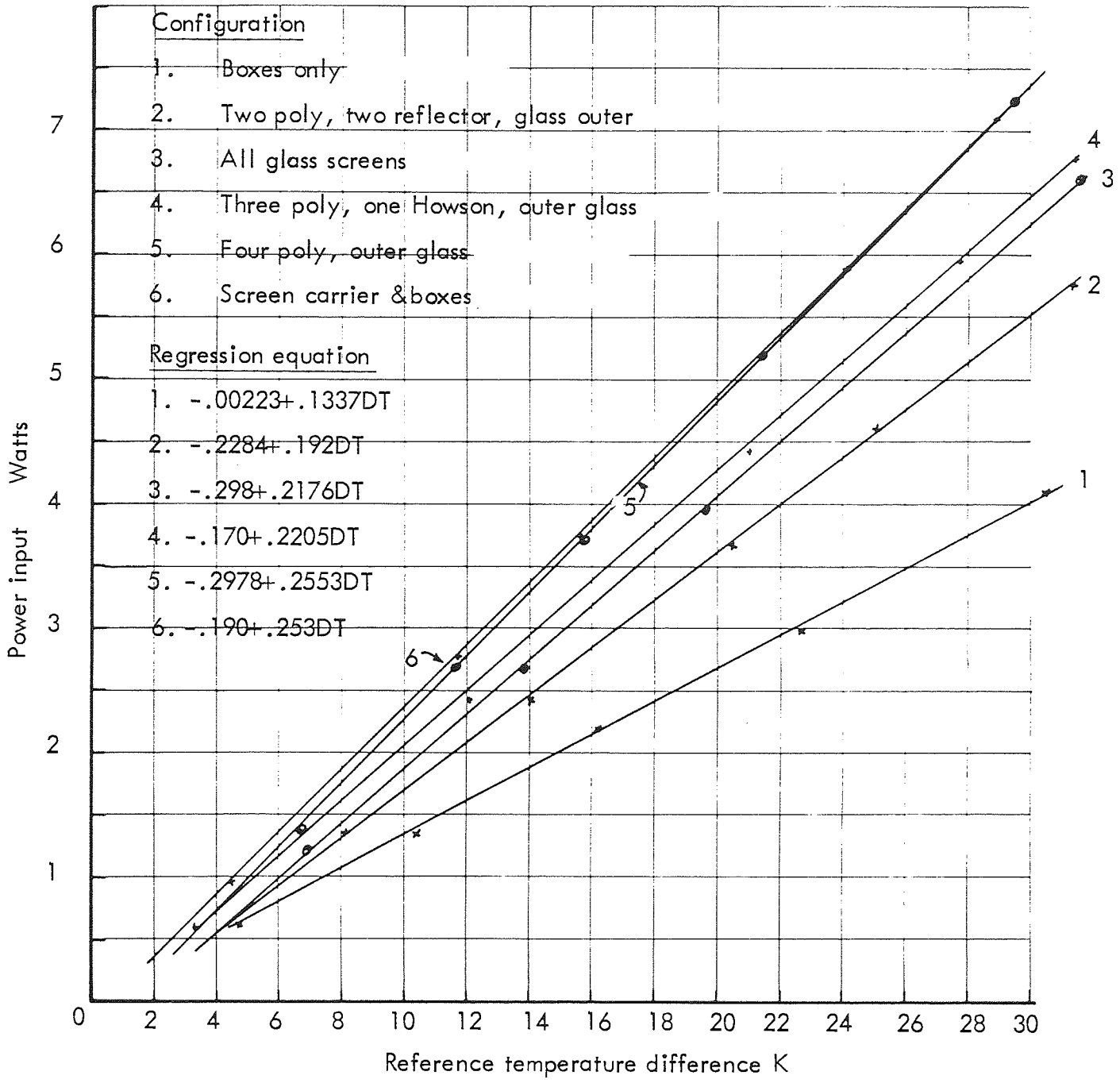

Figure 5.3.

Graph of power input v reference temperature difference for various configurations of experiment.

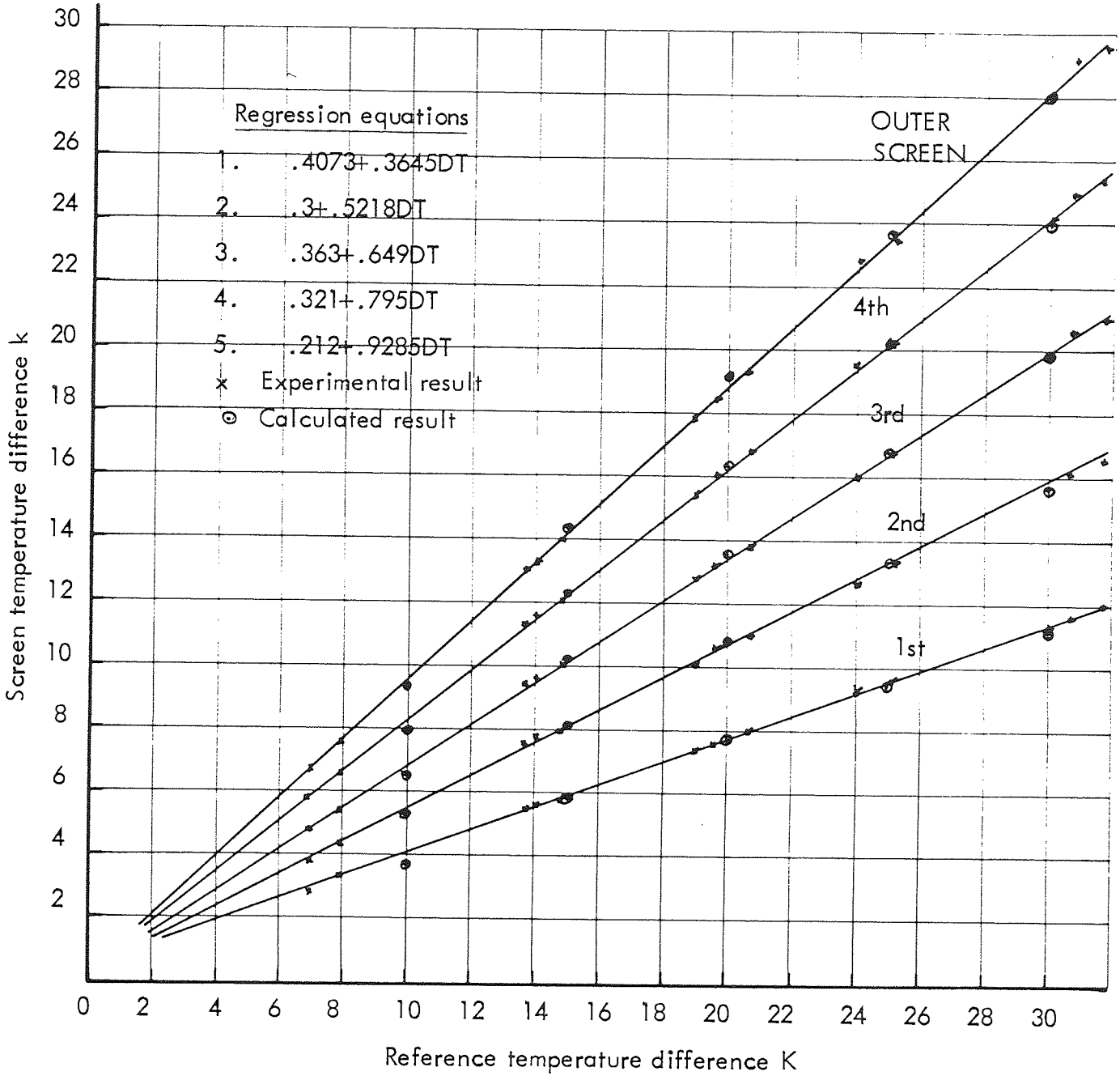

Figure 5.4.

Graphs of screen temperature difference from reference temperature v reference temperature difference for glass screens

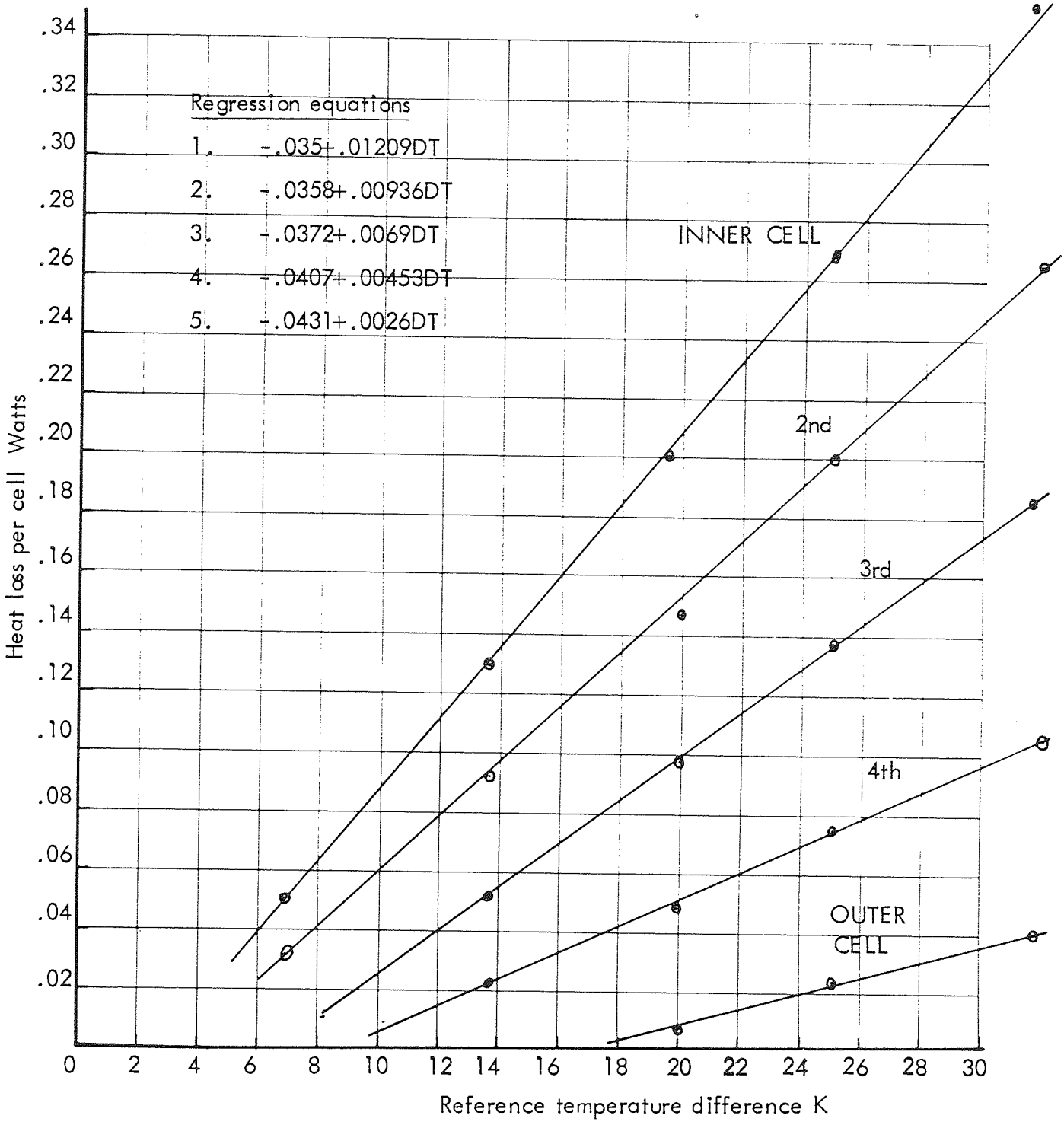

Figure 5.5.

Graphs of cell edge heat loss v reference temperature difference for configuration; glass, glass, glass, glass, glass.

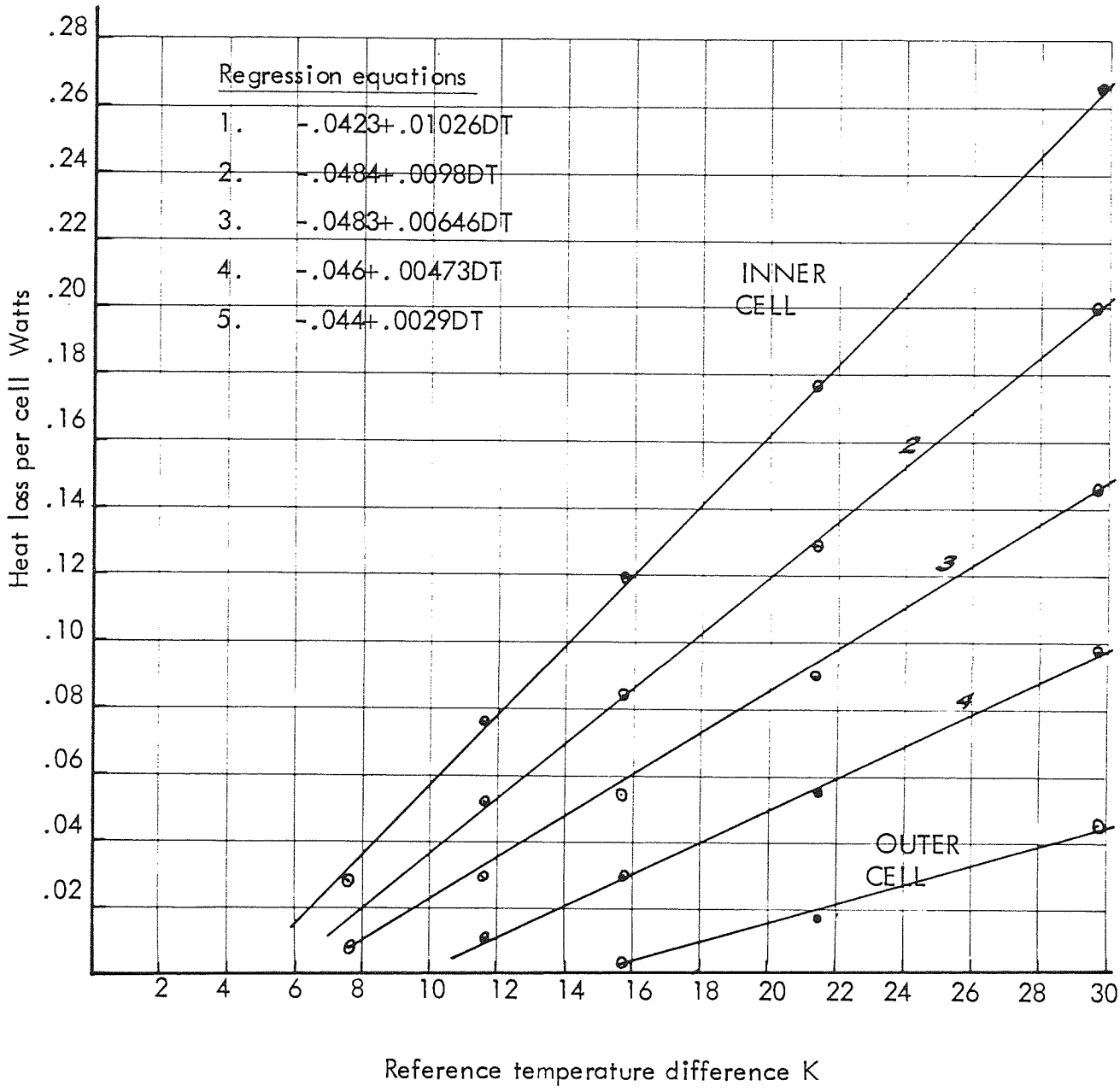

Figure 5.6.

Graphs of cell edge heat loss v reference temperature difference for configuration; poly, poly, poly, poly, glass

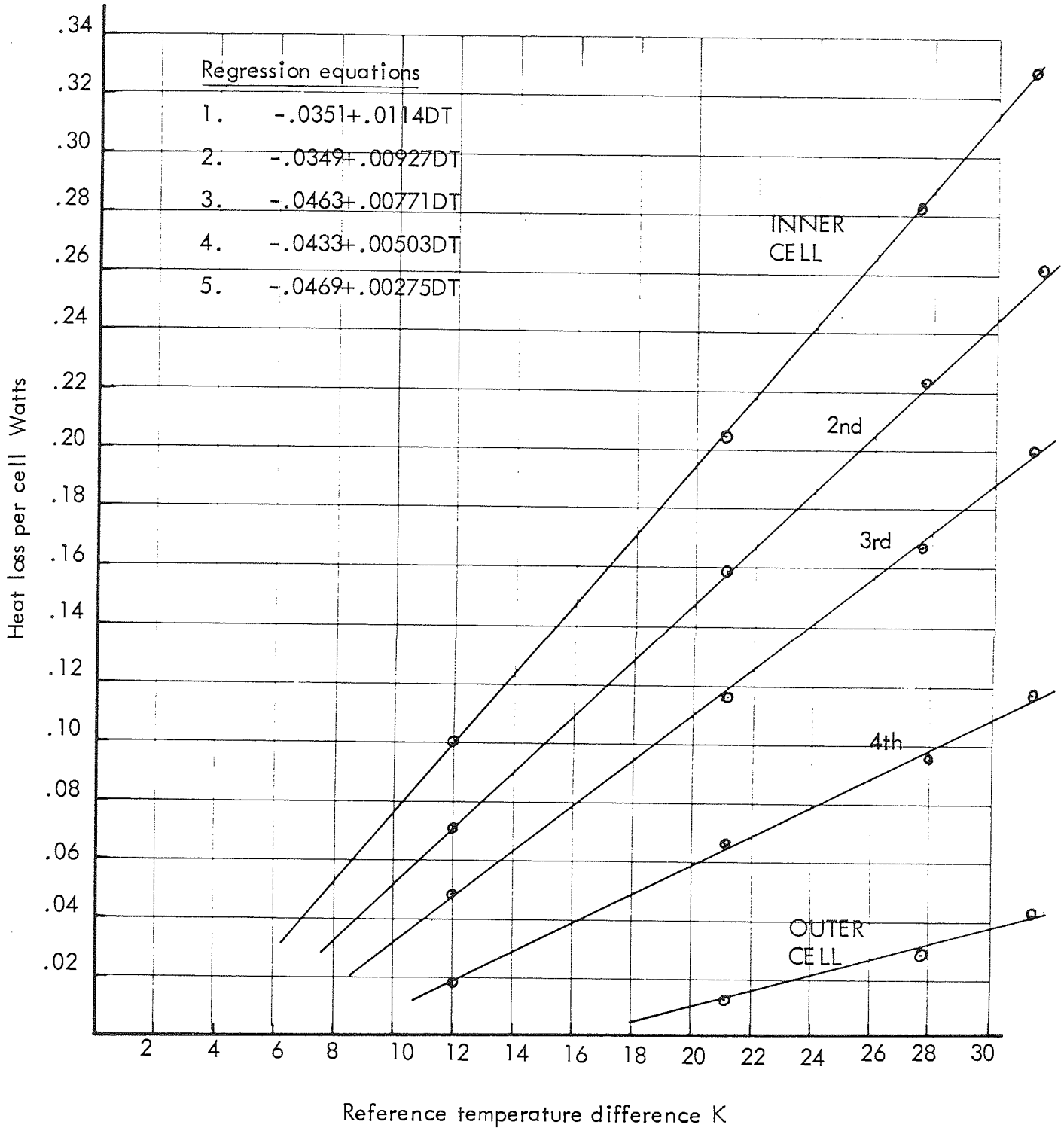

Figure 5.7.

Graphs of cell edge heat loss v reference temperature difference for configuration; poly, poly, poly, Howson, glass.

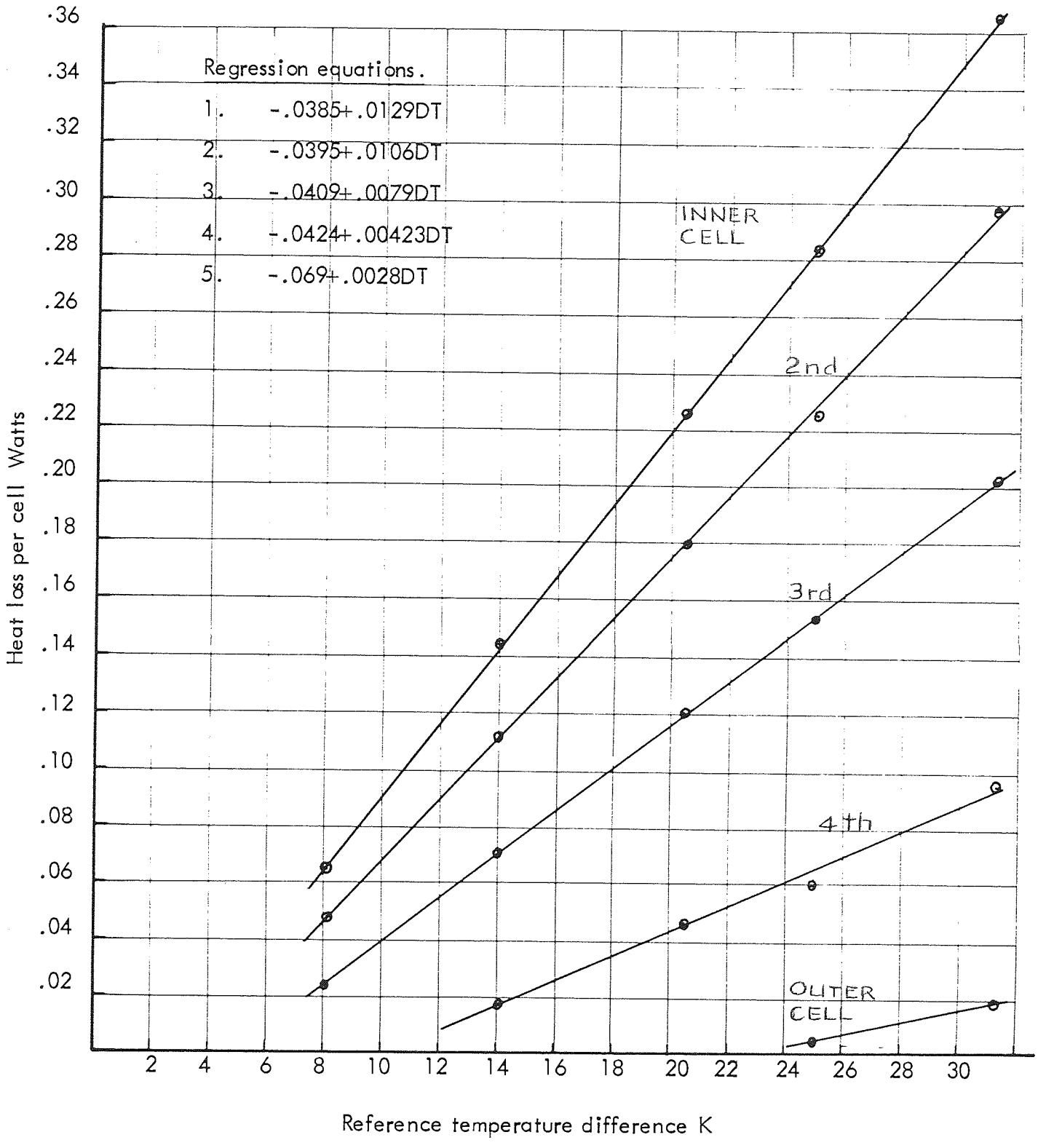

Figure 5.8.

Graphs of cell edge heat loss v reference temperature difference for configuration; poly, poly, reflector reflector, glass.

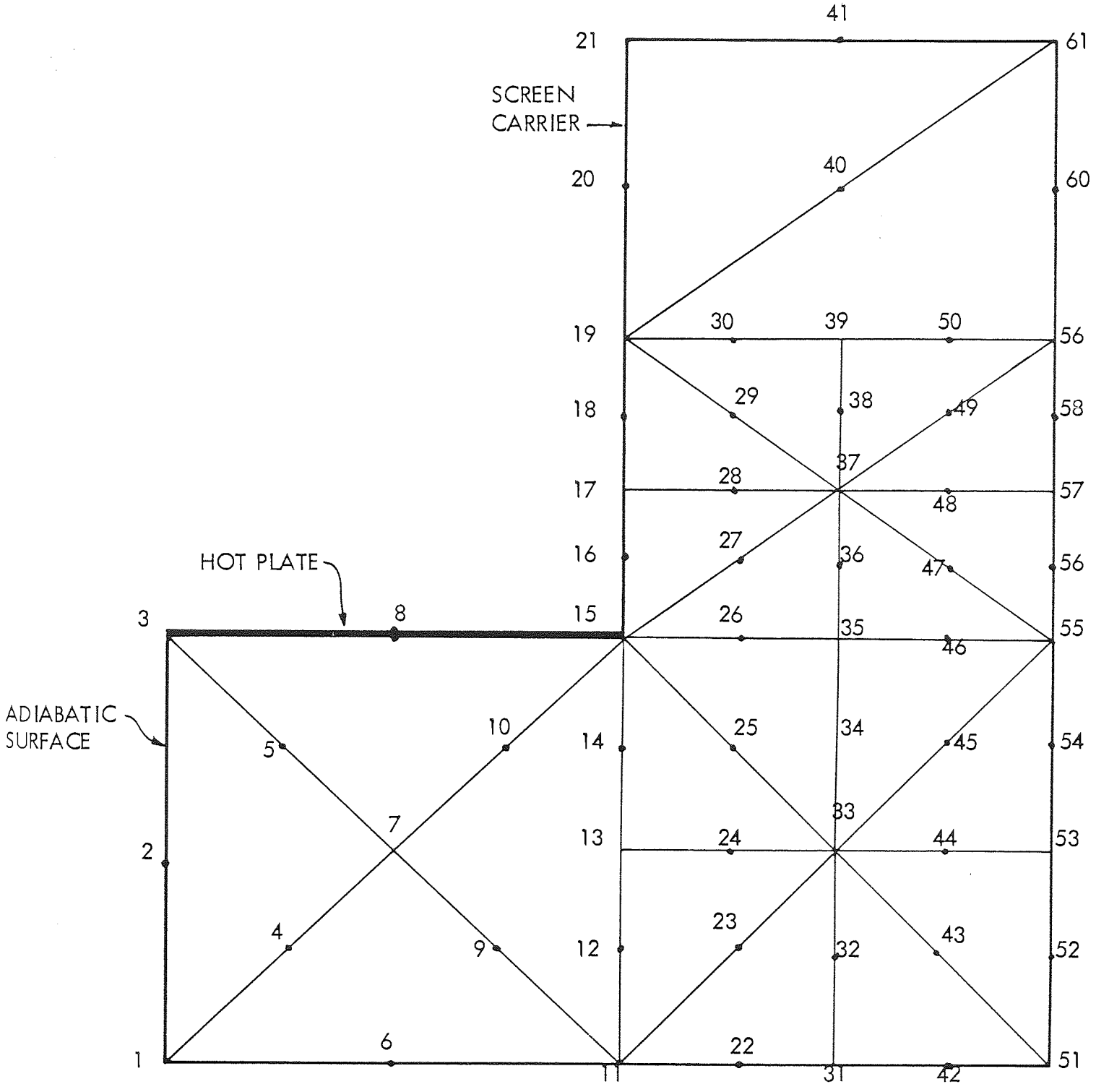

Figure 5.9.

Disposition of nodal points for finite element analysis of heat loss from the hot plate.

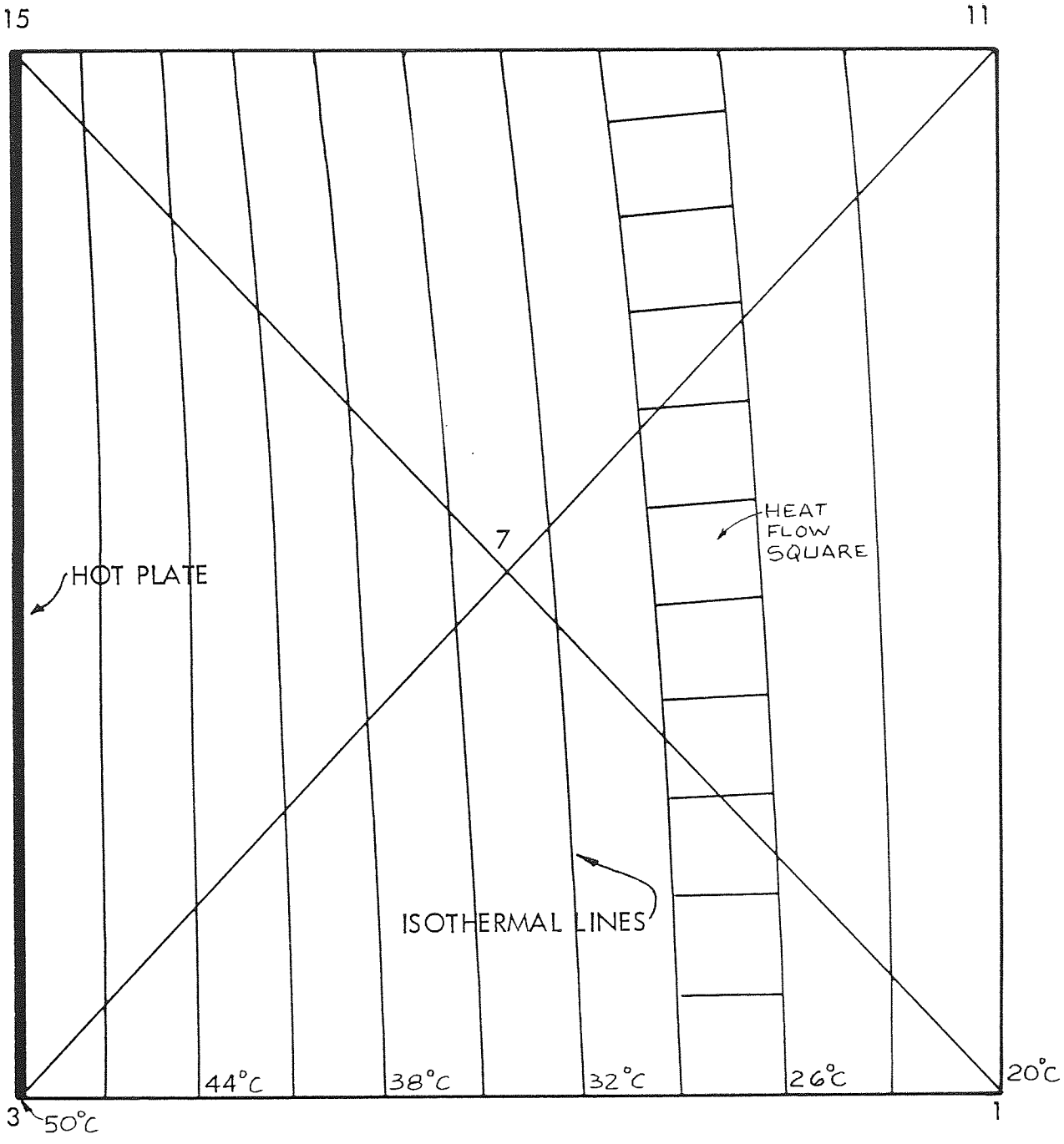

Figure 5.10.

Plot of isotherms and heat flow squares for two end boxes.

(To be read in conjunction with Figure 5.11.)

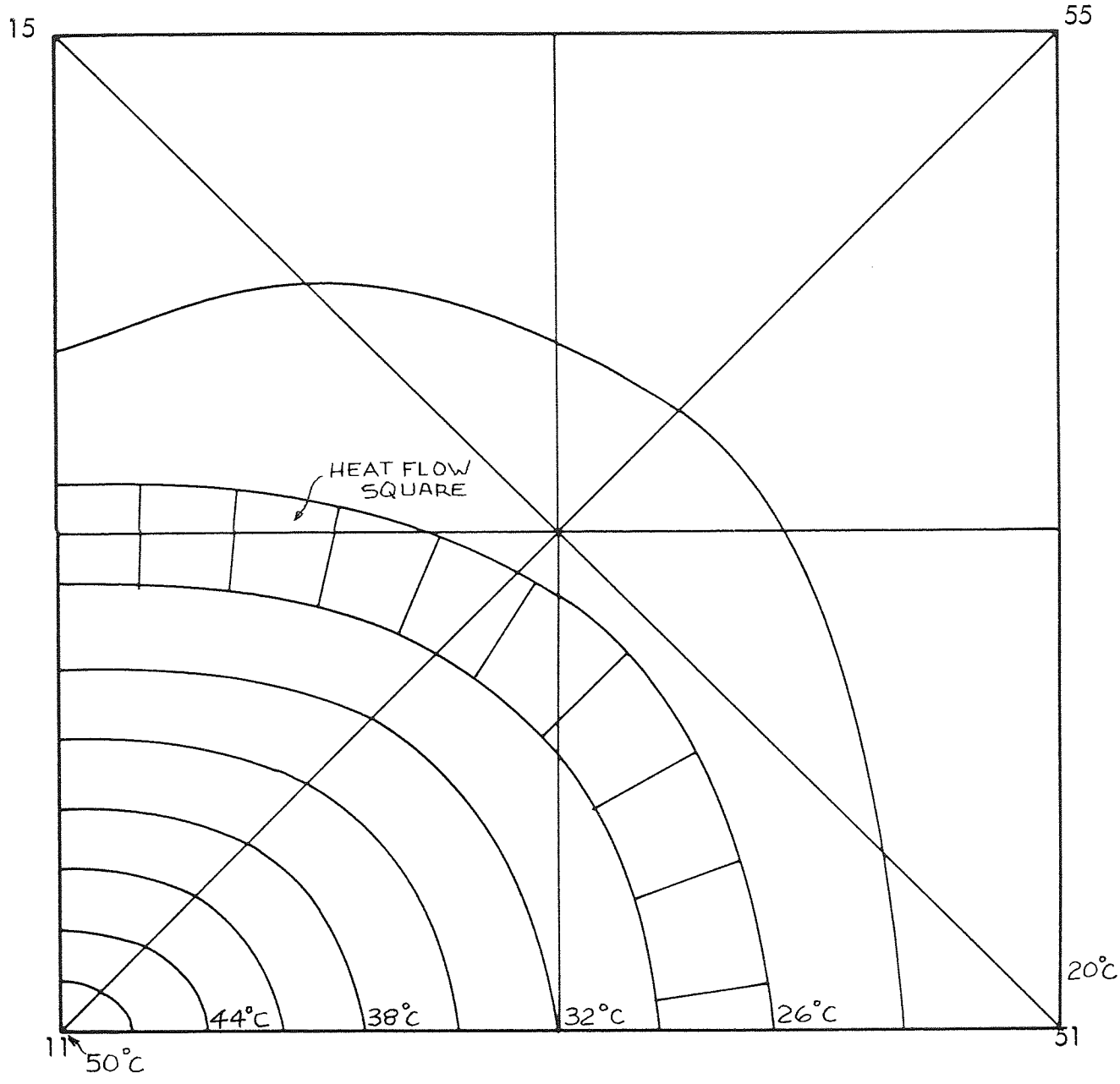

Figure 5.11.

Plot of isotherms and heat squares for two end boxes.

(See also Figure 5.10.)

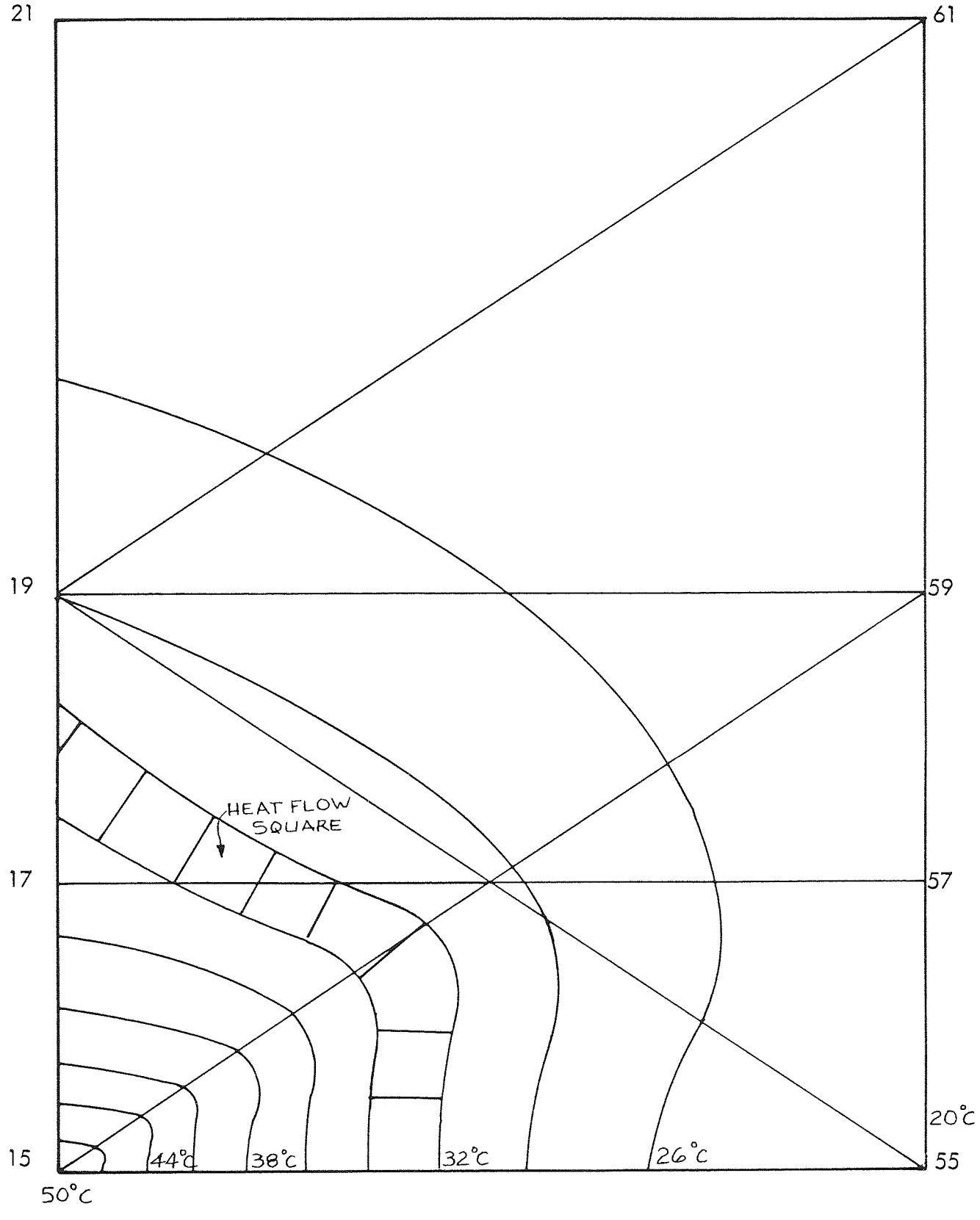

Figure 5.12.

Plot of isotherms and heat flow squares for screen carrier with all glass screens.

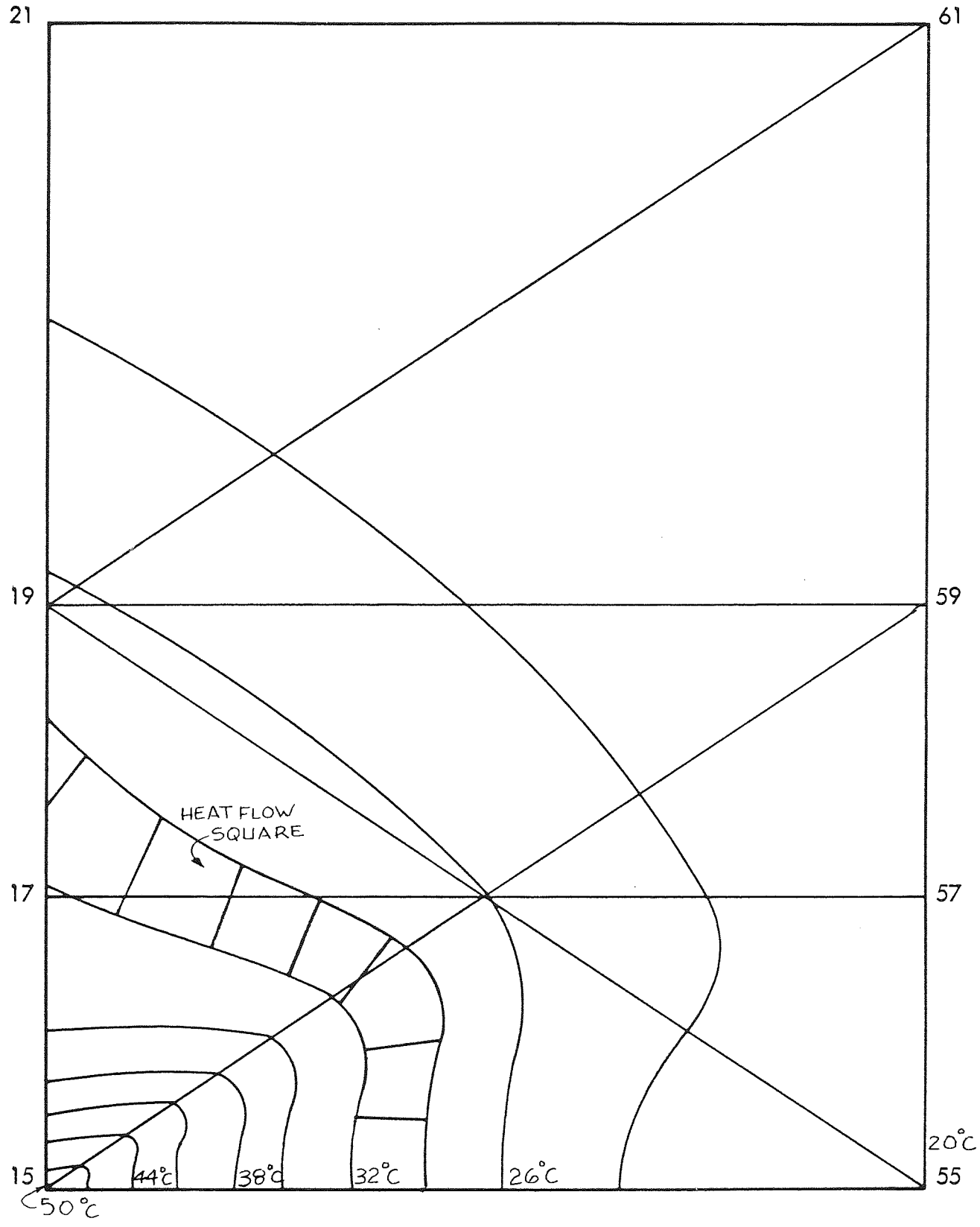

Figure 5.13

Plot of isotherms and heat flow squares for screen carrier with four inner polythene screens and a glass outer screen.

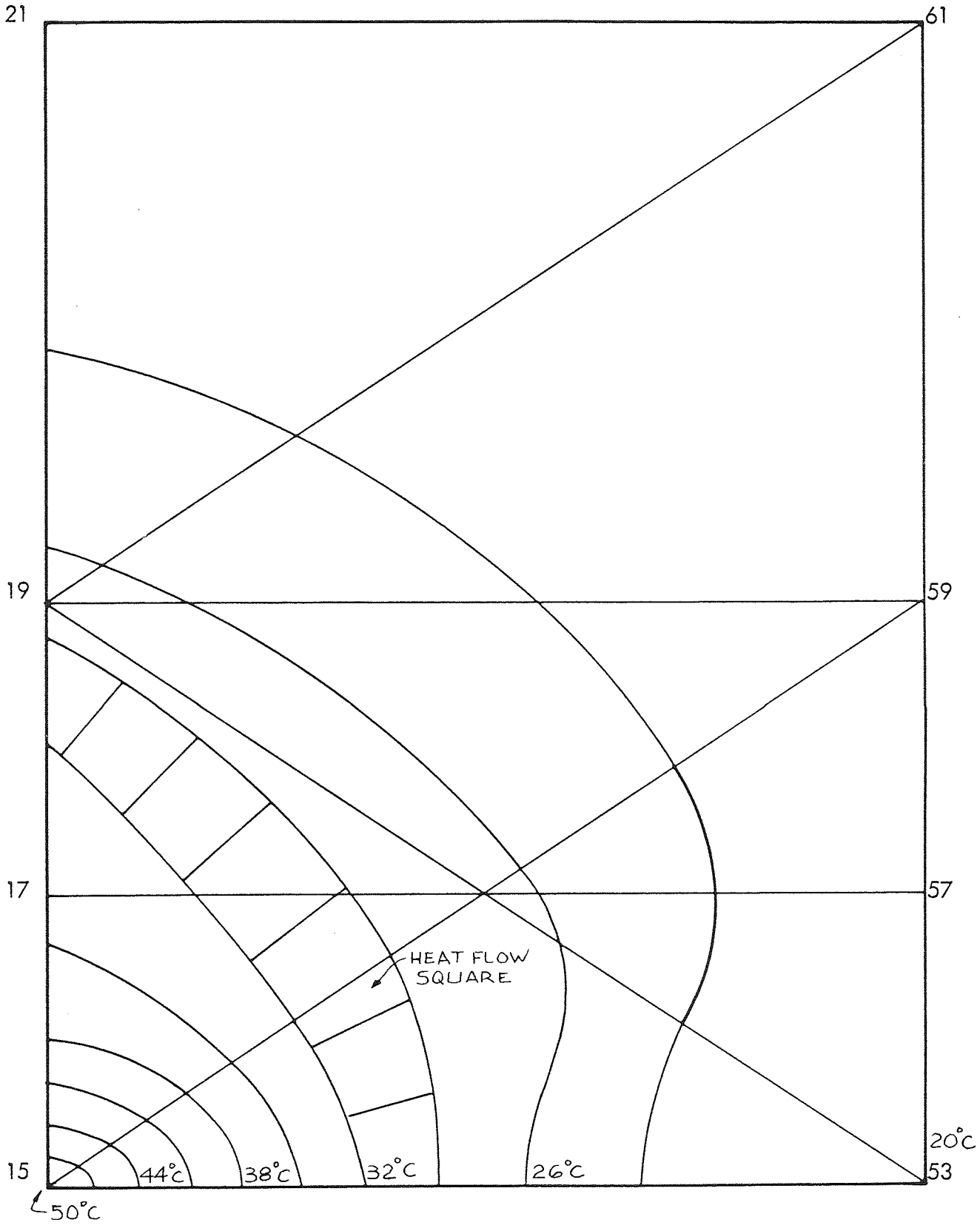

Figure 5.14

Plot of isotherms and heat flow squares for screen carrier with three inner polythene screens, a fourth "Howson" screen, and a glass outer screen.

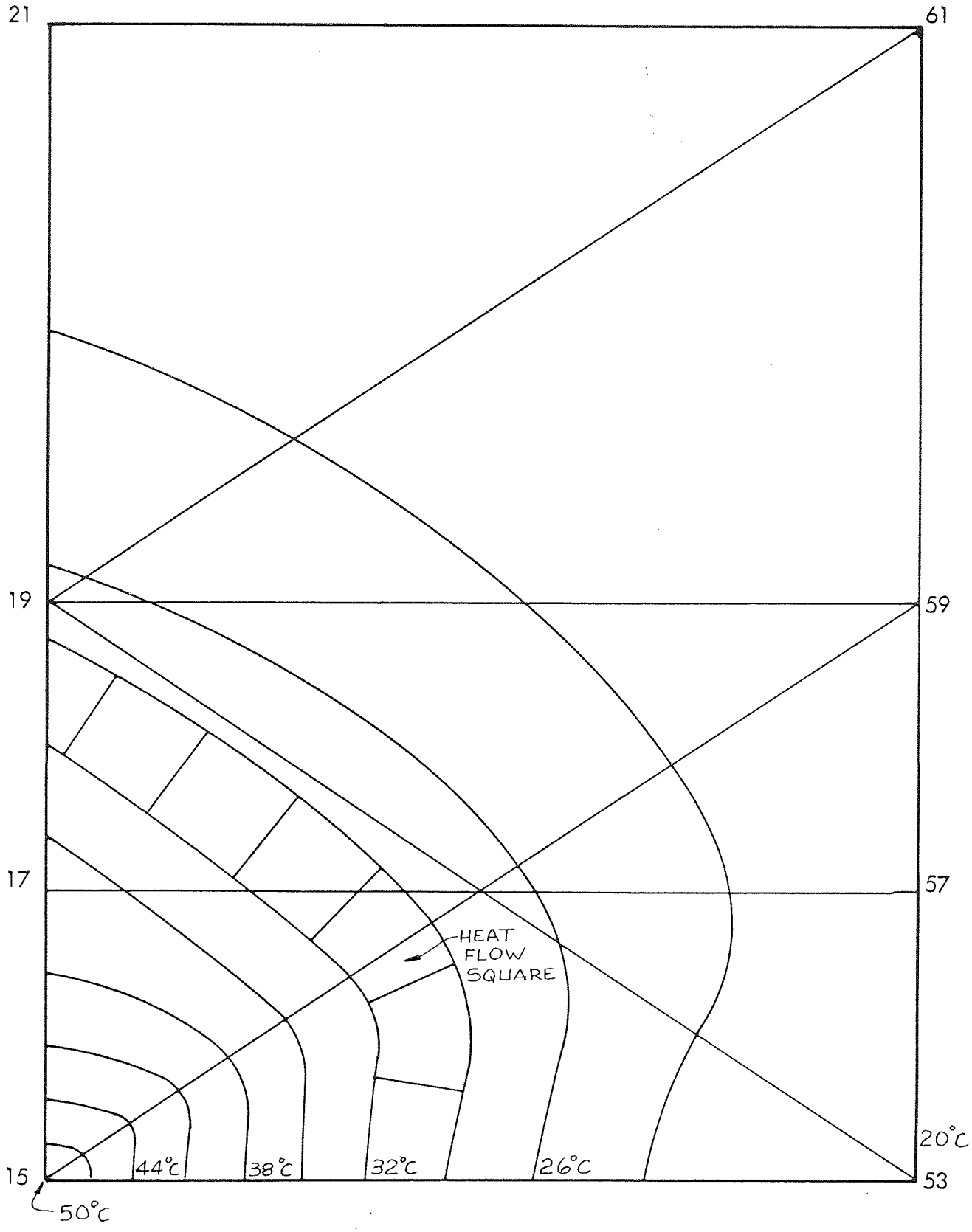

Figure 5.15

Plot of isotherms and heat flow squares for two inner polythene screens, two reflective screens of aluminised polyester, and a glass outer screen.

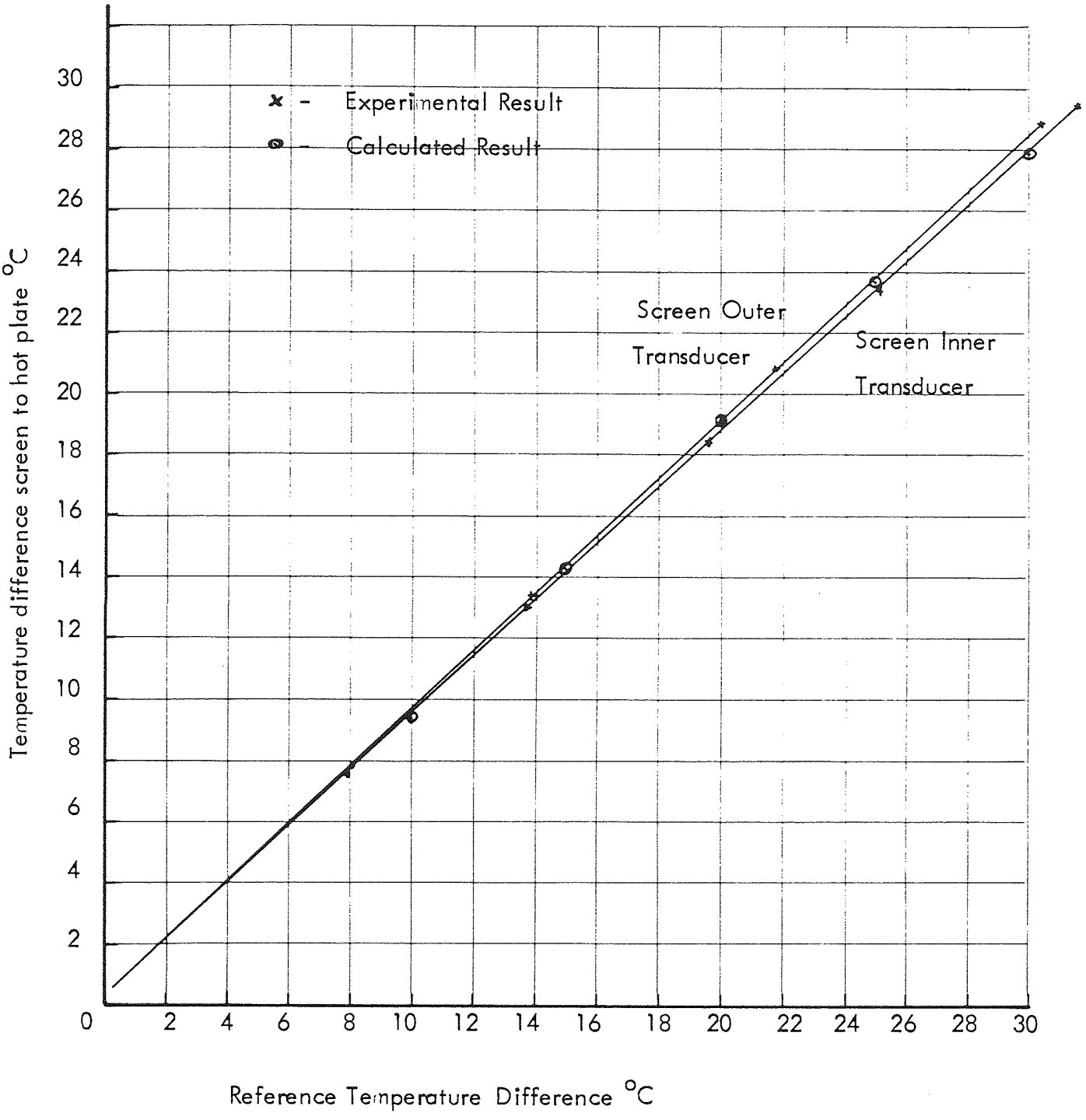

Figure 5.16

Graph of the temperature difference from the hotplate to the outer screen versus the reference temperature difference for all glass screens, showing the similarity of experimental and calculated values.

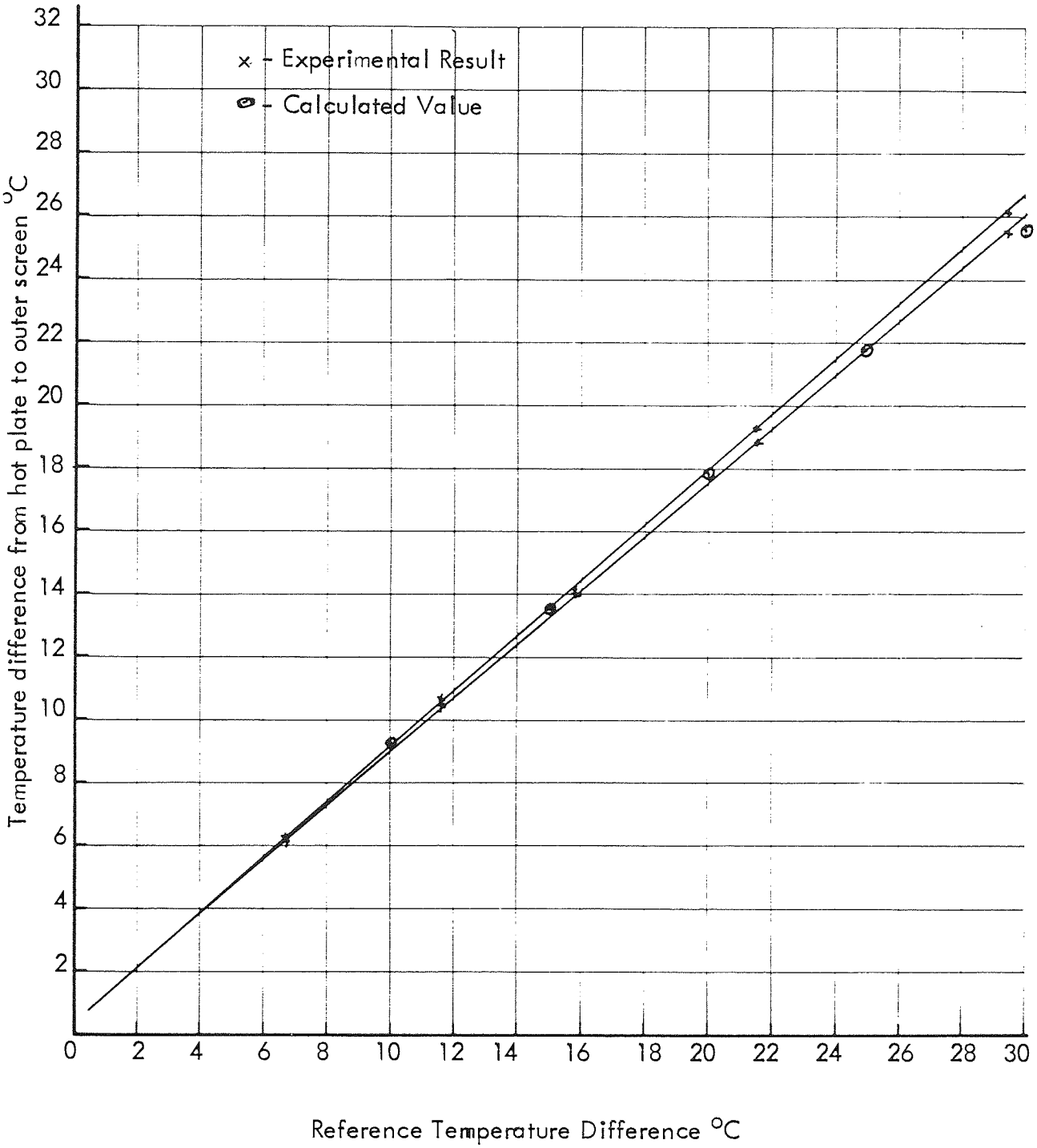

Figure 5.17

Graph of the temperature difference between hotplate and outer screen versus the reference temperature difference for four inner polythene screens and an outer glass screen, showing the similarity between experiment and calculation.

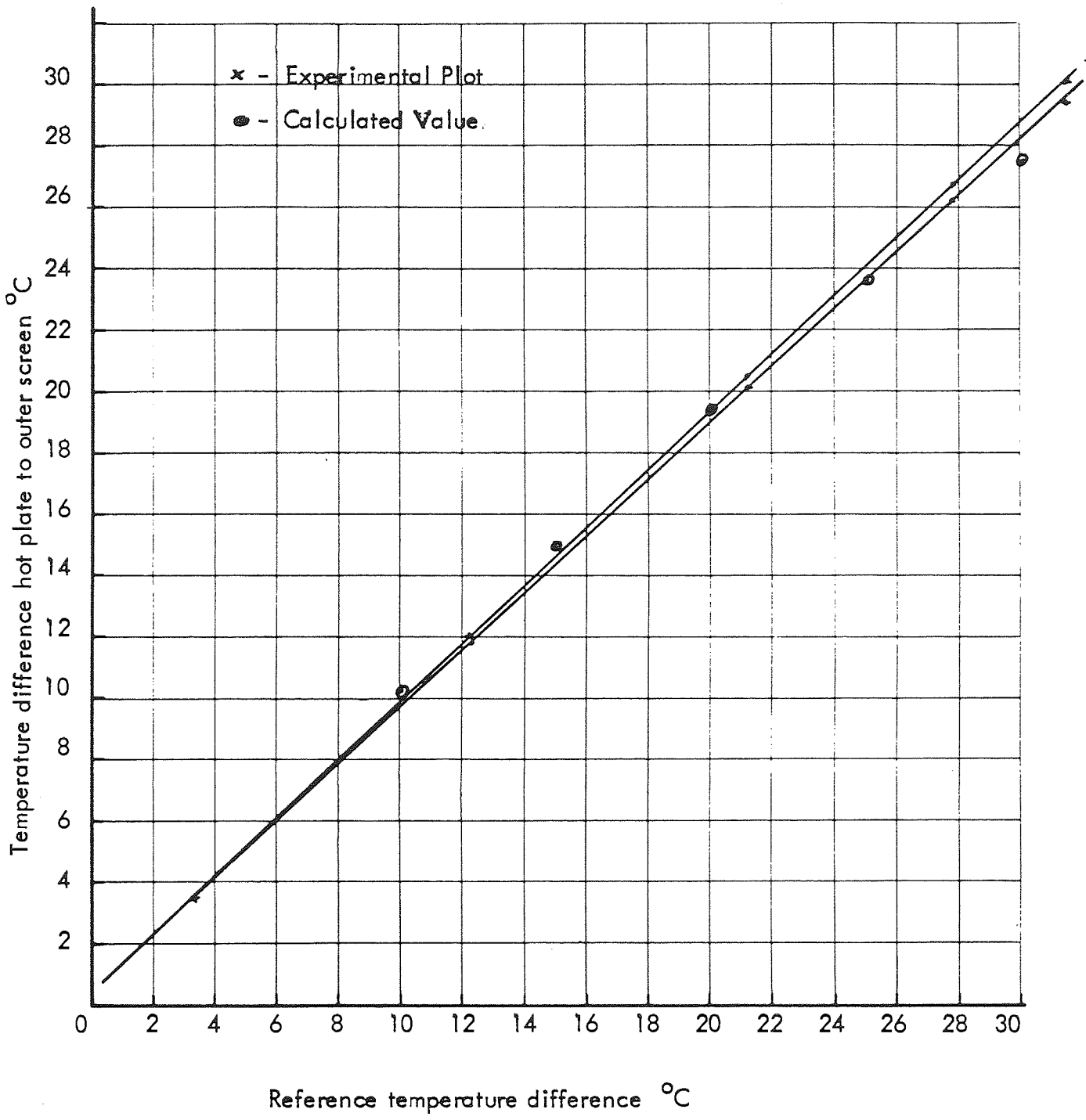

Figure 5.18.

Graph of temperature difference from hot plate to outer screen versus reference temperature difference for three inner polythene screens, a fourth "Howsen" screen and an outer glass screen; showing the similarity of calculated and experimental results.

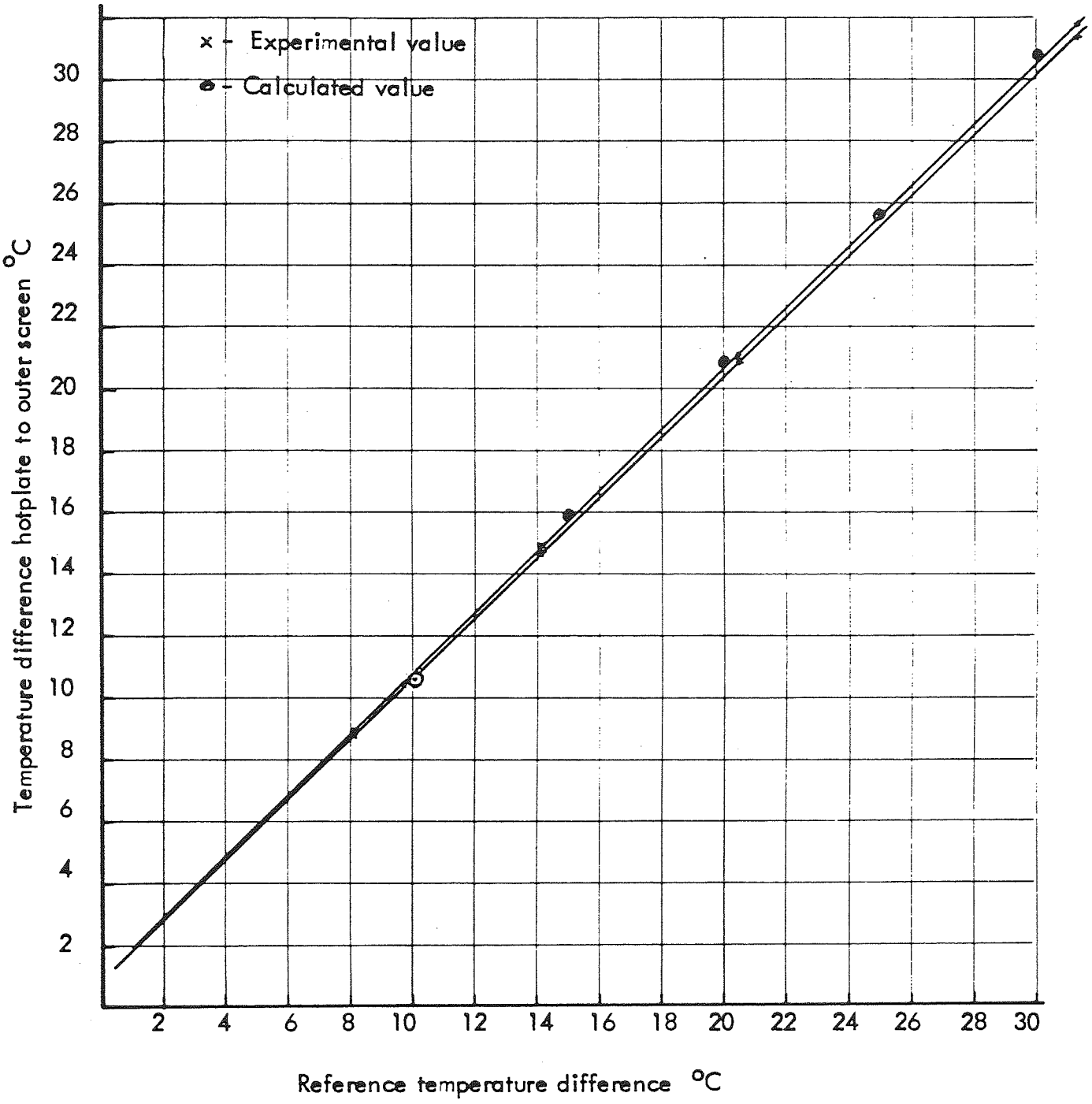

Figure 5.19

Graph of temperature difference from hot plate to outer screen versus the reference temperature difference for two inner polythene screens, two reflect screens and a glass outer screen, showing the similarity of experimental and calculated values.

$-\rho_1$	1	0	0	0	0	0	0	0	0
-1	ρ_2	τ_2	0	0	0	0	0	0	0
0	$-\tau_3$	$-\rho_3$	1	0	0	0	0	0	0
0	0	-1	ρ_4	τ_4	0	0	0	0	0
0	0	0	$-\tau_5$	$-\rho_5$	1	0	0	0	0
0	0	0	0	-1	ρ_6	τ_6	0	0	0
0	0	0	0	0	$-\tau_7$	$-\rho_7$	1	0	0
0	0	0	0	0	0	-1	ρ_8	τ_8	0
0	0	0	0	0	0	0	$-\tau_9$	$-\rho_9$	1
0	0	0	0	0	0	0	0	-1	ρ_{10}

$\times$

G_1
G_2
G_3
G_4
G_5
G_6
G_7
G_8
G_9
G_{10}

$=$

ϵ_1	0	0	0	0	0
0	ϵ_2	0	0	0	0
0	ϵ_3	0	0	0	0
0	0	ϵ_4	0	0	0
0	0	ϵ_5	0	0	0
0	0	0	ϵ_6	0	0
0	0	0	ϵ_7	0	0
0	0	0	0	ϵ_8	0
0	0	0	0	ϵ_9	0
0	0	0	0	0	ϵ_{10}

$\times$

T_1^4
T_2^4
T_3^4
T_4^4
T_5^4
T_6^4
T_7^4
T_8^4
T_9^4
T_{10}^4

Figure 6.1.

Matrices for the analysis of radiant heat transfer for the module neglecting edge effects.

P. Polythene

M. Melinex

H. Howson

G. Glass

——— "Maxorb" absorber

—·—·— Non selective absorber

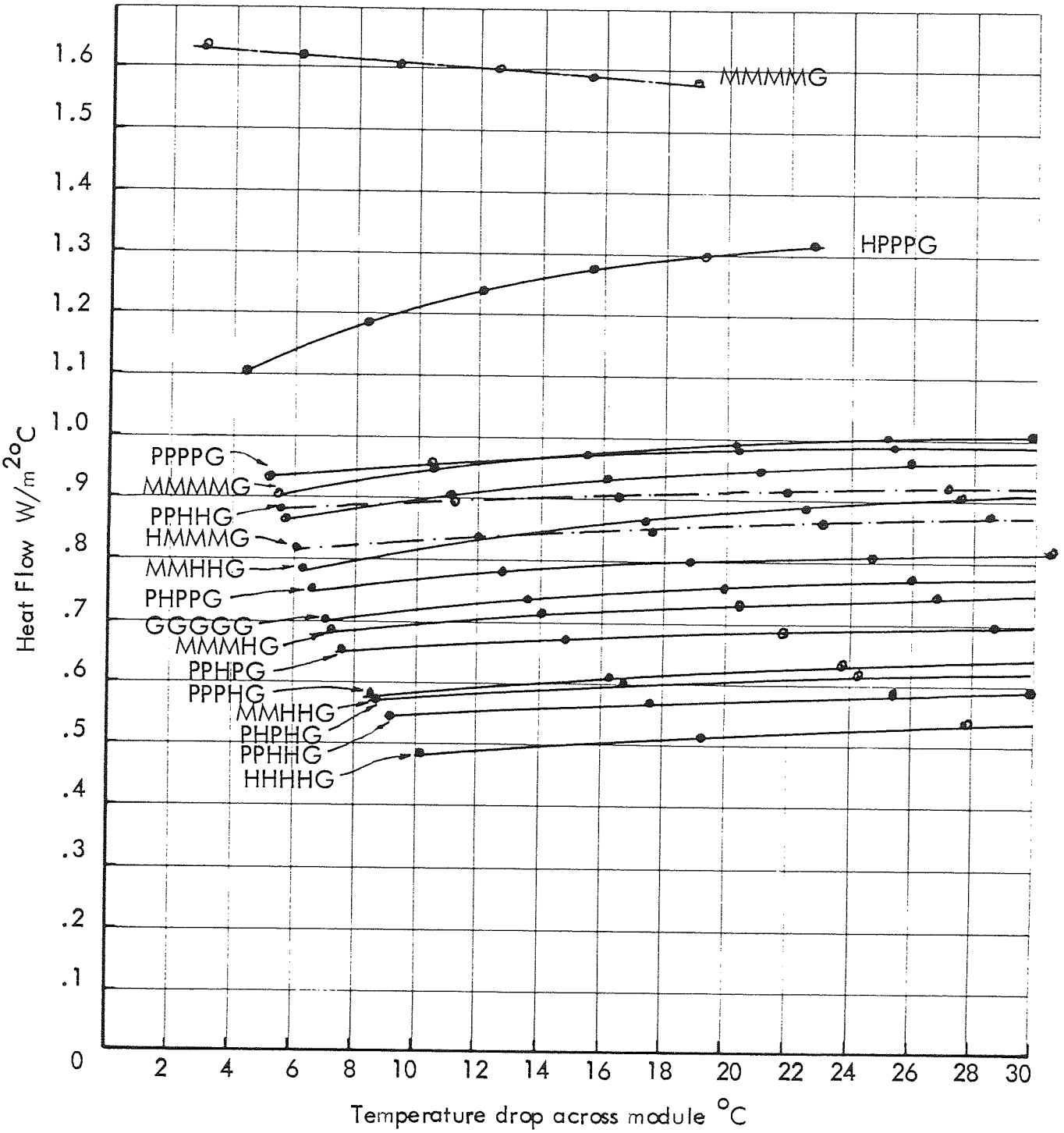

Figure 6.2.

Computed heat transfer characteristics of the solar wall module for various combinations of screens.

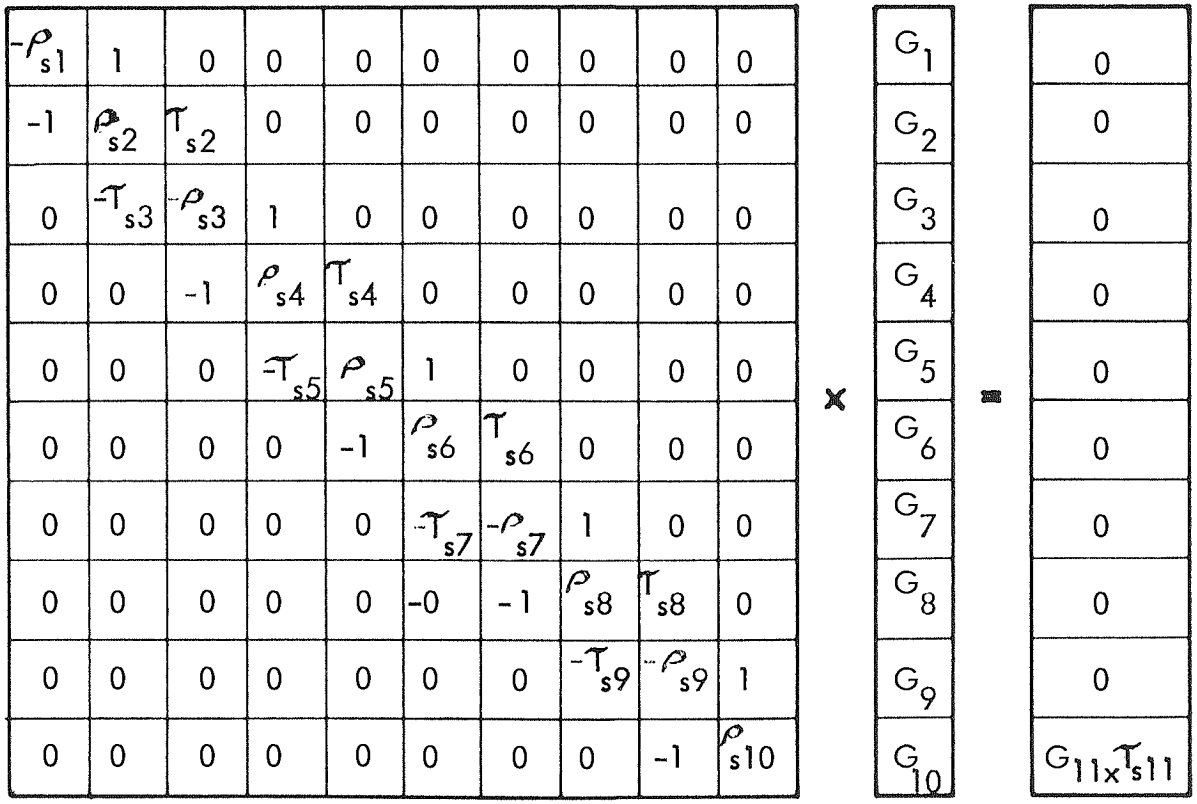

Figure 6.3.

Matrices associated with the computation of the transmission of solar radiation through an array of screens.

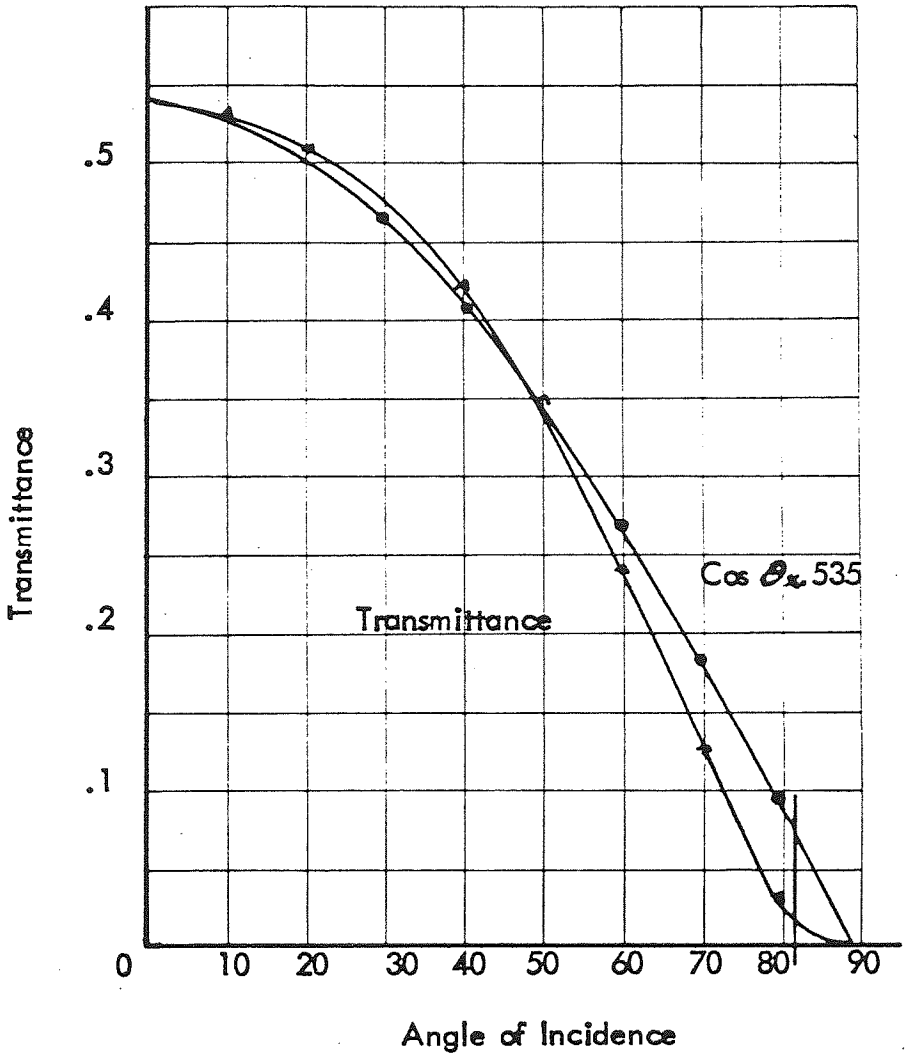

Figure 6.4.

Graph of transmittance versus angle of incidence for a screen array of two inner polythene screens, two "Howson" screens, and a glass outer screen.

GMT	ENERGY W/M^2			
	PAGE		AUTHOR	
	BS	OCST	BS	OCST
6	75	22	59	21
7	193	46	195	47
8	329	70	330	72
9	460	90	461	93
10	571	107	571	109
11	646	117	647	120
12	678	119	679	124
13	663	116	663	121
14	602	109	602	112
15	502	95	502	96
16	375	75	377	76
17	239	51	242	52
18	111	27	75	27
19	25	3	24	0
20	0	0	0	0

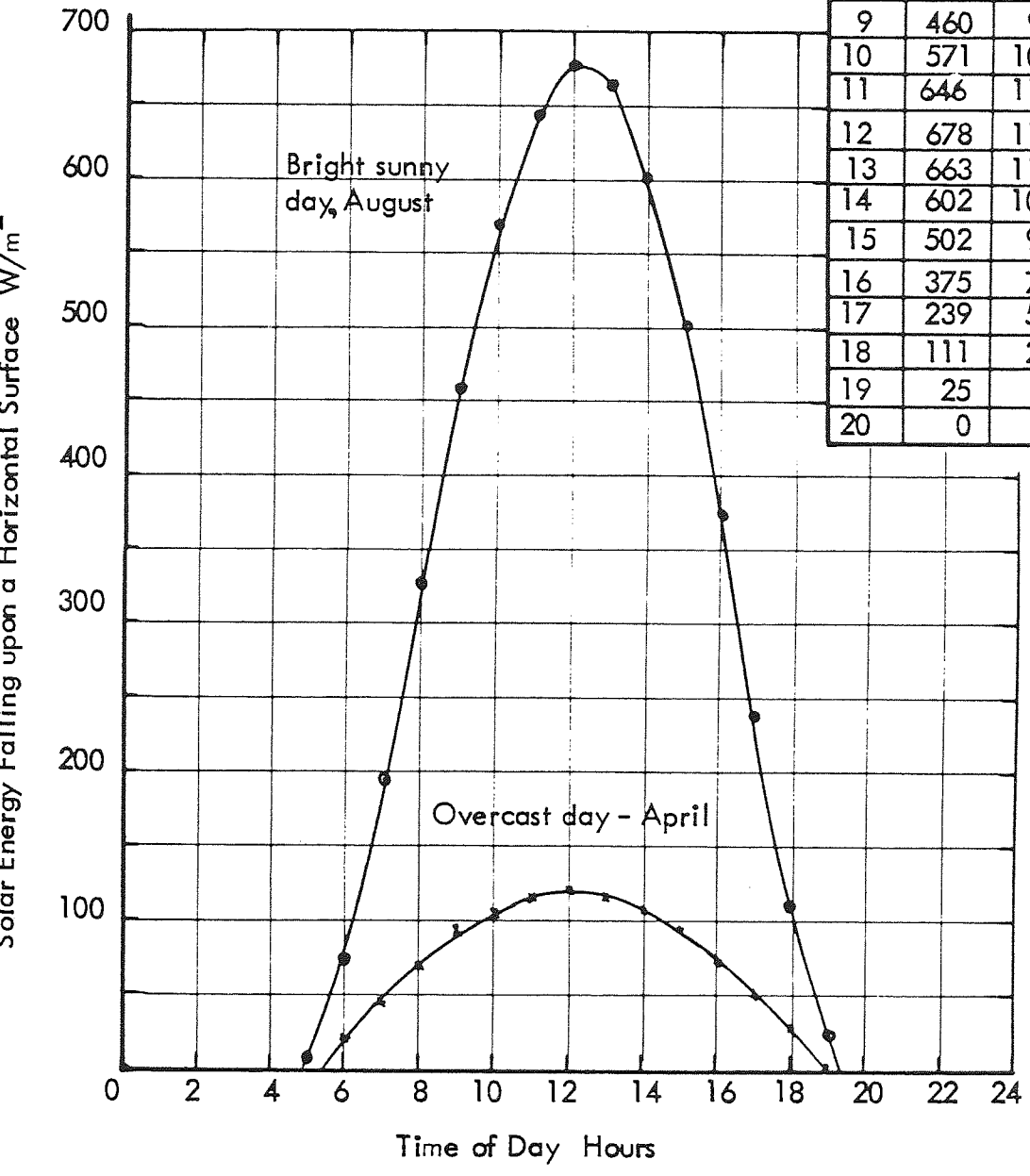

Figure 6.5.

Graph of predicted solar energy falling upon a horizontal surface for clear day and overcast sky conditions, comparing values from Page and the author.

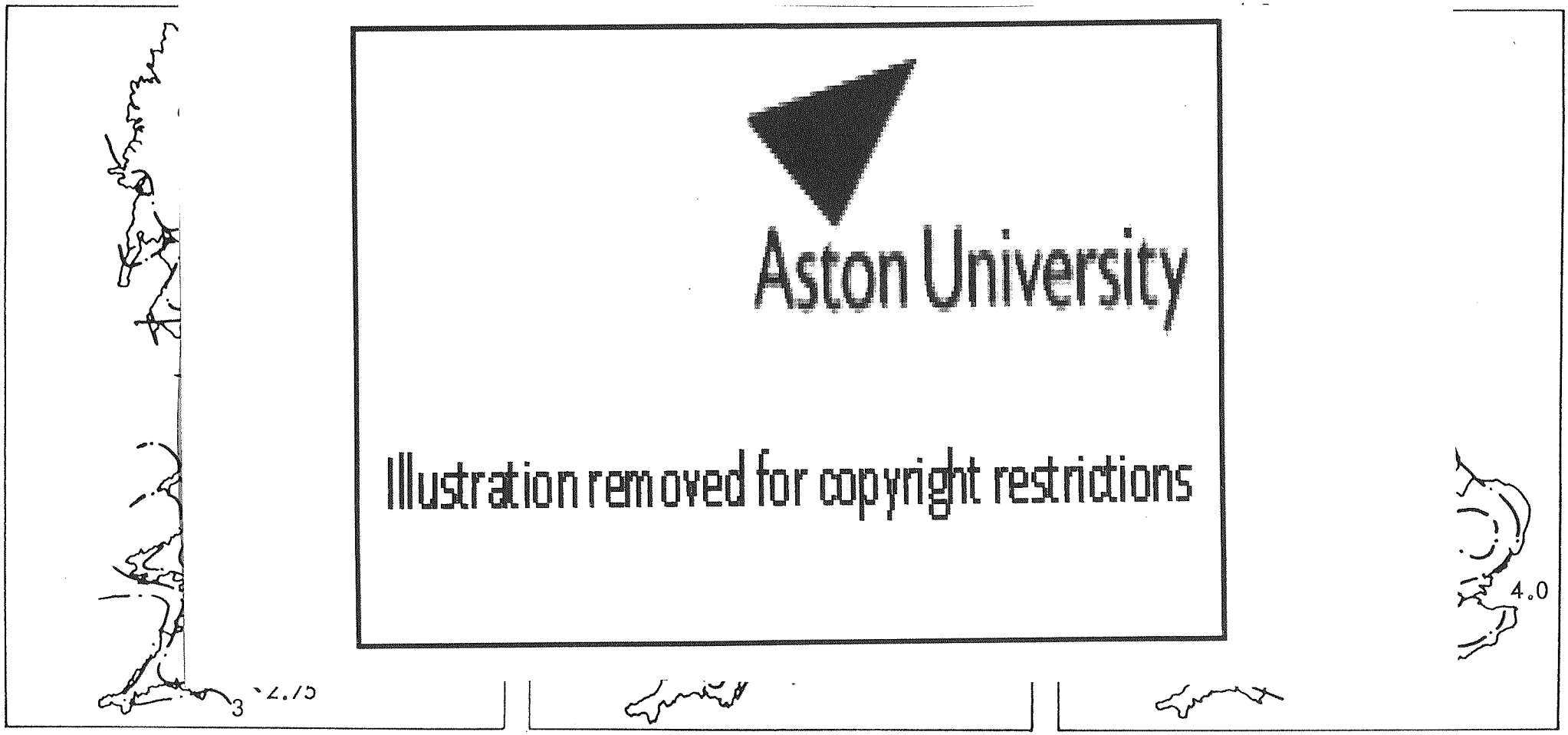

Monthly mean global daily solar irradiation (MJ/M^2). From CIBS (1982)

Monthly mean daily hours of bright sunshine. From Met. Office (1974)

Monthly mean daily temperature °C From Met. Office (1975).

Figure 6.6.

Maps of U.K. monthly mean data for solar irradiation, sunshine hours and temperature for the month of January.

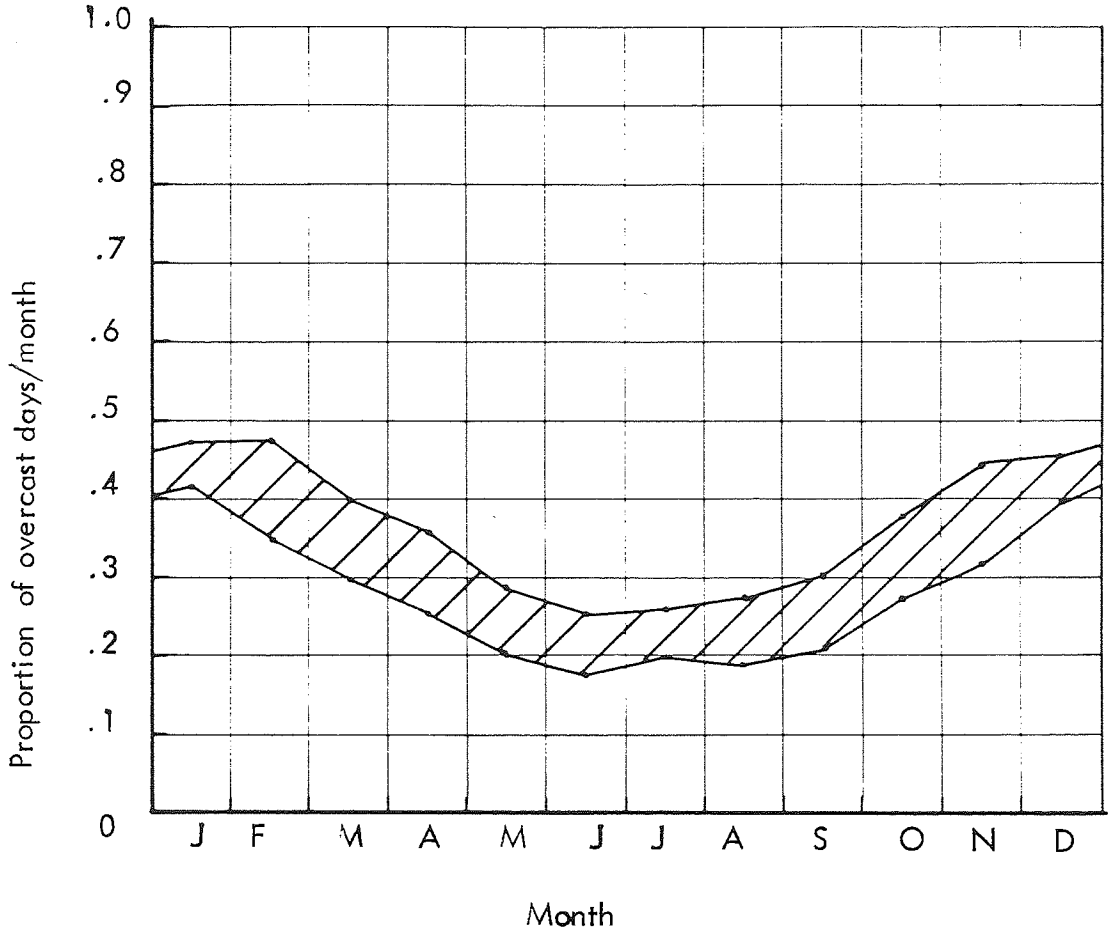

Figure 6.7.

Proportion of overcast days showing the range of values for sites in the north of England and Kew.

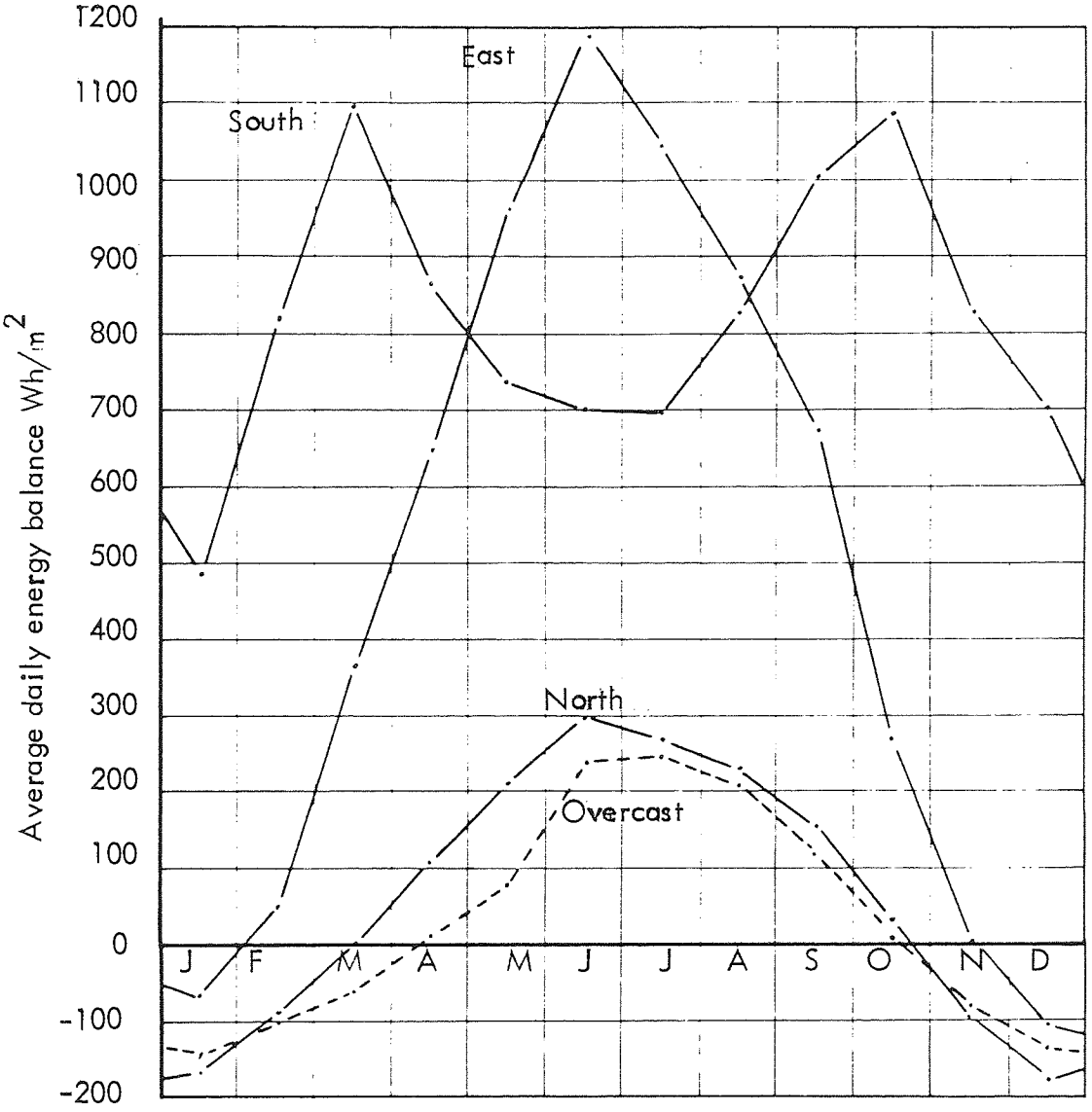

Figure 7.1.

Plot of module energy balance for bright sky conditions with various orientations of wall, and overcast sky conditions.

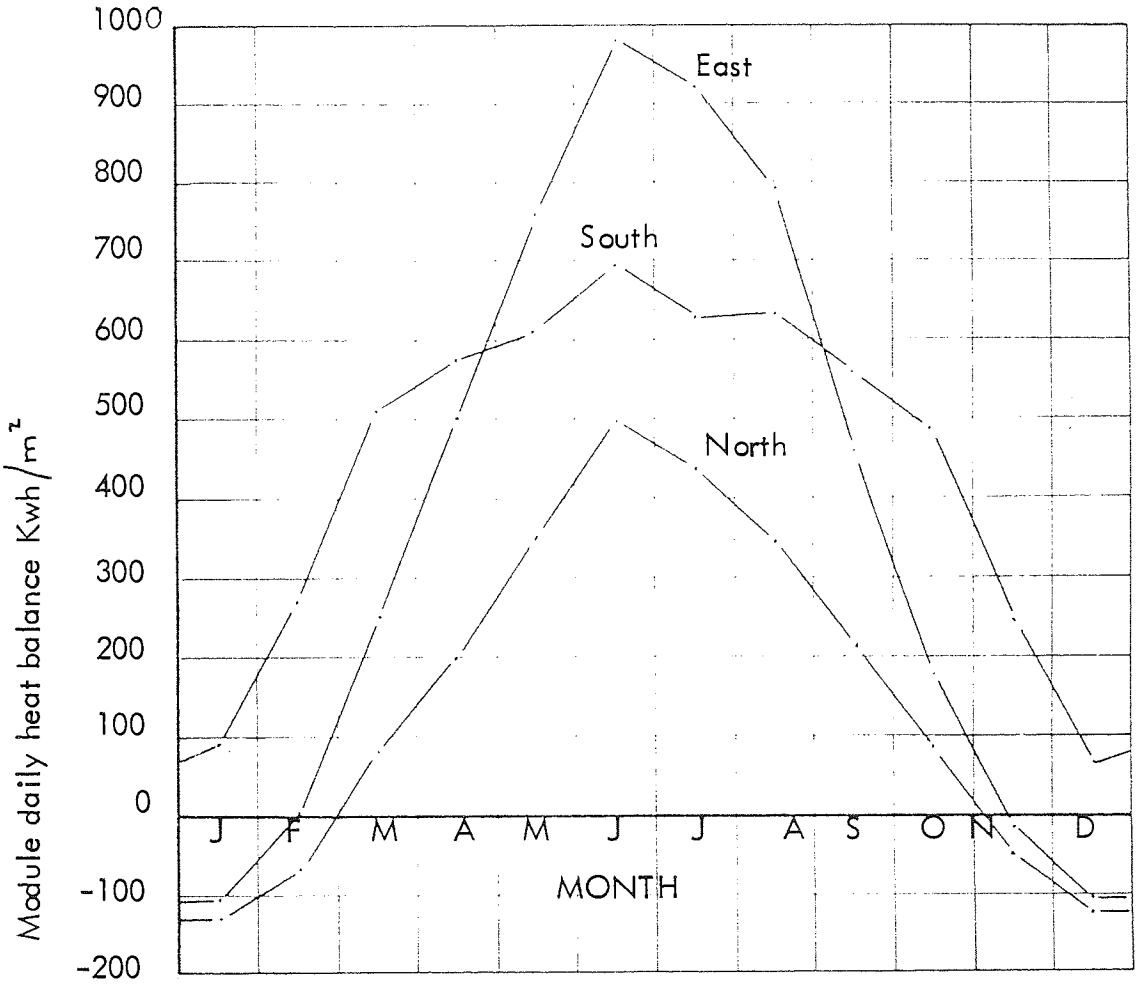

Figure 7.2.

Plot of module daily energy balance for average conditions, module without thermochromic screen.

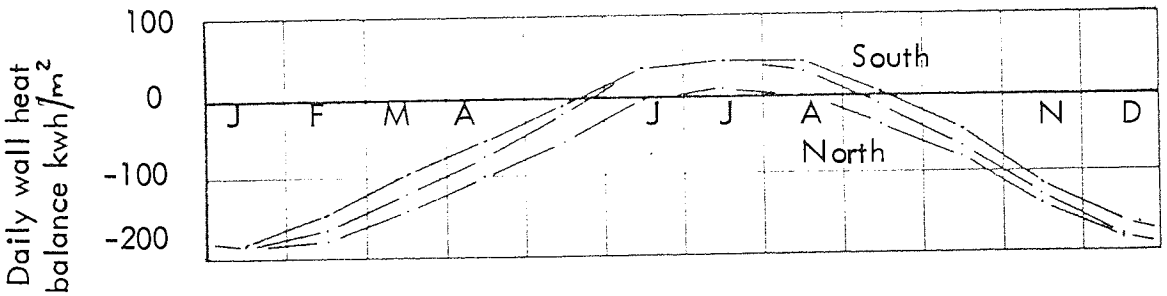

Figure 7.3.

Plot of energy balance for a standard wall with $U = 0.57\ w/m^2K$. Surface absorptance of 0.95.

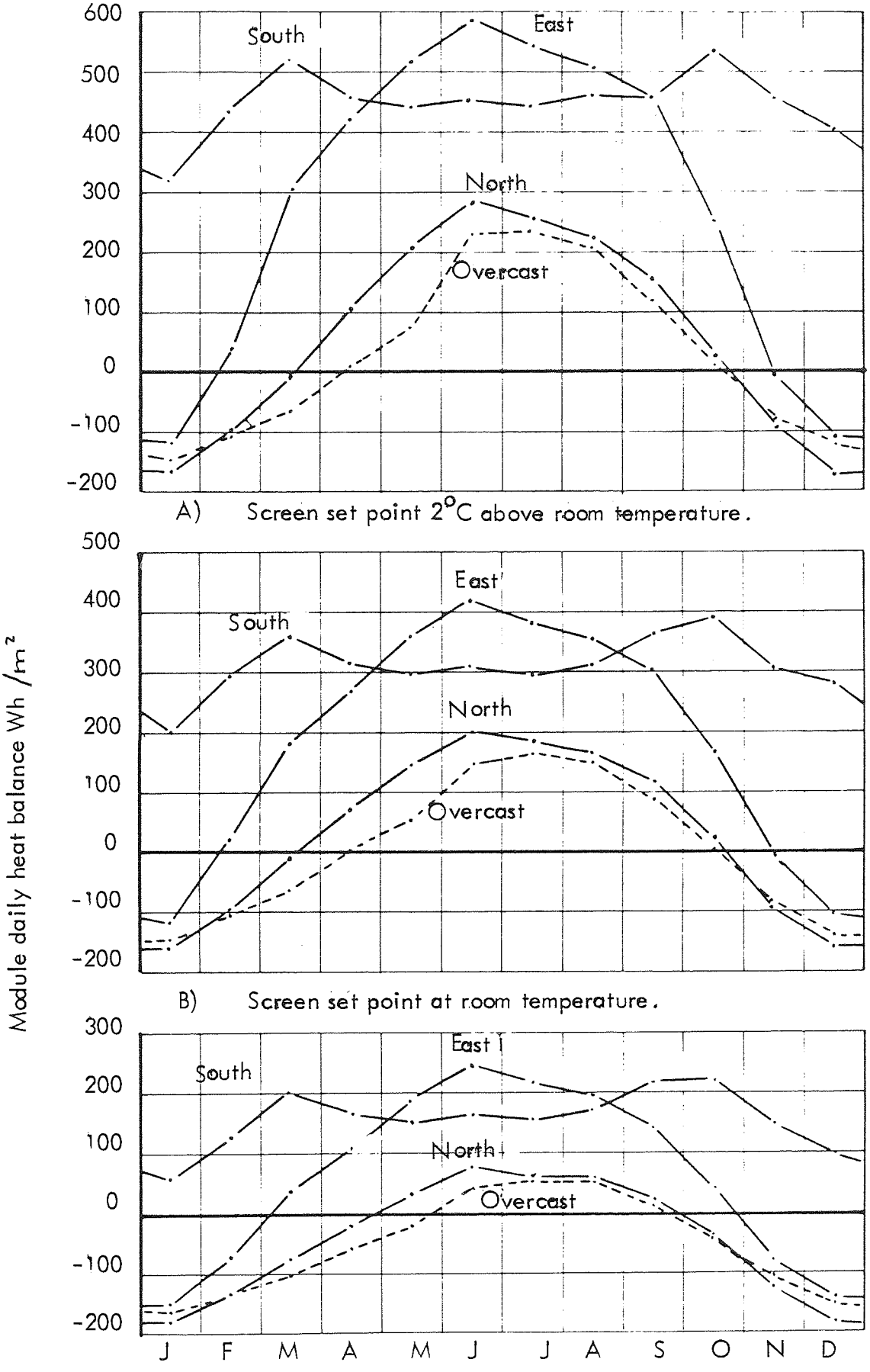

Figure 7.4.

Plots of bright sky and overcast module heat balance for various set points of a thermochromic control screen.

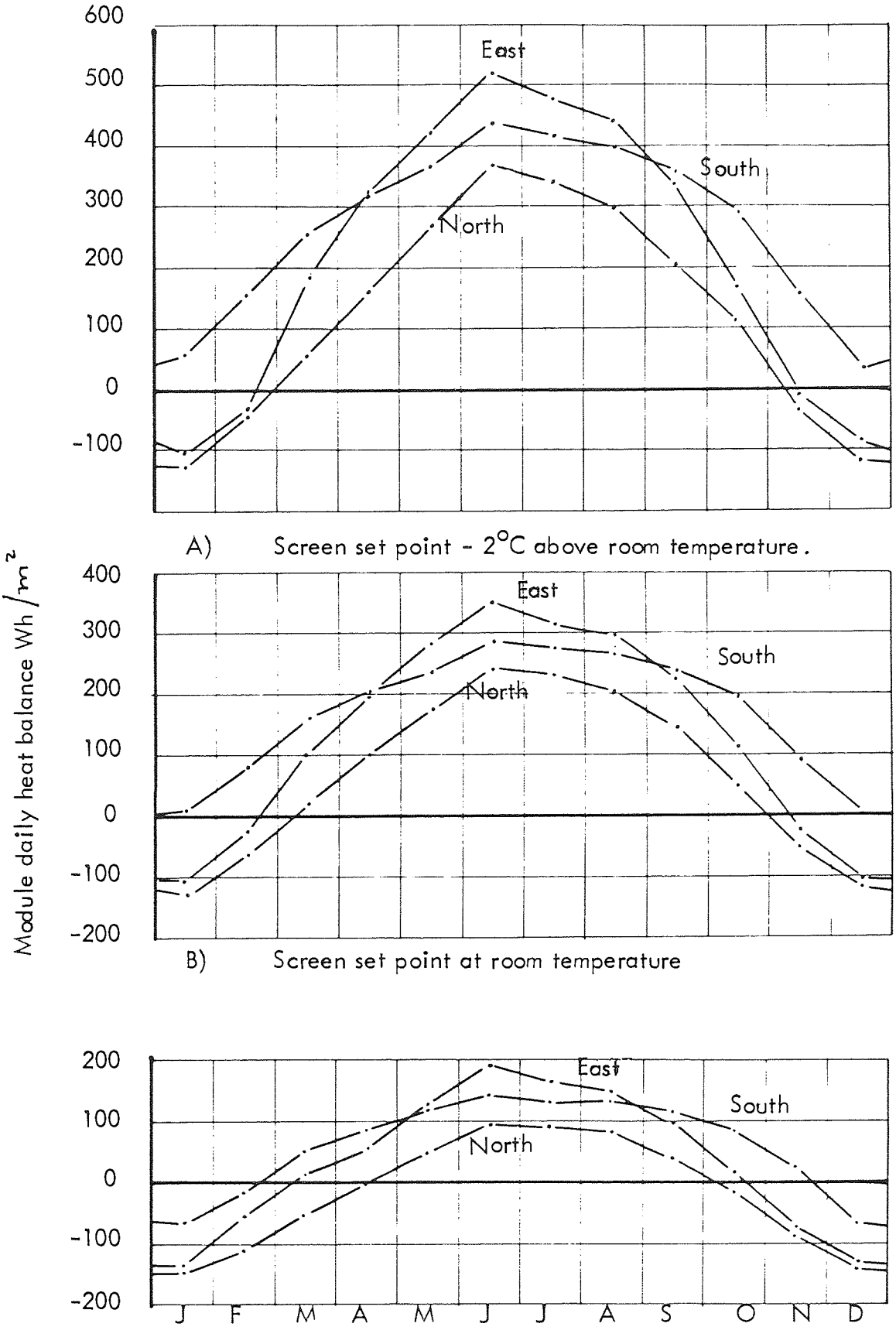

Figure 7.5.

Plots of average module heat balance for various values of thermochromic screen set point.

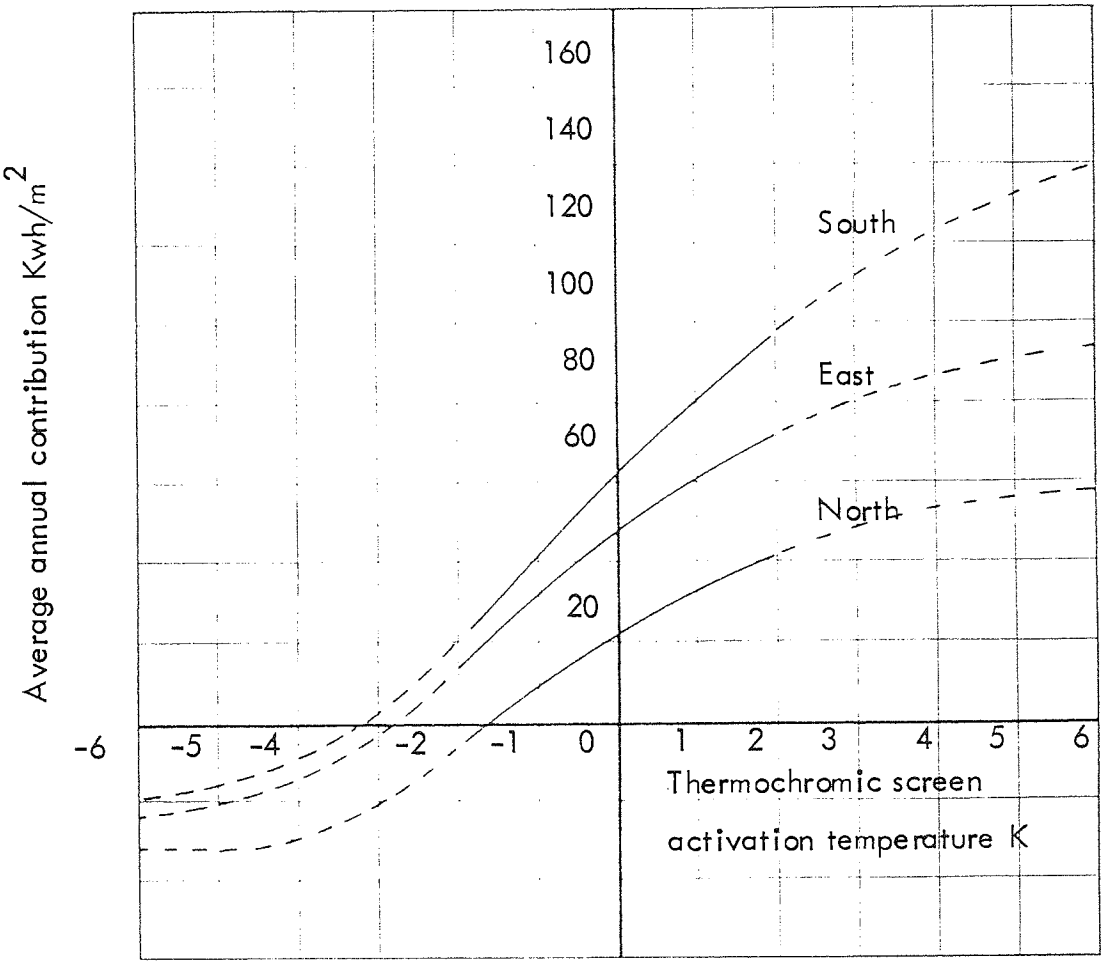

Figure 7.6.

Graph of average annual module energy contribution for various wall orientations and thermochromic screen activation temperatures.

——— interpolated

– – – – extrapolated

Appendix I.

"Maxorb" Solar Foil

MAXORB* Solar Foil

MAXORB* solar foil is a thin nickel foil with a black surface designed for high efficiency solar energy collection. The black surface is produced by a new process which gives the solar foil an outstanding combination of high absorptance, low emittance and high resistance to humidity and thermal degradation. MAXORB* solar foil is supplied as strip, either uncoated or coated with a special pressure-sensitive adhesive which can be used at high temperatures. Coated coils of MAXORB* foil are supplied with a release paper.

Properties:

(a) Foil

Solar absorptance α_s = 0.95 to 0.98

Emissivity (at 100°C) = 0.12 ± 0.03

Tensile Strength > 600 N/mm^2

Resistance to humidity: no degradation of properties after 10 days humidity tests per MIL STD 810C.

Temperature Cycling: no degradation of properties after repeated cycling from −20°C to 200°C.

Breakdown Temperature: adhesive coated foil = 220°C (428°F)

uncoated foil = 315°C (600°F)

(b) Adhesive

The silicone-based adhesive has been used for many years in high temperature applications: for instance, in heat deflectors, high temperature vapour barriers and electrical insulation in aircraft, power plants and motors. It has moisture and weathering resistance, withstanding the effects of sunlight, ozone, fungus and many corrosive chemicals. A clean release may be expected after long term adhesion without leaving a hardened residue or stain.

Availability

MAXORB* solar foil is available in coils with a width of 148 mm and lengths up to 200 metres. Coils in widths up to 1 metre will be available later, and foil of greater thickness could be made available if required.

*Registered Trade Mark

Applications

Principal applications are in flat-plate solar collectors for hot water, air conditioning, de-salination etc.

MAXORB* solar foil can be applied on to flat-plate solar collectors with a minimum of effort and cost compared with other methods of surface preparation such as painting or electroplating. An overall performance increase of 20 to 25% can be expected from a collector made with MAXORB* solar foil compared to black paint in collector systems operating in domestic applications.

Benefits of MAXORB* Solar Foil

- Low capital investment for collector manufacturer — no need for manufacturer to develop expertise in production of large area high quality selective surfaces.
- Prices are very competitive with alternative selective surfaces.
- Minimises collector plate handling and transportation costs that are necessary when using other surface treatments.
- Selective surface of consistent quality.
- Better collector performance than black paint over all weather and hot water conditions.
- Good uniformity.
- Potential of a longer life than painted surfaces.

Appendix 2

Experimental Results.

Results sheet A

Results as calibrated.

Date: 30.6.82

Configuration

Boxes only

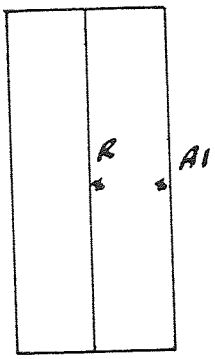

Objective.

Determination of heat loss through boxes

INPUTS	VOLTAGE	CURRENT	REF. t	POWER	RESISTANCE
	2	.33	21.8	.66	6.05
	2.95	.463	29.3	1.36	6.371
	3.8	.577	35.6	2.193	6.584
	4.5	.662	42	2.979	6.797
	5.4	.76	50.3	4.104	7.105

TRANSDUCERS 'A'	1	2	3	4	5	6	7	8	9
	-4.7								
	-10.4								
	-16.2								
	-22.7								
	-30.4								

TRANSDUCERS 'B'	1	2	3	4	5	6	7	8

Results sheet B

Results as calibrated

Date: 25. 6. 82

Configuration.

Boxes with screen carrier

potted transducers

Objective.

Determination of screen carrier heat loss.

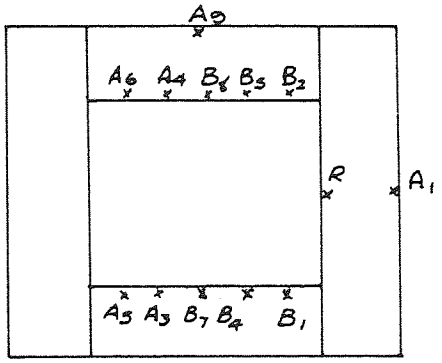

INPUTS	VOLTAGE	CURRENT	REF. t	POWER	RESISTANCE
	3.45	.28	24.4	.966	12.32
	6	.4625	32	2.77	12.97
	7	.531	35.6	3.717	13.182
	9.01	.655	44.2	5.9	13.55
	10	.71	49.3	7.1	14.08

TRANSDUCERS 'A'	1	2	3	4	5	6	7	8	9
	-4.5	—	-.8	-.7	-.7	-.7	—	—	-4.4
	-11.7	—	-2.2	-1.96	-1.95	-1.8	—	—	-11.7
	-15.6	—	-2.85	-2.53	-2.65	-2.35	—	—	-15.7
	- 24	—	-4.3	-3.82	-3.89	-3.44	—	—	-24.1
	-28.8	—	-5.0	-4.5	-4.56	-3.99	—	—	-28.7

TRANSDUCERS 'B'	1	2	3	4	5	6	7	8
	- .8	-.6	—	- .7	- .7	—	- .8	- .7
	-2.14	-1.53	—	-2.03	-1.7	—	-2.18	-1.93
	-2.8	-2.04	—	-2.71	-2.26	—	-2.81	-2.5
	-4.16	-2.97	—	-4.14	-3.37	—	-4.29	-3.73
	-4.92	-3.5	—	-4.8	-3.92	—	-4.45	-4.39

Results sheet C

Results as calibrated

Date: 14. 6.81

Configuration

3mm Glass screens

25mm Gap, sealed with mastic

potted transducers

Objective.

Determination of loss through screen array

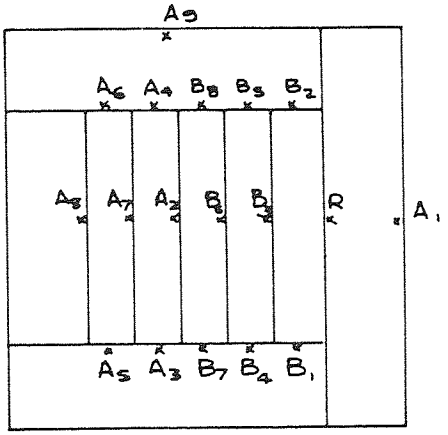

	VOLTAGE	CURRENT	REF. t	POWER	RESISTANCE
INPUTS	2.79	.439	30.3	1.225	6.35
	4.2	.635	37.5	2.667	6.614
	5.2	.762	43.8	3.96	6.82
	6	.858	49	5.148	6.99
	6.9	.96	53.9	6.624	7.185

TRANSDUCERS 'A'	1	2	3	4	5	6	7	8	9
	-6.9	-4.8	- 5.7	- 5.4	- 6.5	- 6.18	- 5.8	- 6.6	- 7.5
	-13.7	-9.4	-11.4	-10.5	-12.9	-11.96	- 11.26	-13	-14.6
	-19.6	-13.2	-16.3	-14.7	-18.4	-16.84	-15.94	-18.4	-20.7
	-25.1	-16.7	-20.8	-18.36	-23.4	-21.23	-20.13	-23.4	-26.2
	-31.7	-20.9	-26.2	-22.96	-29.5	-26.53	-25.23	-29.5	-33.3

TRANSDUCERS 'B'	1	2	3	4	5	6	7	8
	-3.16	-2.12	-2.76	-3.96	-3.34	-3.75	-4.93	-4.37
	-6.43	-3.94	-5.42	-8.14	-6.39	-7.4	-9.95	-8.34
	-9.2	-5.46	-7.58	-11.72	-8.74	-10.36	-14.27	-11.5
	-11.7	-6.67	-9.46	-14.8	-10.9	-13.02	-18.09	-14.38
	-14.66	-8.09	-11.63	-18.6	-13.38	-16.2	-22.8	-17.8

Results sheet D

Results as calibrated.

Date: 16.07.82

Configuration

4 inner screens

polythene, outer-glass

25mm gap

Objective

Determination of heat loss through screens.

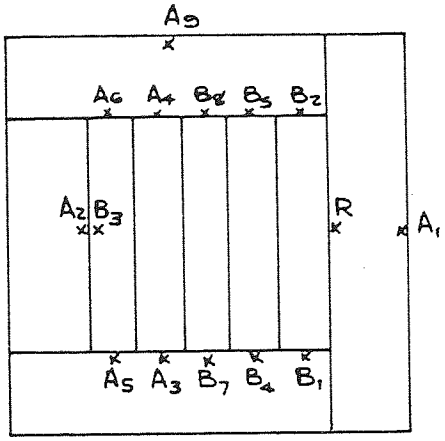

	VOLTAGE	CURRENT	REF. t	POWER	RESISTANCE
INPUTS	3	.46	30	1.38	6.52
	4.2	.643	34.9	2.7	6.53
	5	.741	39.1	3.7	6.75
	6	.87	44.8	5.22	6.89
	7.2	1.01	52	7.27	7.124

TRANSDUCERS 'A'	1	2	3	4	5	6	7	8	9
	- 6.7	- 6.3	- 5.8	- 5.6	- 6.3	- 6.7	-	-	- 7.6
	-11.6	-10.65	- 9.7	- 9.26	-10.76	-10.3	-	-	-12.43
	-15.7	-14.15	- 13	-12.25	-14.25	-13.7	-	-	-16.5
	-21.5	-19.26	- 17.6	-16.55	-19.65	-18.48	-	-	-22.9
	-29.4	-26.2	- 23.75	-22.2	-26.6	-25	-	-	-31.2

TRANSDUCERS 'B'	1	2	3	4	5	6	7	8
	- 4.1	- 3.2	- 6.2	- 4.8	- 4.6	-	- 5.4	- 5.0
	- 6.8	- 5.04	-10.4	- 7.8	- 6.87	-	- 8.9	- 8.12
	- 9.0	- 6.45	- 14	-10.28	- 9.05	-	-11.9	-10.7
	-12.18	- 8.77	-18.8	-14.04	- 12.11	-	-16.12	-14.28
	-16.45	-11.48	-25.5	-18.9	-15.97	-	-21.64	-19.06

Results sheet E

Results as calibrated

Date: 23.07.82

Configuration.

Three polythene inner screens, 4th screen Howson, outer screen glass.

Objective.

Determination of heat loss through screen array

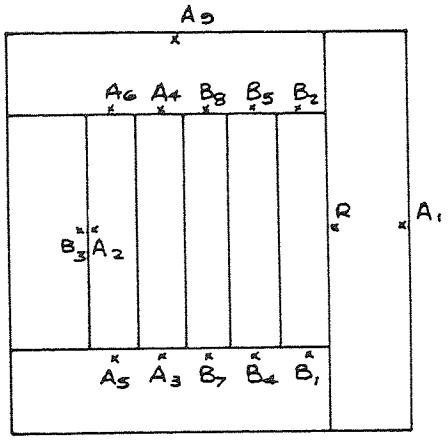

	VOLTAGE	CURRENT	REF. t	POWER	RESISTANCE
INPUTS	3.98	.6125	33.6	2.43	6.49
	5.49	.804	43.2	4.41	6.82
	6.5	.92	50.5	5.98	7.065
	7	.97	54	6.79	7.216
	1.9	.315	23.6	.627	6.03

	1	2	3	4	5	6	7	8	9
TRANSDUCERS 'A'	-.12.1	-12.0	- 9.9	-9.28	-11.4	-10.65	-	-	-12.8
	- 21.1	-20.2	- 16.8	-15.56	- 19.6	-18.12	-	-	- 22.1
	- 27.7	-26.3	- 22	-20.25	- 25.7	-23.6	-	-	- 28.9
	- 31.4	-29.4	-24.6	-22.64	-28.9	-26.38	-	-	-32.6
	- 3.3	- 3.5	- 2.8	-2.6	- 2.9	-2.9	-	-	- 3.4

	1	2	3	4	5	6	7	8
TRANSDUCERS 'B'	-5.93	- 4.33	-12.0	- 7.02	- 6.1	-	- 8.46	- 7.44
	-10.1	- 7.16	-20.5	-11.96	-10.13	-	-14.4	-12.29
	-13.15	- 9.08	-26.8	-15.52	- 12.97	-	-18.64	-15.96
	-14.64	-10.09	-30.1	-17.4	- 14.45	-	-20.75	-17.74
	-1.6	- 1.3	-3.3	- 1.8	- 1.5	-	- 2.2	- 2.1

Results sheet F

Results as calibrated.

Date: 03.08.82

Configuration

Inner two screens polythene outer screen glass.

3rd & 4th screens metalised polyester.

Objective.

Determination of heat loss through screens.

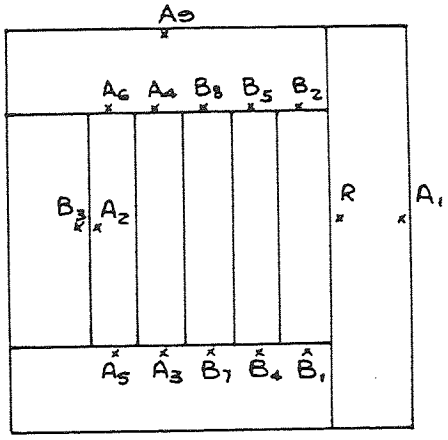

	VOLTAGE	CURRENT	REF. t	POWER	RESISTANCE
INPUTS	2.97	.466	29	1.38	6.37
	4	.605	36.8	2.42	6.61
	5	.733	44.0	3.665	6.82
	5.7	.81	49.8	4.617	7.03
	6.5	.891	56.2	5.79	7.295

	1	2	3	4	5	6	7	8	9
TRANSDUCERS 'A'	-8.1	-8.8	-7.1	-6.5	-8.0	-7.5	-	-	-8.7
	-14.1	-14.7	-12.0	-11.0	-13.8	-12.72	-	-	-14.9
	-20.5	-20.94	-17.3	-15.75	-19.86	-18.29	-	-	-21.5
	-25	-25.35	-21.2	-19.14	-24.45	-22.36	-	-	-26.5
	-31.3	-31.35	-26.0	-23.43	-30.15	-27.34	-	-	-32.6

	1	2	3	4	5	6	7	8
TRANSDUCERS 'B'	-3.35	-2.76	-8.8	-4.3	-3.63	-	-5.54	-4.86
	-5.6	-4.056	-14.8	-7.17	-5.95	-	-9.49	-8.0
	-8.05	-5.67	-21.1	-10.314	-8.38	-	-13.64	-11.36
	-9.82	-6.79	-25.8	-12.57	-10.13	-	-16.67	-13.73
	-12.09	-8.317	-31.7	-15.32	-12.27	-	-20.5	-16.7

Results sheet G

Results as calibrated.

Date: 13.08.82

Configuration.

4 screens only

3 inner screens polythene

outer screen glass

25 mm gap

Objective.

Determination of heat loss through screen array.

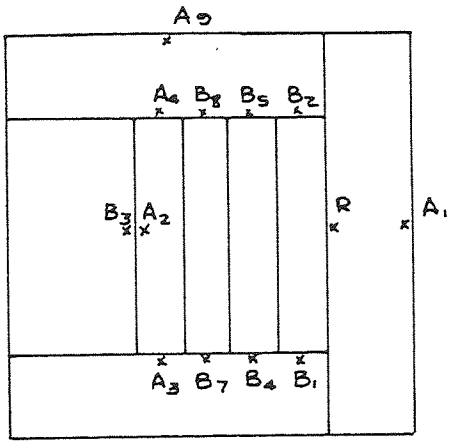

INPUTS	VOLTAGE	CURRENT	REF. t	POWER	RESISTANCE
	1.975	.32	23.8	.632	6.17
	4	.62	32.3	2.48	6.46
	5	.7576	37.9	3.785	6.60
	6.6	.948	47.5	6.256	6.96
	7.2	1.015	51.5	7.308	7.09

TRANSDUCERS 'A'	1	2	3	4	5	6	7	8	9
	-3	-3	-2.8	-2.4	-2.8	-2.4	-	-	-3.1
	-10.6	-9.9	-9.8	-9.2	-10.4	-9.8	-	-	-11.4
	-15.8	-14.2	-14.2	-13.0	-15.3	-14.4	-	-	-16.8
	-24.8	-21.9	-22	-20.0	-23.9	-22.0	-	-	-26.2
	-29.8	-25.2	-25.4	-23.65	-27.7	-25.85	-	-	-30.4

TRANSDUCERS 'B'	1	2	3	4	5	6	7	8
	-1.75	-1.4	-3.1	-2.1	-2.0	-	-2.4	-2.3
	-6.4	-4.8	-10.1	-7.6	-6.6	-	-8.7	-7.8
	-9.5	-6.7	-14.6	-11.1	-9.35	-	-12.73	-11.2
	-14.5	-10.0	-22.4	-17.2	-14.1	-	-19.7	-17.1
	-16.7	-11.4	-25.9	-19.8	-16.3	-	-22.8	-19.6

Results sheet H

Results as recorded

Date: 08.07.82

Configuration.

3mm Glass screens

25mm gap

Transducers on both sides of screens.

Objective.

Screen temperature.

Determination of temperature drop across screens.

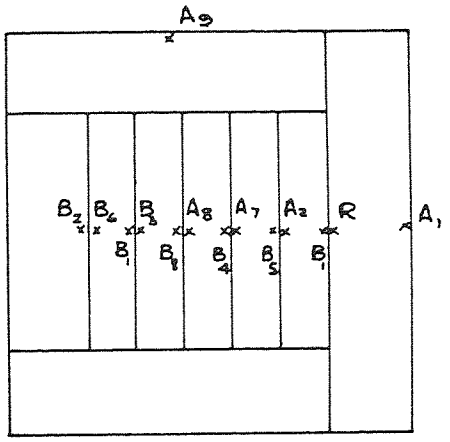

INPUTS	VOLTAGE	CURRENT	REF. t	POWER	RESISTANCE
			28.3		
			33.5		
			42.4		
			52.8		

TRANSDUCERS 'A'	1	2	3	4	5	6	7	8	9
	- 8.2	- 3.3	-	-	-	-	- 4.7	- 5.8	- 8.2
	- 13.9	- 5.1	-	-	-	-	- 7.3	- 9.2	-14.2
	-21.8	-7.8	-	-	-	-	-11.3	-14.2	- 22.3
	-30.4	-10.6	-	-	-	-	-15.5	-19.6	-31.2

TRANSDUCERS 'B'	1.2	2.2	3	4.2	5.2	6	7.2	8.2
	-7	-8.1	-6.8	-4.8	-3.3	-7.9	-.1	-5.8
	-11.6	-13.3	-11.2	-7.6	- 5.3	-13.1	-.2	-9.5
	-18	-20.8	-17.4	-11.6	- 8.1	-20.5	-.2	-14.7
	-24.8	-28.9	-24.2	-16.1	-11.1	-28.6	-.4	-20.3

TRANSDUCER	CALIBRATION SLOPE °C/°C
A1	0
A2	+ .003
A3	0
A4	- .00435
A5	- .00608
A6	- .0143
A7	- .00663
A8	+ .0095
A9	+ .0081
B1	- .00815
B2	+ .0039
B3	- .00967
B4	- .012
B5	- .0126
B6	- .014
B7	+ .0115
B8	- .0095
B22	+.0416
B42	- .0083
B52	- .0093
B7.2	0
B8.2	- .0273

RESULTS SHEET I

TRANSDUCER CALIBRATION SLOPES.

Appendix 3.

Diffuse Radiation Absorbtion

by the Module.

Appendix 3.

Diffuse Radiation Absorption by the Module.

When absorbing diffuse radiation, the module sees a portion of the sky from which radiation is emanating. The sky will be emanating with some sort of distribution of energy, and the absorber of the module will have a proportion of its view of the sky blocked by the sides of the module. Furthermore, the radiation from the sky will be attenuated by the module screen array, and a proportion of it will be reflected by the sides of the module onto the absorber surface.

This results in a complex analysis which is indicated as follows, starting with the simplest case, and progressing towards consideration of the module.

1) Isotropic Sky, Plane Surface

The isotropic sky is that associated with the general constant background irradiation of a bright clear day, as explained in Chapter 6.3.1.

Referring to Figure A.3.1.

The sky vault is considered as the total of a series of elemental areas defined by the element $\delta\theta, \delta\beta$. And we can say that the apparent area of a horizontal surface viewed from that sky vault element is

$$a \cos \theta \qquad \text{A.3.1}$$

The solid angle subtended by this apparent area to the sky element is thus

$$a \cos \theta / r^2 \qquad \text{A3.2.}$$

And the area of the sky vault element is

$$r\,\delta\theta \times r\,\delta\beta \quad \text{Sin}\ \theta = r^2\ \text{Sin}\ \theta\,\delta\theta\,\delta\beta \qquad \text{A 3.3}$$

If the unit radiance of the sky vault is then $\bar{L}$ watts/m^2 steradian, the flux upon the horizontal area is defined by:

$$\bar{L}_r{}^2\ \text{Sin}\ \theta\,\delta\theta\delta\beta \times a\ \text{Cos}\ \theta/_r{}^2$$

$$= \bar{L}a\,\text{Sin}\ \theta\ \text{Cos}\ \theta\ \delta\theta\ \delta\beta \qquad \text{A 3.4.}$$

Integrating for all values of θ and β we have

$$I_H = \bar{L}a \int_{\beta=0}^{2\pi} \int_{\theta=-\pi/2}^{\pi/2} \text{Sin}\ \theta\,\text{Cos}\ \theta\,d\theta\,d\beta$$

$$= \bar{L} \int_0^{2\pi} a\ \tfrac{1}{4}\left[\text{Cos}\ 2\theta\right]_{-\pi/2}^{\pi/2} d\beta = \pi\,\bar{L}a \qquad \text{A 3.5.}$$

Similarly for a vertical surface,

$$I_v = \bar{L}a \int_{\beta=-\pi/2}^{\pi/2} \int_{\theta=0}^{\pi/2} \text{Sin}^2\theta\ \text{Cos}\beta\,d\theta\,d\beta$$

$$= \bar{L} \int_{-\pi/2}^{\pi/2} a\ \frac{\text{Cos}\ \beta}{2} \times \left[\theta - \tfrac{1}{2}\,\text{Sin}\ 2\theta\right]_0^{\pi/2} d\beta \qquad \text{A 3.6.}$$

$$= \pi/2\ \bar{L}a$$

Thus, as might have been expected for an isotropic sky, the ratio of energy falling upon a vertical surface, to that on a horizontal surface is 0.5.

2. Non Isotropic Sky, Plane Surface.

However, the distribution of energy in an overcast sky has been found to be such as to reach a maximum at the apex, and reduce towards the horizon. The precise nature of this variation in radiance is not clear, Moon and Spencer (1942) proposed that this function is:

$$\bar{\bar{L}} \times \tfrac{1}{3}(1 + 2\cos\theta) \quad \text{where } \bar{\bar{L}} \text{ is the zenith radiance.}$$

Substituting this value in the horizontal and vertical expressions for horizontal and vertical surfaces we find:

For horizontal surfaces.

$$I = \frac{\bar{\bar{L}}_a}{3} \int_{B=0}^{2\pi} \int_{\theta=-\pi/2}^{\pi/2} \cos\theta \sin\theta + 2\cos^2\theta \sin\theta \, d\theta \, d\beta$$

$$= \frac{\bar{\bar{L}}_a}{3} \int_{\beta=\theta}^{2\pi} \tfrac{1}{4}\left[-\cos 2\theta\right]_{-\pi/2}^{\pi/2} + \tfrac{2}{3}\left[-\cos\theta\right]_{-\pi/2}^{\pi/2} \, d\beta$$

$$= \frac{7\pi}{9} \times \bar{\bar{L}}_a \qquad \text{A 3.7.}$$

For vertical surfaces.

$$I = \frac{\bar{\bar{L}}_a}{3} \int_{\beta=-\pi/2}^{\pi/2} \int_{\theta=0}^{\pi/2} \sin^2\theta \cos\beta + 2\sin^2\theta \cos\beta \cos\theta \, d\theta \, d\beta$$

$$= \frac{\bar{\bar{L}}_a}{3} \int_{-\pi/2}^{\pi/2} \frac{\cos\beta}{2} \times \left[\theta - \tfrac{1}{2}\sin 2\theta\right]_0^{\pi/2} + \tfrac{2}{3}\cos\beta \left[\sin\theta\right]_0^{\pi/2} d\beta$$

$$= \frac{\bar{\bar{L}}_a}{3} \left(\pi/2 + 4/3\right) \qquad \text{A 3.8.}$$

This indicates a vertical to horizontal ratio of 0.414. These same proportions are reported by Walsh (1961) and Page (1977).

Steven (1977) in his more recent work has established a relationship for the sky vault radiance of

$$\bar{L} \times \frac{(1 + 1.4 \cos\theta)}{1 + 1.4} \qquad \text{A 3.9.}$$

If we consider that the radiance can be represented by a function of the form $\gamma(\alpha + 2 \cos\theta)$ we can use this as a general case which can be employed to establish the vertical/horizontal relationship dependent upon the factors γ and α.

3. Non Isotropic Sky, Module Self Shading

Before considering the situation of the module, it is necessary to define the value of the shading angles which are formed by the sun, or an element of sky vault.

Figure A.3.2. indicates the angles in question. S is termed the vertical wall shadow angle, and β the horizontal wall shadow angle.

The horizontal wall shadow angle is easily determined from the solar bearing and the wall azimath angle, as shown in Chapter 6.3.1.

The vertical wall shadow angle is given by

$$S = \text{Tan}^{-1} (\text{Tan}\ \theta \times \cos\beta) \qquad \text{A.3.10.}$$

The area of absorber which is directly illuminated by a sky vault element is given by

$$A_A = (H - \frac{T}{\tan\theta \cos\beta}) \times (L - T\tan\beta)$$

$$= (HL - \frac{TL}{\tan\theta\cos\beta} - \frac{HT\sin\beta}{\cos\beta} + \frac{T^2\sin\beta\cos\theta}{\cos\beta\sin\theta\cos\beta} \qquad \text{A.3.11.}$$

This area subtended to an element of sky is

$$A_{As} = HL\sin\theta\cos\beta - TL\cos\theta - HT\sin\beta\sin\theta + \frac{T^2\sin\beta\cos\theta}{\cos\beta}$$

This results in the energy falling directly upon the absorber of

$$E_{AD} = I \times \tau \times A_{AS} \qquad \text{A.3.12.}$$

Where τ = transmission of the screen array; but Figure 6.4. indicates that

$\tau \simeq \tau n \cos$ (incidence angle).

Where τn is the normal transmission and this can be shown to be

$$\tau \simeq \tau n \cos\beta \sin\theta \qquad \text{A.3.13.}$$

Substituting this, gives

$$EAD = I \times \tau_n \{HL\cos^2\beta\sin^2\theta - TL\cos\beta\sin\theta\cos\theta - HT\sin\beta\cos\beta\sin^3\theta + T^2\sin\beta\cos\theta\sin\theta\}$$

$$\text{However } I = \bar{L} \times \gamma (\alpha \sin\theta + 2\sin\theta\cos\theta) \qquad \text{A.3.14.}$$

$$\text{Then } EAD = \bar{L} \times \tau n \times \gamma \{(\alpha\sin^3\theta + 2\sin^3\theta\cos\theta)\times(HL\cos^2\beta - HT\sin\beta\cos\beta) + (\alpha\sin^2\theta\cos\theta + 2\sin^2\theta\cos^2\theta)\times(T^2\sin\beta - TL\cos\beta)\} \qquad \text{A.3.15.}$$

However, energy from the sky vault also falls upon the sides of the module and is then reflected onto the absorber. The effect of double reflection from side to base to absorber and vice versa is neglected.

In a similar way to the derivation of EAD, the energy reflected from the sides to the absorber can be determined as follows.

$$\text{Area of base illuminated} = L \times T - \frac{T^2}{2} \tan\beta$$

$$\text{Subtended area} = (L \times T - \frac{T^2}{2} \tan\beta) \cos\theta$$

$$\text{Area of side illuminated} = HT - \frac{T^2}{2 \tan\theta \cos\beta}$$

$$\text{Subtended side area} = (HT - \frac{T^2}{2 \tan\theta \cos\beta}) \times \sin\theta \times \sin\beta \qquad \text{A.3.16.}$$

The total energy reflected onto the absorber is

$$I \times T_n \times \rho \times (\sin\theta \cos\theta (LT\cos\beta - T^2 \sin\beta) + HT \sin\beta \cos\beta \sin^2\theta)$$

Where ρ = reflectance of the module sides.

$$\text{Then } E_{AR} = \bar{L} \times T_n \times \rho \times \gamma \{ \alpha \sin^2\theta \cos\theta (LT\cos\beta - T^2 \sin\beta) + HT\alpha \sin\beta \cos\beta \sin^3\theta + 2\sin^2\theta \times \cos^2\theta (LT\cos\beta - T^2 \sin\beta) + 2HT \sin\beta \cos\beta \sin^3\theta \cos\theta \}$$

Rearranging

$$E_{AR} = \bar{L} T_n \gamma \{ (\rho LT\cos\beta - \rho T^2 \sin\beta) \times (\alpha \sin^2\theta \cos\theta + 2\sin^2\theta \times \cos^2\theta) + \rho HT \sin\beta \cos\beta \times (\alpha \sin^3\theta + 2\sin^3\theta \cos\theta) \} \qquad \text{A.3.17.}$$

Combining E_{AR} and E_{AD} we have the total energy falling on the absorber.

$$ET = \bar{\bar{L}}\,T_n\,\gamma\left\{H\cos\beta\,(L\ \cos\beta + T\sin\beta\,(\rho - 1))x(\alpha\sin^3\theta + 2\sin^3\theta\cos\theta)\right.$$
$$\left.+(T^2\sin\beta(1-\rho)+ TL(\rho-1)\cos\beta)x(\alpha\sin^2\theta\cos\theta + 2\sin^2\theta\cos^2\theta)\right.$$

A.3.17.

This term can now be integrated between the limits defined by the maximum wall shadow angles as follows:

$$E = \bar{\bar{L}} \times T_n \times 2 \times \gamma \int_{\beta=0}^{A_{TN}(L/T)} \int_{\theta = A_{TN}(T/H\cos\beta) = z}^{\pi/2} f(\theta,\beta)\,d\beta\,d\theta \qquad \text{A.3.18.}$$

The integrals involved in this first integration are:

Function	Integral	Definate integral value
$\sin^3\theta$	$\frac{1}{3}\cos^3\theta - \cos\theta$	$\cos Z - \cos^3(Z)/3$
$\sin^3\theta\cos\theta$	$\frac{1}{4}\sin^4\theta$	$.25 - (\sin^4 Z)/4$
$\sin^2\theta\cos\theta$	$\frac{1}{3}\sin^3\theta$	$\frac{1}{3} - (\sin^3 Z)/3$
$\sin^2\theta\cos^2\theta$	$\theta/8 - \frac{\sin 4\theta}{32}$	$\pi/16 - Z/8 + \sin 4Z/32$

Which gives

$$E_T = \bar{\bar{L}} \times T_n \times 2 \times \gamma \int_{\beta=0}^{A_{TN}\,L/T} \left\{H\cos\beta\,(L\cos\beta + T\sin\beta\,(\rho-1))x(\alpha(\cos Z - \frac{\cos^3 Z}{3} + 2(.25 - \frac{\sin^4 Z}{4})) + (T^2\sin\beta(1-\rho)+TL(\rho-1)\cos\beta)\right.$$
$$\left.x(\alpha(\tfrac{1}{3} - \frac{\sin^3 Z}{3}) + 2(\pi/16 - Z/8 + \frac{\sin 4Z}{32})\right\}\,d\beta$$

A.3.19.

For an isotropic sky, the corresponding expression is

$$E_T = \bar{L}\tau_n \times 2 \int_0^{A_{TN}\, L/T} \left\{ H \cos\beta (L \cos\beta + T \sin\beta (\rho - 1)) \times (\cos Z - \frac{\cos^3 Z}{3}) + (T^2 \sin\beta (1-\rho) + T L \cos\beta (\rho - 1) \times (\frac{1}{3} - \frac{\sin^3 Z}{3}) \right\} d\beta$$

These expressions must be integrated numerically, and results are indicated graphically in Figure A.3.3.for a metre square module with .125m sides, neglecting the terms to the left of the integral sign.

As can be seen, the values are relatively insensitive to module depth and side reflectance. The ordinate points are 0.666 for the case of Stevens sky distribution, and 1.047 for the isotropic case.

These can be checked by considering the integral term with T set to zero in which case the integral term is (from A.3.8.):

$$\iint (\alpha \sin^2\theta \cos\beta + 2 \sin^2\theta \cos\theta \cos\beta) \times \sin\theta \cos\beta \, d\beta \, d\theta$$

$$= \int_0^{\pi/2} \cos^2\beta (\alpha - \tfrac{2}{3} + \tfrac{1}{2}) \qquad \text{A.3.20}$$

= 0.664 for the Stevens distribution which compares favourably with the numerical integration value of 0.660 using Simpsons rule.

The equivalent term for a horizontal surface is 2.52 in consequence of which the vertical/horizontal ratio for the Stevens distribution for the module is 0.263, and for the isotropic sky is .312.

From which it follows that the energy falling upon the absorber from the Stevens sky is $0.263 \times \tau_n$ of the horizontal surface value, and

$.312 \times \tau_n$ for an isotropic sky, with perfectly reflecting module sides, and or zero thickness of module.

4. Energy absorbed by the glass screen

From Chapter 4.2. the energy absorbed is given by:

$$E_A = (1 - e^{-KL/\cos\phi})$$

Where ϕ = angle of incidence.

For diffuse radiation, the energy absorbed, assuming a non isotropic sky is:

$$= \frac{\bar{L} \times a}{3} \int_{\beta=-\pi/2}^{\pi/2} \int_{\theta=0}^{\pi/2} (\sin^2\theta \cos\beta + 2\sin^2\theta \cos\beta \cos\theta) \times (1 - e^{-KL/\sin\theta \cos\beta}) d\beta \; d\theta$$

A.3.21

This is a difficult calculation, and to simplify matters, the author has assumed an isotropic sky distribution. For such a distribution, Branden Muhl and Beckman (1980) have demonstrated that the incident radiation can be regarded as having an effective incidence angle of 60°, in which case,

$$E_a = (1 - e^{-KL/\cos\ 60)} \qquad \text{A.3.22}$$

If we assume an extinction coefficient of 10, and a thickness of 5mm, this results in a value of 0.095, and in consequence a value of 0.1 is assumed, i.e. for diffuse radiation, the outer glass screen of the module is assumed to absorb 10% of incident radiation.

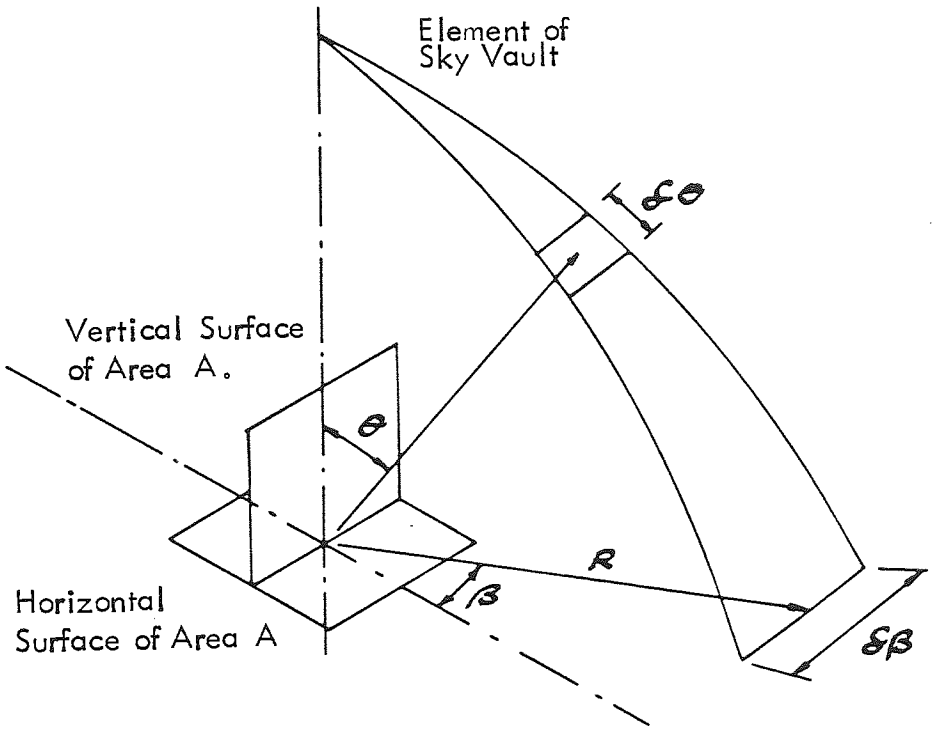

Figure A.3.1.

Showing the relationship between the zenith angle and the horizontal wall shadow angle, for an element of sky vault, in the analysis of diffuse radiation absorption by the module.

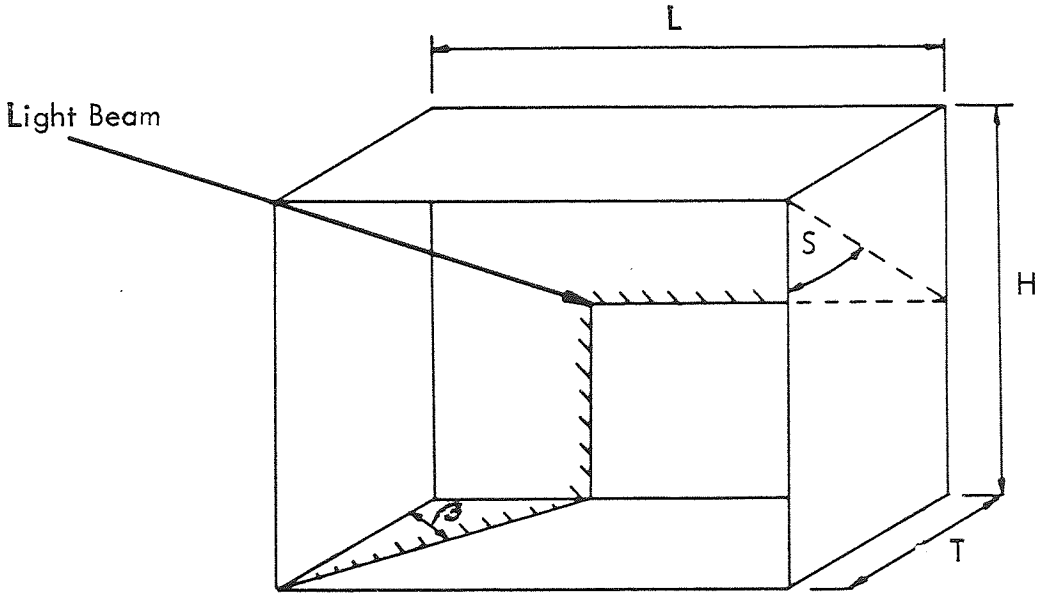

$TAN\,S = TAN\,\theta\,COS\beta$

For vertical side, area of side subtended = $A\,SIN\,\theta\,SIN\beta$

For horizontal side, area of side subtended = $A\,COS\,\theta$

For vertical back face, area of back subtended = $a'\,COS\beta\,SIN\,\theta$

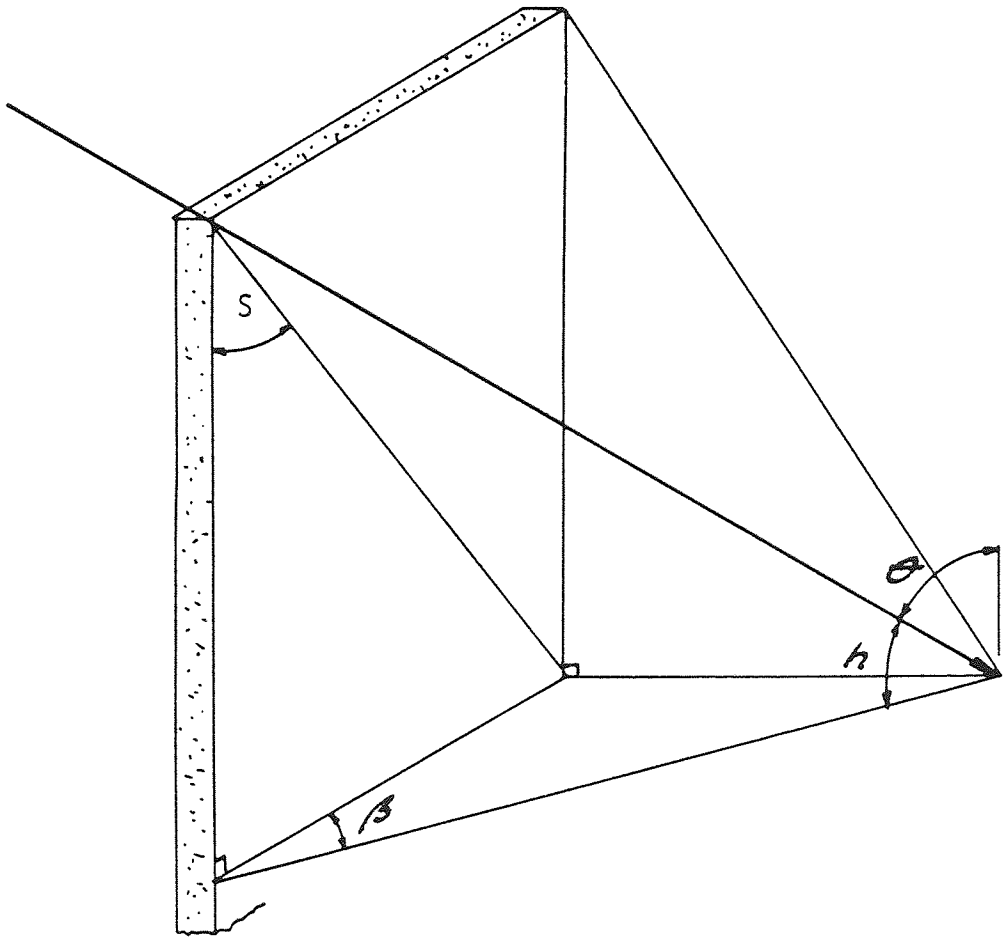

Figure A.3.2.

Relationship between the horizontal and vertical wall shadow angles, and the solar azimuth and altitude.

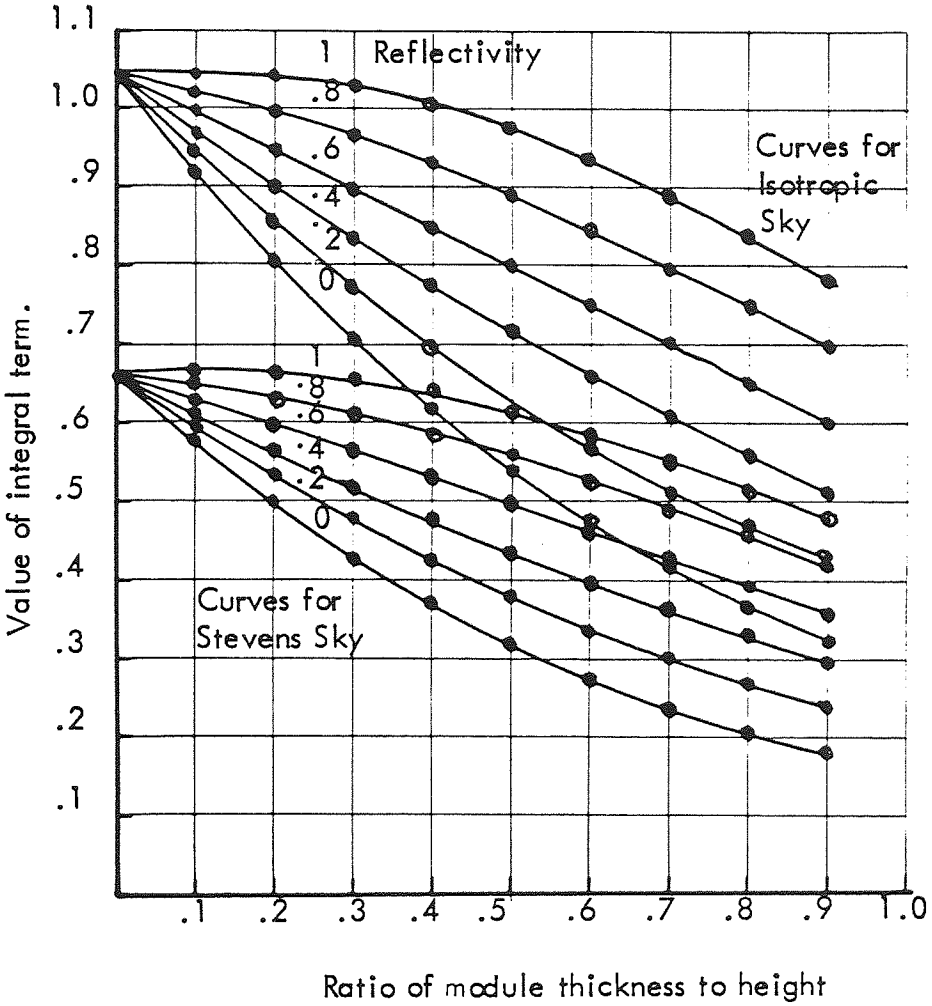

Figure A.3.3.

Graph of the integral terms for isotropic and Steven's skies versus the ratio of module thickness to height for a square module, for various values of wall reflectance.

Appendix 4.

Computer Programes.

Appendix 4.1.

Thermal Losses From The Experimental Apparatus.

```
10    REM    PROG5
20    REM     THIS PROGRAM CALCULATES THE HEAT FLOW THROUGH THE EXPERIMENTAL
30    REM     EQUIPMENT DESCRIBED IN CHAPTER 5.  THE OUTPUT INDICATES THE
40    REM     APPROPRIATE OUTER SCREEN MEAN TEMPERATURE FOR A GIVEN
50    REM     COMBINATION OF SCREEN ARRAYS, AND REFERENCE TEMPERATURE DIFFERENCE.
60    REM
70    REM    ETAS IS THE EMITTANCE OF THE SCREEN CARRIER SIDES
80    REM    ROS IS THE REFLECTANCE OF THE SCREEN CARRIER SIDES
90 ETAS=.9: ROS=.1
100    REM
110    REM    A1 IS THE AREA OF THE SCREEN, A2 THE AREA OF THE CELL SIDES
120    REM
130    REM    FA, FC, FB AND FD ARE RADIATION FORM FACTORS DESCRIBED IN CHAPTER 411
140 FA=.86: FB=.14: FC=.45: FD=.1
150    REM
160    REM     THE FOLOWING LINES SET THE RADIANT CHARACTERISTICS OF
170    REM     THE SCREENS
180    REM     ETA, RHO AND TOR ARE EMITTANCE, REFLECTANCE AND TRANSMITTANCE.
190 M1$="MAXORB"
200 MTEL$=M1$
210 GOSUB 550
220 ETA1=ETAB : RO1=1-ETA1
230    REM
240 INPUT "1ST SCREEN MATERIAL", M2$
250 MTEL$=M2$
260 GOSUB 550
270 ETA2=ETAA : ETA4=ETAB : TOR2=TORA: TOR4=TORB: RO2=1-ETA2-TOR2
280 RO4=1-ETA4-TOR4
290    REM
300 INPUT "2ND SCREEN MATERIAL", M3$
310 MTEL$=M3$
320 GOSUB 550
330 ETA5=ETAA: ETA7=ETAB: TOR5=TORA: TOR7=TORB
340 RO5=1-ETA5-TOR5: RO7=1-ETA7-TOR7
```

```
350   REM
360 INPUT "THIRD SCREEN MATERIAL",M4$
370 MTEL$=M4$
380 GOSUB 550
390 ETA8=ETAA :ETA10=ETAB :TOR8=TORA:TOR10=TORB
400 RO8=1-ETA8-TOR8:RO10=1-ETA10-TOR10
410   REM
420 INPUT "4TH SCREEN MATERIAL",M5$
430 MTEL$=M5$
440 GOSUB 550
450 ETA11=ETAA :ETA13=ETAB :TOR11=TORA:TOR13=TORB
460 RO11=1-ETA11-TOR11:RO13=1-ETA13-TOR13
470   REM
480 INPUT "OUTER SCREEN MATERIAL",M6$
490 MTEL$=M6$
500 GOSUB 550
510 ETA14=ETAA :RO14=1-ETA14
520   REM
530 GOTO 790
540   REM
550 IF MTEL$="MAXORB" THEN GOTO 680
560 IF MTEL$="NONSEL" THEN GOTO 690
570 IF MTEL$="GLASS" THEN GOTO 700
580 IF MTEL$="HOWSON" THEN GOTO 710
590 IF MTEL$="POLYTHENE"THEN GOTO 720
600 IF MTEL$="POLYPROPYLENE" THEN GOTO 730
610 IF MTEL$="REFLECTOR" THEN GOTO 740
620 IF MTEL$="MELINEX"THEN GOTO 750
630 IF MTEL$="TEDLAR" THEN GOTO 760
640 PRINT "NO MATERIAL DEFINITION"
650 GOTO 4390
660   REM
670   REM   THE FOLLOWING 8 LINES SET THE SCREEN RADIATION PROPERTIES.
680 ETAA=0:ETAB=.125:TORA=0:TORB=0:GOTO 770
```

```
690 ETAA=0   : ETAB=. 9    : ROA=0   : ROB=. 1    : TORA=0   : TORB=0   : GOTO 770
700 ETAA=. 9: ETAB=. 9: TORA=0: TORB=0: GOTO 770
710 ETAA=. 246: ETAB=. 805: ROA=. 743: ROB=. 184: TORA=. 011: TORB=. 011: GOTO 770
720 ETAA=. 064: ETAB=. 064: ROA=. 067: ROB=. 067: TORA=. 869: TORB=. 869: GOTO 770
730 ETAA=. 091: ETAB=. 091: ROA=. 067: ROB=. 067: TORA=. 842: TORB=. 842: GOTO 770
740 ETAA=. 031: ETAB=. 475: ROA=. 969: ROB=. 525: TORA=0    : TORB=0    : GOTO 770
750 ETAA=. 665: ETAB=. 665: ROA=. 074: ROB=. 074: TORA=. 261: TORB=. 261: GOTO 770
760 ETAA=. 7   : ETAB=. 7   : ROA=. 05  : ROB=. 05  : TORA=. 25  : TORB=. 25  : GOTO 770
770 RETURN
780   REM
790 EL "OUTPUT"
800 GE "OUTPUT"
810 AS #12="OUTPUT"
820 OPEN #12
830 PRINT #12; "MATERIALS"
840 PRINT #12; M1$; M2$; M3$; M4$; M5$; M6$
850 PRINT #12
860   REM   GAP=THE SCREEN SPACING.
870 GAP=. 025
880 IF M5$="GLASS" THEN 920
890   REM
900   REM   GCON=CONDUCTIVITY OF SCREEN MATERIAL.
910 GCON=200: GOTO 930
920 GCON=26
930 PRINT #12; "GAPS"
940 PRINT #12; GAP1; GAP2; GAP3; GAP4; GAP5
950 PRINT #12
960 HEIGHT=. 32
970 PRINT #12 "HEIGHT", HEIGHT
980 WIDTH=. 32
990 PRINT #12 "WIDTH", WIDTH
1000 PRINT #12
1010 OPTION BASE=1
1020   REM   GCF IS THE G COEFFICIENT MATRIX DESCRIBED IN CHAPTER 4. 2
1030   REM   GRA IS THE INCIDENT RADIATION VECTOR.
```

```
1040    REM    T4CF IS THE TEMPERATURE COEFFICIENT MATRIX.
1050    REM    T4VA IS THE TEMPERATURE^4 VECTOR.
1060 DIM GCF(1:15,1:15)
1070 DIM GRA(1:15,1:1)
1080 DIM T4CF(1:15,1:15)
1090 DIM T4VEC(1:15,1:1)
1100 DIM T4VA(1:15,1:1)
1110 GE "DATIN"
1120 AS #13="DATIN"
1130 OPEN #13
1140    REM    THE FOLLOWING LINES SET THE G COEFFICIENT MATRIX AS IN FIG 4.7
1150 PRINT #13; RO1*FA*A1; -A1; RO5*FC*A2; 0; 0; 0; 0; 0; 0; 0; 0; 0; 0; 0; 0
1160    REM
1170 PRINT #13; RO1*FB*A1; RO2*FB*A1; RO5*FD*A2-A2; TOR4*FB*A1; 0; 0; 0; 0; 0->
; 0; 0; 0; 0; 0; 0
1180    REM
1190 PRINT #13; -A1; RO2*FA*A1; RO5*FC*A2; TOR4*FA*A1; 0; 0; 0; 0; 0; 0; 0; 0; 0; 0; 0
1200    REM
1210 PRINT #13; 0; TOR2*FA*A1; 0; RO4*FA*A1; -A1; RO5*FC*A2; 0; 0; 0; 0; 0; 0; 0; 0; 0
1220    REM
1230 PRINT #13; 0; TOR2*FB*A1; 0; RO4*FB*A1; RO5*FB*A1; RO5*FD*A2-A2; ->
TOR7*FB*A1; 0; 0; 0; 0; 0; 0; 0; 0
1240    REM
1250 PRINT #13; 0; 0; 0; -A1; RO5*FA*A1; RO5*FC*A2; TOR7*FA*A1; 0; 0; 0; 0; 0; 0; 0; 0
1260    REM
1270 PRINT #13; 0; 0; 0; 0; TOR5*FA*A1; 0; RO7*FA*A1; -A1; RO5*FC*A2; 0; 0; 0; 0; 0; 0
1280    REM
1290 PRINT #13; 0; 0; 0; 0; TOR5*FB*A1; 0; RO7*FB*A1; RO8*FB*A1; RO5*FD*A2-A2; ->
TOR10*FB*A1; 0; 0; 0; 0; 0
1300    REM
1310 PRINT #13; 0; 0; 0; 0; 0; 0; -A1; RO8*FA*A1; RO5*FC*A2; TOR10*FA*A1; 0; 0; 0; 0; 0
1320    REM
1330 PRINT #13; 0; 0; 0; 0; 0; 0; 0; TOR8*FA*A1; 0; RO10*FA*A1; -A1; RO5*FC*A2; 0; 0; 0
1340    REM
```

```
1350 PRINT #13; 0; 0; 0; 0; 0; 0; 0; TOR8*FB*A1; 0; RO10*FB*A1; RO11*FB*A1; ->
ROS*FD*A2-A2; TOR13*FB*A1; 0; 0
1360    REM
1370 PRINT #13; 0; 0; 0; 0; 0; 0; 0; 0; 0; -A1; RO11*FA*A1; ROS*FC*A2; TOR13*FA*A1; 0; 0
1380    REM
1390 PRINT #13; 0; 0; 0; 0; 0; 0; 0; 0; 0; 0; 0; TOR11*FA*A1; 0; RO13*FA*A1; -A1; ROS*FC*A2
1400    REM
1410 PRINT #13; 0; 0; 0; 0; 0; 0; 0; 0; 0; 0; 0; TOR11*FB*A1; 0; RO13*FB*A1; ->
RO14*FB*A1; ROS*FD*A2-A2
1420    REM
1430 PRINT #13; 0; 0; 0; 0; 0; 0; 0; 0; 0; 0; 0; 0; 0; -A1; RO14*FA*A1; ROS*FC*A2
1440    REM
1450 RW #13
1460 MAT INPUT #13, GCF
1470 RW #13
1480    REM    DATA FOR T4CF FOLLOWS
1490 PRINT #13; ETA1*FA*A1; 0; ETAS*FC*A2; 0; 0; 0; 0; 0; 0; 0; 0; 0; 0; 0; 0
1500 PRINT #13; ETA1*FB*A1; ETA2*FB*A1; ETAS*FD*A2; 0; 0; 0; 0; 0; 0; 0; 0; 0; 0; 0; 0
1510 PRINT #13; 0; ETA2*FA*A1; ETAS*FC*A2; 0; 0; 0; 0; 0; 0; 0; 0; 0; 0; 0; 0
1520 PRINT #13; 0; 0; 0; ETA4*FA*A1; 0; ETAS*FC*A2; 0; 0; 0; 0; 0; 0; 0; 0; 0
1530 PRINT #13; 0; 0; 0; ETA4*FB*A1; ETA5*FB*A1; ETAS*FD*A2; 0; 0; 0; 0; 0; 0; 0; 0; 0
1540 PRINT #13; 0; 0; 0; 0; ETA5*FA*A1; ETAS*FC*A2; 0; 0; 0; 0; 0; 0; 0; 0; 0
1550 PRINT #13; 0; 0; 0; 0; 0; 0; ETA7*FA*A1; 0; ETAS*FC*A2; 0; 0; 0; 0; 0; 0
1560 PRINT #13; 0; 0; 0; 0; 0; 0; ETA7*FB*A1; ETA8*FB*A1; ETAS*FD*A2; 0; 0; 0; 0; 0; 0
1570 PRINT #13; 0; 0; 0; 0; 0; 0; 0; ETA8*FA*A1; ETAS*FC*A2; 0; 0; 0; 0; 0; 0
1580 PRINT #13; 0; 0; 0; 0; 0; 0; 0; 0; 0; 0; ETA10*FA*A1; 0; ETAS*FC*A2; 0; 0; 0
1590 PRINT #13; 0; 0; 0; 0; 0; 0; 0; 0; 0; 0; ETA10*FB*A1; ETA11*FB*A1; ETAS*FD*A2; 0; 0; 0
1600 PRINT #13; 0; 0; 0; 0; 0; 0; 0; 0; 0; 0; 0; ETA11*FA*A1; ETAS*FC*A2; 0; 0; 0
1610 PRINT #13; 0; 0; 0; 0; 0; 0; 0; 0; 0; 0; 0; 0; 0; ETA13*FA*A1; 0; ETAS*FC*A2
1620 PRINT #13; 0; 0; 0; 0; 0; 0; 0; 0; 0; 0; 0; 0; 0; ETA13*FB*A1; ETA14*FB*A1; ETAS*FD*A2
1630 PRINT #13; 0; 0; 0; 0; 0; 0; 0; 0; 0; 0; 0; 0; 0; 0; ETA14*FA*A1; ETAS*FC*A2
1640 RW #13
1650 MAT INPUT #13, T4CF
1660 EL "DATIN"
```

```
1670   REM
1680 PRINT M1$;M2$;M3$;M4$;M5$;M6$
1690   REM
1700   REM   DT IS THE REFERENCE TEMPERATURE DIFFERENCE SEE CHAPTER 5.7
1710 INPUT "TEMP DIF",DT
1720   REM
1730   REM   TMAX=HOTPLATE TEMP.
1740 TMAX=290+DT
1750   REM
1760   REM BCLOS=EXPERIMENTAL VALUE OF HEAT LOSS FROM BACK.
1770 BCLOS=-.00223+.1337*DT
1780 IF M5$="GLASS" THEN 1840
1790 IF M5$="HOWSON" THEN 1850
1800 IF M5$="POLYTHENE" THEN 1860
1810 IF M5$="REFLECTOR" THEN 1870
1820   REM   THE FOLLOWING HEATIN VALUES ARE THE VALUES OBTAINED BY
1830   REM   EXPERIMENT SEE CHAPTER 5.7 AND FIG 5.3
1840 HEATIN=-.298+.2176*DT-BCLOS*1.4/2:GOTO 1890
1850 HEATIN=-.1701+.22088*DT-BCLOS*1.325/2:GOTO 1890
1860 HEATIN=-.2505+.2578*DT-BCLOS*1.35/2:GOTO 1890
1870 HEATIN=-.2284+.19206*DT-BCLOS*1.325/2
1880   REM   .95 IS AMMETER CORRECTION FACTOR
1890 HEATIN=HEATIN*.95
1900   REM   CON IS THE CORRECTION FACTOR FOR EACH CELL TO CALIBRATE FOR ALL
1910   REM   GLASS SCREEN CONFIGURATION AT DT=30
1920 CON1=1.35
1930 CON2=.5
1940 CON3=1.5
1950 CON4=1.5
1960 CON5=1.5
1970 PRINT
1980 PRINT DT
1990 PRINT
2000 IF M5$="GLASS" THEN 2060
2010 IF M5$="POLYTHENE" THEN 2120
```

```
2020 IF M5$="HOWSON" THEN 2180
2030 IF M5$="REFLECTOR" THEN 2240
2040   REM   THE FOLLOWING HLOS FACTORS ARE THE EXPERIMENTALLLY DETERMINED
2050   REM   EDGE LOSS VALUES AS DESCRIBED IN CHAPTER 5.8
2060 H1LOS=-.035+.01209*DT
2070 H2LOS=-.0358+.009367*DT
2080 H3LOS=-.0372+.006902*DT
2090 H4LOS=-.0407+.004526*DT
2100 H5LOS=-.0431+.0026*DT
2110 GOTO 2290
2120 H1LOS=-.0423+.01026*DT
2130 H2LOS=-.0484+.0098*DT
2140 H3LOS=-.0483+.00646*DT
2150 H4LOS=-.046+.00473*DT
2160 H5LOS=-.044+.0029*DT
2170 GOTO 2290
2180 H1LOS=-.0351+.0114*DT
2190 H2LOS=-.0349+.00927*DT
2200 H3LOS=-.0463+.00771*DT
2210 H4LOS=-.0433+.00503*DT
2220 H5LOS=-.0469+.00275*DT
2230 GOTO 2290
2240 H1LOS=-.0385+.0129*DT
2250 H2LOS=.0395+.0106*DT
2260 H3LOS=-.0409+.0079*DT
2270 H4LOS=-.0424+.00423*DT
2280 H5LOS=-.069+.0028*DT
2290 IF H1LOS>0 THEN 2310
2300 H1LOS=0
2310 IF H2LOS>0 THEN 2330
2320 H2LOS=0
2330 IF H3LOS>0 THEN 2350
2340 H3LOS=0
2350 IF H4LOS>0 THEN 2370
2360 H4LOS=0
```

```
2370 IF H5LOS>0 THEN 2390
2380 H5LOS=0
2390 PRINT
2400 H1LOS=H1LOS*CON1
2410 H2LOS=H2LOS*CON2
2420 H3LOS=H3LOS*CON3
2430 H4LOS=H4LOS*CON4
2440 H5LOS=H5LOS*CON5
2450   REM
2460   REM THE FOLOWING HEAT1 TO 5 VALUES ARE THE CUMPUTED HEAT
2470   REM FLOWS THROUGH THE APPROPRIATE CELLS.
2480 HEAT1=HEATIN-H1LOS
2490 HEAT2=HEAT1-H2LOS
2500 HEAT3=HEAT2-H3LOS
2510 HEAT4=HEAT3-H4LOS
2520 HEAT5=HEAT4-H5LOS
2530   REM
2540 MAT GCF=INV(GCF)
2550 MAT T4CF=(5.669E-8)*T4CF
2560 MAT T4CF=(-1)*T4CF
2570   REM
2580   REM     THE FOLLOWING TEMPERATURE VALUES ARE THE FIRST GUESS
2590   REM     AT THE SCREEN TEMPERATURES.
2600 T1=TMAX: T2=TMAX-3: T3=T2: T4=T2: T5=T4-3: T6=T5: T7=T5: T8=T7-3
2610 T9=T8: T10=T8: T11=T10-3: T12=T11: T13=T11: T14=T13-3
2620 T15=(T13+2*T14)/3
2630   REM
2640   REM    THE FOLLOWING TEMPERATURE VALUES ARE THE ITERATED
2650   REM    COMPUTED VALUES.
2660 T4VEC(1,1)=T1^4: T4VEC(2,1)=T2^4: T4VEC(3,1)=T3^4: T4VEC(4,1)=T4^4
2670 T4VEC(5,1)=T5^4: T4VEC(6,1)=T6^4: T4VEC(7,1)=T7^4: T4VEC(8,1)=T8^4
2680 T4VEC(9,1)=T9^4: T4VEC(10,1)=T10^4: T4VEC(11,1)=T11^4
2690 T4VEC(12,1)=T12^4: T4VEC(13,1)=T13^4: T4VEC(14,1)=T14^4
2700 T4VEC(15,1)=T15^4
2710   REM
```

```
2720    REM    MATRIX MANIPULATION.
2730 MAT T4VA=T4CF*T4VEC
2740 MAT GRA=GCF*T4VA
2750 MAT GRA=(A1)*GRA
2760    REM
2770 TA=T1: TB=T2: TC=T3: GRAX=GRA(2, 1): ETA=ETA2: RO=RO2: TOR=TOR4: GRAY=GRA(4, 1)
2780 GRAZ=GRA(1, 1)
2790 GOSUB 3560
2800 HEATA=HEAT
2810    REM
2820 TA=T4: TB=T5: TC=T6: GRAX=GRA(5, 1): ETA=ETA5: RO=RO5: TOR=TOR7: GRAY=GRA(7, 1)
2830 GRAZ=GRA(4, 1)
2840 GOSUB 3560
2850 HEATB=HEAT
2860    REM
2870 TA=T7: TB=T8: TC=T9: GRAX=GRA(8, 1): ETA=ETA8: RO=RO8: TOR=TOR10: ->
GRAY=GRA(10, 1)
2880 GRAZ=GRA(7, 1)
2890 GOSUB 3560
2900 HEATC=HEAT
2910    REM
2920 TA=T10: TB=T11: TC=T12: GRAX=GRA(11, 1): ETA=ETA11: RO=RO11: TOR=TOR13: ->
GRAY=GRA(13, 1)
2930 GRAZ=GRA(10, 1)
2940 GOSUB 3560
2950 HEATD=HEAT
2960    REM
2970 TA=T13: TB=T14: TC=T15: GRAX=GRA(14, 1): ETA=ETA14: RO=RO14: TOR=0: GRAY=0
2980 GRAZ=GRA(13, 1)
2990 GOSUB 3560
3000 HEATE=HEAT
3010    REM
3020    REM    X AND Y ARE ACCURACY CRITERIA.
3030 X=1.001: Y=.999
3040 IF HEATA<HEAT1*Y THEN 3200
```

```
3050 IF HEATA<HEAT1*X THEN 3070
3060 GOTO 3200
3070 IF HEATB<HEAT2*Y THEN 3200
3080 IF HEATB<HEAT2*X THEN 3100
3090 GOTO 3200
3100 IF HEATC<HEAT3*Y THEN 3200
3110 IF HEATC<HEAT3*X THEN 3130
3120 GOTO 3200
3130 IF HEATD<HEAT4*Y THEN 3200
3140 IF HEATD<HEAT4*X THEN 3160
3150 GOTO 3200
3160 IF HEATE<HEAT5*Y THEN 3200
3170 IF HEATE<HEAT5*X THEN 3430
3180   REM
3190   REM   HTRN VALUES ARE COMPUTED HEAT TRANSFER COEFS.
3200 HTRN1=HEATA/(T1-T2)
3210 HTRN2=HEATB/(T4-T5)
3220 HTRN3=HEATC/(T7-T8)
3230 HTRN4=HEATD/(T10-T11)
3240 HTRN5=HEATE/(T13-T14)
3250   REM
3260   REM   NEW TEMPERATURE VALUES ARE CALCULATED.
3270 T1=TMAX
3280 T2=TMAX-HEAT1/HTRN1
3290 T3=T2
3300 T4=T2-HEAT1/GCON
3310 T5=T4-HEAT2/HTRN2
3320 T6=T5
3330 T7=T5-HEAT2/GCON
3340 T8=T7-HEAT3/HTRN3
3350 T9=T8
3360 T10=T8-HEAT3/GCON
3370 T11=T10-HEAT4/HTRN4
3380 T12=T11
3390 T13=T11-HEAT4/GCON
```

```
3400 T14=T13-HEAT5/HTRN5
3410 T15=T14
3420 GOTO 2660
3430   REM
3440 PRINT "TEMP DIFFS"
3450 PRINT TMAX-T2, TMAX-T5, TMAX-TB, TMAX-T11, TMAX-T14
3460   REM
3470 GOTO 4390
3480   REM    ******
3490   REM    ******
3500   REM    ******
3510   REM    SUBROUTINE FOR CALCULATING THE CONVECTIVE HEAT TRANSFER
3520   REM    COEFFICIENT THROUGH A SINGLE CELL, AND COMBINED HEAT
3530   REM    FLOW
3540   REM
3550   REM    ASPR=ASPECT RATIO.
3560 ASPR=HEIGHT/GAP
3570   REM    AIRVIS=AIR VISCOSITY.
3580 AIRVIS=9E-8*(TA+TB)/2-1.132E-5
3590   REM    AIRDIF=AIR THERMAL DIFFUSIVITY.
3600 AIRDIF=13.8E-8*(TA+TB)/2-1.961E-5
3610   REM    AIRCON=AIR THERMAL CONDUCTIVITY.
3620 AIRCON=7.84E-5*(TA+TB)/2+2.72E-3
3630   REM    RANO=RALEIGH NUMBER.
3640 RANO=2*9.81*(TA-TB)*GAP^3/AIRVIS/AIRDIF/(TA+TB)
3650 IF RANO>10^((190-ASPR)/25) THEN GOTO 4370
3660 RANO1=RANO/GAP^3*(HEIGHT/5)^3
3670   REM    NUS=NUSSELT NUMBER.
3680   REM  SUFFIX NUMBER ON NUS RELATES TO THE APPROPRIATE ASPECT
3690   REM  RATIO FOR HOLLANDS RELATIONSHIPS, SEE CHAPTER 4.1.
3700 NUS11=(1+(.193*RANO1^.25/(1+(1800/RANO1)^1.29))^3)^(1/3)
3710 NUS12=.0605*RANO1^(1/3)
3720 IF NUS11>NUS12 THEN 3740
3730 NUS1=NUS12: GOTO 3770
3740 NUS1=NUS11
```

```
3750    REM
3760    REM    NOD IS THE CONVECTIVE HEAT FLOW AT APPROPRIATE ASPRS.
3770 NOD1=NUS1*(TA-TB)*AIRCON/(HEIGHT/5)
3780    REM
3790 RAN02=RAN0/GAP^3*(HEIGHT/10)^3
3800 NUS21=(1+(.125*RAN02^.28)^9)^(1/9)
3810 NUS22=.061*RAN02^(1/3)
3820 IF NUS21>NUS22 THEN 3840
3830 NUS2=NUS22: GOTO 3850
3840 NUS2=NUS21
3850 NOD2=NUS2*(TA-TB)*AIRCON/(HEIGHT/10)
3860    REM
3870 RAN03=RAN0/GAP^3*(HEIGHT/20)^3
3880 NUS3=(1+(.064*RAN03^(1/3))^6.5)^(1/6.5)
3890 NOD3=NUS3*(TA-TB)*AIRCON/(HEIGHT/20)
3900    REM
3910 RAN04=RAN0/GAP^3*(HEIGHT/40)^3
3920 PEX4=.31*40^.81
3930 NUS4=(1+(.064*RAN04^(1/3))^PEX4)^(1/PEX4)
3940 NOD4=NUS4*(TA-TB)*AIRCON/(HEIGHT/40)
3950    REM
3960 PEX=.31*ASPR^.81
3970    REM NUS IS THE NUSSELT NUMBER FOR HIGH ASPECT RATIOS.
3980 NUS=(1+(.064*RAN0^(1/3))^PEX)^(1/PEX)
3990    REM
4000 IF ASPR=5 THEN GOTO 4060
4010 IF ASPR=10 THEN GOTO 4070
4020 IF ASPR=20 THEN GOTO 4080
4030 IF ASPR=40 THEN GOTO 4090
4040 GOTO 4130
4050    REM
4060 HCON=NOD1: GOTO 4300
4070 HCON=NOD2: GOTO 4300
4080 HCON=NOD3: GOTO 4300
4090 HCON=NOD4: GOTO 4300
```

```
4100   REM
4110   REM    THE FOLOWING CALCULATES CONVECTIVE HEAT FLOWS FOR
4120   REM    INTERMEDIATE ASPECT RATIOS, LINEARLY.
4130 IF ASPR<5 THEN GOTO 4380
4140 IF ASPR<10 THEN GOTO 4180
4150 IF ASPR<20 THEN GOTO 4190
4160 IF ASPR<40 THEN GOTO 4200
4170 GOTO 4230
4180 X=NOD1: Y=NOD2: GOTO 4260
4190 X=NOD2: Y=NOD3: GOTO 4250
4200 X=NOD3: Y=NOD4: GOTO 4240
4210   REM
4220   REM    HCON IS THE CONVECTIVE HEAT FLOW
4230 HCON=NUS*(TA-TB)*AIRCON/GAP: GOTO 4300
4240 HCON=X+(Y-X)/20*(ASPR-20): GOTO 4300
4250 HCON=X+(Y-X)/10*(ASPR-10): GOTO 4300
4260 HCON=X+(Y-X)/5*(ASPR-5): GOTO 4300
4270   REM
4280   REM    HCOND IS THE CONVECTIVE HEAT FLOW CORRECTED TO ALLOW
4290   REM    FOR EDGE EFFECTS.
4300 HCOND=HCON*.9*A1
4310   REM    HREF IS THE NET RADIANT HEAT FLOW.
4320 HREF=GRAX-GRAZ
4330   REM
4340   REM    HEAT IS THE COMBINED CELL HEAT FLOW
4350 HEAT=HREF+HCOND
4360 RETURN
4370 PRINT "OUT OF RANG": GOTO 4390
4380 PRINT "TOO LOW ASPR": GOTO 4390
4390 END
```

Appendix 4.2.

Thermal losses from the Wall Module

```
10      REM   PROGRAM 7
20      REM   THIS PROGRAM CALCULATES THE ENERGY LOST THROUGH THE SCREEN
30      REM   ARRAY OF THE MODULE, EDGE EFFECTS ARE NEGLECTED, SEE CHAPTER 6.1..
40 EL "OUTPUT"
50 QE "OUTPUT"
60 AS #12="OUTPUT"
70 OPEN #12
80 PRINT #12 "OUT LOSS FOR 5 SCREEN ARRAY, VARIOUS COMBINATIONS OF MATERIALS"
90 PRINT #12 "NO EDGE LOSSES"
100 PRINT #12
110 PRINT #12
120   REM
130 WIDTH=1
140 PRINT #12 "WIDTH", WIDTH
150 HT=1
160 PRINT #12 "HEIGHT", HT
170   REM
180   REM   GAP IS THE SCREEN SPACING.
190 GAP1=.025
200 GAP2=.025
210 GAP3=.025
220 GAP4=.025
230 GAP5=.025
240   REM
250 PRINT #12 USING ->
"CELL GAPS   #.###   #.###   #.###   #.###   #.####", ->
GAP1, GAP2, GAP3, GAP4, GAP5
260   REM
270   REM   TMAX=ABSORBER TEMPERATURE.
280 TMAX=293
290 PRINT #12 "ABSORBER TEMPERATURE    ", TMAX
300 PRINT #12
310   REM
320 INPUT "ABSORBER MATERIAL MAXORB, OR NONSEL", M1$
```

```
330 PRINT "SCREEN MATERIALS MAY BE:-POLYTHENE, MELINEX, TEDLAR"
340 PRINT "GLASS, POLYPROPYLENE OR HOWSON. "
350 PRINT
360 INPUT "1ST SCREEN MATERIAL", M2$
370 INPUT "SECOND SCREEN MATERIAL", M3$
380 INPUT "THIRD SCREEN MATERIAL", M4$
390 INPUT "FOURTH SCREEN MATERIAL", M5$
400 INPUT "OUTER SCREEN MATERIAL, GLASS OR RGLASS", M6$
410 PRINT #12
420   REM
430 M$=M1$
440 GOSUB 700
450   REM
460   REM   ETA, RHO AND TOR ARE EMITTANCE, REFLECTANCE AND TRANSMITTANCE.
470 RHO1=RHOB: ETA1=ETAB
480 REM
490 M$=M2$
500 GOSUB 700
510 RHO2=RHOA: RHO3=RHOB: ETA2=ETAA: ETA3=ETAB: TOR2=TORA: TOR3=TORB
520   REM
530 M$=M3$
540 GOSUB 700
550 RHO4=RHOA: RHO5=RHOB: ETA4=ETAA: ETA5=ETAB: TOR4=TORA: TOR5=TORB
560   REM
570 M$=M4$
580 GOSUB 700
590 RHO6=RHOA: RHO7=RHOB: ETA6=ETAA: ETA7=ETAB: TOR6=TORA: TOR7=TORB
600   REM
610 M$=M5$
620 GOSUB 700
630 RHO8=RHOA: RHO9=RHOB: ETA8=ETAA: ETA9=ETAB: TOR8=TORA: TOR9=TORB
640   REM
650 M$=M6$
660 GOSUB 700
670 RHO10=RHOA: ETA10=ETAA
```

```
680 GOTO 1140
690   REM
700 IF M$="MAXORB" THEN GOTO 830
710 IF M$="NONSEL" THEN GOTO 860
720 IF M$="GLASS" THEN GOTO 890
730 IF M$="HOWSON" THEN GOTO 920
740 IF M$="POLYTHENE"THEN GOTO 950
750 IF M$="POLYPROPYLENE" THEN GOTO 980
760 IF M$="REFLECTOR" THEN GOTO 1010
770 IF M$="MELINEX"THEN GOTO 1040
780 IF M$="TEDLAR" THEN GOTO 1070
790 IF M$="RGLASS" THEN GOTO 1100
800 PRINT "NO MATERIAL DEFINITION": GOTO 3030
810   REM
820   REM THE FOLLOWING LINES SET ETA RHO AND TOR FOR SCREENS.
830 ETAA=0   : ETAB=. 08   : RHOA=0   : RHOB=. 92   : TORA=0   : TORB=0
840 GOTO 1120
850   REM
860 ETAA=0   : ETAB=. 9    : RHOA=0   : RHOB=. 1    : TORA=0   : TORB=0
870 GOTO 1120
880   REM
890 ETAA=. 9: ETAB=. 9   : RHOA=. 1: RHOB=. 1   : TORA=0   : TORB=0
900 GOTO 1120
910   REM
920 ETAA=. 246: ETAB=. 805: RHOA=. 743: RHOB=. 184: TORA=. 011: TORB=. 011
930 GOTO 1120
940   REM
950 ETAA=. 064: ETAB=. 064: RHOA=. 067: RHOB=. 067: TORA=. 869: TORB=. 869
960 GOTO 1120
970   REM
980 ETAA=. 091: ETAB=. 091: RHOA=. 067: RHOB=. 067: TORA=. 842: TORB=. 842
990 GOTO 1120
1000   REM
1010 ETAA=. 031: ETAB=. 745: RHOA=. 969: RHOB=. 525: TORA=0    : TORB=0
1020 GOTO 1120
1030   REM
```

```
1040 ETAA=.665:ETAB=.665:RHOA=.074:RHOB=.074:TORA=.261:TORB=.261
1050 GOTO 1120
1060    REM
1070 ETAA=.7   :ETAB=.7   :RHOA=.05 :RHOB=.05 :TORA=.25 :TORB=.25
1080 GOTO 1120
1090    REM
1100 ETAA=.257:ETAB=.816:RHOA=.743:RHOB=.184:TORA=0    :TORB=0
1110    REM
1120 RETURN
1130    REM
1140 PRINT #12;"MATERIALS"
1150 PRINT #12 "ABSORBER",M1$
1160 PRINT #12;M2$,M3$,M4$,M5$,M6$
1170 PRINT #12
1180 PRINT #12 ->
"ETA1   ETA2   ETA3   ETA4   ETA5   ETA6   ETA7   ETA8   ETA9   ETA10"
1190    REM
1200 PRINT #12 USING ->
".###   .###   .###   .###   .###   .###   .###   .###   .###   .###",->
ETA1,ETA2,ETA3,ETA4,ETA5,ETA6,ETA7,ETA8,ETA9,ETA10
1210 PRINT #12->
"RHO1   RHO2   RHO3   RHO4   RHO5   RHO6   RHO7   RHO8   RHO9   RHO10"
1220    REM
1230 PRINT #12 USING->
".###   .###   .###   .###   .###   .###   .####   .###   .###   .###",->
RHO1,RHO2,RHO3,RHO4,RHO5,RHO6,RHO7,RHO8,RHO9,RHO10
1240    REM
1250 PRINT #12->
"TOR1   TOR2   TOR3   TOR4   TOR5   TOR6   TOR7   TOR8   TOR9   TOR10"
1260    REM
1270 PRINT #12 USING->
".###   .###   .###   .###   .###   .###   .###   .###   .###   .###",->
TOR1,TOR2,TOR3,TOR4,TOR5,TOR6,TOR7,TOR8,TOR9,TOR10
1280    REM
1290 PRINT #12
```

```
1300    REM
1310 OPTION BASE=1
1320 DIM GCF(1:10,1:10)
1330 DIM T4CFA(1:10,1:6)
1340 DIM T4VEC(1:6,1:1)
1350 DIM TVEC(1:6,1:1)
1360 DIM T4CFB(1:10,1:6)
1370 DIM GCFA(1:10,1:10)
1380 DIM T4VA(1:10,1:1)
1390 DIM GRA(1:10,1:1)
1400 DIM GVAL(1:5,1:1)
1410 DIM GCELL(1:5,1:10)
1420    REM
1430 GE "PUTIN"
1440 AS #13="PUTIN"
1450 OPEN #13
1460    REM
1470    REM DATA FOR GCF FOLLOWS, SEE FIGURE 6.1.
1480 PRINT #13; -RHO1; 1; 0; 0; 0; 0; 0; 0; 0; 0
1490 PRINT #13; -1; RHO2; TOR2; 0; 0; 0; 0; 0; 0; 0
1500 PRINT #13; 0; -TOR3; -RHO3; 1; 0; 0; 0; 0; 0; 0
1510 PRINT #13; 0; 0; -1; RHO4; TOR4; 0; 0; 0; 0; 0
1520 PRINT #13; 0; 0; 0; -TOR5; -RHO5; 1; 0; 0; 0; 0
1530 PRINT #13; 0; 0; 0; 0; -1; RHO6; TOR6; 0; 0; 0
1540 PRINT #13; 0; 0; 0; 0; 0; -TOR7; -RHO7; 1; 0; 0
1550 PRINT #13; 0; 0; 0; 0; 0; 0; -1; RHO8; TOR8; 0
1560 PRINT #13; 0; 0; 0; 0; 0; 0; 0; -TOR9; -RHO9; 1
1570 PRINT #13; 0; 0; 0; 0; 0; 0; 0; 0; -1; RHO10
1580 RW #13
1590 MAT INPUT #13, GCF
1600 RW #13
```

```
1610   REM DATA FOR T4CFA FOLLOWS.
1620 PRINT #13;ETA1;0;0;0;0;0
1630 PRINT #13;0;-ETA2;0;0;0;0
1640 PRINT #13;0;ETA3;0;0;0;0
1650 PRINT #13;0;0;-ETA4;0;0;0
1660 PRINT #13;0;0;ETA5;0;0;0
1670 PRINT #13;0;0;0;-ETA6;0;0
1680 PRINT #13;0;0;0;ETA7;0;0
1690 PRINT #13;0;0;0;0;-ETA8;0
1700 PRINT #13;0;0;0;0;ETA9;0
1710 PRINT #13;0;0;0;0;0;-ETA10
1720 RW #13
1730 MAT INPUT #13,T4CFA
1740 RW #13
1750   REM
1760   REM DATA FOR QCELL FOLLOWS,QCELL SUMS QRA FOR HEAT FLOW/CELL.
1770 DATA -1,1,0,0,0,0,0,0,0,0
1780 DATA 0,0,-1,1,0,0,0,0,0,0
1790 DATA 0,0,0,0,-1,1,0,0,0,0
1800 DATA 0,0,0,0,0,0,-1,1,0,0
1810 DATA 0,0,0,0,0,0,0,0,-1,1
1820 DIM QCELL(1:5,1:10)
1830 MAT READ QCELL
1840   REM
1850   REM  HEAT=HEAT FLOW THROUGH SCREEN ARRAY.
1860 FOR HEAT=30 TO 1 STEP -5
1870 REM THE FOLLOWING TEMPERATURES ARE IST GUESS VALUES
1880 TVEC(1,1)=TMAX
1890 TVEC(2,1)=TMAX-3
1900 TVEC(3,1)=TVEC(2,1)-3
1910 TVEC(4,1)=TVEC(3,1)-3
1920 TVEC(5,1)=TVEC(4,1)-3
1930 TVEC(6,1)=TVEC(5,1)-3
1940   REM
1950   REM
1960 T4VEC(1,1)=TMAX^4
```

```
1970 T4VEC(2,1)=TVEC(2,1)^4
1980 T4VEC(3,1)=TVEC(3,1)^4
1990 T4VEC(4,1)=TVEC(4,1)^4
2000 T4VEC(5,1)=TVEC(5,1)^4
2010 T4VEC(6,1)=TVEC(6,1)^4
2020   REM
2030   REM**********
2040   REM
2050    REM MATRIX MANIPULATION
2060 MAT T4CFB=(5.699E-8*HT*WIDTH)*T4CFA
2070 MAT QCFA=INV(QCF)
2080 MAT T4VA=T4CFB*T4VEC
2090 MAT QRA=QCFA*T4VA
2100   REM
2110   REM**********
2120   REM
2130 T1=TMAX: T2=TVEC(2,1): T3=TVEC(3,1): T4=TVEC(4,1): T5=TVEC(5,1): T6=TVEC(6,1)
2140   REM
2150   REM H VALUES ARE CONVECTIVE HEAT TRANSFER COEFFICIENTS.
2160 TA=T1: TB=T2
2170 QAP=QAP1
2180 QOSUB 3110
2190 H1=HTX
2200   REM
2210 TA=T2: TB=T3
2220 QAP=QAP2
2230 QOSUB 3110
2240 H2=HTX
2250   REM
2260 TA=T3: TB=T4
2270 QAP=QAP3
2280 QOSUB 3110
2290 H3=HTX
2300   REM
2310 TA=T4: TB=T5
```

```
2320 GAP=GAP4
2330 GOSUB 3110
2340 H4=HTX
2350   REM
2360 TA=T5: TB=T6
2370 GAP=GAP5
2380 GOSUB 3110
2390 H5=HTX
2400   REM
2410   REM
2420 MAT GVAL=GCELL*GRA
2430   REM
2440   REM HEATF VALUES ARE COMPUTED CELL HEAT FLOWS
2450 HEATF1=GVAL(1,1)+H1*(T1-T2)
2460 HEATF2=GVAL(2,1)+H2*(T2-T3)
2470 HEATF3=GVAL(3,1)+H3*(T3-T4)
2480 HEATF4=GVAL(4,1)+H4*(T4-T5)
2490 HEATF5=GVAL(5,1)+H5*(T5-T6)
2500   REM
2510   REM HTRN VALUES ARE COMPUTED COMBINED HEAT TRANSFER COEFFICIENTS
2520 HTRN1=HEATF1/(T1-T2)
2530 HTRN2=HEATF2/(T2-T3)
2540 HTRN3=HEATF3/(T3-T4)
2550 HTRN4=HEATF4/(T4-T5)
2560 HTRN5=HEATF5/(T5-T6)
2570   REM
2580   REM Y IS ACCURACY LEVEL
2590 Y=.01
2600 IF HEATF1<HEAT-Y THEN 2770
2610 IF HEATF1<HEAT+Y THEN 2630
2620 GOTO 2770
2630 IF HEATF2<HEAT-Y THEN 2770
2640 IF HEATF2<HEAT+Y THEN 2660
2650 GOTO 2770
2660 IF HEATF3<HEAT-Y THEN 2770
```

```
2670 IF HEATF3<HEAT+Y THEN 2690
2680 GOTO 2770
2690 IF HEATF4<HEAT-Y THEN 2770
2700 IF HEATF4<HEAT+Y THEN 2720
2710 GOTO 2770
2720 IF HEATF5<HEAT-Y THEN 2770
2730 IF HEATF5<HEAT+Y THEN 2860
2740   REM
2750   REM
2760   REM FOLLOWING TVEC VALUES ARE IMPROVED ITERATION.
2770 TVEC(1,1)=TMAX
2780 TVEC(2,1)=TVEC(1,1)-HEAT/HTRN1
2790 TVEC(3,1)=TVEC(2,1)-HEAT/HTRN2
2800 TVEC(4,1)=TVEC(3,1)-HEAT/HTRN3
2810 TVEC(5,1)=TVEC(4,1)-HEAT/HTRN4
2820 TVEC(6,1)=TVEC(5,1)-HEAT/HTRN5
2830   REM
2840 GOTO 1960
2850   REM
2860 PRINT "HEAT FLOW   ",HEAT
2870 PRINT #12 "HEAT FLOW   ",HEAT
2880 PRINT
2890   REM
2900 PRINT USING ->
"SCREEN TEMPERATURES- ###.### ###.### ###.### ###.### ###.### ###.###",->
      TMAX,TVEC(2,1),TVEC(3,1),TVEC(4,1),TVEC(5,1),TVEC(6,1)
2910 PRINT #12 USING ->
"SCREEN TEMPERATURES  ###.### ###.### ###.### ###.### ###.### ###.###",->
      TMAX,TVEC(2,1),TVEC(3,1),TVEC(4,1),TVEC(5,1),TVEC(6,1)
2920 PRINT
2930 PRINT USING ->
"HEAT TX COEFFICIENT  ###.###",HEAT/(TMAX-TVEC(6,1))/HT/WIDTH
2940 PRINT #12 USING ->
"HEAT TX COEFFICIENT  ###.###",HEAT/(TMAX-TVEC(6,1))/HT/WIDTH
2950 PRINT "TEMP DIF",TMAX-TVEC(6,1)
```

```
2960 PRINT #12 "TEMP DIF",TMAX-TVEC(6,1)
2970 PRINT
2980 PRINT #12
2990 PRINT #12
3000 NEXT HEAT
3010   REM
3020   REM
3030 GOTO 3890
3040   REM
3050   REM*********
3060   REM*********
3070   REM*********
3080   REM
3090   REM SUBROUTINE FOR CONVECTIVE HEAT FLOW THROUGH CELLS.
3100   REM ASPR=ASPECT RATIO
3110 ASPR=HT/GAP
3120   REM AIRVIS=AIR VISCOSITY
3130 AIRVIS=9E-8*(TA+TB)/2-1.132E-5
3140   REM AIRDIF=AIR THERMAL DIFFUSIVITY
3150 AIRDIF=13.8E-8*(TA+TB)/2-1.961E-5
3160   REM AIRCON=AIR THERMAL CONDUCTIVITY
3170 AIRCON=7.84E-5*(TA+TB)/2+2.72E-3
3180   REM RANO=RALEIGH NUMBER
3190 RANO=2*9.81*(TA-TB)*GAP^3/AIRVIS/AIRDIF/(TA+TB)
3200   REM
3210 IF RANO>10^((190-ASPR)/25) THEN GOTO 3860
3220   REM
3230 RANO1=RANO/GAP^3*(HT/5)^3
3240   REM NUS=NUSSELT NUMBER
3250   REM CALCULATE CELL HEAT FLOWS FOR HOLLANDS ASPECT RATIOS
3260   REM NOD=CELL HEAT FLOW
3270 NUS11=(1+(.193*RANO1^.25/(1+(1800/RANO1)^1.29))^3)^(1/3)
3280 NUS12=.0605*RANO1^(1/3)
3290 IF NUS11>NUS12 THEN 3310
3300 NUS1=NUS12:GOTO 3320
```

```
3310 NUS1=NUS11
3320 NOD1=NUS1*(TA-TB)*AIRCON/(HT/5)
3330    REM
3340    REM
3350 RANO2=RANO/GAP^3*(HT/10)^3
3360 NUS21=(1+(.125*RANO2^.28)^9)^(1/9)
3370 NUS22=.061*RANO2^(1/3)
3380 IF NUS21>NUS22 THEN 3400
3390 NUS2=NUS22: GOTO 3410
3400 NUS2=NUS21
3410 NOD2=NUS2*(TA-TB)*AIRCON/(HT/10)
3420    REM
3430    REM
3440 RANO3=RANO/GAP^3*(HT/20)^3
3450 NUS3=(1+(.064*RANO3^(1/3))^6.5)^(1/6.5)
3460 NOD3=NUS3*(TA-TB)*AIRCON/(HT/20)
3470    REM
3480    REM
3490 RANO4=RANO/GAP^3*(HT/40)^3
3500 PEX4=.31*40^.81
3510 NUS4=(1+(.064*RANO4^(1/3))^PEX4)^(1/PEX4)
3520 NOD4=NUS4*(TA-TB)*AIRCON/(HT/40)
3530    REM
3540 PEX=.31*ASPR^.81
3550 NUS=(1+(.064*RANO^(1/3))^PEX)^(1/PEX)
3560    REM
3570    REM
3580 IF ASPR=5 THEN GOTO 3630
3590 IF ASPR=10 THEN GOTO 3640
3600 IF ASPR=20 THEN GOTO 3650
3610 IF ASPR=40 THEN GOTO 3660
3620 GOTO 3680
3630 HCON=NOD1: GOTO 3830
3640 HCON=NOD2: GOTO 3830
3650 HCON=NOD3: GOTO 3830
```

```
3660 HCON=NOD4: GOTO 3830
3670   REM
3680 IF ASPR<5 THEN GOTO 3870
3690 IF ASPR<10 THEN GOTO 3740
3700 IF ASPR<20 THEN GOTO 3750
3710 IF ASPR<40 THEN GOTO 3760
3720 GOTO 3770
3730   REM CALC HEAT FLOW AT ACTUAL ASPECT RATIO.
3740 X=NOD1: Y=NOD2: GOTO 3800
3750 X=NOD2: Y=NOD3: GOTO 3790
3760 X=NOD3: Y=NOD4: GOTO 3780
3770 HCON=NUS*(TA-TB)*AIRCON/GAP: GOTO 3830
3780 HCON=X+(Y-X)/20*(ASPR-20): GOTO 3830
3790 HCON=X+(Y-X)/10*(ASPR-10): GOTO 3830
3800 HCON=X+(Y-X)/5*(ASPR-5): GOTO 3830
3810   REM
3820   REM
3830 HTX=HCON/(TA-TB)*HT*WIDTH: GOTO 3880
3840   REM
3850   REM
3860 PRINT "OUT OF RANO": GOTO 3880
3870 PRINT "TOO LOW ASPR": GOTO 3880
3880 RETURN
3890 END
```

Appendix 4.3.

Solar Transmission of the Wall Module

```
10     REM PROGRAM 9
20     REM THIS PROGRAM CALCULATES THE SOLAR TRANSMITTANCE OF A
30     REM SCREEN ARRAY. SEE CHAPTER 6.2
40 EL "OUTPUT"
50 QE "OUTPUT"
60 AS #12="OUTPUT"
70 OPEN #12
80      REM
90      REM
100 WIDTH=1
110 HT=1
120      REM    GAP=SCREEN SPACING.
130 GAP1=.025
140 GAP2=.025
150 GAP3=.025
160 GAP4=.025
170 GAP5=.025
180 INPUT "DIRECT SOLAR RADIATION W/M^2"
190 INPUT "ANGLE OF INCIDENCE, DEGREES (GREATER THAN 0)"
200     REM
210 THETA1=THETA1*PI(1/180)
220     REM
230     REM    BEAM1=ENERGY FALLING UPON OUTER COVER.
240 BEAM1=BEAM*COS(THETA1)
250     REM
260 INPUT "ABSORBER MATERIAL, MAXORB OR NONSEL"
270 PRINT "SCREEN MATERIAL MAY BE: -POLYTHENE, MELINEX, TEDLAR"
280 PRINT "GLASS, POLYPROPYLENE OR HOWSON"
290 PRINT
300 INPUT "1ST SCREEN MATERIAL", M2$
310 INPUT "SECOND SCREEN MATERIAL", M3$
320 INPUT "THIRD SCREEN MATERIAL", M4$
330 INPUT "FOURTH SCREEN MATERIAL", M5$
340 INPUT "OUTER SCREEN MATERIAL", M6$
350      REM
```

```
360      REM    RHOSB=SCREEN REFLECTANCE TO BEAM RADIATION
370      REM    TORSB=SCREEN TRANSMITTANCE.
380 M$=M1$
390 GOSUB 710
400 RHOSB1=1-BLACK
410 RHOSD1=1-BLACK
420      REM
430      REM
440 M$=M2$
450 GOSUB 710
460 RHOSB2=RHOSE: RHOSB3=RHOSF: TORSB2=TORSE: TORSB3=TORSF
470      REM
480      REM
490 M$=M3$
500 GOSUB 710
510 RHOSB4=RHOSE: RHOSB5=RHOSF: TORSB4=TORSE: TORSB5=TORSF
520      REM
530      REM
540 M$=M4$
550 GOSUB 710
560 RHOSB6=RHOSE: RHOSB7=RHOSF: TORSB6=TORSE: TORSB7=TORSF
570      REM
580      REM
590 M$=M5$
600 GOSUB 710
610 RHOSB8=RHOSE: RHOSB9=RHOSF: TORSB8=TORSE: TORSB9=TORSF
620      REM
630      REM
640 M$=M6$
650 GOSUB 710
660 RHOSB10=RHOSE
670 GOTO 1440
680      REM
690      REM
700      REM
```

```
710 IF M$="MAXORB" THEN GOTO 830
720 IF M$="NONSEL" THEN GOTO 860
730 IF M$="GLASS" THEN GOTO 930
740 IF M$="HOWSON" THEN GOTO 960
750 IF M$="POLYTHENE"THEN GOTO 990
760 IF M$="POLYPROPYLENE" THEN GOTO 1020
770 IF M$="MELINEX"THEN GOTO 1070
780 IF M$="TEDLAR" THEN GOTO 1100
790 IF M$="RGLASS" THEN GOTO 1130
800 PRINT "NO MATERIAL DEFINITION":GOTO 1890
810     REM
820     REM
830 BLACK=.95:GOTO 1410
840     REM
850     REM
860 BLACK=.95:GOTO 1410
870     REM
880     REM
890     REM
900     REM   RIND=REFRACTIVE INDEX.
910     REM   EXTCF=EXTINCTION COEFFICIENT
920     REM   THK=SCREEN THICKNESS
930 RIND=1.526:EXCF=10:THK=.005:GOTO 1180
940     REM
950     REM
960 GOSUB 1940
970 GOTO 1390
980     REM
990 RIND=1.51:EXCF=300:THK=3E-5:GOTO 1180
1000    REM
1010    REM
1020 RIND=1.51:EXCF=300:THK=3E-5:GOTO 1180
1030    REM
1040    REM
1050    REM
```

```
1060      REM
1070 RIND=1.62: EXCF=240: THK=75E-6: GOTO 1180
1080      REM
1090      REM
1100 RIND=1.684: EXCF=280: THK=100E-6: GOTO 1180
1110      REM
1120      REM
1130 PRINT "GLASS NOT YET DEFINED": GOTO 1890
1140      REM
1150      REM
1160      REM
1170      REM    CALC EFFECTIVE REFLECTANCE AND TRANSMITTANCE.
1180 THETAA=THETA1
1190      REM
1200      REM THETAB=REFRACTED ANGLE. TABS=TRANSMITTANCE TO ABSORBTION.
1210 THETAB=ASN(SIN(THETAA/RIND)): TABS=EXP(-EXCF*THK/COS(THETAB))
1220      REM
1230      REM RPERP=REFLECTION PERPENDICULAR
1240 RPERP=(SIN(THETAB-THETAA))^2/(SIN(THETAB+THETAA))^2
1250      REM
1260      REM RLEL= REFLECTION PARALLEL
1270 RLEL=(TAN(THETAB-THETAA))^2/(TAN(THETAB+THETAA))^2
1280      REM
1290      REM TREFL=TRANSMITTANCE DUE TO REFLECTION
1300 TREFL=1/2*((1-RLEL)/(1+RLEL)+(1-RPERP)/(1+RPERP))
1310      REM
1320      REM TORS=TOTAL TRANSMITTANCE.
1330 TORS=TABS*TREFL
1340      REM
1350 RHOS=1-TREFL
1360      REM
1370 RHOSE=RHOS: RHOSF=RHOS: TORSE=TORS: TORSF=TORS
1380      REM
1390 IF M$><M6$ THEN 1410
1400 TOR11B=TORS
```

```
1410 RETURN
1420      REM
1430      REM
1440 OPTION BASE=1
1450 DIM GCFSB(1:10,1:10)
1460 DIM GCFSBA(1:10,1:10)
1470 DIM SOLINB(1:10,1:1)
1480 DIM GRASB(1:10,1:1)
1490      REM
1500      REM
1510 GE "PUTIN"
1520AS #13="PUTIN"
1530 OPEN #13
1540 RW #13
1550      REM
1560      REM DATA FOR G COEFFICIENT MATRIX FOLLOWS.
1570 PRINT #13;-RHOSB1;1;0;0;0;0;0;0;0;0
1580 PRINT #13;-1;RHOSB2;TORSB2;0;0;0;0;0;0;0
1590 PRINT #13;0;-TORSB3;-RHOSB3;1;0;0;0;0;0;0
1600 PRINT #13;0;0;-1;RHOSB4;TORSB4;0;0;0;0;0
1610 PRINT #13;0;0;0;-TORSB5;-RHOSB5;1;0;0;0;0
1620 PRINT #13;0;0;0;0;-1;RHOSB6;TORSB6;0;0;0
1630 PRINT #13;0;0;0;0;0;-TORSB7;-RHOSB7;1;0;0
1640 PRINT #13;0;0;0;0;0;0;-1;RHOSB8;TORSB8;0
1650 PRINT #13;0;0;0;0;0;0;0;-TORSB9;-RHOSB9;1
1660 PRINT #13;0;0;0;0;0;0;0;0;-1;RHOSB10
1670 RW #13
1680 MAT INPUT #13,GCFSB
1690 RW #13
1700      REM
1710      REM
1720      REM DATA FOR SOLAR INPUT THROUGH OUTER SCREEN FOLLOWS.
1730 PRINT #13;0;0;0;0;0;0;0;0;0;-BEAM1*WIDTH*HT*TOR11B
1740 RW #13
1750 MAT INPUT #13,SOLINB
```

```
1760      REM
1770      REM
1780 EL "PUTIN"
1790      REM
1800      REM
1810      REM
1820      REM      **************
1830      REM
1840      REM MATRIX MANIPULATION.
1850 MAT GCFSBA=INV(GCFSB)
1860 MAT GRASB=GCFSBA*SOLINB
1870 PRINT "TRANSMITTANCE=",GRASB(1,1)/BEAM
1880 STOP
1890 END
1900     REM
1910     REM      ***************
1920      REM SUBROUTINE FOR "HOWSON" SCREEN.
1930      REM "MELINEXR"IS MELINEX WITH ANTI-REFLECTION COATING.
1940 IF M$="MELINEXR" THEN RIND1=1.4 ELSE RIND1=1.51
1950 RIND2=2.1:EXCF1=300:EXCFL=.01635:THK=75E-6
1960 THETAA=THETA1
1970 THETAB=ASN(SIN(THETAA/RIND1))
1980 THETAC=ASN(SIN(THETAB/RIND2))
1990 TABS1=EXP(-EXCF1*THK/COS(THETAB))
2000 TABS2=EXP(-EXCFL/COS(THETAC))
2010 RPERP1=SIN(THETAB-THETAA)^2/(SIN(THETAB+THETAA)^2)
2020     REM
2030 RLEL1=TAN(THETAB-THETAA)^2/(TAN(THETAB+THETAA)^2)
2040 RPERP2=SIN(THETAC-THETAB)^2/(SIN(THETAC+THETAB)^2)
2050 RLEL2=TAN(THETAC-THETAB)^2/(TAN(THETAB+THETAC)^2)
2060 TPERP=(1-RPERP1)*(1-RPERP2)/(1-RPERP1*RPERP2)
2070 TLEL=(1-RLEL1)*(1-RLEL2)/(1-RLEL1*RLEL2)
2080 TREF=(TPERP+TLEL)/2
2090 TORS=TREF*TABS1*TABS2
2100 RHOS=1-TREF
2110 RHOSE=RHOS:RHOSF=RHOS:TORSE=TORS:TORSF=TORS
2120 RETURN
```

Appendix 4.4.

Daily Thermal Performance of the Wall Module

```
10          REM      PROGRAM 14
20          REM      THIS PROGRAM CALCULATES THE ENERGY BALENCE UPON THE WALL
30          REM      MODULE FOR A SHEFFIELD URBAN SITE. THE PROGRAM CALCULATES
40          REM      THE SOLAR ENERGY ABSORBED BY A VERTICAL MODULE FOR NORTH
50          REM      SOUTH EAST AND WEST ORIENTATIONS, FOR BRIGHT, OVERCAST OR
60          REM      PARTIALLY CLOUDY CONDITIONS. THE PROGRAM ALSO CALCULATES
70          REM      HOURLY OUTSIDE AIR TEMPERATURES, AND THE APPROPRIATE LOSS
80          REM      OF ENERGY THROUGH THE MODULE WITH A CONSTANT ROOM TEMP-
90          REM      OF 20C. THE ABOVE IS COMPUTED FOR THE 15TH OF EACH MONTH,
100          REM      AND THE RESULTING MONTHLY ENERGY BALENCE ESTABLISHED.
110         REM      SEE CHAPTER 6.
120 DIM WLCF(1:8,1:8)
130 DIM WLTEM(1:8,1:1)
140 DIM WLHT(1:8,1:1)
150 DIM TEMT(0:25,1:1)
160 DIM EATT(0:25,1:1)
170 DIM BSGND(0:25,1:1)
180 DIM BSBGD(0:25,1:1)
190 DIM BSBGC(0:25,1:1)
200 DIM BSB(0:25,1:1)
210 DIM INCA(0:25,1:1)
220 DIM OCD(0:25,1:1)
230          REM      TST IS THE INITIAL SLAB TEMPERATURE ASSUMED
240 TST=293:T11,T21,T31,T41,T51,T61,T71,T81=TST
250          REM
260 GE "PUTMOD"
270 AS #13="PUTMOD"
280 OPEN #13
290 GE "OUTMOD"
300 AS #12="OUTMOD"
310 OPEN #12
320          REM
330          REM      CORR1=HORIZ TO VERT CORRECTION FACTOR FOR "STEVENS" SKY
340          REM      CORR2=              DITTO                ISOTROPIC SKY
350          REM      SEE CHAPTER 6.3 AND APPENDIX 3.
```

```
360 CORR2=.264
370 CORR1=.318
380         REM      RHO IS REFLECTANCE OF MODULE SIDES.
390 RHO=.5
400         REM      LN,HIT,TK=MODULE LENGTH,HEIGHT AND SLAB THICKNESS.
410 LN=1:HIT=1:TK=.125
420         REM      AB=CORRECTION FACTOR FOR DEVIATION OF TRANSMITTANCE
430         REM      FROM COSINE FORM,SEE APPENDIX 3.
440 AB=.95
450 NAME$="SHEFFIELD"
460         REM
470         REM      LONG=LONGITUDE
480 LONG=1.5*PI(1/180)
490 CONV=PI(1)/180
500         REM
510         REM      LAT=LATITUDE
520 LAT=53.5*PI(1/180)
530         REM
540         REM      SLOP=SLOPE OF MODULE FROM HORIZ,SET TO VERT.
550 SLOP=PI(.5)
560         REM
570         REM      ALT=ALTITUDE,METRES
580 ALT=140
590         REM
600         REM      MDY=DAY OF MONTH
610 MDY=15
620         REM      ALB=GROUND ALBEDO
630 ALB=.2
640         REM      CUTOF=TEMPERATURE OF MODULE ROOM SURFACE AT WHICH THE
650         REM      THE THERMOCHROMIC SCREEN BEGINS TO OPERATE.
660 CUTOF=320
670         REM      MT=MONTH NUMBER.
680 FOR MT=1 TO 12 STEP 1
690 IF MT=1 THEN MTH$="JANUARY"
700 IF MT=2 THEN MTH$="FEBRUARY"
```

```
710 IF MT=3 THEN MTH$="MARCH"
720 IF MT=4 THEN MTH$="APRIL"
730 IF MT=5 THEN MTH$="MAY"
740 IF MT=6 THEN MTH$="JUNE"
750 IF MT=7 THEN MTH$="JULY"
760 IF MT=8 THEN MTH$="AUGUST"
770 IF MT=9 THEN MTH$="SEPTEMBER"
780 IF MT=10 THEN MTH$="OCTOBER"
790 IF MT=11 THEN MTH$="NOVEMBER"
800 IF MT=12 THEN MTH$="DECEMBER"
810         REM
820 IF MTH$="JANUARY" THEN 1000
830 IF MTH$="FEBRUARY" THEN 1010
840 IF MTH$="MARCH" THEN 1020
850 IF MTH$="APRIL" THEN 1030
860 IF MTH$="MAY" THEN 1040
870 IF MTH$="JUNE" THEN 1050
880 IF MTH$="JULY" THEN 1060
890 IF MTH$="AUGUST" THEN 1070
900 IF MTH$="SEPTEMBER"THEN 1080
910 IF MTH$="OCTOBER" THEN 1090
920 IF MTH$="NOVEMBER" THEN 1100
930 IF MTH$="DECEMBER" THEN 1110
940         REM
950         REM      SEA$=SEASON; TURB=ATMOSPHERIC TURBIDITY COEFFICIENT
960         REM      FOR KEW; SN=NUMBER OF BRIGHT SUNSHINE HOURS PER DAY;
970         REM      TBARC=MEAN DAILY TEMPERATURE C; PCM=PARTIAL CLOUD
980         REM      MULTIPLIER.
990        REM
1000 DAYNO=MDY: SEA$="WINT": MN=1: MMN=1: TURB=.3: SN=1.25: TBARC=4: ->
     PCM=1.61: GOTO 1130
1010 DAYNO=MDY+31: SEA$="WINT": MN=2: MMN=2: TURB=.35: SN=2.25: TBARC=4.9: ->
     PCM=1.63: GOTO 1130
1020 DAYNO=MDY+59: SEA$="SPRG": MN=3: MMN=3: TURB=.30: SN=3.25: TBARC=6.8: ->
     PCM=2.31: GOTO 1130
```

```
1030 DAYNO=MDY+90: SEA$="SPRG": MN=4: MMN=4: TURB=.40: SN=4.75: TBARC=9.4: ->
    PCM=2.43: GOTO 1130
1040 DAYNO=MDY+120: SEA$="SPRG": MN=5: MMN=5: TURB=.34: SN=5.5: TBARC=12.5: ->
    PCM=2.54: GOTO 1130
1050 DAYNO=MDY+151: SEA$="SUMMER": MN=6: MMN=6: TURB=.25: ->
    SN=6.25: TBARC=15.9: PCM=2.8: GOTO 1130
1060 DAYNO=MDY+181: SEA$="SUMMER": MN=7: MMN=6: TURB=.33: ->
    SN=5: TBARC=15: PCM=2.18: GOTO 1130
1070 DAYNO=MDY+212: SEA$="SUMMER": MN=8: MMN=5: TURB=.36: ->
    SN=4.75: TBARC=16.5: PCM=2.12: GOTO 1130
1080 DAYNO=MDY+234: SEA$="AUTM": NM=9: MMN=4: TURB=.34: ->
    SN=3.5: TBARC=14.7: PCM=1.69: GOTO 1130
1090 DAYNO=MDY+273: SEA$="AUTM": MN=10: MMN=3: TURB=.31: ->
    SN=2.75: TBARC=11.8: PCM=1.8: GOTO 1130
1100 DAYNO=MDY+304: SEA$="AUTM": MN=11: MMN=2: TURB=.25: ->
    SN=1.5: TBARC=7.5: PCM=1.73: GOTO 1130
1110 DAYNO=MDY+334: SEA$="WINT": MN=12: MMN=1: TURB=.17: ->
    SN=1: TBARC=4.9: PCM=1.65: GOTO 1130
1120          REM
1130 TBARK=TBARC+273
1140 IF DAYNO>0 THEN 1160
1150 PRINT "PLEASE INPUT DATE AGAIN": GOTO 780
1160          REM
1170          REM      CALC WATER PRECIPITATION
1180 WPREC=10.44+(-6.47*COS(2*PI(1)/366*DAYNO)-3.492*SIN(2*PI(1)/366*DAYNO))->
     +(1.056*COS(4*PI(1)/366*DAYNO)+2.049*SIN(4*PI(1)/366*DAYNO))->
     +(-.128*COS(6*PI(1)/366*DAYNO)+.579*SIN(6*PI(1)/366*DAYNO))
1190          REM
1200          REM      TERR$=TERRIAN
1210 TERR$="URBAN"
1220          REM
1230          REM      TORAT IS THE ATMOSPHERIC TURBIDITY COEFFICIENT
1240          REM      CORRECTED FOR THE SITE.
1250 IF TERR$="OPEN" THEN TORAT=TURB-.07
1260 IF TERR$="FIELD" THEN TORAT=TURB-.03
```

```
1270 IF TERR$="URBAN" THEN TORAT=TURB
1280 IF TERR$="CITY" THEN TORAT=TURB+.1
1290         REM
1300 PRINT #12; "CUTOFF=", CUTOF
1310 PRINT #12;  "SITE "; NAME$; "    LATITUDE "; LAT*180/PI(1); ->
     "    LONGITUDE "; LONG*180/PI(1)
1320 PRINT #12;  "ALTITUDE                        "; ALT
1330 PRINT #12;  "MONTH & DAY                     "; MTH$; " "; MDY
1340 PRINT #12;  "GROUND ALBEDO                   "; ALB
1350 PRINT #12;  "TURBIDITY COEFFICIENT           "; TORAT
1360 PRINT #12;  "TERRIAN                         "; TERR$
1370 PRINT #12;  "WATER PRECIPITATION             "; WPREC; "MM"
1380         REM
1390         REM      DTYP$=TYPE OF DAY
1400 DTYP$="AVCST"
1410 IF DTYP$="BS" THEN 1450
1420 IF DTYP$="AVCST" THEN 1460
1430 IF DTYP$="CST10" THEN 1470
1440 IF DTYP$="PC" THEN 1480
1450 PRINT #12;  "BRIGHT CLEAR DAY": GOTO 1490
1460 PRINT #12;  "AVERAGE OVERCAST DAY": GOTO 1490
1470 PRINT #12;  "10% WORST OVERCAST DAY"
1480 PRINT #12;  "PARTIALY CLOUDY SKY"
1490         REM
1500         REM      AZP=WALL AZIMUTH ANGLE; SOUTH 0, WEST +VE.
1510 AZP=0
1520 PRINT #12;  "WALL ORIENTATION                "; AZP*180/PI(1); ->
     "DEGREES FROM SOUTH"
1530 PRINT #12;
1540 PRINT #12; ->
     "TIME    SOLAR      AIR     WALL     WALL    HEAT    COVER    TRANS"
1550 PRINT #12; ->
     "          INPUT      TEMT    OUTER    INNER   FLOW    TEMP      MITCE"
1560         REM
1570 GBEAM1=0: GBEAM2=0: GBEAM3=0: GBEAM4=0: SBGSUF=0: SCCSU1=0: SCCSU2=0
```

```
1580 SUFTOT=0
1590          REM
1600         REM      SOLAR ENERGY CALCULATIONS FOLLOW, SEE CHAPTER 6.3.
1610         REM
1620          REM      CALC CORRECTED EXTRA TERRESTRIAL SOLAR NORMAL RADIATION
1630 WN=PI(2)/366*DAYNO
1640 SLXCOR=1/1353*(1353+45.326*COS(WN)+1.8037*SIN(WN)+.88018*COS(2*WN)->
    +.09746*SIN(2*WN)-.00461*COS(3*WN)+.18412*SIN(3*WN))
1650          REM      SOLXN=EXTRATERRESTRIAL NORMAL SOLAR RADIATION
1660 SOLXN=SLXCOR*1353
1670          REM
1680          REM      CALC EQUATION OF TIME
1690 STIMEQ=.00037+.43177*COS(WN)-7.3764*SIN(WN)-3.165*COS(2*WN)->
    -9.3893*SIN(2*WN)+.07272*COS(3*WN)-.24498*SIN(3*WN)
1700          REM
1710          REM      CALC SOLAR DECLINATION
1720 SOLDEC=.33281-22.984*COS(WN)+3.7872*SIN(WN)-.3499*COS(2*WN)->
    +.03205*SIN(2*WN)-.1398*COS(3*WN)+.07187*SIN(3*WN)
1730 SOLDEC=SOLDEC*CONV
1740          REM
1750          REM      CALC SUNSET ANGLE
1760 SUNSET=ACS(-TAN(LAT)*TAN(SOLDEC))
1770          REM
1780          REM      CALC DAYLIGHT HOURS
1790 DAYHRS=2/15*180/PI(1)*SUNSET
1800          REM
1810          REM      ITN=ITERATION NUMBER
1820 ITN=0
1830          REM      TAT=TOTALISED AIR TEMPERATURE.
1840 TAT=0
1850 HTFLT=0
1860 ITN=ITN+1
1870          REM      GMT= GREENWICH MEAN-TIME, MINUTES.
1880 FOR GMT=0 TO 24*60 STEP 60
1890          REM
```

```
1900          REM      CALC SOLAR TIME
1910 SOLTIM=GMT-4*LONG/CONV+STIMEQ
1920          REM
1930          REM      CALC HOUR ANGLE
1940 HRAN=(12-SOLTIM/60)*15*CONV
1950          REM
1960          REM
1970          REM      CALC ANGLE OF INCIDENCE
1980          REM      HRAN2 IS HOUR ANGLE WITH MORNING -VE.
1990 HRAN2=-HRAN
2000          REM
2010          REM      CALCULATE ANGLE OF BEAM INCIDENCE.
2020 SOLINC= (SIN(SOLDEC)*SIN(LAT)*COS(SLOP)->
     -SIN(SOLDEC)*COS(LAT)*SIN(SLOP)*COS(AZP)->
     +COS(SOLDEC)*COS(LAT)*COS(SLOP)*COS(HRAN2)->
     +COS(SOLDEC)*SIN(LAT)*SIN(SLOP)*COS(AZP)*COS(HRAN2)->
     +COS(SOLDEC)*SIN(SLOP)*SIN(AZP)*SIN(HRAN2))
 2030 SOLINC=ACS(SOLINC)
 2040          REM
 2050          REM
 2060          REM      CALC SOLAR ZENITH ANGLE
 2070 SOLZEN=ACS(COS(SOLDEC)*COS(LAT)*COS(HRAN)+SIN(SOLDEC)*SIN(LAT))
 2080          REM
 2090          REM      CALC SOLAR ALTITUDE ANGLE
 2100 SOLALT=ASN(SIN(LAT)*SIN(SOLDEC)+COS(LAT)*COS(SOLDEC)->
      *COS(HRAN))
 2110          REM
 2120 IF SOLALT<.001 THEN 2150
 2130 IF SOLALT>PI(.999) THEN 2150
 2140 GOTO 2220
 2150 GBEAM1=0: GBEAM2=0: GBEAM3=0: GBEAM4=0: SBGSUF=0: SCCSU1=0: SCCSU2=0
 2160 SBGDIF=0
 2170 SBGGND=0
 2180 SUFTOT=0
 2190 GOTO 3050
```

```
2200          REM
2210          REM      CALCULATE AIR MASS
2220 IF SOLALT<10*PI(1)/180 THEN 2250
2230          REM
2240 AMAS=1/SIN(SOLALT):GOTO 2260
2250 AMAS=EXP(3.67985-24.4465*SIN(SOLALT)+154.017*SIN(SOLALT)^2->
     -742.181*SIN(SOLALT)^3+2263.36*SIN(SOLALT)^4-3804.89*SIN(SOLALT)^5->
     +2661.05*SIN(SOLALT)^6)
2260          REM
2270 AMAS=AMAS*EXP(ALT/1000*(-.1174-.0017*ALT/1000))
2280          REM
2290          REM      CALC DIRECT BEAM NORMAL RADIATION
2300 GIND1=((-12.9641E-2)+(.412828E-2*WPREC)+(-1.12096E-4*WPREC^2))->
     +((-6.4211E-2)+(-.80104E-2*WPREC)+(1.53069E-4*WPREC^2))*AMAS->
     +((-.46883E-2)+(.220414E-2*WPREC)+(-.429818E-4*WPREC^2))*AMAS^2->
     +((.0844097E-2)+(-.0191442E-2*WPREC)+(.0374176E-4*WPREC^2))*AMAS^3
2310 GBEAM1=SOLXN*EXP(GIND1)
2320          REM
2330          REM      GBEAM2=NORMAL BRIGHT SKY RADIATION AT SITE
2340 GBEAM2=GBEAM1*EXP(-TORAT*AMAS)
2350          REM
2360          REM      CALC SOLAR AZIMUTH
2370 SOLAZA=ACS((SIN(SOLDEC)*COS(LAT)-COS(SOLDEC)*SIN(LAT)*COS(HRAN))->
     /COS(SOLALT))
2380 IF SOLTIM/60>12 THEN 2410
2390          REM      BRING=SOLAR BEARING FROM NORTH
2400 SOLAZ=SOLAZA-PI(1):BRING=SOLAZA:GOTO 2440
2410 SOLAZ=PI(1)-SOLAZA:BRING=2*PI(1)-SOLAZA
2420          REM
2430          REM      CALC DIRECT BEAM RADIATION ON SURFACE
2440 GBEAM3=GBEAM2*COS(SOLINC)
2450 IF GBEAM3<0 THEN GBEAM3=0
2460          REM
2470          REM      CALC HORIZONTAL WALL SHADOW ANGLE, SEE APP 3.
2480 IF AZP>=PI(1) THEN AZP1=AZP-PI(1)
```

```
2490 IF AZP<PI(1) THEN AZP1=AZP+PI(1)
2500 IF BRING<AZP1 THEN WLHSHD=AZP1-BRING
2510 IF BRING>AZP1 THEN WLHSHD=BRING-AZP1
2520         REM
2530         REM      CALC VERTICAL WALL SHADOW ANGLE, SEE APP 3.
2540 WLVSHD=ATN(TAN(SOLALT)/COS(WLHSHD))
2550         REM
2560         REM      CALCULATE BACKGROUND AND CIRCUMSOLAR DIFFUSE COEFFS
2570         REM      FOR A BRIGHT SKY
2580 ELV=SIN(SOLALT)
2590         REM
2600 BDIFB0=2+331.965*ELV-658.223*ELV^2+4356.27*ELV^3-15563*ELV^4->
    +26253.8*ELV^5-20505.8*ELV^6+6037.43*ELV^7
2610         REM
2620 BDIFB1=.272+.371162*ELV-9.33202*ELV^2+45.8221*ELV^3-108.407*ELV^4->
    +137.668*ELV^5-89.6616*ELV^6+23.4606*ELV^7
2630         REM
2640 CDIFC0=1+536.917*ELV-802.612*ELV^2+3836.53*ELV^3-12557*ELV^4->
     +20257.8*ELV^5-15276.3*ELV^6+4358.42*ELV^7
2650 CDIFC1=.4524+1.54901*ELV-12.2948*ELV^2+36.6472*ELV^3-60.846*ELV^4->
     +59.7328*ELV^5-32.3132*ELV^6+7.3817*ELV^7
2660         REM
2670         REM      CALC DIRECT SOLAR RADIATIO ON HORIZONTAL SURFACE
2680 GBEAM4=GBEAM2*SIN(SOLALT)
2690         REM
2700         REM      CALC SOLAR BACKGROUND DIFFUSE RADIATION ON A
2710         REM      HORIZONTAL SURFACE.
2720 SBGDIF=SLXCOR*BDIFB0-BDIFB1*GBEAM4
2730         REM
2740         REM      CALC CIRCUMSOLAR DIFFUSE RADIATION UPON A
2750         REM      HORIZONTAL SURFACE.
2760 SBGCCS=SLXCOR*CDIFC0-CDIFC1*GBEAM4
2770         REM
2780         REM      CALC BACKGROUND DIFFUSE ON SURFACE
2790 SBGSUF=SBGDIF/2*(1+COS(SLOP))
```

```
2800          REM
2810          REM      CALC CIRCUMSOLAR DIFFUSE UPON SURFACE
2820 SCCSU1=SBGCCS*COS(SOLINC)
2830 IF SCCSU1<0 THEN SCCSU1=0
2840          REM
2850          REM      CALC CORRECTION FOR SURFACES AT LARGE ANGLES TO SUN
2860 SCCSU2=.4*SBGCCS*(1-COS(SLOP))*SIN(2*(WLHSHD-PI(.25)))->
     *SIN(SOLALT)*COS(SOLALT)
2870 IF WLHSHD<PI(.25) THEN SCCSU2=0
2880 IF WLHSHD>PI(.75) THEN SCCSU2=0
2890          REM
2900          REM      CALC TOTAL RADIATION ON HORIZONTAL SURFACE
2910 GHTOT=GBEAM4+SBGDIF+SBGCCS*SIN(SOLALT)
2920          REM
2930          REM      CALC CONTRIBUTION FROM GROUND REFLECTION
2940 SBGGND=.5*ALB*GHTOT*(1-COS(SLOP))
2950          REM
2960          REM      CALC TOTAL RADIATION ON SURFACE
2970 SUFTOT=GBEAM3+SBGSUF+SCCSU1+SCCSU2+SBGGND
2980          REM
2990          REM      TORN=NORMAL SOLAR TRANSMITTANCE OF MODULE
3000          REM      T81=MODULE ROOM SURFACE TEMPERATURE.
3010 TORN=(.5-.4/3*(T81-CUTOF))
3020 IF TORN>.5 THEN TORN=.5
3030 IF TORN<.1 THEN TORN=.1
3040          REM
3050 IF DTYP$="BS" THEN GOSUB 3390
3060 IF DTYP$="AVCST" THEN GOSUB 3760
3070 IF DTYP$="CST10" THEN GOSUB 3920
3080 IF DTYP$="PC" THEN GOSUB 3390
3090 GOSUB 4050
3100 EATT(GMT/60,1)=EATOT
3110 TEMT(GMT/60,1)=TEMP
3120 BSGND(GMT/60,1)=SBGGND
3130 BSBGD(GMT/60,1)=SBGSUF
3140 BSBGC(GMT/60,1)=SCCSU1+SCCSU2
```

```
3150 BSB(GMT/60,1)=GBEAM3
3160 INCA(GMT/60,1)=SOLINC
3170 OCD(GMT/60,1)=OCH*.396+OCH*.5*ALB
3180          REM
3190 IF GMT=0 THEN 3230
3200          REM
3210 GOSUB 5260
3220          REM
3230 NEXT GMT
3240          REM
3250 IF ITN<2 THEN 1840
3260          REM
3270 PRINT #12,->
          "MEAN AIR TEMPERATURE                    =",TAMN
3280 PRINT #12,->
          "AVERAGE HEAT TRANSFER COEFFICIENT=",HTCF
3290 PRINT #12,->
          "ENERGY BALANCE                          =",HTFLT,"WATT HOURS"
3300 PRINT #12
3310 PRINT #12
3320 PRINT #12
3330 NEXT MT
3340          REM
3350 STOP
3360          REM      ***********
3370          REM      ***********
3380          REM      ***********
3390          REM      SUBROUTINE FOR SUN ON BRIGHT DAYS
3400 EAD=0:EAR=0:EABG=0:EAGND=0
3410 IF SOLALT>0 THEN GOTO 3450
3420 EATOT=0:DAREA=0:RAREA=0:GOTO 3720
3430          REM
3440          REM      IGNORE SOLAR INPUT IF SHADOW FALLS PAST ABSORBER.
3450 IF WLHSHD>ATN(LN/TK) THEN 3490
3460 IF WLVSHD>ATN(HIT/TK) THEN 3490
```

```
3470 GOTO 3540
3480          REM      EATOT= TOTAL SOLAR ENERGY ABSORBED.
3490 EATOT=(((SBGDIF)*CORR1*TORN*AB)+SBGGND*TORN*COS(60*CONV)*AB)
3500 IF DTYP$="PC" THEN EATOT=PCM*EATOT
3510 GOTO 3720
3520          REM
3530          REM      DAREA=ABSORBER AREA DIRECTLY ILLUMINATED.
3540 DAREA=(HIT*LN-TK*LN*TAN(WLVSHD)-HIT*TK*TAN(WLHSHD)->
          +TK^2*TAN(WLVSHD)*TAN(WLHSHD))
3550          REM
3560          REM      RAREA=AREA OF MODULE SIDES ILLUMINATED.
3570 RAREA=((LN*TK-TK^2/2*TAN(WLHSHD))*COS(SOLZEN)->
          +HIT*TK-TK^2/2*TAN(WLVSHD)*SIN(SOLZEN)*SIN(WLHSHD))
3580          REM
3590          REM      EAD=BEAM RADIATION DIRECTLY ABSORBED.
3600 EAD=DAREA*COS(SOLINC)*TORN*COS(SOLINC)*AB->
       *(GBEAM2+(SCCSU1+SCCSU2)/COS(SOLINC))
3610          REM
3620          REM      EAR=BEAM RADIATION REFLECTED ONTO ABSORBER.
3630 EAR=RAREA*TORN*COS(SOLINC)*AB*RHO*(GBEAM2+(SCCSU1+SCCSU2)/COS(SOLINC))
3640          REM
3650          REM      EABG=DIFFUSE RADIATION ABSORBED.
3660 EABG=SBGDIF*CORR1*TORN*AB
3670          REM
3680          REM      EAGND=GROUND REFLECTED DIFFUSE RADIATION ABSORBED.
3690 EAGND=SBGGND*TORN*AB*COS(60*CONV)
3700 EATOT=EAD+EAR+EABG+EAGND
3710 IF DTYP$="PC" THEN EATOT=SBGDIF*CORR1*TORN*AB*PCM->
      +EAGND*PCM->
      +PCM*((SCCSU1+SCCSU2)*TORN*AB*(DAREA*COS(SOLINC)+RAREA*RHO))
3720 RETURN
```

```
3730          REM       ************
3740          REM       ************
3750          REM       ************
3760          REM       SUBROUTINE FOR AVERAGE OVERCAST DAYS
3770 IF SOLALT>.01 THEN GOTO 3810
3780 EATOT=0:GOTO 3880
3790          REM
3800          REM       OCIND=OVERCAST SKY ENERGY INDEX,SEE 6.3.2.
3810 IF SEA$="WINT" THEN OCIND=230
3820 IF SEA$="SPRG" THEN OCIND=170
3830 IF SEA$="SUMMER" THEN OCIND=260
3840 IF SEA$="AUTM" THEN OCIND=230
3850          REM       OCH=OVERCAST SKY ENERGY ON HORIZ SURFACE.
3860 OCH=2+OCIND*SIN(SOLALT)
3870 EATOT=OCH*CORR2*TORN*AB+.5*OCH*ALB*TORN*AB*COS(60*CONV)
3880 RETURN
3890          REM************
3900          REM       ************
3910          REM       ************
3920          REM       SUBROUTINE FOR 10% WORST DAYS SUN
3930 IF SOLALT>.01 THEN 3950
3940 EATOT=0:GOTO 4010
3950 IF SEA$="WINT" THEN OCIND=64
3960 IF SEA$="SPRG" THEN OCIND=116
3970 IF SEA$="SUMMER" THEN OCIND=213
3980 IF SEA$="AUTM" THEN OCIND=118
3990 OCH=2+OCIND*SIN(SOLALT)
4000 EATOT=OCH*CORR2*TORN*AB+OCH*.5*ALB*TORN*AB*COS(60*CONV)
4010 RETURN
4020          REM       ************
4030          REM       ************
4040          REM       ************
4050          REM       SUBROUTINE FOR AIR TEMPERATURE,SEE 6.3.3
4060          REM       WMEAN=MEAN WIND SPEED M/S.
4070 WMEAN=6
```

```
4080 IF TERR$="OPEN" THEN 4150
4090 IF TERR$="FIELD" THEN 4160
4100 IF TERR$="URBAN" THEN 4170
4110 IF TERR$="CITY" THEN 4180
4120 PRINT "TERRIAN NOT DEFINED":GOTO 1160
4130          REM
4140          REM      KS AND LS ARE WIND SPEED INDICES.
4150 KS=.68:LS=.17:GOTO 4210
4160 KS=.52:LS=.17:GOTO 4210
4170 KS=.35:LS=.25:GOTO 4210
4180 KS=.21:LS=.33:GOTO 4210
4190          REM
4200          REM      WIND=WIND SPEED M/S.
4210 WIND=WMEAN*KS*10^LS
 4220          REM
4230          REM
4240 FMN=4.62-2.3*MMN+.43*MMN^2-.0267*MMN^3
4250          REM
4260          REM      AVERAGE @ MAX TEMP
4270          REM      AVEF=AVERAGE FUNDAMENTAL TEMPERATURE.
 4280 AVEF=TBARK
 4290 IF MN=1 GOTO 4430
 4300 IF MN=2 GOTO 4430
 4310 IF MN=3 GOTO 4430
 4320 IF MN=4 GOTO 4430
 4330 IF MN=5 GOTO 4580
 4340 IF MN=6 GOTO 4580
 4350 IF MN=7 GOTO 4580
 4360 IF MN=8 GOTO 4580
 4370 IF MN=9 GOTO 4650
 4380 IF MN=10 GOTO 4650
 4390 IF MN=11 GOTO 4650
 4400 IF MN=12 GOTO 4650
  4410          REM
  4420          REM      AVE1ST=AVERAGE 1ST HARMONIC OF AIR TEMPERATURE.
  4430 AVE1ST=2.73*SN/WIND
```

```
4440          REM
4450          REM       AVE2ND=2ND HARMONIC OF AIR TEMPERATURE.
4460 AVE2ND=-(.1+(.4-.1*AVE1ST)*AVE1ST)
4470          REM
4480          REM       MAXF=FUNDAMENTAL OF MAX AIR TEMPERATURE.
4490 MAXF=273+(-3.63+2.01*TBARC-.056*TBARC^2-.165*LONG/CONV)
4500          REM
4510          REM       MAX1ST=1ST HARMONIC OF MAX AIR TEMPERATURE.
4520 MAX1ST=-.49+4.32*SN/WIND+.003*ALT
4530          REM
4540          REM       MAX2ND=2ND HARMONIC OF MAX AIR TEMPERATURE.
4550 MAX2ND=-(.22+(.455-.074*MAX1ST)*MAX1ST)
4560 GOTO 4720
4570          REM
4580 AVE1ST=1+SN*(.85-.125*WIND)
4590 AVE2ND=0
4600 MAXF=(6.14+.36*TBARC+.025*TBARC^2-.347*WIND)+273
4610 MAX1ST=1+SN*(1.61-.28*WIND+.042*(LAT/CONV-50))
4620 MAX2ND=-(4.09+.0013*ALT-1.3*MN+.1*MN^2)
4630 GOTO 4720
4640          REM
4650 AVE1ST=2.73*SN/WIND-.488*(SN/WIND)^2
4660 AVE2ND=-(.1+(.43-.082*AVE1ST)*AVE1ST)
4670 MAXF=(-3.73+1.67*TBARC-.023*TBARC^2-.165*LONG/CONV)+273
4680 MAX1ST=(2.79+.006*ALT)*SN/WIND
4690 MAX2ND=-(.38+(.404-.05*MAX1ST)*MAX1ST)
4700          REM
4710          REM       AVEPS1=AVERAGE TEMP 1ST HARMONIC PHASE ANGLE.
4720 AVEPS1=13+(AVE1ST)*FMN
4730          REM
4740          REM       AVEPS2=AVERAGE TEMP 2ND HARMONIC PHASE ANGLE.
4750 AVEPS2=.5*AVEPS1
4760          REM
4770          REM       MAXPS1=MAX TEMP 1ST HARMONIC PHASE ANGLE.
4780 MAXPS1=13+.7*MAX1ST*FMN
```

```
4790          REM
4800          REM      MAXPS2=MAX TEMP 2ND HARMONIC PHASE ANGLE.
4810 MAXPS2= .5*MAXPS1
4820          REM
4830          REM      AVTEMP=AVERAGE AIR TEMPERATURE.
4840 AVTEMP=AVEF+AVE1ST*COS(PI(1/12)*(SOLTIM/60-AVEPS1))->
              +AVE2ND*COS(PI(1/6)*(SOLTIM/60-AVEPS2))
4850          REM
4860          REM      MATEMP=MAXIMUM AIR TEMPERATURE.
4870 MATEMP=MAXF+MAX1ST*COS(PI(1/12)*(SOLTIM/60-MAXPS1))->
              +MAX2ND*COS(PI(1/6)*(SOLTIM/60-MAXPS2))
4880          REM      MINIMUM TEMP DAYS
4890 IF MN=1 GOTO 5010
4900 IF MN=2 GOTO 5010
4910 IF MN=3 GOTO 5010
4920 IF MN=4 GOTO 5010
4930 IF MN=5 GOTO 5010
4940 IF MN=6 GOTO 5010
4950 IF MN=7 GOTO 5080
4960 IF MN=8 GOTO 5080
4970 IF MN=9 GOTO 5080
4980 IF MN=10 GOTO 5080
4990 IF MN=11 GOTO 5080
5000 IF MN=12 GOTO 5010
5010 IF TBARC<2 GOTO 5060
5020          REM
5030          REM      MINF=MINIMUM TEMP FUNDAMENTAL.
5040 MINF=(.68*TBARC+1.5+.2*LONG/CONV+MN/15)+273
5050 GOTO 5110
5060 MINF=(2.86+.2*LONG/CONV+MN/15)+273
5070 GOTO 5110
5080 MINF=(.85*TBARC+.9+MN/10)+273
5090          REM
5100          REM      MIN1ST=MIN TEMP 1ST HARMONIC.
5110 MIN1ST=.5+.16*SN-.1*(.9+1.4*SIN(PI(MN/12)))*(WIND-3.7)+.0013*ALT
```

```
5120          REM      MINPS1=MIN TEMP 1ST HARMONIC PHASE ANGLE.
5130 MINPS1=15.6-.1*(WIND-4)-.1*(MN-1)
5140          REM
5150          REM      MITEMP=MINIMUM TEMPERATURE.
5160 MITEMP=MINF+MIN1ST*COS(PI(1/12)*(SOLTIM/60-MINPS1))
5170 IF DTYP$="BS" THEN TEMP=MATEMP
5180 IF DTYP$="AVCST" THEN TEMP=MITEMP
5190 IF DTYP$="PC" THEN TEMP=MITEMP
5200 IF DTYP$="CST10" THEN TEMP=MITEMP
5210 RETURN
5220          REM      **********
5230          REM      **********
5240          REM      **********
5250          REM      **********
5260          REM      SUBROUTINE FOR WALL STORAGE.
5270          REM
5280          REM      ETSKY=SKY EMITTANCE.
5290 IF DTYP$="BS" THEN ETSKY=(.7+.09*(.5+LN(WPREC/10)))*.5+.09*.35
5300 IF DTYP$="AVCST" THEN ETSKY=(.952+.0144*(.5+LN(WPREC/10)))*.5+.0144*.35
5310 IF DTYP$="CST10" THEN ETSKY=(.952+.0144*(.5+LN(WPREC/10)))*.5+.0144*.35
5320 IF DTYP$="PC" THEN ETSKY=(.952+.0144*(.5+LN(WPREC/10)))*.5+.0144*.35
5330          REM
5340          REM      ETGND=GROUND EMITTANCE.
5350 IF SEA$="WINT" THEN ETGND=.4925 ELSE ETGND=.5
5360          REM
5370          REM      EXCF=EXTINCTION COEFFICIENT OF GLASS COVER.
5380 EXCF=10
5390          REM
5400          REM      COVTK=GLASS COVER THICKNESS MM.
5410 COVTK=.005
5420          REM      WALL DENSITY, DEN
5430 DEN=2400
5440          REM      WALL SPECIFIC HEAT, CP
```

```
5450 CP=1000
5460          REM      WALL THICKNESS THK
5470 THK=.075
5480          REM      WALL CONDUCTIVITY COND
5490 COND=1.44
5500          REM      FINITE TIME DIFFERENCE, TIM
5510 TIM=300
5520          REM      HEAT TRANSFER COEF.  FROM WALL TO AIR VIA SCREENS
5530 H1=.6
5540          REM      ROOM TEMP, TRM
5550 TRM=293
5560          REM      OUTSIDE AIR TEMP TAIR
5570          REM
5580          REM      TAIR=AIR TEMPERATURE,
5590 TAIR=(TEMT(GMT/60,1)+TEMT((GMT/60-1),1))/2
5600          REM
5610          REM      TGND=GROUND TEMPERATURE.
5620 IF SEA$="WINT" THEN TGND=TAIR-1.5 ELSE TGND=TAIR
5630          REM
5640          REM      THETAV=MEAN ANGLE OF INCIDENCE FOR HOUR.
5650 THETAV=(INCA(GMT/60,1)+INCA((GMT/60-1),1))/2
5660          REM
5670          REM      HWIND=WIND HEAT TRANSFER COEFFICIENT.
5680 HWIND=2.8+3*WIND
5690          REM      SOLAR INPUT SLR
5700 SLR=(EATT(GMT/60,1)+EATT((GMT/60-1),1))/2
5710          REM
5720          REM      CALC SOLAR ENERGY ABSORBED BY GLASS COVER.
5730 IF DTYP$="BS" THEN 5760
5740 SOL=.1*(OCD(GMT/60,1)+OCD((GMT/60-1),1))/2
5750 GOTO 5790
5760 SOL=.1*((BSGND(GMT/60,1)+BSGND((GMT/60-1),1))/2->
              +(BSBGD(GMT/60,1)+BSBGD((GMT/60-1),1))/2->
              +(BSBGC(GMT/60,1)+BSBGC((GMT/60-1),1))/2)->
              +(1-EXP(-EXCF*COVTK/COS(THETAV)))->
              *(BSB(GMT/60,1)+BSB((GMT/60-1),1))/2
```

```
5770          REM
5780          REM      TGUS=GUESS AT COVER TEMPERATURE.
5790 TGUS=TAIR
5800          REM
5810          REM      TCOV=COVER TEMPERATURE.
5820 TCOV=(.6*T11+HWIND*TAIR+5.669E-8*->
       (ETSKY*TAIR^4+ETGND*TGND^4-.95*TGUS^4)+SOL)/(HWIND+.6)
5830 IF TCOV<TGUS-.01 THEN 5850
5840 IF TCOV<TGUS+.01 THEN 5870
5850 TGUS=TCOV: GOTO 5820
5860          REM      DEX=FINITE DIFFERENCE NODAL DISTANCE FOR 8 NODES.
5870 DEX=THK/7
5880 ALPH=DEN*CP*DEX/TIM
5890 BET=COND/DEX
5900          REM
5910          REM      LAPSE=FINITE DIFFERENCE TIME INTERVAL.
5920 FOR LAPSE=TIM TO 3600 STEP TIM
5930          REM      HEA TRANSFER COEF. INTO ROOM, H2
5940 H2=3+.95*5.699E-8*(T81^2+TRM^2)*(T81+TRM)
5950 PRINT #13; ALPH/2+BET+H1; -BET; 0; 0; 0; 0; 0; 0
5960 PRINT #13; -BET; ALPH+2*BET; -BET; 0; 0; 0; 0; 0
5970 PRINT #13; 0; -BET; ALPH+2*BET; -BET; 0; 0; 0; 0
5980 PRINT #13; 0; 0; -BET; ALPH+2*BET; -BET; 0; 0; 0
5990 PRINT #13; 0; 0; 0; -BET; ALPH+2*BET; -BET; 0; 0
6000 PRINT #13; 0; 0; 0; 0; -BET; ALPH+2*BET; -BET; 0
6010 PRINT #13; 0; 0; 0; 0; 0; -BET; ALPH+2*BET; -BET
6020 PRINT #13; 0; 0; 0; 0; 0; 0; -BET; ALPH/2+BET+H2
6030 RW #13
6040 MAT INPUT #13, WLCF
6050 RW #13
6060 PRINT #13; H1*TCOV+ALPH/2*T11+SLR; ALPH*T21; ALPH*T31
6070 PRINT #13; ALPH*T41; ALPH*T51; ALPH*T61; ALPH*T71; ALPH/2*T81+H2*TRM
6080 RW #13
6090 MAT INPUT #13, WLHT
6100 RW #13
6110 MAT WLCF=INV(WLCF)
```

```
6120 MAT WLTEM=WLCF*WLHT
6130 T11=WLTEM(1,1):T21=WLTEM(2,1):T31=WLTEM(3,1):T41=WLTEM(4,1)
6140 T51=WLTEM(5,1):T61=WLTEM(6,1):T71=WLTEM(7,1):T81=WLTEM(8,1)
6150 NEXT LAPSE
6160         REM
6170         REM      HTFL=HOURLY HEAT FLOW.
6180 HTFL=SLR-.6*(T11-TCOV)
6190 TAT=TAT+(TAIR-273)
6200         REM
6210         REM      HTFLT=DAILY HEAT BALENCE.
6220 HTFLT=HTFLT+HTFL
6230 IF ITN=2 THEN PRINT #12,USING->
     "##     ####.#     ###.#    ##.#    ###.#    ###.#    ###.#    .##", ->
     GMT/60,SLR,TAIR-273,T11-273,T81-273,HTFL,TCOV-273,TORN
6240 TAMN=TAT/24
6250 HTFLD=HTFLT/24
6260 HTCF=HTFLD/(TRM-273-TAMN)
6270 RETURN
```

REFERENCES

Analogue Devices. Data Acquisition Components and Sub-systems catalogue. Analogue Devices, Central Avenue, East Molesly, Surrey. (1981).

E.C. Barrett. Cloud and Thunder. The Climate of the British Isles. Ed. Chandler & Gregory, Longman, New York (1976).

S. Batty. Some Social Factors Affecting the Market in Solar Energy Thermal Systems. U.K. ISES Conference C31 pp. 55 - 59, (1982)

F. Benford & J.E. Bock. A Time Analysis of Sunshine. Transactions of the American Illumination Engineering Society 34(200) 1939.

Berkeley Energy Efficient Window System. Final report (California University Berkely USA) Lawrence Berkeley Laboratory (1977).

J.W. Bugler. The determination of hourly insolation on an inclined plane using a diffuse irradiance model based upon hourly measured global horizontal insolation. Solar Energy 21(171) (1978).

Building Research Establishment. Energy conservation: A study of energy consumption and a possible means of saving energy in housing. BRE (1975)

D. Charoudi. Variable transmission solar membrane. Proc. 2nd National Passive Solar Conference, Phil adelphia. pp. 602-609 (1978)

Cibs Guide A2. Weather and Solar Data. The Chartered Institute of Building Services. (1982).

F. Clark. NPL Teddington. Private discussion with the author. August 1982.

Cole & Sturrock. The convective heat exchange at the external surface of buildings. Building and Environment 12 pp. 207-214. Pergammon (1977).

Department of Energy (1) Fuel Efficiency Booklet 7, Degree Days. Department of Energy (undated)

D.R. Croft & D.G. Lilley. Heat transfer calculations using finite difference equations. Applied Sciences, London (1977).

R. Dogniaux & Doyem P. Inst. Roy. Met. de Belgique. Contribution No. 18, (1954).

R. Dogniaux. Paper 130. Conf. Sun in the Service of Mankind, UNESCO, Paris, (1973)

J.A. Duffie & W.J. Beckman. Solar Engineering of Thermal Processes. Wiley Interscience. New York (1980).

D.K. Edwards. Solar Absorption by each element in a cover glass array. Solar Energy 19 (4). pp. 401-402 (1977).

A.J. Elder. Guide to the Building Regulations 1976 7th editions. Architectural Press, London (1981)

R. Everett. How do we Know if we've Saved any Energy? ISES Solar World Forum Vol. 3 pp.1792-1796 Pergammon (1982)

D.J. Fisk. Thermal Control of Buildings. Applied Science (1981).

J.M. Gordon & Y. Zarmi. Analytical Models for Passively Heated Solar Houses. Parts 1 & 2. Solar Energy 27(4) pp. 331-347 (1981).

S.T. Hendeson. Daylight and its Spectrum. Hilger (1970).

Hickey etal. Extra terrestrial solar irradiance variability. Two and one half years of measurements from nimbus 7. Solar Energy Vol 29, No.2 pp 125-127, 1982.

K G T Hollands etal. Free convective heat transfer across inclined air layers, Journal of Heat Transfer, pp. 189-193 ASME 1976.

K G T Hollands etal Heat transfer by natural convection across vertical and inclined air layers. ASME 80-HT-67 (1980)

K G T Hollands Heat loss coefficients and effective $\tau\alpha$ products for flat plate collectors with diatermanous covers. Solar Energy 30 (3) pp.211-216 (1983).

K G T Hollands & R.G. Huget. A Probability Density Function for the Clearness Index with Applications. Solar Energy 30.(3). pp. 195-200 (1983).

J. P. Holman — Heat Transfer 3rd Edition, McGraw Hill. (1972).

R.P. Howson, J.N. Avratsiotis, M.I. Ridge, C.A. Bishop — Properties of conducting transparent oxide films produced by ION plating onto room temperature substrates. Applied physics letters 35(2) (1979)

M.G. Hutchins, K. Haywand, J. P. Kenda — Thermal performance of evacuated tubular solar collectors an experimental and theoretical evaluation. ISES Solar World Forum pp. 136-141, Pergamon 1982

M.G. Hutchins — Recent advances in selective surfaces. U.K. ISES Conference C25 pp. 43-50 (1981).

R. Ivimy — Discussion with the author, R. Ivimy of Barton Concrete. Herstmoncevx. (May 1983)

M. Jacob. — Heat transfer, Wiley (1949).

L.F. Jesch. — Solar Energy Today, U.K. ISES, (1981)

P. C. Jones — Discussion with the author, 17.9.81

J.P. Kenna — Materials and design methods to improve the performance of flat plate collectors. U.K. ISES Conference (C25) Discussion (1981).

M.M. Koltun — Selective optical surfaces for solar energy converters. Allerton Press, New York (1981).

K. YA. Kondratyev — Radiation in the atmosphere. Academic Press, (1969).

F. Kreith & W.Z.Black — Basic Heat Transfer. Harper & Row, New York (1980.)

G. Lof. Comments made during the structured discussion of active heating and cooling of buildings. ISES Solar World Forum (1981).

G.Long. Solar Heating Prospects - A personal view. U.K. ISES Conference C31 pp. 85 - 94 (1982).

C. M. Lampert. Heat Mirror Coatings for Energy Conserving Windows. Solar Energy Materials 6 pp.1-41 (1981)

R.M. Lebens. Passive Solar Heating Design. Applied Science (1980)

B.Y.H. Liu and R.C. Jordan. The interrelationship and characteristic distribution of direct, diffuse and total radiation. Solar energy 19 (325) (1977).

A. G. Louden. Overheating of Buildings by Solar Radiation, B.R.S. Internal note no. IN/65. Building Research Establishment, Garston.

A.W.K. MacGregor. A comparison of the suitability of various locations in the European community for Solar Space Heating. ISES Solar World Forum. pp. 1852 - 1857. Pergammon (1982).

D.N. Manning. So You Think You Know About Discount Rates? U.K. ISES Conference C31. pp. 35-44 (1982).

J.J. Mason.

a. The Commercial Prospects for Selective Surfaces on Nickel and Stainless Steel. U.K. ISES Conference M3. pp. 111-116, (1982).

b. To be published in Surface Technology 1983

PERIODIC HEATING/COOLING BY SOLAR RADIATION.
PROC. INT SOLAR ENERGY SOC. CONGRESS. PERGAMON 78.

A.B. Meinel — "Applied Solar Energy" Addison-Wesley, (1978).

Met. Office — Maps of average duration of Bright Sunshine over the United Kingdom 1941-70. Climatological Memorandum No. 72. Met. Office, Bracknell (1974).

Met. Office — Tables of Total Cloud Ammount for the United Kingdom 1957-76. Climatological memorandum No. 110, Met. Office, Bracknell (1980).

Met. Office — Solar Radiation data for the United Kingdom 1951-75. Met. Office, Bracknell (1980).

P. Moon & D.E. Spencer — Illumination Engineering 37 p. 707 (1942).

W.E.J. Neal & A.H. Musa — Observations on Black Nickel Foil Selective Surfaces, Surface Technology 14, 345-352 (1981).

B. Norton, L.J. Petts, D. Smellie & S.J. Probert — Opinions of prospective purchasers concerning water heating by solar energy. U.K. ISES Conference C31. pp. 69 - 78 (1982).

J.F. Orgill & K.G.T. Hollands. — Correlation Equation for Hourly Diffuse Radiation on a Horizontal Surface. Solar Energy 19 (357) (1976).

D. Oppenheim. — An evaluation of all the Solar Heated Buildings in Britain. ISES Solar World Forum, pp. 342 - 347, Pergammon (1982).

J.K. Page. The estimation of Monthly Mean Values of daily Short Wave Irradiation on Vertical and Inclined Surfaces from Sunshine Records for latitudes 60°N to 40°S. University of Sheffied, Dept. of Building Sciences. Report BS32 (1977).

J.K. Page. Methods for the estimation of Solar Energy on Vertical and Inclined Surfaces. University of Sheffield, Dept. of Building Science. Report No. BS46 (1978)

J.K. Page. Systematic techniques of Design for Solar Houses in high latitudes. University of Sheffield, Dept. of Building, Science Report No. BS47 (1979).

J.K. Page, C.G. Souster & S. Sharples. Mathematical modelling of hourly variations in temperature, wind speed and long wave radiation for different classes of radiation day in the United Kingdom. U.K. ISES Conference C.18 (1979).

J.K. Page & R.J. Flynn The development of a Meteorologically Validated model for the prediction of inclined surface irradiation for the EEC area. ISES Solar World Forum pp. 2386 - 2390 - Pergammon (1982).

J.K.R. Page, R.E.B. Swayne, I.K. Mead, & C. Hayman. Thermal storage materials and components for Solar Heating. ISES Solar World Forum, pp. 723 - 730. Pergammon (1982).

G.D. Raithby, K.G.T. Hollands & Tunny. Analysis of heat transfer by natural convection across vertical fluid layers. Journal of heat transfer 99 pp. 439 - 444 (1973)

R.W. Richardson & S.M. Berman. Optimum lumped parameters for modelling building thermal performance. The International Journal of Ambient Energy 2 (4) (1981).

C.G. Rogers, J.K.Page & C.G. Souster. Mathematical models for estimating the Irradiance falling upon inclined surfaces for clear, overcast and average conditions U.K. ISES Conference C18. (1979).

G.G. Rodgers, C.G. Souster & J.K. Page. The development of an interactive computer program SUN 1 for the calculation of Solar Irradiances and Daily Irradiations on Horizontal Surfaces on cloudless days for given conditions of sky clarity and atmospheric water content. University of Sheffield, Dept. of Building, Sciences Report BS28 (Revised) (1981).

R. Sadler. How Does the Consumer View Solar Heating? What Could Make the Market Take Off? U.K. ISES Conference C31 pp. 60 - 68 (1982).

B.O. Seraphin. Spectrally selective surfaces and their impact on photothermal solar energy conversion. Solar Energy Conversion Ed. Dixon & Lesley Pergammon (1979).

S. Sharples. Modelling the short wave, longwave and convective heat transfer at glazing surfaces for the detailed computation of the thermal performance of unshuttered and shuttered windows. University of Sheffield, Dept. of Building. Science Report BS54 (1980).

S. Sharples & J.K.Page Natural convective heat transfer across parallel sided air cavities in building components - A review of current knowledge. University of Sheffield, Dept. of Building Science. (1979).

W.A. Shurcliff. Thermal Shutters and Shades. Brick House Publishing Co. Inc. (1980).

C.G. Souster. University of Sheffield, Dept. of Building Science, Internal research note (1977).

E.M. Sparrow & R.D. Cess. Radiation Heat Transfer. McGraw Hill (1978).

J.R. Stammers. Solar Energy Trades Association, Private discussion (1980).

J.R. Stammers. Developing the market in solar energy thermal systems, an industry view. U.K. ISES Conference C31, pp. 1-10 (1982).

B. Stay. ICI Plastics Division, Private discussion and correspondence with the author, January, 1982.

M.D. Steven. Angular distribution and interception of diffuse solar radiation. Ph.D. thesis University of Nottingham (1977).

H. Tabor. Bulletin, Research Council of Israel, SA No. 2 pp. 119 - 134 (1956).

H. Tabor. Farrington Daniels Address, Solar World Forum, Ed. Hall and Morton, Pergammon (1982).

J.L. Threlkeld. Thermal environmental engineering. Prentice Hall (1962).

J.B. Thring. Hypothesising the diffusion of solar heating. UK ISES Conference C'31, pp. 25 - 34 (1982).

T.S. Toloukian. Thermophysical properties of matter. Vol. 7 Thermal radiative properties of metallic elements & alloys. Heyden & Son, (1970).

M.H. Unsworth. Longwave radiation at the ground. Quarterly Journal of the Royal Meteorological Society. 101 pp. 25 - 34 (1975).

Unsworth & Montieth. Longwave radiation at the ground. Quarterly Journal of the Royal Meteorological Society 101 pp. 13 - 24 (1975).

U.K. ISES Solar Energy, a U.K. Assessment (1976)

J. Walker. Discussion with the author by J. Walker of Serac UK Ltd., Haywards Heath. (1983).

J.W.T. Walsh. The Science of Daylight. MacDonald (1961).

A. Whillier. Solar energy collection and its utilisation for house heating. Ph.D. Thesis, M.I.T, Cambridge, Mass., USA. (1953)

A. Whillier. Prediction of performance of solar collectors. Applications of solar energy for heating and cooling of buildings. ASHRAE GRP 170 (1977).